Part I The Adsorption of Capillary-Active Substances at the Dropping Mercury Electrode

Part II The Polarographic Analysis of Nitrite and of Nitrite-Nitrate Mixtures

Part III An Electron Diffraction Investigation of the Structure of Some Organic Molecules

a) Some Cyclic Derivatives of Ethylene Glycol

b) Naphthalene and Anthracene

Thesis by

Bertram Keilin

In Partial Fulfillment of the Requirements for the

Degree of Doctor of Philosophy

California Institute of Technology
Pasadena, California
1950

TABLE OF CONTENTS

ACKNOWLEDGEMENT

I wish to express my sincere and warm appreciation for the aid, the guidance and the encouragement afforded to me by Professor Verner Schomaker in all phases of the work described in this thesis.

I wish also to thank Professor Linus Pauling and Dr. Robert B. Corey for their direction of this work in the absence of Professor Schomaker.

I am indebted to Mrs. G. Guthrie, Mr. C.N. Scully and Mr. H. Garner for the preparation and purification of the various derivatives of ethylene glycol which were investigated in Part III of this thesis.

I am grateful to my colleagues Mr. G. Guthrie, Mr. K. Hedberg, and Mr. H.G. Pfeiffer for their aid in preparing photographs and for many helpful discussions in the field of electron diffraction.

The work described in Part II of this thesis was carried out with the collaboration of Dr. John W. Otvos, who has never failed to afford me good advice and good friendship.

## ABSTRACT

Part I. The Adsorption of Capillary-Active Materials at the Dropping Mercury Electrode

It has been found that the addition of a capillary-active substance to a solution which is to be analyzed at the dropping mercury electrode brings about a decrease in the diffusion current which passes as a result of the discharge of the reducible ion. Molecules of the capillary-active compound, adsorbed on the surface of the growing drop, appear to deactivate a portion of this electrode surface. As a result, some of the reducible ions or molecules which reach the electrode vicinity by diffusion do not actually reach the electrode surface, and the current which passes as a result of the reduction is consequently decreased. As the concentration of capillary-active material is increased, the diffusion current decreases to a limiting value which is apparently dependent upon the amount of surface still left free on the electrode after a monomolecular layer of material has been adsorbed. Experimental verification and theoretical consequences of the foregoing are described in Part I of this thesis.

Part II. The Polarographic Analysis of Nitrite and of Nitrite-Nitrate Mixtures

It has been found that a solution containing both nitrate and nitrite ions can be analyzed for both constituents in two polarographic experiments. With one aliquot part, the diffusion current due to the two constituents in the original solution is measured. In another aliquot part, the nitrite present is quantitatively oxidized to nitrate and the diffusion current of the resulting solution is measured as before. The two experiments provide sufficient data for determining the quantity of each ion in the solution. The oxidation of nitrite is conveniently carried out with hydrogen peroxide in acid solution and the excess peroxide is destroyed catalytically by manganese dioxide in basic solution.

Part III. An Electron Diffraction Investigation of the Structure of Some Organic Molecules

a) Some Cyclic Derivatives of Ethylene Glycol

The results of an electron diffraction investigation of some cyclic derivatives of ethylene glycol (chlorophosphite ester, sulfite ester, and acetal) confirm the configuration assigned by the organic chemist to these molecules. Non-planarity of the five-membered ring may be demonstrated only in the chlorophosphite ester, in which also there is found an abnormally long phosphorus-to-chlorine bond distance and a subnormally short phosphorus-to-oxygen bond distance. The covalent bond distances in the other molecules were shown to be normal but no conclusion could be drawn concerning the planarity or non-planarity of the ring systems.

b) Naphthalene and Anthracene

In an electron diffraction investigation of naphthalene, the average carbon-to-carbon bond distance has been found to be $1.39_7 \pm 0.02$ Å. The limits of error cannot be narrowed sufficiently to permit a definite choice to be made among the theoretical models proposed by various workers, but the configuration suggested by Penney and Coulson appears to be in best agreement with the observations.

In anthracene, the mean carbon-to-carbon bond distance has been found to be $1.41_9 \pm 0.02$ Å. Although no statement of the limits of error for the individual distances could be made, it was concluded that

the best model in the region investigated is different than that proposed by Robertson, in which the atoms lie at the corners of regular hexagons.

# PART I

## The Adsorption of Capillary-Active Substances at the Dropping Mercury Electrode

# THE ADSORPTION OF CAPILLARY-ACTIVE SUBSTANCES AT THE DROPPING MERCURY ELECTRODE

The polarographic method of analysis was invented by Jaroslav Heyrovsky[1] in 1922, when, at the suggestion of Professor G. Kucera, he attempted to explain some anomalous inflections in the electrocapillary curve of mercury in electrolyte solutions containing reducible substances. The method of analysis is based upon the interpretation of the current-voltage (c.-v.) curve which is obtained when a dilute solution of a reducible or an oxidizable substance is electrolyzed in a cell in which one electrode consists of mercury falling dropwise from a fine-bore capillary tube. The value of the polarographic method lies in its suitability for a simultaneous qualitative and quantitative analysis of very dilute solutions ($10^{-6}$ to $10^{-2}$ molar).

As the potential applied to a dropping mercury electrode dipped into a solution of a reducible substance is made more negative, a sharp rise in the current passing between the electrodes is observed at a voltage approximately corresponding to the equilibrium reduction potential of the material in solution. The current gradually approaches a limiting value, and finally becomes constant and almost independent of further increase in the applied electromotive force. In the presence of a comparatively large concentration of a non-reducible electrolyte (which is used to render negligible the transference number of a reducible ion) and with all other factors constant, the limiting current is a function

of the concentration of the electroreducible substance. The limiting current is due to a virtually complete state of concentration polarization at the dropping electrode. The reaction which takes place at the electrode surface brings about a decrease in the concentration of the reducible substance in the immediate vicinity, and a radial concentration gradient is set up between the electrode and the body of the solution. Diffusion of the reducible substance to the electrode is controlled by this gradient and reaches a limit when the concentration at the electrode surface is effectively zero at all times. With an excess of some indifferent salt (a "supporting electrolyte") present in the solution, the effect of migration (induced by the electric field gradient in the solution) in aiding the approach of the reducible substance to the electrode is negligible and the limiting current is determined almost entirely by the rate of diffusion; hence, it is called a "diffusion current." The potential of the dropping electrode (with respect to an external reference electrode) at that point in the c.-v. curve at which the diffusion current is one-half of its limiting value is characteristic, for reversible electrode reactions, of the particular substance which is being reduced, and is independent of the concentration. This voltage is termed the "half-wave potential."

A quantitative description of diffusion to a growing spherical electrode was first given by Ilkovic[2] in 1934. MacGillavry and Rideal[3] later succeeded in carrying out a more rigorous derivation of the Ilkovic equation, but with an identical result. The fundamental equation relating the average diffusion current, $i_d$, (observed at the

dropping mercury electrode) to the concentration, C, of the reducible substance is

$$i_d = KnD^{1/2}Cm^{2/3}t^{1/6}, \qquad (1)$$

where K is a dimensional constant depending on the units employed in the description of the various quantities, n is the number of faradays of electricity required per mole of the electrode reaction, D is the diffusion coefficient of the reducible substance in the given medium, m is the rate of flow of mercury from the dropping electrode and t is the drop time. The proportionality, under a given set of conditions, between the diffusion current and the concentration of a reducible substance is valid only up to concentrations of the order of $10^{-2}$M. In less dilute solutions, the current which passes is limited by the saturation of the electrode surface; that is, the electrode surface is not large enough to accommodate all of the reducible material which may approach it by diffusion.

The shape of the polarographic wave (c.-v. curve) is determined by the nature of the reaction which takes place at the electrode. For a reversible electrode reaction in an efficiently buffered solution, in which the concentration of the products is effectively zero at all times, the relation between the instantaneous current and the applied voltage is given by

$$E_{d.e.} = E_{1/2} - \frac{0.059}{n} \log \frac{i}{i_d - i}, \qquad (2)$$

where i is the instantaneous current passing to the electrode under the applied potential, $E_{d.e.}$, $i_d$ is the limiting diffusion current and $E_{1/2}$

is the half-wave potential.[4]

The current-voltage curves do not always exhibit the ideal shape described above. In the polarographic analysis of certain molecules or ions, one of the general characteristics of the c.-v. curve is the pronounced maximum which occurs unless special measures are taken to suppress it. The maximum is perfectly reproducible[5] and usually independent of the direction in which the applied electromotive force is changed. As the applied voltage is increased, this feature of the curve always begins at a point approximately corresponding to the toe of the normal c.-v. curve and is characterized by a linear increase in current until a maximum is reached. The shape of the maximum may vary, for different substances, from a sharp, almost discontinuous peak, to a well-rounded hump followed by a more or less rapid decrease to approximately the expected value of the diffusion current, as predicted from the Ilkovic equation.

Many attempts have been made to explain the nature and the origin of the polarographic maximum. Heyrovsky[6] and Ilkovic[7] attributed the phenomenon to the adsorption of the reducible substance at the surface of the drop, whereby the concentration of reducible substance in the immediate electrode area is increased above that in the body of the solution and normal concentration polarization is prevented. This theory has been strongly opposed by Antweiler and von Stackelberg[8,9] who interpret maxima as an electrokinetic effect. These workers, and also Frumkin and his coworkers,[10,11,12] have shown conclusively that there is a pronounced streaming of the liquid around the mercury drop

at that stage in the reduction at which a maximum occurs in the c.-v. curve. Although many attempts have been made to explain the polarographic maximum, none of them has thus far been accepted as a completely satisfactory explanation of the phenomenon; all, including the two mentioned above, appear to meet with serious theoretical difficulties.

Early in the development of the polarographic method of analysis, it was discovered that maxima could be suppressed by the addition to the solution of small traces of certain capillary-active ions (or molecules) or of various non-capillary-active ions or charged colloids. According to Heyrovsky,[5] the Hardy-Schultze rule, with some exceptions, has been found to hold for the suppression of maxima by non-capillary-active substances. For the most part, investigators, interested mainly in practical polarographic analysis, have treated the phenomenon as a nuisance, to be eliminated in whatever way possible. The small effect on the limiting current which sometimes occurred as a result of the addition of capillary-active substances to the solution was ignored, especially since incomplete data on diffusion coefficients often render predictions of the diffusion currents from the Ilkovic equation uncertain, and accurate polarographic analysis is, for the most part, empirical. In the few cases in which the effect was large, attempted explanations were short, scanty, and highly unsatisfactory.

Although the phenomenon of maximum suppression was early associated with the adsorption of molecules at the dropping electrode, the steric hindrance and concomitant deactivation of portions of the electrode surface which one should expect as a result of the adsorption has

apparently not been considered or discussed. It will be shown here that the adsorption of a protein at the dropping mercury electrode may have a large effect in decreasing the limiting current of a reducible substance, that the decrease is a function of the protein concentration, and that there is a limiting concentration of protein above which no further decrease in the diffusion current is observed.

## EXPERIMENTAL PROCEDURES AND RESULTS

### a) Preparation of Solutions and Recording of Polarograms

Polarograms were recorded at 25°C. (±1°) on a Heyrovsky Polarograph, Type XII, manufactured by E. H. Sargent and Co., Chicago, Illinois. Oxygen was removed by bubbling nitrogen through the solution, since it was found to have a large effect on the properties of the c.-v. curves. Potentials were measured with respect to a saturated calomel electrode (S.C.E.) which acted as a standard. The polarograms were analyzed according to the graphical method, a correction being made as usual for the residual current.

Experiments were carried out with the dye p-hydroxyphenyl-azophenylarsonic acid (HPA),

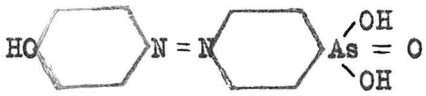


or with cystine, $(HOOC - CH(NH_2) - CH_2S -)_2$, as the reducible substance. Sodium chloride, 0.15 M., was used as the supporting electrolyte and the solutions were buffered at pH 8 with 0.02 M. veronal, the monosodium salt of diethyl barbituric acid,

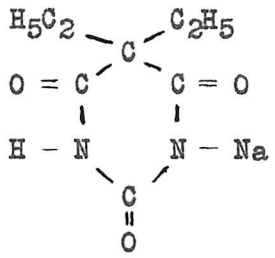


. In solutions of the reducible azo dye, no maximum suppressor is needed in the range of concentrations which were of interest, although a pronounced

maximum occurs in the c.-v. curve at concentrations above $10^{-3}$M. In the reduction of cystine, thymol was used as a maximum suppressor.[13]

A variety of protein substances were used. Quantitative observations were made on solutions containing purified horse albumin (prepared by Dr. G. Wright at this laboratory) or crystallized human albumin (supplied by the Harvard Medical School). The protein content of these preparations was determined by an estimation of the amino nitrogen with Nessler's reagent (analyses by Mr. D. Rice). The results in similar experiments were identical in the two cases. Qualitative comparisons were made with normal rabbit serum, normal sheep serum, purified rabbit globulin, azo albumin (diazo-p-arsanilic acid coupled to purified albumin), and anti-$R_p$ serum (rabbit serum which contains antibodies for the haptenic p-azophenylarsonic acid group).

b) Diffusion Current Constant of p-Hydroxyphenylazophenylarsonic Acid

A test of the accuracy of the Ilkovic equation (1) and a determination of the ratio (known as the "diffusion current constant") between the diffusion current and the concentration of HPA was first carried out. The results of this series of experiments are tabulated in Table I, and are illustrated in Figure 1, wherein the diffusion current is plotted directly against the concentration. A typical polarogram is reproduced in Figure 2.

Table I

p-Hydroxyphenylazophenylarsonic Acid

The Ratio of the Diffusion Current to the Concentration of Azo Dye

All solutions 0.15 M. in NaCl, 0.02 M. in Veronal; pH 8;

temp. 25°C.; $m^{2/3}t^{1/6} = 1.503$ mg.$^{2/3}$-sec.$^{-1/2}$.

| Conc. of Azo Dye, C (millimoles/liter, mm./l.) | Diffusion Current, $i_d$ (microamperes, $\mu$a.) | Diffusion Current Constant, $K' = \frac{i_d}{Cm^{2/3}t^{1/6}}$)* | Half-Wave Potential, $E_{1/2}$** (volts vs. S.C.E.) |
|---|---|---|---|
| 0.986 | 3.72 | 2.50 | -0.419 |
| .906 | 3.38 | 2.48 | .418 |
| .725 | 2.76 | 2.53 | .419 |
| .362 | 1.36 | 2.50 | .416 |
| .181 | 0.69 | 2.55 | .416 |
| .136 | .51 | 2.49 | .417 |
| .0906 | .34 | 2.46 | .422 |
| .0453 | .18 | 2.60 | .421 |
| .0181 | .07 | 2.53 | .420 |
| | Average | 2.52 | -0.419 |
| | Average Deviation | 0.03 | 0.002 |

* Units of K' are $\mu$a.-l.-mm.$^{-1}$-mg.$^{-2/3}$-sec.$^{1/2}$

** The last figure is considered to be unreliable

It may be seen from Table I and from Figure 1 that with all other factors held constant, there is strict linearity between the diffusion current and the concentration of the azo dye in the concentration range investigated. The average diffusion current constant, K', is 2.52 microamperes-liters-millimoles$^{-1}$-milligrams$^{-2/3}$-seconds$^{1/2}$, with an average deviation of 1.3% and a maximum deviation of 3.2%, well within the limits of experimental error. The half-wave potential was found to remain constant (within the limits of error of measurement) at -0.42 volts with respect to a saturated calomel electrode.

From the studies of Shikata and Tachi[14,15] and of Nga,[16] it appears that two electrons are involved in the reduction of the azo group at the dropping mercury electrode and that hydrazo compounds are the reduction products:

$$R - N = N - R + 2H^{+} + 2e^{-} \longrightarrow R - NH - NH - R. \qquad (3)$$

If the Ilkovic equation (1) is written in the form

$$K' = KnD^{1/2} = \frac{i_d}{Cm^{2/3}t^{1/6}}, \qquad (4)$$

then, with K' in the units employed in Table I and D in cm.$^2$/sec., the dimensional constant K has the value 605 $\mu$a.-sec.-cm.-mg.$^{-2/3}$-$\ell$.-mm.$^{-1}$-$F_y^{-1}$, where $F_y$ is the faraday. Substituting in equation (4) the average value of K' (from Table I) and setting n equal to 2, the value for the diffusion coefficient of the azo dye is seen to be

$$D = 4.53 \times 10^{-6} cm^2/sec.$$

This value is in reasonably good agreement with the value

$$D = 5.55 \times 10^{-6} cm.^2 /sec.$$

which is calculated from the Stokes-Einstein relation between the diffusion coefficient and the molecular weight of a spherical molecule.* This result serves to confirm the conclusion of Shikata and Tachi and of Nga (loc. cit.) with respect to the end-product which is formed as a result of the reduction. It is evident then that the concentration of hydrogen ion will affect the position of the wave and that the solutions must be efficiently buffered to insure reproducible results.

Analysis of a typical c.-v. curve of HPA gives a result which throws question upon the general conclusion of Conant and Pratt[17] and of Tachi[18] that the azo-hydrazo systems are reversible. According to equation (2), a plot of the applied potential against log $(\frac{i_d}{i_d - i})$ should result in a straight line with a slope of 0.0295 for a reversible

---

* The assumption of a spherical molecule in this case is a poor one and accounts partly for the disagreement between the calculated and the observed values of the diffusion coefficient. This azo dye molecule undoubtedly has an elongated ellipsoidal shape rather than a spherical one.

The Stokes-Einstein relation is given by

$$D = \frac{RT}{6\pi\eta N (\frac{3M}{4\pi\rho N})^{1/3}}$$

where R is the gas constant, T is the absolute temperature, $\eta$ is the viscosity of the medium, N is Avogadro's number, M is the molecular weight of the dye, and $\rho$ is the density of the dye. The value 0.00895 poises (dyne-sec.-cm.$^{-2}$) was used for the viscosity of the saline solution (I.C.T.), and the density of the dye was found by Dr. Arthur B. Pardee to be 1.5 gms./cc.

two-electron reduction. The results of such an analysis are given in Table II and are plotted in Figure 3.

Table II

p-Hydroxyphenylazophenylarsonic Acid

Reversibility of the Electrode Reaction

| $E_{d.e.}$ (volts vs. S.C.E.) | $\frac{i}{(i_d - i)}$ |
|---|---|
| -0.380 | 0.148 |
| .390 | .239 |
| .400 | .474 |
| .410 | .866 |
| .420 | 1.640 |
| .430 | 2.781 |
| .440 | 4.602 |
| .450 | 8.340 |

These data correspond to 1.50 electrons per molecule for a reversible reduction. The reproducibility of this result in curves obtained from solutions of different dye concentrations makes it improbable that the deviation from the value of 2 for the number of electrons involved in the overall reduction is attributable to an error in measurement. It may well be that the electrode reaction takes place in two stages, one being reversible, the other irreversible. In any case, it must be concluded that the overall electrode reaction is irreversible.

c) Effect of Protein on the Diffusion Current of p-Hydroxyphenylazophenylarsonic Acid

The characteristics of what might be called the normal polarographic reduction of the azo dye having been determined, it is now possible to consider the effect on the diffusion current of the addition of protein to the solutions. A series of solutions were prepared containing constant concentrations of dye, sodium chloride, and veronal, but various concentrations of purified horse albumin. A similar series was prepared with crystallized human albumin. The hydrogen ion concentration was carefully adjusted to pH 8, and a polarogram was recorded for each of the solutions. The composition of the solutions and the results obtained from the polarograms are tabulated in Tables III and IV.

Table III

p-Hydroxyphenylazophenylarsonic Acid

Diffusion Current of Dye in the Presence of Horse Albumin

All solutions $9.86 \times 10^{-4}$ M. in dye, 0.15 M. in NaCl, 0.02 M. in Veronal; pH 8; temp. 25°C., $m^{2/3}t^{1/6} = 1.503$ mg.$^{2/3}$sec.$^{-1/2}$.

| Conc. of Horse Albumin (moles/ℓ. x $10^7$) | Diffusion Current (μa.) | Half-Wave Potential (volts vs. S.C.E.)* |
|---|---|---|
| 228 | 0.94 | -0.515 |
| 114 | 1.01 | .513 |
| 79.9 | 1.17 | .512 |
| 68.5 | 1.26 | .514 |
| 57.1 | 1.48 | .510 |
| 45.7 | 1.76 | .508 |
| 40.0 | 1.84 | .503 |
| 28.6 | 2.28 | .475 |
| 22.8 | 2.74 | .448 |
| 11.4 | 3.30 | .431 |
| 7.99 | 3.48 | .426 |
| 6.85 | 3.55 | .420 |
| 5.71 | 3.75 | .419 |
| 4.57 | 3.68 | .418 |
| 1.14 | 3.79 | .416 |
| 0.114 | 3.71 | .412 |

* The last figure is considered to be unreliable.

Table IV

p-Hydroxyphenylazophenylarsonic Acid

Diffusion Current of Dye in the Presence of Human Albumin

All solutions $9.86 \times 10^{-4}$ M. in dye, 0.15 M. in NaCl, 0.02 M. in Veronal; pH 8; temp. 25°C.; $m^{2/3}t^{1/6} = 1.503$ mg.$^{2/3}$-sec.$^{-1/2}$.

| Conc. of Human Albumin (moles/ℓ. x $10^7$) | Diffusion Current ($\mu$a.) | Half-Wave Potential (volts vs. S.C.E.)* |
|---|---|---|
| 228 | 0.94 | -0.517 |
| 114 | 1.01 | .514 |
| 79.9 | 1.19 | .512 |
| 68.5 | 1.24 | .511 |
| 57.1 | 1.45 | .510 |
| 45.7 | 1.75 | .506 |
| 40.0 | 1.84 | .502 |
| 28.6 | 2.30 | .472 |
| 22.8 | 2.76 | .453 |
| 11.4 | 3.31 | .430 |
| 7.99 | 3.52 | .427 |
| 6.85 | 3.59 | .420 |
| 5.71 | 3.68 | .418 |
| 4.57 | 3.70 | .418 |
| 1.14 | 3.73 | .415 |
| 0.114 | 3.74 | .414 |

* The last figure is considered to be unreliable.

The similarity of the results recorded in Table III to those in Table IV is immediately striking. It is apparent that horse albumin and human albumin have the same effect on the diffusion current of the azo dye. A comparison of a typical current-voltage curve obtained from a dye solution containing protein with that from a slightly less concentrated dye solution containing no protein is made in Figure 6. The diffusion current of the former has been suppressed far below its normal value. Control solutions containing protein, salt, and buffer at pH 8, but no reducible ion, exhibit no diffusion current. In such solutions, the slowly increasing residual current shows a sharp change in slope in the neighborhood of the electrocapillary zero, indicating a change in the cell resistance, due perhaps to the beginning of desorption of the protein from the mercury surface. It should be noted (Figure 6) that the diffusion current of a dye solution containing protein does not reach a true limiting value, but that after leveling off, it begins to increase sharply again in the neighborhood of the electrocapillary zero, almost reaching its normal value before the discharge of hydrogen ion. It seems likely that the decrease in the diffusion current of the dye which is brought about by the addition of albumin to the solution may be attributed to a decrease in the electrode surface available for reduction. The protein molecules which are adsorbed at the interface may constitute a real barrier to the approach of dye molecules to the electrode, and thus prevent a portion of those which reach the electrode vicinity by diffusion from undergoing reduction. The adsorption of protein at the

mercury surface may also be expected to be diffusion-controlled; if so, the average fraction of surface covered by protein during the life of the drop should increase with increasing concentration in the solution to a limiting value which corresponds to a monomolecular layer being effectively maintained over the surface. The diffusion current is found to decrease to a limiting value which, however, is not zero. It may well be that the interstices in a monomolecular layer of protein are of such a size that a portion of the dye molecules may still reach the electrode surface although no further protein can be absorbed. The abrupt increase in current which is observed after the initial attainment of the diffusion current occurs in the neighborhood of the electrocapillary zero, and may be due to desorption of the protein from the electrode surface. The initiation of the desorption process is perhaps attributable to the change in the sign of the charge on the mercury drop as the applied potential becomes more negative than that corresponding to the electrocapillary zero. The electrostatic repulsion of the negatively charged electrode for the similarly charged protein molecules (at pH 8) may then begin to overcome the adsorptive attraction of the mercury surface, and desorption occurs with a resultant increase in diffusion current.

The shift in the half-wave potential brought about by increasing the protein concentration in the solution should be pointed out here. This result is not necessarily indicated by the foregoing hypotheses. The character of the initial wave appears to change in the presence of protein, with the current increase becoming more diffuse so that at large concentrations of protein, the attainment of the pseudo-limiting current

is almost coincident with the initiation of the desorption process; however, at low protein concentrations, a half-wave shift in the initial wave is observed although the resolution of the two waves is complete (See Figure 6, curve B). It must be noted that the composition of the solutions and the cell characteristics are changed by the addition of protein, the effects of which are not easy to predict in this irreversible system. It is well known that changes in the concentration or in the nature of a supporting electrolyte may bring about unexplained changes in the half-wave potential of a reducible ion, even in a reversible system. In this light, it is difficult to determine whether the half-wave shift in the present work is significant or important. Similar data for some reversible redox systems would be desirable and enlightening for the resolution of this difficulty.

The data in Tables III and IV are plotted in Figure 4, from which it may be shown that an empirical equation which describes the experimental data extremely well is of the form

$$\ln k(i_d - i_d^l) = -k'C_p, \qquad (5)$$

where $i_d$ is the diffusion current observed in a solution of azo dye with albumin concentration $C_p$, and $i_d^l$ is the minimum diffusion current observed in similar solutions containing increasingly larger concentrations of the protein. The validity of this relation is illustrated in Figure 5, in which a plot of log $(i_d - i_d^l)$ against the protein concentration, $C_p$, results in a straight line. An explanation of these phenomena is pre-

sented later in this thesis and a theoretical expression which is in reasonable agreement with the experimental data, but which is not of the form of equation (5) is deduced. It appears that either the validity of equation (5) in this form is coincidental, or the assumptions made in the development of the equations later in this thesis are not adequate.

d) Saturation Current at the Dropping Mercury Electrode

In a previous section of this thesis, it has been mentioned that the ratio of the diffusion current of a reducible substance to its concentration in solution is constant only over a limited range of concentration. As the concentration is increased, the limited amount of electrode surface available for reduction becomes important in determining the current density; that is, above some limiting concentration, the electrode can no longer reduce all of the molecules or ions which would reach its surface if complete concentration polarization were to occur. Consequently, there is a concentration of dye above which the polarization is incomplete and the diffusion current attains a maximum value. If, as postulated in the preceding section, a protein molecule adsorbed at the mercury-solution interface immobilizes a portion of the electrode for use in reduction, it would be expected that in the presence of protein, the saturation current will be decreased accordingly. The dropping electrode, in a solution containing protein, should act toward a reducible ion as if its surface area were smaller than that calculated from the capillary constants, and at a given protein concentration, the fractional decrease of the diffusion current should be independent of the dye concentration. In order to

examine the effect of protein on the maximum diffusion current, an experiment was carried out in which the diffusion current was measured in solutions having a constant protein concentration but various concentrations of dye. The results are tabulated in Table V.

Table V

p-Hydroxyphenylazophenylarsonic Acid

Variation of the Diffusion Current with Concentration in the Presence and in the Absence of Proteins

All solutions 0.15 M. in NaCl; 0.02 M. in Veronal, pH 8; temp. 25°C.; $m^{2/3}t^{1/6} = 1.503$ mg.$^{2/3}$-sec.$^{-1/2}$.

| Conc. of dye (millimoles/ℓ.) | Diffusion Current, $i_d'$, in presence of protein* (microamperes) | Diffusion Current in absence of protein, $i_d$ (microamperes) | $\frac{i_d'}{i_d}$ |
|---|---|---|---|
| 0.181 | 0.25 | 0.69 | 0.36 |
| 0.362 | 0.50 | 1.36 | .37 |
| 0.725 | 0.99 | 2.76 | .36 |
| 0.906 | 1.21 | 3.38 | .36 |
| 0.986 | 1.36 | 3.72 | .37 |
| 1.36 | 1.80 | 5.09 | .35 |
| 1.81 | 2.04 | 5.82 | .35 |
| 2.27 | 2.13 | 6.03 | .35 |
| 2.72 | 2.11 | 5.98 | .35 |

* These solutions were $6.1 \times 10^{-6}$M. in crystallized human albumin.

It may be noted in Figure 7 that the maximum current, both in the presence and in the absence of proteins is reached at almost exactly the same dye concentration, although the current density is greatly decreased in the former case, and that the ratio $i'_d/i_d$ remains constant over the entire range investigated. The results of this series of experiments appear to support very strongly the hypothesis of reduced electrode surface.

e) Effect of Other Proteins on the Diffusion Current of Azo Dye

Qualitative observations have indicated that other proteins have an effect similar to that of albumin on the diffusion current of HPA. Lack of pure materials, however, rendered quantitative studies unattractive. The addition, to buffered saline solutions of HPA, of any of the following materials was found to suppress the diffusion current of the azo dye appreciably:*

Normal Rabbit Serum

Normal Sheep Serum

Purified Rabbit Globulin

Azoalbumin (diazo-p-arsanilic acid coupled to albumin)

Anti-$R_p$ Serum (rabbit serum containing antibodies for the haptenic p-azophenylarsonic acid group)

No protein-containing substances were found which did not materially affect the diffusion current of HPA. Control solutions of the above

---

* In preliminary experiments, a similar qualitative effect was observed in the reduction of cadmium ions in the presence of gelatin, but this result may be due largely to a change in the viscosity of the solution, which would affect the diffusion coefficient of the cadmium ions.

proteins ( in the absence of a reducible substance) characteristically exhibited no diffusion wave, but there was evident, in each polarogram, a sharp change in the slope of the residual current line at applied potentials in the neighborhood of that corresponding to the electrocapillary zero.

### f) Effect of Thymol on the Reduction of Cystine

A survey of the literature revealed an example in which a decrease in the diffusion current from solutions of a reducible substance was attributed to the effect of maximum suppressors. Kolthoff and Barnum[13] investigated extensively the effects of gelatin, phenol, resorcinol, thymol, methylene blue, methyl red and camphor in suppressing the maximum in the reduction wave of cystine. They observed current suppressions, half-wave shifts and changes in the shape of the wave. These authors propose that "cystine must be oriented in a favorable position at the surface of the electrode before it can be reduced" and that "the capillary-active substances inhibit this orientation." This picture seems rather unclear and it is difficult to say whether the authors had in mind an explanation similar to the present one, or whether they intended to imply only that the effect was due to the capillary-active substance in a way which they did not clearly understand.

A brief and very incomplete confirmation of the results of Kolthoff and Barnum is reported in this section. A series of solutions was prepared in which the concentration of cystine was held constant as the concentration of thymol was varied. The composition of these solutions is given in Table VI.

Table VI

Composition of Cystine Solutions

All solutions 0.001 M. in cystine, 0.15 M. in NaCl; pH 1; temp. 25°C.;
$m^{2/3}t^{1/6} = 1.503$ mg.$^{2/3}$-sec.$^{-1/2}$

| Solution Number | Concentration of Thymol (moles/ℓ. x $10^5$) |
|---|---|
| 1 | 0.00 |
| 2 | 1.00 |
| 3 | 3.00 |
| 4 | 9.00 |
| 5 | 10.0 |
| 6 | 15.0 |
| 7 | 20.0 |

The polarograms of these solutions are reproduced in Figure 8. The trend is clearly indicated. As the concentration of thymol is increased, the reduction wave of cystine is shifted to more negative potentials. From these curves, it appears that the adsorption of a monomolecular layer of thymol completely suppresses the reduction wave of cystine, which is observed only after desorption has begun. At low concentrations of thymol, the desorption from the electrode appears to occur at a potential which is only slightly greater than that corresponding to the beginning of the reduction of cystine. However, as the concentration of thymol is increased, there is observed a decrease in the slope of the initial portion of the reduction wave and an increase in the slope of the final portion which are analogous respectively to the small diffusion current observed for HPA in the presence of proteins, and the increase

in current observed as the desorption of protein occurs. The shift in the half-wave potential is probably due to the increasing difficulty with which thymol is desorbed as its concentration increases. Further discussion of the curves is given later.

g) Effect of Adsorbed Protein Molecules on the Mercury Droplet

The polarographic experiments carried out with solutions of azo dye in the presence of proteins were characterized by a reluctance of the mercury drops to coalesce at the bottom of the electrolysis vessel. The droplets remained separate and failed to coalesce even after violent shaking or profuse washing. In order to study the adsorption more directly, a cell was devised in which the mercury droplets formed at the electrode just above a liquid boundary between a solution which was $2.2 \times 10^{-5}$M. in horse albumin, 0.02 M. in veronal, and 0.15 M. in NaCl at pH 8, and another solution which was simply 0.75 M. in NaCl. In this way, an attempt was made to preclude the adsorption of protein on the droplet after it had detached itself from the capillary. When the droplets were allowed to form at an applied voltage less negative than -2.2 volts (vs. S.C.E.), the drops did not coalesce. When the applied potential was more negative than -2.2 volts, however, the drops coalesced immediately. Moreover, when the drops were allowed to fall, at -2.2 volts or greater into a previously collected pool of individual droplets, the entire pool slowly fused, a few drops at a time, as each fresh spherule joined the group. A collection of discrete globules of mercury could also be made to coalesce by passing a platinum electrode, at a potential more negative than -0.7 volts, through the array. The speed of fusion increased as the voltage was increased, being extremely slow up to -1.1 volts and extremely rapid in the neighborhood of -2.0 volts.

It seems likely that the apparent discrepancy between -0.7 volts for coalescence of the mercury droplet pool by a platinum electrode and -2.2 volts for immediate coalescence upon leaving the capillary may be explained as follows: desorption of the albumin from the mercury surface occurs at any applied voltage more negative than -0.7 volts (vs. S.C.E.). However, between -0.7 and -2.2 volts, the charge on the drop, after it leaves the electrode, is rapidly dissipated and, despite the precautions taken, albumin is adsorbed on the surface before the drop leaves the protein medium. When the applied voltage is more negative than -2.2 volts, it is to be expected that during the growth of the drop, sodium ions from the solutions are reduced; consequently, the surface of the falling drop consists of a dilute sodium amalgam. The discharge of sodium from this amalgam, as the drop falls through the solution, may maintain a potential sufficient to preclude the adsorption of protein.

These experiments, supporting very strongly the adsorption hypothesis, lend added credibility to the explanations presented in the preceding sections which are more fully developed in the following discussion.

## DISCUSSION

It seems likely from the results of the experiments described that the large effect which proteins have on the polarographic properties of a solution of a reducible substance may be attributed to adsorption of the protein molecules on the surface of the dropping mercury electrode. That such adsorption does occur was recognized early in the history of polarography and is further borne out in the present work by the reluctance of the individual mercury droplets to fuse with one another after departing from the end of the capillary.

In general, the number of solute molecules adsorbed from any solution onto a surface increases with increasing concentration, but reaches a limit when the concentration is such that a monomolecular layer of adsorbed molecules is maintained over the surface. It will be assumed, in the following discussion, that these considerations apply to the adsorption of proteins at the dropping electrode, and inferences will be drawn to explain the observed phenomena.

That the presence of adsorbed molecules may impede the approach of other particles to the electrode and thus by a steric effect hinder the reduction has not heretofore been considered. The diffusion current which passes in a polarographic experiment is dependent upon the number of particles which reach the electrode for reduction. If a particle is unable to undergo immediate reduction because that portion of the electrode toward which it is approaching is covered by a protein molecule, it may be deflected back toward the body of the solution. Of those molecules which

enter the electrode vicinity at a given time the fraction which cannot make contact with the reducing surface and are consequently deflected should be just equal to the fraction of the surface which is covered by the adsorbed material. Complete concentration polarization would hence not be achieved, the concentration gradient between the electrode surface and the body of the solution would be less than predicted and a decrease from the normal diffusion current would be observed.

It seems likely that at any given instant in the life of the drop the fraction of electrode surface which is covered by protein molecules increases with the protein concentration in the solution to a limiting value which corresponds to the adsorption of a monomolecular layer. Such a monomolecular layer, however, need not completely inactivate the entire surface of the electrode. If it be assumed that for secondary layers of protein molecules the adsorptive forces are weak or absent, as will be true for a soluble protein, except possibly at the isoelectric point, the adsorbed film, consisting of a single layer of large ellipsoidal particles, may, even in closest packing, have holes of a size large enough to permit some of the reducible material, usually smaller in size, to reach the electrode and undergo reduction. On the other hand, the holes in the adsorbed film would be too small to allow other protein molecules to fit among those which are adsorbed in the primary layer. Thus in increasing the concentration of albumin the effect would be to decrease the diffusion current of an azo dye to a limiting value which would <u>not necessarily</u> be zero (Figure 4). In this case, the diffusion current is suppressed by protein adsorption to about twenty-five percent of its normal value. For

comparison, it may be noted that a layer of ellipsoids in closest packing projected onto a flat surface leave interstices which total about 9.1 percent of the area. The percentage of voids in simple rectangular packing of ellipses is about 21.5 percent. In view of the present hypotheses, the monomolecular layer of protein molecules apparently does not arrange itself into a closest packed array.

Further evidence in support of the present hypotheses is afforded by an examination of the characteristic effects of saturation of the electrode. It has been shown, for example, that the capacity of a mercury electrode in saturated solutions of capillary-active organic substances depends inversely upon the chain length of the molecule.[19] In Figure 7, the variation of the diffusion current with concentration of azo dye in the presence of a constant concentration of protein is compared with that in the absence of protein. It is striking that the fractional decrease in current brought about by a given amount of protein is constant. It may be inferred that the average fraction of surface covered during the life of the mercury drop remains constant in the presence of a given concentration of protein, and that the diffusion current is affected accordingly. It must be pointed out that the effects which are discussed here are average ones, over the surface of the drop, since with portions of the electrode surface inactivated, the spherical symmetry of the diffusion layer would be destroyed.

Since the adsorption process at the electrode surface would also be diffusion dependent, it may be asked whether, at a protein concentration at which the limiting suppression is achieved, it is possible for enough protein molecules to reach the electrode to maintain a monomolecular layer over the surface. Such a calculation must of needs be idealized since in

the actual case such factors as the electrostatic forces between the electrode and the protein molecules and the competition between dye and albumin molecules for the electrode surface must be considered as well as the fact that the spherical symmetry of the concentration gradients is destroyed by molecules which are neither adsorbed nor reduced at the mercury surface, even though they reach the electrode vicinity.

Let it be assumed, for simplicity, that the diffusion of protein to the mercury drop may be described by the Ilkovic equation (1); that is to say, that all protein molecules which reach the electrode vicinity are immediately adsorbed on the surface and are thus effectively removed from the solution. The Ilkovic equation (1) may be alternately written

$$N = 0.63\ C m^{2/3} t_{max}^{1/6}\ D^{1/2}\ , \qquad (6)$$

where N is the number of moles of diffusing substance reaching the electrode during the life of the drop, $t_{max}$ (secs.); D is the diffusion coefficient ($cm.^2/sec.$); C is the concentration (moles/cc.); and m is the dropping rate of mercury (mg./sec.).

In the present experiments, m = 1.22 mg./sec. and $t_{max}$ = 5.33 secs. at approximately the reduction potential of the dye: The diffusion coefficient of horse albumin is approximately $6 \times 10^{-7} cm^2/sec.$ Consequently,

$$N = 3.9 \times 10^{-5} C, \qquad (7)$$

Since the concentration of albumin at which the diffusion current of azo dye reaches its minimum value is approximately $1 \times 10^{-8}$ moles per cubic centimeter, it is seen that $3.9 \times 10^{-13}$ moles of protein may reach the electrode under the stated conditions. Assuming again, for simplicity, a spherical albumin molecule with a density of 1 gm./cc., and a molecular

weight of 70000, the radius of each molecule is calculated to be 3.03 x $10^{-7}$cm. The projected area of a sphere of this radius onto a flat surface is then 2.88 x $10^{-13}$sq. cm., and the projected area for all molecules which may reach the electrode during the life of a drop is 0.0676 sq. cm. From the known weight of each droplet, 6.6 mg., the maximum area of the surface is calculated to be 0.0264 sq. cm. Thus, under the ideal conditions set forth, approximately two and a half times as much protein may diffuse to the electrode during the life of the drop as is actually needed to cover the maximum surface attained. The agreement in order of magnitude is good.

An approximate expression for the reduction of azo dye under conditions similar to those specified in the preceding calculation may be derived. Let us assume the Ilkovic equation (1) for the flux of diffusing molecules to a growing surface to hold, both for protein and for reducible substance, with the exceptions only that the instantaneous reduction current is diminished by a fraction equal to the fraction of the electrode surface which has become covered by protein and that the rate of deposition of protein molecules is similarly decreased but with a different proportionality constant. The assumption (which would appear to become increasingly inadequate as the protein concentration is increased) is that in effect the molecules which are not permitted to reach the electrode surface simply cease to exist insofar as the diffusion problem is concerned. Let us denote by X the area of the electrode per unit area covered by protein at a given time, t, in the life of the drop. The amount of protein on the electrode in units of (area excluded to other protein molecules) per unit area is then $k_1$ X, where $k_1$ may be described as the protein-protein blocking factor,

introduced to express the hypothesis that the inactivation of the surface with respect to the adsorption of more protein is greater than the area actually covered by the previously adsorbed albumin molecules. Let us then write

$$i = i_o(1 - X), \tag{8}$$

where i is the instantaneous reduction current at time, t, in the presence of a concentration, $C_p$, of protein and $i_o$ is the corresponding instantaneous current in the absence of protein. Let us denote by T the amount of protein on the drop in the units of area covered. Then

$$T = S_o X = 4\pi^{1/3}\left(\frac{3m}{d}\right)^{2/3} t^{2/3} X = pt^{2/3}X, \tag{9}$$

where $S_o$ is the surface area of the drop at time, t; m is the dropping rate of mercury and d is the density of mercury. Let us now write

$$\frac{dT}{dt} = \left(\frac{dT}{dt}\right)_o (1 - k_1 X), \tag{10}$$

where $\left(\frac{dT}{dt}\right)_o$ is the rate at which protein diffuses toward the drop which, under our assumptions, is given by the Ilkovic equation. Hence,

$$\left(\frac{dT}{dt}\right)_o = \frac{0.73}{k_2} D^{1/2} C_p m^{2/3} t^{1/6}, \tag{11}$$

where D is the diffusion coefficient of the protein and $k_2$ is introduced to convert to units of area. $k_2$ is then the number of moles of protein which cover unit surface area of the drop. From equation (10) and (11), then,

$$\frac{dT}{dt} = at^{1/6} - \frac{bT}{t^{1/2}}, \tag{12}$$

where $a = \frac{0.73}{k_2} D^{1/2} C_p m^{2/3}$, and $b = \frac{ak_1}{p}$. Equation (12) is a linear differential equation, the solution of which may be found in any elementary

treatise on differential equations. For this particular equation, a solution in terms of a useful, convergent, infinite series is:

$$T = 6/7\ at^{7/6} - 6/7\ 6/10\ abt^{10/6} + 6/7\ 6/10\ 6/13\ ab^2t^{13/6} - + \text{---}. \quad (13)$$

From equation (9), then,

$$X = \frac{T}{pt^{2/3}} = 6/7\ a/p\ t^{1/2} - 6/7\ 6/10\ \frac{ab}{p}\ t + 6/7\ 6/10\ 6/13\ \frac{ab^2}{p}t^{3/2} \text{--}, \quad (14)$$

and from equation (8),

$$i = i_o(1 - X) = At^{1/6}\left(1 - \frac{6}{7}\frac{a}{p}\ t^{1/2} + \frac{6}{7}\frac{6\,ab}{10\ p}\ t - \frac{6}{7}\frac{6\ 6}{10\ 13}\frac{ab^2}{p}\ t^{3/2} + \text{--}\right), \quad (15)$$

where $i_o = At^{1/6}$ is given by the Ilkovic equation. The average current, which is measured experimentally, is then given by

$$\bar{i} = \frac{1}{\tau}\int_o^\tau i\,dt = 6/7\ A\tau^{1/6} - 6/7\ 6/10\ \frac{Aa}{p}\tau^{4/6} + 6/7\ 6/10\ 6/13\ \frac{Aab}{p}\tau^{7/6} - + \text{--} \quad (16)$$

where $\tau$ is the drop time. But

$$\bar{i}_o = \frac{1}{\tau}\int_o^\tau i_o\,dt = \frac{1}{\tau}\int_o^\tau At^{1/6}dt = 6/7\ At^{7/6}$$

$$\therefore\ \bar{i} \quad \bar{i}_o - \bar{i}_o\left(6/10\ \frac{a}{p}\tau^{1/2} - 6/10\ 6/13\ \frac{ab}{p}\tau + 6/10\ 6/13\ 6/16\ \frac{ab^2}{p}\tau^{3/2} \text{--}\right). \quad (17)$$

Let $\bar{i}_o - \bar{i} = \delta\bar{i}$, and let $u = 6b\tau^{1/2}$. Then, from equation (17), since

$a/b = p/k_1$ ,

$$\frac{k_1\,\delta\bar{i}}{\bar{i}_o} = (u/10 - u^2/10\cdot13 + u^3/10\cdot13\cdot16 - + \text{----}), \quad (18)$$

or $$\frac{k_1 \overline{\delta i}}{\overline{i}_o} = f(u), \tag{19}$$

when $$f(u) = u/10 - \frac{u^2}{10.13} + \frac{u^3}{10.13.16} - + - - -. \tag{20}$$

It may be shown that $f(u)$ is a convergent series which approaches unity as $u$ becomes large. The expression $f(u)$ has been evaluated as a function of $u$. A number of values are given in Table VII and a plot of $f(u)$ against $u$ is made in Figure 9.

Table VII

Evaluation of $f(u)$ as a Function of $u$

| u | f(u) |
|---|---|
| 0 | 0.000 |
| 1 | .093 |
| 2 | .172 |
| 3 | .242 |
| 5 | .355 |
| 7 | .442 |
| 10 | .540 |
| 14 | .630 |
| 15 | .648 |
| 20 | .716 |
| 30 | .797 |
| 50 | .871 |
| 70 | .900 |

From equation (12),

$$u = 6bT^{1/2} = 6\left(\frac{0.73K_1}{K_2 P} D^{1/2} C_p m^{2/3}\right) T^{1/2}, \qquad (21)$$

or from equation (9),

$$u = \frac{4.38 D^{1/2} C_p K_1 T^{1/2} d^{2/3}}{K_2 (4\pi)^{1/3} (3)^{2/3}} \qquad (22)$$

In the present experiments, $T$ = 5.33 secs.; from the known values $D_{albumin} = 6 \times 10^{-7}$ cm.$^2$/sec. and $d_{Hg}$ = 13.55 gms./cc., it may be shown that

$$u = 0.925 \frac{k_1 C_p}{k_2}. \qquad (23)$$

Assuming a spherical albumin molecule with a molecular weight of 70000 and a density of 1, it may be shown that $k_2$, the number of moles of albumin which, projected, may cover unit area of surface, is $5.76 \times 10^{-12}$ moles/cc. Since the asymptotic value of the reduction current in the present experiments is about 25 percent of the "true" value, it may be inferred that $k_1$, the protein-protein blocking factor, is approximately 1.33. Hence,

$$u = 0.214 \times 10^{10} C_p. \qquad (24)$$

The reduction current to be expected under the stated conditions may now be calculated. In Table VIII and in Figure 10, the calculated values are compared with those observed. In each calculation, $u(C_p)$ was obtained from equation (24). The corresponding value for $f(u) = \frac{K_1 \delta i}{\bar{i}_o}$ was read from Figure 9; from this, $\bar{i}_{calc.}$ was obtained.

Table VIII

p-Hydroxyphenylazophenylarsonic Acid

Comparison of $\bar{i}_{calc.}$ with $\bar{i}_{obs.}$

| $C_p$ (moles/cc. x $10^{10}$) | u | f(u) | $\bar{i}_{calc.}$ | $\bar{i}_{obs.}$ |
|---|---|---|---|---|
| 228 | 48.70 | 0.87 | 1.29 | 0.94 |
| 114 | 24.35 | .76 | 1.60 | 1.01 |
| 79.9 | 17.08 | .68 | 1.82 | 1.17 |
| 68.5 | 14.65 | .64 | 1.93 | 1.26 |
| 57.1 | 12.21 | .59 | 2.07 | 1.48 |
| 45.7 | 9.75 | .53 | 2.24 | 1.76 |
| 40.0 | 8.55 | .49 | 2.35 | 1.84 |
| 28.6 | 6.10 | .40 | 2.60 | 2.28 |
| 22.8 | 4.87 | .35 | 2.74 | 2.74 |
| 11.4 | 2.44 | .21 | 3.13 | 3.30 |
| 7.99 | 1.71 | .16 | 3.27 | 3.48 |
| 6.85 | 1.47 | .14 | 3.33 | 3.55 |
| 5.71 | 1.22 | .12 | 3.38 | 3.68 |
| 4.57 | 0.98 | .09 | 3.47 | 3.70 |
| 1.14 | 0.24 | .02 | 3.66 | 3.73 |
| 0.114 | 0.02 | .00 | 3.72 | 3.74 |

The agreement between the experimental and the calculated curves is reasonably good in the light of the assumptions made. It is

possible to bring about somewhat better agreement by a suitable variation of the constant, $k_2$, or at the expense of adding another parameter; however, these modifications would be of an empirical nature, and although there is much justification for them, they would seem to contribute little to our knowledge of the system. The agreement afforded by the present treatment appears to be at least as instructive as the better agreement that could be obtained by the addition of further constants.

A reasonable theoretical background having been established for the hypotheses herein presented, it is possible to inquire further into the nature of the phenomena at the electrode. The effects of electrostatic forces between the electrode and the protein molecule should be considered. At pH 8, the albumin molecule has an overall negative charge, and should be attracted to an electrode which is positively charged, a situation which obtains when the applied voltage is more positive than that corresponding to the electrocapillary zero ( which varies from solution to solution in the neighborhood of -0.6 volts vs. S.C.E.). On the other hand, as the applied voltage becomes more negative than the potential corresponding to zero charge, the electrostatic repulsion between the electrode and the protein molecule would be expected to counterbalance and finally overcome the adsorptive forces, eventually effecting a desorption from the electrode surface. The experiments described in section (g) bear out these contentions, since it was shown that a platinum electrode at a potential more negative than -0.7 volts, when passed through a collection of individual mercury droplets formed in a protein solution, brings about their fusion, and that the rate of fusion increases with increasing voltage.

The difference in appearance between the current-voltage curve obtained from an azo dye solution in the absence of protein and that from a similar solution containing a comparatively large concentration of protein (Figure 6) may easily be explained. In the former case, the diffusion current reaches a limiting value and remains practically constant thereafter, whereas in the presence of protein, the diffusion current flattens, but in the region corresponding to the electrocapillary zero, takes a sharp turn upward and increases with voltage, finally approaching the normal limiting current as the hydrogen-ion discharge begins. This is attributed to the gradual desorption of albumin from the electrode with a concomitant increase of available space at which the dye may be reduced.

The results, summarized in Figure 8, of adding thymol to solutions of cystine may be similarly explained. Apparently, adsorption of the thymol molecule (which is smaller than the albumin molecule and consequently leaves only very small holes in the adsorption layer) almost completely suppresses the reduction of cystine. As desorption occurs at more negative voltages, reduction may take place. Since the desorption may be expected to become more difficult as the thymol concentration is increased, there is observed an apparent shift in the half-wave potential of cystine. These results confirm the experimental observations of Kolthoff and Barnum (loc. cit.)

The explanation for the desorption of thymol is probably not based on a simple electrostatic repulsion in this case for at pH 1, thymol would be expected to exist almost completely as a neutral molecule. How-

ever, Tachi[18] and Kolthoff and Barnum[13] have shown that camphor is desorbed from the electrode at increasing negative potentials, and that the desorption is complete at -1.24 volts (vs. S.C.E.). It seems probable that thymol is similarly desorbed at high negative potentials and that the desorption is due rather to the preferential adsorption of cystine or of water molecules than to electrostatic repulsion.

In part (e) of the experimental section, it was mentioned that in polarograms of control solutions containing various protein mixtures (but no reducible substance), no diffusion current is observed, and that in each case, a sharp change in the slope of the residual current line occurs at applied potentials which are in the region of the electrocapillary zero of potential. Although no diffusion layer is to be expected in such solutions, the desorption of proteins from the electrode surface would bring about a change in the electrokinetic potential at the interface and would disrupt the linearity of the residual current line usually observed in such solutions.

The shift in the half-wave potential brought about by the addition of proteins to a solution of HPA is not yet understood. We are not at all positive that the shift is related to the present phenomena. It is often true in polarographic analysis that a shift in half-wave occurs as a result of changing certain constituents in the solution. On the other hand, it may be that there is a very definite relationship between the shift in the half-wave potential and the decrease in diffusion current. We have not yet arrived at a satisfactory explanation for the observed shift and we feel that this may constitute a serious flaw in our proposed explanation. In the absence of further experimental evidence, however, we are forced to leave

this point unexplained.

In reference to the half-wave potential of a reducible ion in the presence of capillary-active substances, it must be recognized that adsorption at an electrode is dependent on the applied voltage. The desorption potential of a surface active material is a characteristic of the molecule or ion and is probably dependent upon the strength of adsorption and on the relative charge of the mercury and the adsorbate. We may then recognize three possible effects on the half-wave potential. If the desorption takes place at a more positive potential than that corresponding to the beginning of discharge of the reducible ion, there should be no effect on the diffusion current or on the half-wave potential. Secondly, if desorption takes place at a much greater negative potential than that at which the ion reduces, two waves should result. The first will correspond to the normal polarographic wave, but will be suppressed by the immobilization of electrode surface and will reach a limiting value which may or may not be zero. The second wave will occur when desorption suddenly increases the available electrode surface for reduction of the ion in question. Such a situation apparently obtains in the reduction of HPA in the presence of albumin, in the reductions of methylene blue and of riboflavin which are cited below, and in the reduction of cystine in the presence of high concentrations of thymol, where the wave is completely suppressed. In this last case, the wave is sharpened considerably because of the sudden desorption at a higher negative potential than that at which the normal reduction occurs. Thirdly, the desorption may occur in the region of the normal reduction wave. The potential of the inception of reduction will be unaffected, but as the current is building up to its limiting value, desorption

may begin, and the current will continue to increase until the surface is completely free of adsorbed material. The effect will be to spread out the wave and give an apparent shift in half-wave potential to more negative voltages. Apparently, one observes this in the reduction of cystine at low concentrations of thymol. Depending upon how small is the difference between the reduction potential and the desorption potential and upon how sharply the desorption occurs, the wave may simply be a very diffuse one, or it may involve a more or less sharp break in the current-voltage curve.

In addition to the work of Kolthoff and Barnum, a few examples of phenomena similar to those reported herein have been noted. For example, Salac[20] reports that substances, including albumin, possessing high surface activity interfere with the polarographic determination of saccharin in beer, decreasing the observed diffusion currents. The original paper is unavailable at this writing, and no detailed consideration can be given to the work.

Brdicka[21] reports that in the polarographic reduction of methylene blue and of riboflavin, a small anomalous wave, independent of concentration when the concentration of reducible ion is above a given value, precedes the large reduction wave. He suggests that this may be due to the adsorption of reduction products and he suggests that the so-called anomalous wave corresponds to the beginning of reduction, which is suppressed by the adsorption of reduction products. The second wave, representing the true diffusion current, occurs at a more negative potential where the products are desorbed from the electrode. This explanation fits well with the present work and is apparently a satisfactory explanation of the observations.

The effect of protein in reducing the diffusion current of the dye is so large that the possibility of attributing the results to an inter-

action between dye and protein molecules in solution is immediately excluded. If it is assumed that the decrease in current is due to compound formation with the concomitant decrease in diffusion coefficient, and if the data are then treated in a manner analogous to that of Klotz, Walker and Pivan[22] according to their derived equation,

$$\frac{1}{r} = \frac{K}{n[A]} + \frac{1}{n},$$

where r is the ratio of molecules of bound dye to total moles of protein, $[A]$ is the concentration of free dye, and n is the maximum number of dye molecules which may be bound to a single protein molecule, it may then be shown that n is of the order of 1000. Spatially, this result is, of course, impossibly large, especially since Klotz has shown that, for calcium ion, which is much smaller than the protein molecule, n is 22. In addition, the data of Figure 7, from which it may be seen that a given concentration of protein decreases the diffusion current by a constant fraction, independent of the dye concentration, is in disagreement with the hypothesis that an equilibrium between dye, protein, and combined dye-protein is of importance here. It is not improbable that there is some small effect of interaction, but of the total decrease in current observed, this can be, at most, of the order of a few percent.

The confused state of present theories of polarographic maxima makes it a difficult task to present an accurate picture of the role of capillary-active substances in maximum suppression. However, it seems very likely that the suppression of maxima is closely related to adsorption on the electrode surface. We may, as a result of the present work, attempt to place the use of maximum suppressors upon a less empirical basis. It seems likely that a capillary-active substance which is desorbed from the

electrode at a more positive potential than that at which reduction of the substance in question occurs will be inactive as a maximum suppressor. A maximum suppressor should be used in accurate polarographic work only when absolutely required, and then in a minimal concentration. The choice should probably be such that desorption of the capillary-active material occurs rather sharply at a potential just slightly more negative than that at which the maximum in the c.-v. curve is reached. (We cannot, of course, state just what the optimum criterion will prove to be.) The measurement of the current should be made just beyond this desorption point. A systematic tabulation of the desorption characteristics of the commonly used maximum suppressors would be very convenient for these purposes.

The relation of the present work to the phenomenon of maxima and their suppression should be explored briefly. Antweiler and von Stackelberg[8,9] have shown conclusively that a pronounced streaming occurs about the electrode during the stage in the reduction at which a maximum is observed in the c.-v. curve. There appears to be no diffusion layer, the reducible substance reaching the electrode by the streaming process. Antweiler points out that the tip of the capillary exerts a screening effect and prevents the free diffusion of reducible material at this point with the result that the current density at the bottom is greater than at the top; there remains in the solution an unequal distribution of the indifferent ions between the bottom and the top of the drop and consequently, a tangential potential gradient exists in the solution about the drop. The double layer migrates along this gradient, inducing a streaming of the solution. This flow brings more reducible ions to the incipient "hot spot,"

bringing about a further inequality in the distribution of indifferent ions,* and thus the cycle continues. It seems almost certain that the adsorption of capillary-active substances on these centers of high current density with consequent immobilization of the given area as an electrode surface is the mode of action of such substances as maximum suppressors. The incipient center being deactivated, the whole mechanism for production of the anomalous current loses its driving force. The concentration of capillary-active substance, according to this interpretation, need not be so high as to produce a notable effect on the normal diffusion current because at any incipient center, the suppressor will be brought to the electrode by flow as well as by diffusion and because the whole phenomenon obviously represents a rather narrow choice between the two types of behavior which may depend quite sensitively on very small changes in a considerable number of factors including the reactivity of the electrode surface which we have been discussing.

---

* This explanation is set forth by Antweiler, but it has been pointed out by Kolthoff and Lingane[4] that no consistent picture of the charge distribution about the drop can be drawn for the general case. In addition, the specific effects observed in the study of maxima are unexplained.

## SUMMARY

A search of the literature reveals that although adsorption of capillary-active materials at the dropping mercury electrode was considered important in polarographic work almost from its inception, consideration has never been given to the actual inhibiting effect an adsorbed ion might have on the reduction of other ions. It has been shown in this paper that under certain conditions, the effect may be extremely large although only a small trace of the capillary-active substance is present.

Polarograms prepared from solutions which contained various concentrations of serum albumin (either human or horse) buffered at pH 8 with veronal and which, in each case, contained the same concentration of a dye (p-hydroxyphenylazophenylarsonic acid) and of sodium chloride indicated that the diffusion current was suppressed to approximately 90% of its true value at a protein concentration of $1 \times 10^{-6}$M. and to an asymptotic value of about 25% at $1 \times 10^{-5}$M.

It seems likely that the albumin, a capillary-active substance, is adsorbed on the growing mercury drops, decreasing the surface available for reaction with the reducible molecules or ions, and thus decreasing the diffusion current. The fraction of inactivated surface and the consequent reduction of the instantaneous diffusion current is, at any stage in the life of the drop, proportional to the diffusion rate of the protein or accordingly, its concentration. At moderately high concen-

trations of protein, however, a monomolecular layer would be formed and an asymptotic diffusion current would be attained which may or may not be zero, for a monomolecular layer of adsorbed molecules may well have interstices large enough so that some of the reducible material can reach the electrode. The hypothesis of reduced electrode surface is supported by the observation that at a given concentration of protein, the fractional decrease in the diffusion current is constant, independent of the concentration of reducible material.

Such considerations clarify, in part, the decrease in diffusion current which is observed in this and a number of other cases upon the addition to the solution of capillary-active molecules or ions.

## ADDENDUM

In a paper published in 1945, S. Fiala[23] reported that the reduction potential of oxygen at the dropping mercury electrode is shifted to more negative values when dyes of the eosine group are present in the solution. At low concentrations of the dye, only part of the oxygen wave is shifted. With increasing dye concentration, the shifted wave increases at the expense of the original wave until finally, a single wave occurs at the more negative potential. Fiala attributed this to the combination of molecular oxygen with the dye.

K. Wiesner in a recent paper[24] has pointed out that, according to Henry's Law, unbound molecular oxygen could not be absent from a solution open to the atmosphere and that one should expect the normal oxygen wave to appear in all the polarograms even if some oxygen were bound to the dye. Wiesner investigated more thoroughly the role of eosine and its derivatives in the polarographic depolarization process with a study of some reversible redox systems, such as quinone, hydroquinone, and a number of quinone derivatives. He concluded that the observations could be attributed to the adsorption of dye on the electrode with a concomitant suppression of the diffusion current. Furthermore, the effect was observed only when the dye concentration was above a minimum value. Wiesner concentrated his attention on this last observation. He concluded that the dye, when first adsorbed, behaves as a two-dimensional gas (after Langmuir[25] and Volmer[26]) which cannot inhibit the approach of reducible ions or molecules, but that after a time (the length of which is dependent

on the dye concentration), the adsorbate crystallizes, acquiring a definite structure, and then hinders the reduction process. At low concentrations of dye, the incubation period (during which the adsorbate acts as a two-dimensional gas) is longer than the drop time, and no effect is observed. At higher concentrations, the crystallization occurs during the life of the drop, and a suppression of the current may be observed. Wiesner supported his conclusions with oscillographic current-time curves.

As the eosine concentration was increased in solutions containing a constant concentration of a reducible dye, the current was suppressed in a manner similar to that recorded in Figure 4 of this thesis. The curve analogous to Figure 4 was shifted, however, being preceded by a flat portion, the length of which varied with the drop time. It appears that the phenomenon is very similar to that observed in the HPA-albumin system, except that here no evidence of an incubation period is observed. The work and the conclusions of Wiesner are in good agreement with the observations reported in the preceding sections.

## REFERENCES


1. J. Heyrovsky, Chem. Listy. 16, 256 (1922); Phil. Mag. 45, 303 (1923)

2. D. Ilkovic, Collection Czechoslov. Chem. Commun. 6, 498 (1934); J. chim. phys. 35, 129 (1938)

3. D. MacGillavry and E. K. Rideal, Rec. trav. chim. 56, 1013 (1937)

4. I. M. Kolthoff and J. J. Lingane, "Polarography," Interscience Publishers, New York, N.Y. (1941), p. 168

5. J. Heyrovsky and E. Vascantzann, Collection Czechoslov. Chem. Commun. 3, 418 (1931)

6. J. Heyrovsky, Actualities scientifiques et industrielles, No. 90, Paris, 1934

7. D. Ilkovic, Collection Czechoslov. Chem. Commun. 8, 13 (1936)

8. H. J. Antweiler, Z. Electrochemie, 43, 896 (1937); 44, 719, 813, 888 (1938)

9. M. Von Stackelberg, H. J. Antweiler, and Keisenbach, Z. Electrochemie 44, 663 (1938)

10. A. Frumkin and B. Bruns, Acta physicochim., U.R.S.S. 1, 232 (1934)

11. B. Bruns, A Frumkin, S. Jofa, L. Vanjukova and S. Zolotarevskaja, Acta physicochim., U.R.S.S. 9, 359 (1938)

12. S. Jofa and A. Frumkin, Compt. rend. acad. sciences, U.R.S.S. 20, 293 (1938)

13. I. M. Kolthoff and C. Barnum, J.A.C.S. 63, 520 (1941)

14. M. Shikata and I. Tachi, Mem. Coll. Agr. Kyoto Imp. Univ. 17, 45 (1931)

15. I. Tachi, Mem. Coll. Agr. Kyoto Imp. Univ. 40, 1, 11 (1937); 42, 1 (1938)

16. N. T. Nga, J. chim. phys. 35, 345 (1938)

17. J. B. Conant and M. F. Pratt, J.A.C.S. 48, 2468 (1926)

18. I. Tachi, Mem. Coll. Agr. Kyoto Imp. Univ., 42, 36 (1938)

19. A. Ksenofontov, M. Proskurnin, A. Gorodetzkaya, J. Phys. Chem., U.S.S.R. 12, 408 (1938)

20. Salac, Kvas 64, 383 (1936)

21. R. Brdicka, Z. Electrochemie 47, 721 (1941); 48, 278, 686 (1942)

22. I. M. Klotz, F. M. Walker, and R. B. Pivan, J.A.C.S. 68, 1486 (1946)

23. S. Fiala, Chem. listy 39, 14 (1945)

24. K. Wiesner, Collection Czechoslov. Chem. Commun. 12, 594 (1947)

25. I. Langmuir, Chem. Reviews 13, 147 (1933)

26. M. Volmer, Z. phys. chem. 119, 46 (1925)

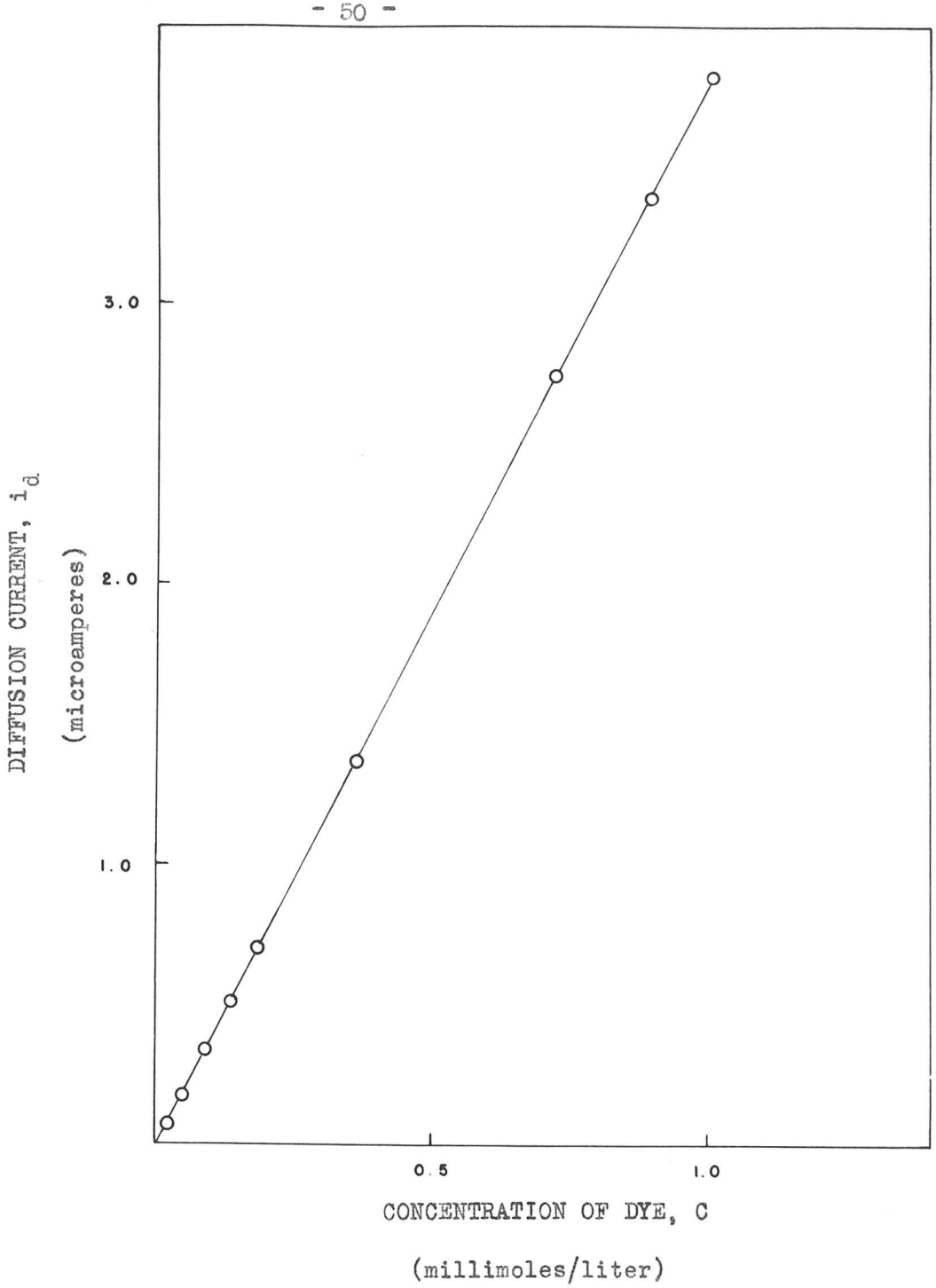


Figure 1: p-Hydroxyphenylazophenylarsonic Acid. A Test of the Ilkovic Equation.(See Table I) All solutions 0.15 M. in NaCl, 0.02 M. in veronal; pH 8

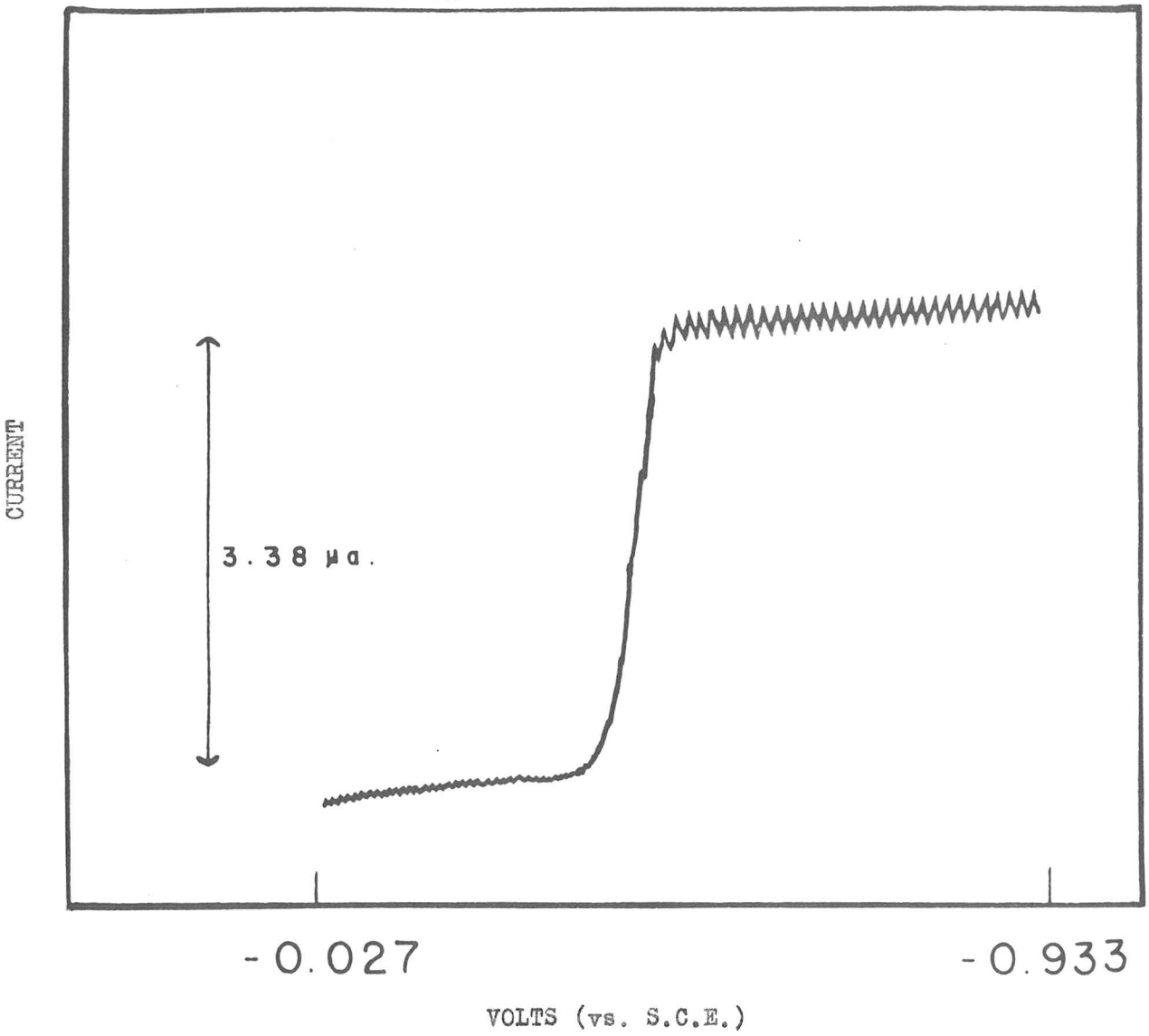


Figure 2: A Typical Polarogram of p-Hydroxyphenylazophenylarsonic Acid. The solution is 9.06 X $10^{-4}$ M. in dye, 0.15 M. in NaCl, 0.02 M. in veronal; pH 8

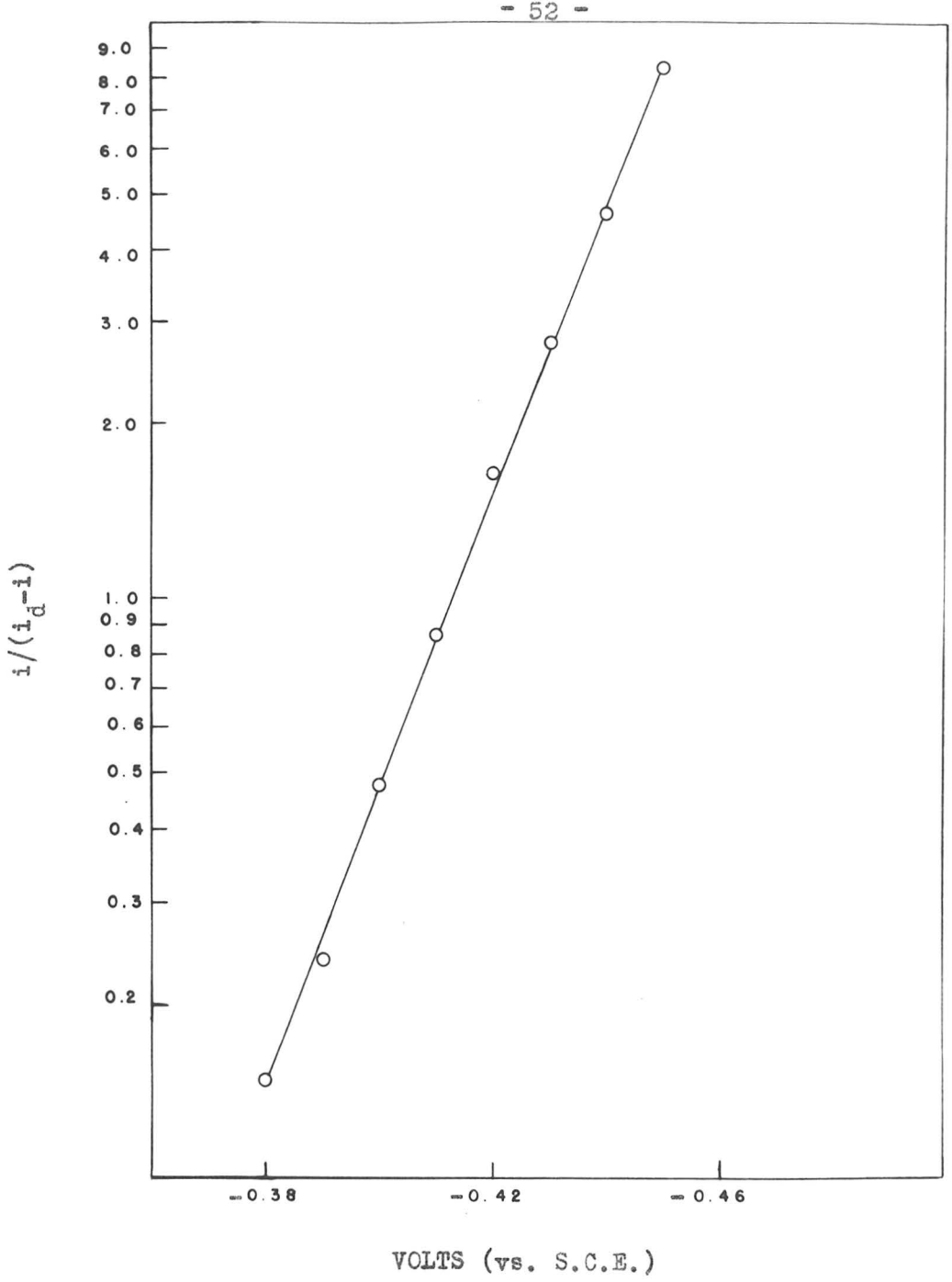


Figure 3: p-Hydroxyphenylazophenylarsonic Acid. A Test of the Reversibility of the Electrode Reaction (See Table II). The solution is 5 X $10^{-4}$ M. in dye, 0.15 M. in NaCl, 0.02 M. in veronal; pH 8

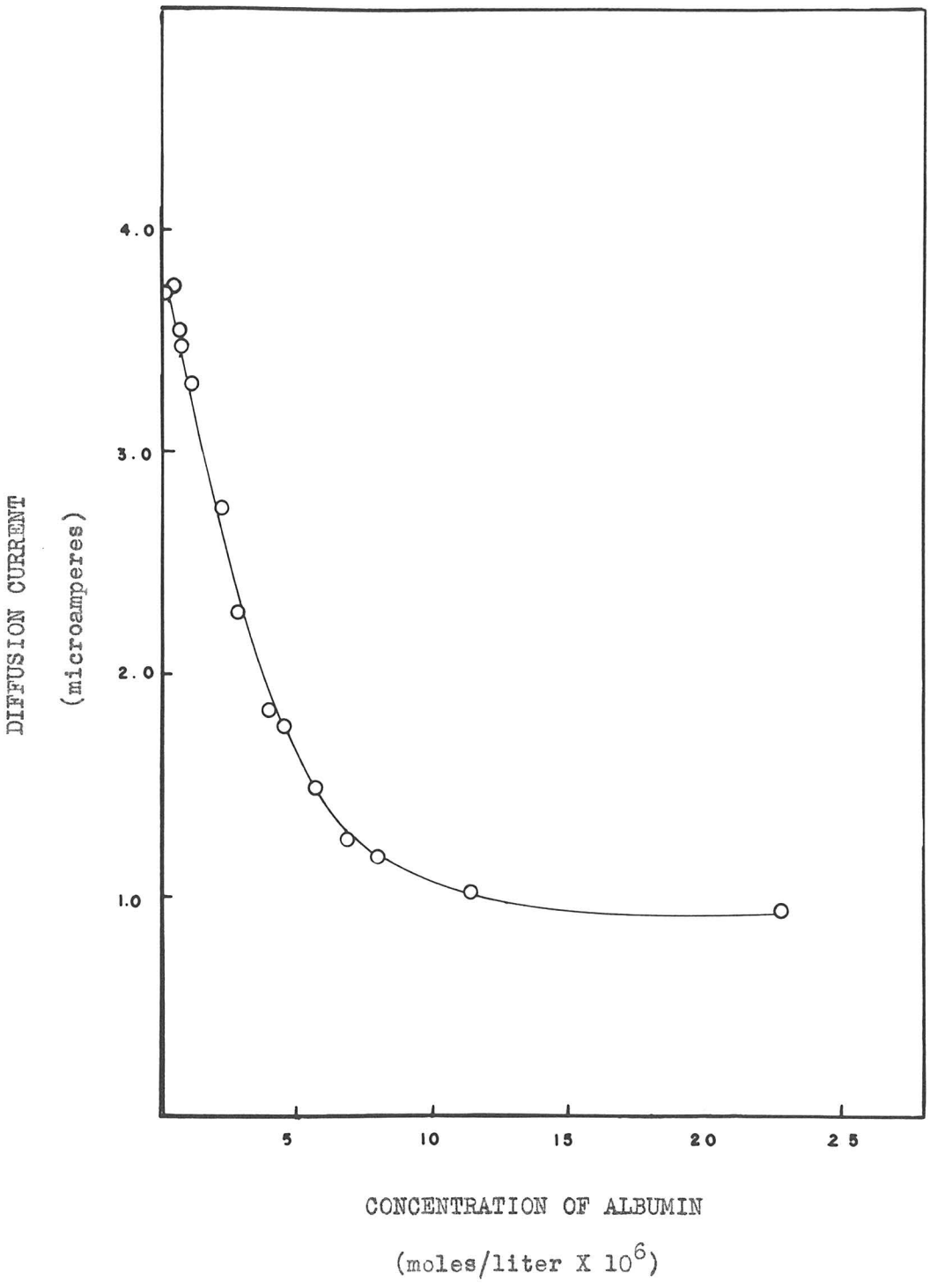


Figure 4: p-Hydroxyphenylazophenylarsonic Acid. The Effect of Increasing Albumin Concentration on the Diffusion Current of the Dye (See Tables III and IV). All solutions are 9.86 X $10^{-4}$ M. in dye, 0.15 M. in NaCl, 0.02 M. in veronal; pH 8

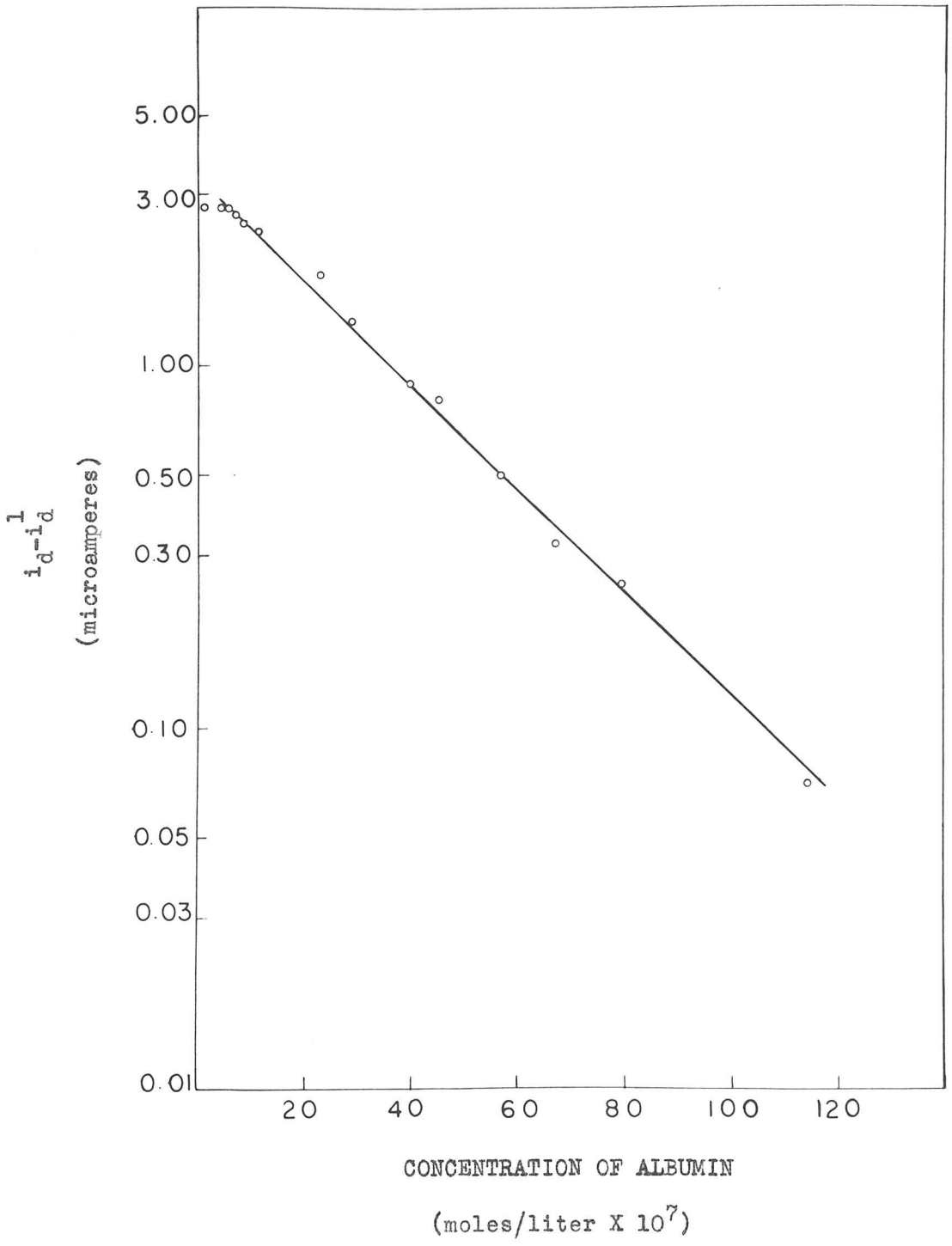


Figure 5: p-Hydroxyphenylazophenylarsonic Acid. The Linear Relationship Between log $(i_d - i_d^1)$ and the Concentration of Protein. All solutions are 9.86 X $10^{-4}$ M. in dye, 0.15 M. in NaCl, 0.02 M. in veronal; pH 8

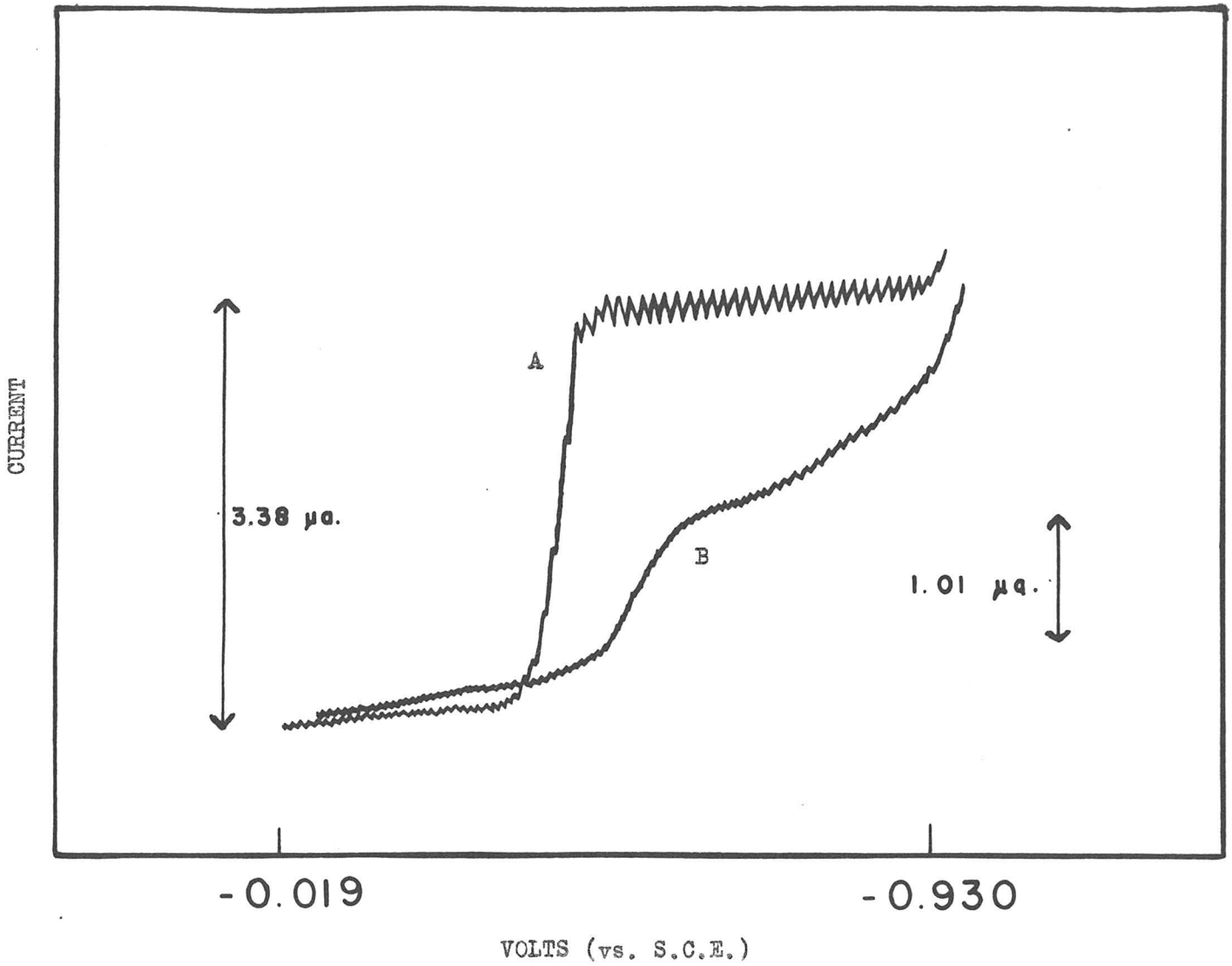


Figure 6: p-Hydroxyphenylazophenylarsonic Acid. A Comparison Between c.-v. Curves Obtained in the Absence and in the Presence of Albumin. Curve A was obtained from a solution 9.06 X $10^{-4}$ M. in dye, curve B from a solution 9.86 X $10^{-4}$ M. in dye and 7.99 X $10^{-6}$ M. in horse albumin. Both solutions were 0.15 M. in NaCl, 0.02 M. in veronal; pH 8

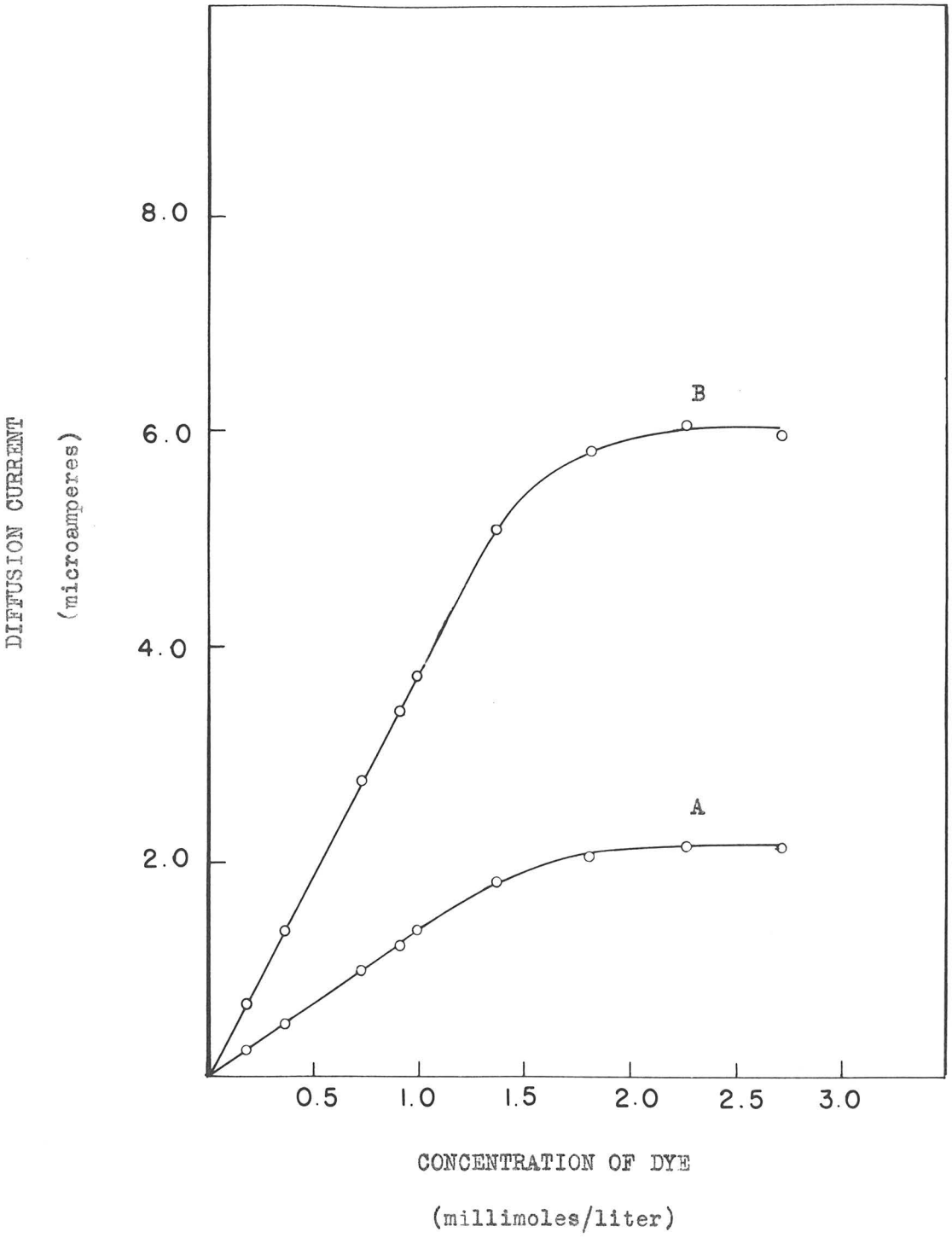


Figure 7: p-Hydroxyphenylazophenylarsonic Acid. The Variation of the Diffusion Current with Concentration of Dye in the Presence (Curve A) and in the Absence (Curve B) of Albumin (See Table V). All solutions were 0.15 M. in NaCl, 0.02 M. in veronal; pH 8. The solutions along curve A were $6.1 \times 10^{-6}$ M. in albumin

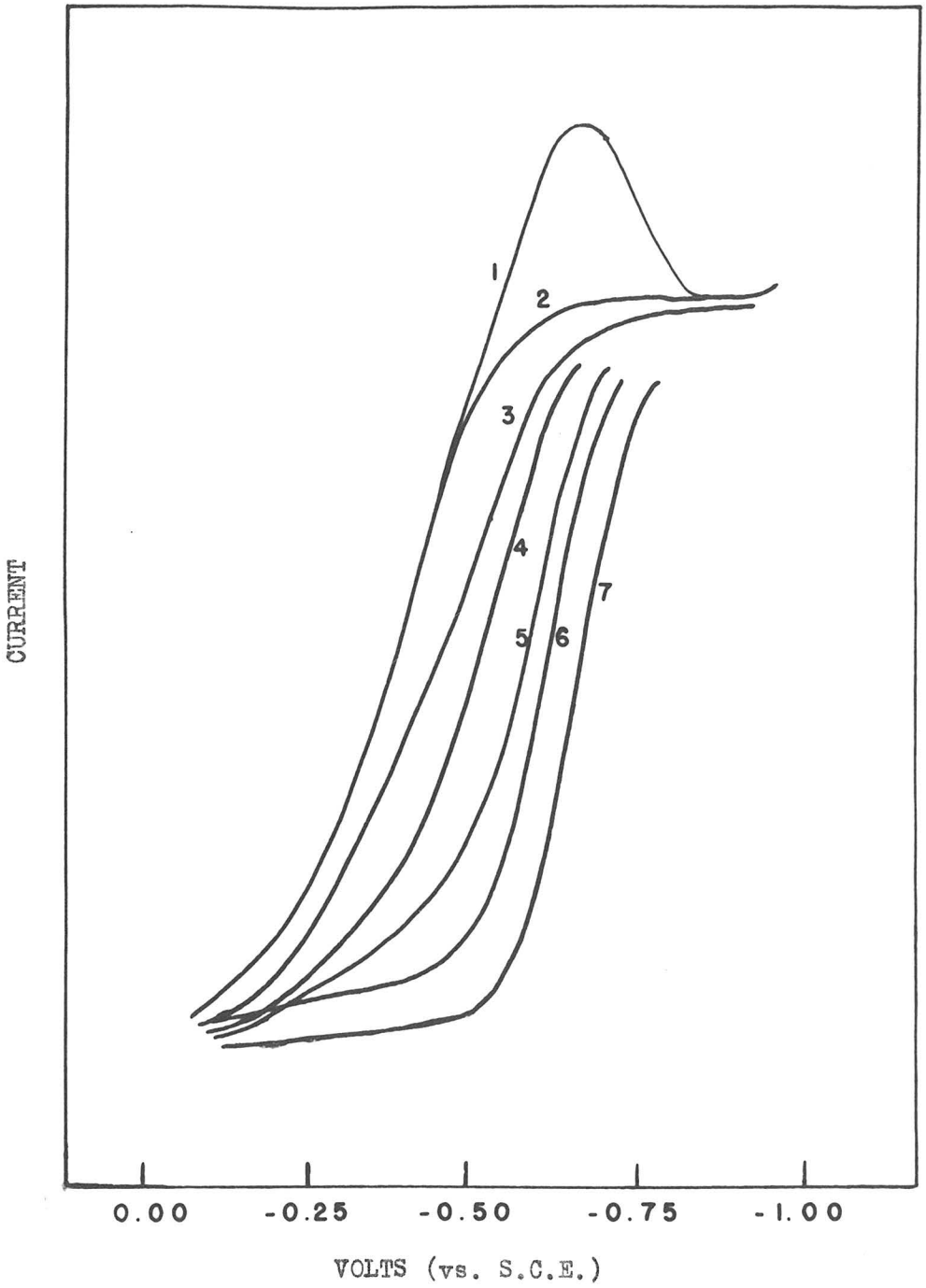


Figure 8: The Effect of Thymol on the c.-v. Curves of Cystine (See Table VI). All solutions are 0.001 M. in cystine, 0.15 M. in NaCl; pH 1 -

The concentrations of thymol are as follows:

1) 0.00 X $10^{-5}$ M.
2) 1.00 X $10^{-5}$ M.
3) 3.00 X $10^{-5}$ M.
4) 9.00 X $10^{-5}$ M.
5) 10.0 X $10^{-5}$ M.
6) 15.0 X $10^{-5}$ M.
7) 20.0 X $10^{-5}$ M.

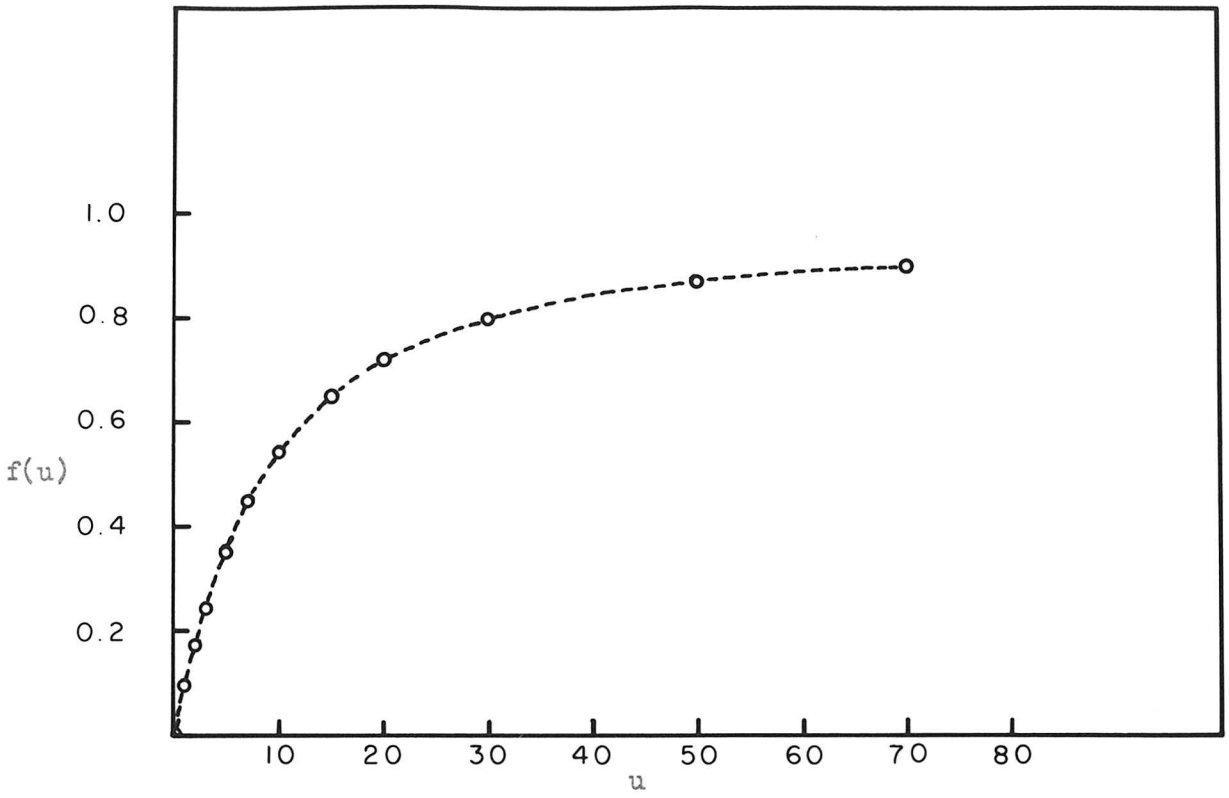


Figure 9: The Variation of the Function f(u) with u. (See Table VII and Equation (20))

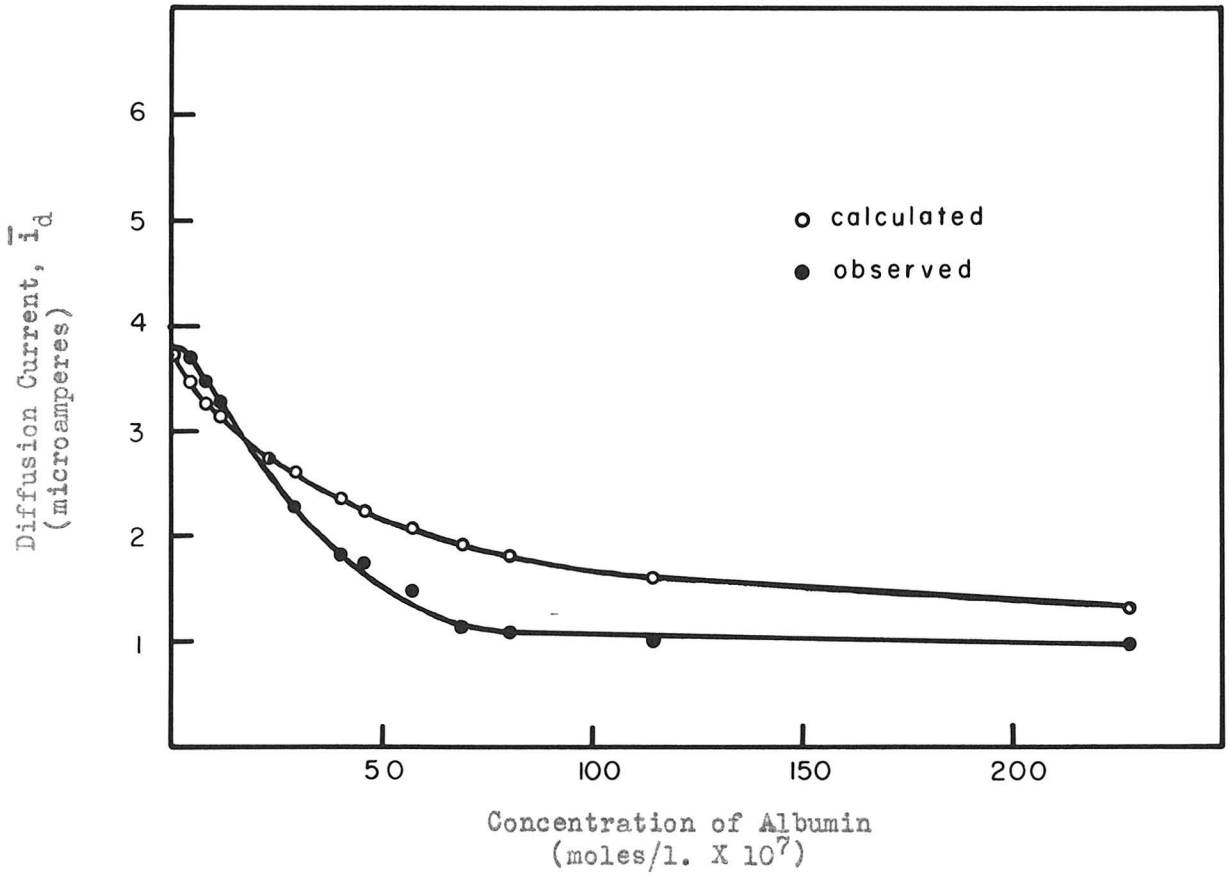


Figure 10: Comparison of the Observed and the Calculated Diffusion Current of HPA as a Function of the Albumin Concentration

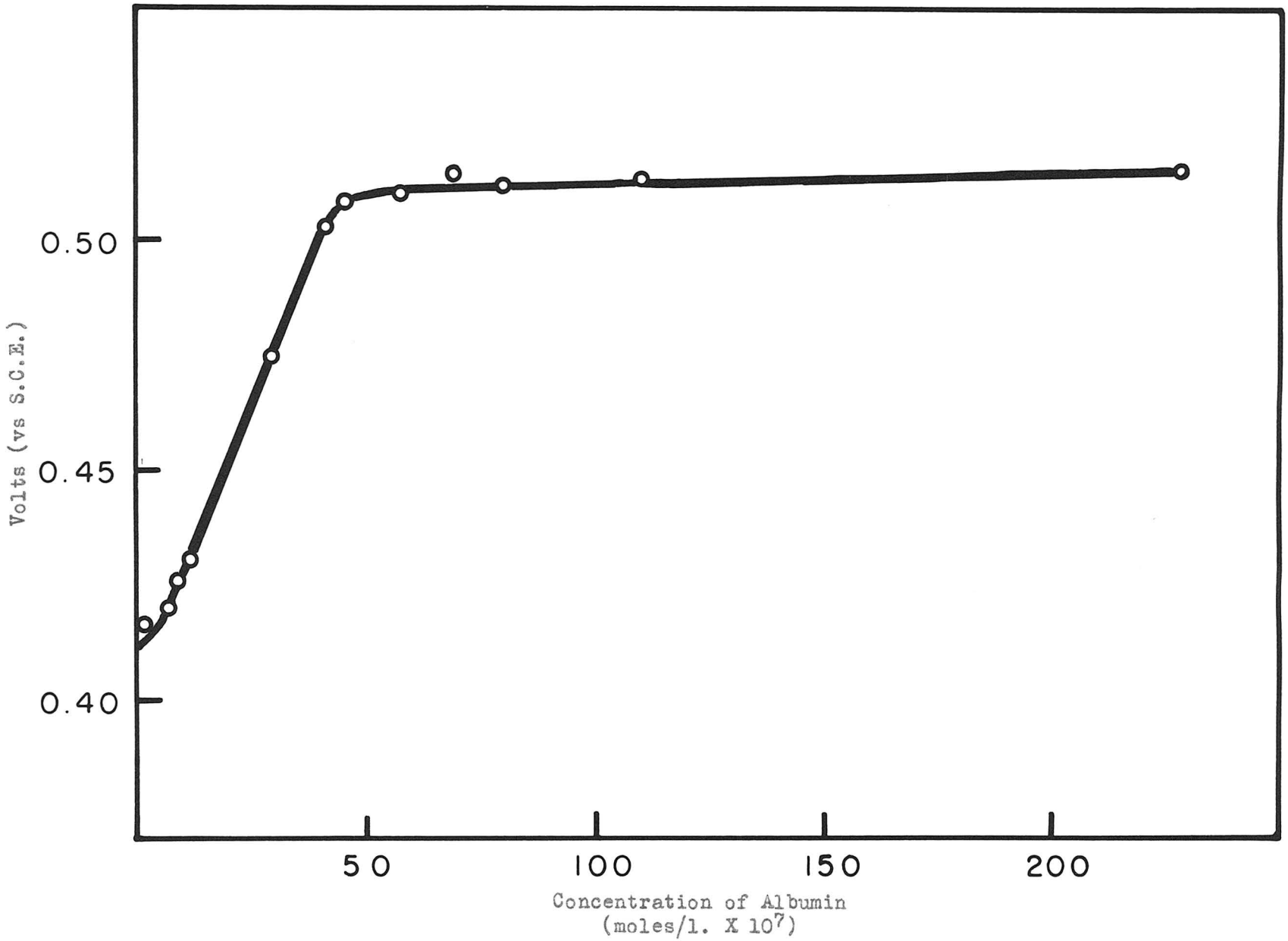


Figure 11: Variation of the Half-Wave Potential of HPA with Change in the Albumin Concentration

# Part II

## The Polarographic Analysis of Nitrite and of Nitrite-Nitrate Mixtures

[Reprinted from the Journal of the American Chemical Society, 68, 2665 (1946).]

CONTRIBUTION FROM THE GATES AND CRELLIN LABORATORIES OF CHEMISTRY, CALIFORNIA INSTITUTE OF TECHNOLOGY, No. 1031]

# The Polarographic Analysis of Nitrite and of Nitrite–Nitrate Mixtures[1]

BY BERTRAM KEILIN AND JOHN W. OTVOS[2]

A method for the polarographic determination of nitrate in the presence of uranyl ion in acid solution has been described by Kolthoff, Harris and Matsuyama.[3] Since in the earlier methods studied by Tokuoka and Ruzicka[4,5] in which other cations were used as "activators," the reduction potentials for nitrate and nitrite were always found to be identical, it was of interest to us to examine the polarographic behavior of nitrite in the presence of uranyl ion.

At the acid concentrations necessary for suppressing the hydrolysis of uranyl ion, all but a few per cent. of nitrite exists as nitrous acid and the similarity between nitrate and nitrite is thus greatly decreased. Nevertheless the waves for the two substances are very similar in appearance and occur at the same potential.

A method for the separate estimation of nitrate and nitrite in solutions containing both ions is described in this paper. Use is made of the additivity of the waves, and of a simple chemical conversion of nitrite to nitrate without the introduction of new ions which might interfere with the determination.

## Experimental

**Apparatus and Materials.**—A Heyrovsky Type XII Polarograph was used in all experiments. Measurements were made at 25°. Dissolved oxygen was removed by passing nitrogen through the solutions. All chemicals were of reagent grade. The sodium nitrite used in quantitative experiments was standardized against permanganate in acid solution, the primary standard being sodium oxalate.[6]

**Decomposition of Nitrous Acid.**—It is known that in cold dilute solutions and in the absence of air nitrous acid decomposes to nitric acid and nitric oxide; in the presence of oxygen, nitric acid alone is produced. Because of the instability of nitrous acid, a polarographic procedure for the determination of nitrite in acid solution must involve some error. Experiments performed in connection with this investigation have shown that in air and at concentrations which are of interest in polarography the decomposition of nitrous acid[7,8] is first order and that about six per cent. decomposes in a half hour at room temperature. If the nitrite solution is polarographed as soon as possible after it is acidified, the error arising from nitrous acid decomposition can be kept below 3%.

**Comparison of the Nitrous Acid and Nitrate Waves.**—Figure 1 shows a nitrous acid wave and a nitrate wave, each obtained with a solution $4 \times 10^{-4}$ $M$ in the nitrous acid[9] or nitrate, $2 \times$

(1) This paper is based in whole or in part on work done for the Office of Scientific Research and Development under Contract OEMsr-881 with the California Institute of Technology.

(2) Present address: Shell Development Company, Emeryville, California.

(3) I. M. Kolthoff, W. E. Harris and G. Matsuyama, THIS JOURNAL, **66**, 1782 (1944).

(4) M. Tokuoka, *Coll. Czechoslov. Chem. Comm.*, **4**, 444 (1932).

(5) M. Tokuoka and J. Ruzicka, *ibid.*, **6**, 339 (1934).

(6) J. S. Laird and T. C. Simpson, THIS JOURNAL, **41**, 524 (1919).

(7) Abel, *Z. physik. Chem.*, **148**, 337 (1930).

(8) Bray *et al.*, *Chem. Rev.*, **10**, 161 (1932).

(9) Concentrations of nitrous acid, as given in this paper, include both un-ionized and ionized forms.

$10^{-4}$ $M$ in uranyl acetate, 0.01 $M$ in hydrochloric acid, and 0.1 $M$ in potassium chloride. The two waves are almost identical in shape. There is no trace of the nitric oxide wave at $-0.77$ volt (*vs.* S.C.E.) reported by Heyrovsky and Nejedly[10] for acid solutions of nitrite, probably because nitrogen was bubbled through the solutions immediately before the polarograms were made.

In neutral or alkaline solutions the reduction potentials of nitrate and nitrite are known to become more positive in the presence of polyvalent cations.[5] This effect has been attributed to the formation of loose "ion pairs" which, because of their positive charge, facilitate the access of nitrate or nitrite to the negative electrode. Presumably the same phenomenon occurs with nitrate in acid solution in the presence of uranyl ion. Nitrous acid, however, is uncharged and should not require the assistance of polyvalent cations for its approach to the cathode. In preliminary experiments in this Laboratory, nitrous acid in the absence of uranyl ion has indeed been found to produce a wave at about $-1.0$ volt (*vs.* S.C.E.), which is approximately the half-wave potential of the uranyl-activated nitrite wave. This wave may correspond to that reported by Schwarz[11] for nitrite in acetic acid solution, which extends from $-0.6$ to $-1.6$ volts. Although the uranyl ion has little effect on the half-wave potential of the nitrous acid wave, its presence causes an increase in the nitrous acid diffusion current.

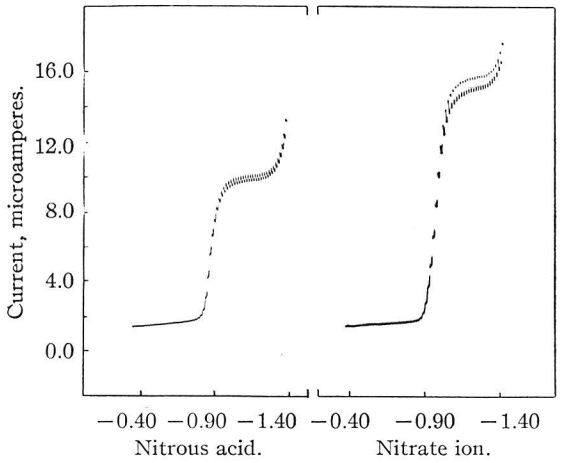


Fig. 1.—Comparison of nitrous acid and nitrate waves. Solutions are 0.1 $M$ in hydrochloric acid, 0.1 $M$ in potassium chloride, $2 \times 10^{-4}$ $M$ in uranyl acetate, and $4 \times 10^{-4}$ $M$ in nitrous acid and nitrate, respectively; $m^{2/3}t^{1/6} = 2.08$ mg.$^{2/3}$ sec.$^{-1/2}$.

The nitrous acid wave shown in Fig. 1 is a little over half as high as the nitrate wave, after correction has been made for the blank uranyl wave. The diffusion current constants for nitrous acid at several concentrations are given in Table I. For the more dilute solutions the concentration of uranyl ion was reduced to $5 \times 10^{-5}$ $M$ from the usual value of $2 \times 10^{-4}$ $M$. Over a hundred-fold concentration range of nitrous acid ($2 \times 10^{-5}$ $M$ to $2 \times 10^{-3}$ $M$), the mean value of $i_d/Cm^{2/3}t^{1/6}$ is 7.45 and the average deviation of the points from the mean is 4.5%. Probably a large part of the deviation is due to the instability of nitrous acid and variations in the time required to run a polarogram.

TABLE I

DIFFUSION CURRENT CONSTANT FOR NITROUS ACID AT 25°

$m^{2/3}t^{1/6} = 2.08$ mg.$^{2/3}$ sec.$^{-1/2}$ at $-1.2$ volts *vs.* S.C.E.; diffusion current is measured at $-1.2$ volts *vs.* S.C.E.; residual current at $-1.2$ volts = 2.00 microamperes

| Concn. of nitrous acid, millimoles/liter, $C$ | Diffusion current of nitrous acid, microamperes, $i_d$ | $K = i_d/Cm^{2/3}t^{1/6}$ |
|---|---|---|
| A. Solutions 0.1 $M$ in KCl, 0.01 $M$ in HCl, and $2 \times 10^{-4}$ $M$ in $UO_2(OOCCH_3)_2$ | | |
| 5.125 | 47.8 | 4.50[a] |
| 2.050 | 31.5 | 7.40 |
| 1.025 | 15.6 | 7.30 |
| 0.820 | 12.3 | 7.20 |
| .512 | 7.52 | 7.06 |
| .205 | 2.92 | 6.87 |
| .102 | 1.56 | 7.35 |
| .082 | 1.17 | 6.87 |
| .0512 | 0.87 | 8.16 |
| B. Solutions 0.1 $M$ in KCl, 0.01 $M$ in HCl, $5 \times 10^{-5}$ $M$ in $UO_2(OOCCH_3)_2$ | | |
| 0.102 | 1.66 | 7.83 |
| .082 | 1.32 | 7.74 |
| .0512 | 0.83 | 7.78 |
| .0205 | .324 | 7.60 |
| .0102 | .214 | 10.1[a] |
| .00512 | .111 | 10.4[a] |
| C. Average diffusion current constant | | 7.45 |

[a] Not included in the average.

The number of electrons involved in the reduction of nitrous acid can be calculated with the use of Ilkovic's equation:

$$i_d = 605nD^{1/2}Cm^{2/3}t^{1/6} \quad (1)$$

where $i_d$ is the average diffusion current obtained at the dropping mercury electrode in microamperes, $n$ is the number of faradays transferred per mole, $D$ is the diffusion coefficient of the reducible substance in cm.$^2$ sec.$^{-1}$, $C$ is its concentration in millimoles per liter, $m$ is the rate of flow of mercury in mg. sec.$^{-1}$ and $t$ is the drop time in seconds. The diffusion current constant, $K = i_d/Cm^{2/3}t^{1/6}$, as given in Table I, is 7.45. The value of $D$ for nitrite ion, calculated from its equivalent conductance,[12] is $1.92 \times 10^{-5}$ cm.$^2$ sec.$^{-1}$. With the assumption that the diffusion coefficient for nitrous acid is the same as that for nitrite ion, $n$ can be calculated from these figures

(10) J. Heyrovsky and V. Nejedly, *Coll. Czechoslov. Chem. Comm.*, **3**, 126 (1931).

(11) K. Schwarz, *Z. anal. Chem.*, **115**, 161 (1939).

(12) Niementowski and Roszkowski, *Z. physik. Chem.*, **22**, 147 (1897).

The value obtained for the electron transfer, $n$, is 2.8 faradays per mole.

Kolthoff, Harris and Matsuyama[3] report a five-electron reduction for nitrate in the presence of uranyl ion. The present result of 2.8 or 3 electrons for nitrous acid indicates that it, as well as nitrate, is reduced to nitrogen at the dropping mercury cathode in acid solution in the presence of uranyl ion.

It is interesting to compare this value of the electron transfer for nitrous acid, $n = 3$, with the value obtained by direct analysis of the nitrous acid wave according to the fundamental equation for a polarographic wave, first derived by Heyrovsky and Ilkovic.[13]

$$E_{d.e.} = E_{1/2} - \frac{0.0591}{n} \log \frac{i}{i_d - i} \qquad (2)$$

In this equation $E_{d.e.}$ and $i$ are corresponding values for the potential of the dropping mercury electrode and the current at any point on the wave, $E_{1/2}$ is the half-wave potential, and $n$ is the number of electrons involved reversibly in the reduction. When $\log i/(i_d - i)$ is plotted against the voltage, a slope is obtained which corresponds to a value of $n = 1$ (Fig. 2). An electron transfer of $n = 1$ was also obtained by Kolthoff, Harris and Matsuyama in an analysis of the nitrate wave, although the over-all reduction of nitrate appears to involve 5 electrons. It may be inferred that, under these conditions, neither the reduction of nitrous acid nor that of nitrate is reversible. A similar effect has been found by Orlemann and Kolthoff[14] in the irreversible reduction of iodate and bromate.

**Solutions Containing both Nitrate and Nitrite Ions.**—In polarograms of solutions containing both nitrate ion and nitrous acid, the diffusion current, above that due to the blank uranyl wave, is the sum of the diffusion currents due to nitrate ion and nitrous acid independently. In Table II, the observed diffusion currents of some solutions containing these ions together are compared with values calculated from the additivity relationship

$$i_d = m^{2/3}t^{1/6}(7.45C_1 + 13.8C_2) \qquad (3)$$

where $C_1$ and $C_2$ are the concentrations of nitrite and nitrate in millimoles per liter and $m$ and $t$ are expressed in the conventional units. The coefficients of $C_1$ and $C_2$ are the experimentally determined diffusion current constants reported here and in the paper of Kolthoff, Harris and Matsuyama.[3]

TABLE II

ADDITIVITY OF NITRATE AND NITROUS ACID WAVES

Solutions 0.1 $M$ in KCl, 0.01 $M$ in HCl, $2 \times 10^{-4}$ $M$ in $UO_2(OOCCH_3)_2$; $m^{2/3}t^{1/6} = 2.08$ mg.$^{2/3}$ sec.$^{-1/2}$

| Concn. of nitrate, millimoles/liter | Concn. of nitrous acid, millimoles/liter | Diffusion current, microamperes Obs. | Calcd. |
|---|---|---|---|
| 0.100 | 0.096 | 4.35 | 4.37 |
| .100 | .192 | 5.75 | 5.86 |
| .100 | .384 | 8.85 | 8.83 |
| .100 | .768 | 14.9 | 14.8 |

(13) J. Heyrovsky and D. Ilkovic, *Coll. Czechoslov. Chem. Comm.*, **7**, 198 (1935).

(14) E. F. Orlemann and I. M. Kolthoff, THIS JOURNAL, **64**, 1044 (1942).

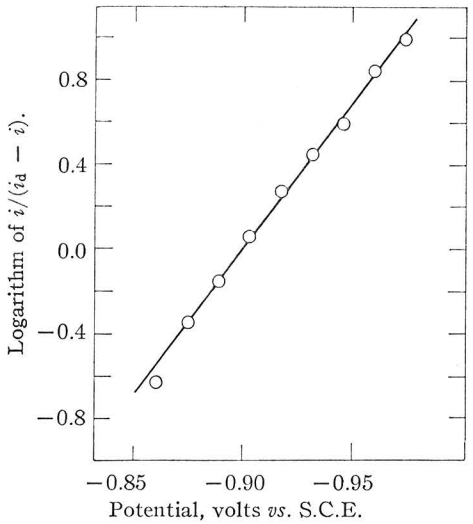


Fig. 2.—Analysis of nitrite reduction wave in 0.1 $M$ potassium chloride, 0.01 $M$ hydrochloric acid and $2 \times 10^{-4}$ $M$ uranyl acetate.

From a single polarogram of a solution containing uranyl ion, only a figure representing the weighted sum of nitrous acid and nitrate concentrations can be obtained. To obtain the concentrations of the substances separately by the methods described above it is necessary to run another polarographic experiment on an aliquot of the solution after altering the relative amounts of the two substances in a known way. It is convenient to do this by transforming one of them quantitatively to the other. A satisfactory and convenient method of achieving this transformation is the quantitative oxidation of nitrite to nitrate by hydrogen peroxide in acid solution.

$$HNO_2 + H_2O_2 \longrightarrow NO_3^- + H^+ + H_2O$$

If the solution is then made basic, the excess peroxide may be catalytically decomposed with manganese dioxide. The only products of these two reactions that remain in solution are nitrate, water and oxygen; no new ionic species are produced. The uranyl ion must not be added until the reactions described above are completed and the solution is again acidified.

A polarogram of the oxidized solution, after the addition of uranyl acetate, potassium chloride and hydrochloric acid in the usual concentrations, gives a diffusion current

$$i_d' = 13.8m^{2/3}t^{1/6}(C_1 + C_2) \qquad (4)$$

since all of the nitrite has been converted to nitrate. From equations (3) and (4), the separate concentrations $C_1$ and $C_2$ of nitrite and nitrate, respectively, can be calculated.

$$C_1 = \frac{i_d' - i_d}{6.35m^{2/3}t^{1/6}} \quad (5)$$

$$C_2 = \frac{i_d'}{13.8m^{2/3}t^{1/6}} - C_1 \quad (6)$$

**Procedure for the Polarographic Determination of Nitrite.**—For the determination of nitrite in solutions where its concentration is between $5 \times 10^{-5}$ and $5 \times 10^{-3}$ $M$, the following procedure is recommended.

Prepare two stock solutions, one being 0.2 $M$ in potassium chloride, 0.02 $M$ in hydrochloric acid, and $4 \times 10^{-4}$ $M$ in uranyl acetate; the other having the same composition except that it is only $1 \times 10^{-4}$ $M$ in uranyl acetate.

Dilute 25.00 ml. of the uranyl acetate stock solution to 50.00 ml. with redistilled water, bubble with nitrogen gas to make oxygen-free, and measure the apparent diffusion current due to the reduction of uranyl ion at a potential of −1.2 volts *vs.* S.C.E. This current is taken as the "blank" or "residual" current for the nitrous acid wave.

Measure a suitable volume of an unknown nitrite solution into a 50-ml. volumetric flask, add 25.00 ml. of the appropriate uranyl acetate stock solution and dilute to volume with redistilled water. (It may be necessary to make a preliminary run in order to determine the concentration of uranyl ion to be used. In general, if the final concentration of the nitrite ion is to be above $1 \times 10^{-4}$ $M$, the stock solution containing the higher concentration of uranyl acetate is used. If the concentration is below this value, the one containing the lower concentration is employed.) Make the resulting solution oxygen-free and measure the apparent diffusion current at a potential of −1.2 volts *vs.* S.C.E. Subtract the "residual" current due to the reduction of uranyl ion from the diffusion current to obtain the diffusion current due to nitrous acid. The amount of nitrite in the unknown solution can be found from this diffusion current by referring to a standard curve, which is constructed by plotting diffusion current against concentration. Such a plot is prepared with data, such as are given in Table I, that are obtained with known solutions.

**Analysis of Solutions Containing Both Nitrate and Nitrite.**—Divide the solution to be analyzed into two equal portions. Add to the first portion 25.00 ml. of the appropriate uranyl acetate stock solution, and dilute to 50.00 ml. with redistilled water. Make the resulting solution air-free, measure the apparent diffusion current, and subtract the "residual" current as described above to obtain the total diffusion current due to nitrate ion and nitrous acid. To the second portion, add 2 $N$ hydrochloric acid until it is just neutral and then add an excess of five drops. Add 1 ml. of 30% hydrogen peroxide and allow the mixture to stand at room temperature for thirty minutes. Add eight drops of 2 $N$ sodium hydroxide and then introduce a small quantity of manganese dioxide. After the evolution of gas has ceased, decant the solution quantitatively into a 50-ml. volumetric flask. Add three drops of 2 $N$ hydrochloric acid and then 25.00 ml. of the appropriate uranyl acetate stock solution, and dilute to volume. Measure the apparent diffusion current as before, and again subtract the "residual" current. From the two values of the diffusion current thus obtained, the concentrations of nitrite and nitrate originally present in the unknown solution may be calculated as described above.

**Interferences.**—In general, interferences which have been described for the estimation of nitrate[3] will also be encountered in this determination. The presence in solution of substances such as strong bases and phosphates, which precipitate the uranyl ion, or complex-formers such as citrate or tartrate will interfere, as will also those substances, such as oxalates and strong acids, which discharge at voltages near to that of nitrous acid. Sulfate ion in a concentration twenty times that of the nitrite was found to reduce the wave height somewhat.

**Acknowledgment.**—We wish to express our thanks to Mr. F. D. Ordway of this Laboratory for his kind assistance in carrying out the chemical analyses necessary for this work. We are also greatly indebted to Mr. Joseph C. Guffy of the University of Wisconsin for his interest in this problem and for many most helpful conversations on the subject.

## Summary

1. In the presence of uranyl ion, nitrous acid in dilute solutions of hydrochloric acid is reduced at the same potential at which nitrate is reduced (*ca.* −1 volt *vs.* S.C.E.). The diffusion current is proportional to the nitrous acid concentration when the ratio of uranyl ion to nitrous acid is above a critical minimum. The reduction of nitrous acid under these conditions involves three electrons, indicating a reduction to nitrogen, but analysis of the wave shows that the reduction is irreversible.

2. A solution containing both nitrate and nitrite ions can be analyzed for both constituents in two polarographic experiments. First, the diffusion current due to the two constituents in the original solution is measured. With another aliquot, the nitrite present is oxidized to nitrate and the diffusion current of the resulting solution is measured as before. The nitrite can be conveniently oxidized by hydrogen peroxide in acid solution, and the excess peroxide can be destroyed catalytically by manganese dioxide in basic solution.

3. Interferences are similar to those encountered by Kolthoff, Harris and Matsuyama[3] in the analysis of nitrate solutions, except that large amounts of sulfate seem to reduce the diffusion current.

PASADENA, CALIFORNIA RECEIVED JULY 18, 1946

# Part III

## An Electron Diffraction Investigation of the Structure of Some Organic Molecules

a) Some Cyclic Derivatives of Ethylene Glycol

b) Naphthalene and Anthracene

# AN ELECTRON DIFFRACTION INVESTIGATION OF THE STRUCTURE OF SOME ORGANIC MOLECULES

Part III of this thesis is devoted to an account of the results obtained in a series of molecular structure determinations by the electron diffraction method. It is convenient to describe the five compounds which were investigated in two sections. Section (a) is given to the structure determinations of ethylene glycol sulfite ester, ethylene glycol chlorophosphite ester, and ethylene glycol acetal, and section (b) to those of naphthalene and anthracene. The account of the work is preceded by a brief description of the electron diffraction method as practised in these laboratories.

The electron diffraction apparatus has been described by Brockway:[1] A collimated beam of electrons originating from a hot tungsten filament and accelerated through a potential drop of approximately 40,000 volts is allowed to intersect a stream of gas emanating from a pinhole in a nozzle placed just below the path of the beam. The electrons interact with the molecules of the gas and then fall upon a flat photographic plate which, after development, shows a radially symmetric diffraction pattern that to the eye appears to consist of a series of alternate maxima and minima.

The diffracted intensity, which is a function of the scattering angle, may be described as the resultant of the contributions from the incoherent and the atomic scattering, which are structure insensitive and decline monotonically with increasing angle, and from the molecular

scattering, which is the particular component of interest in the determination of the structure of the molecule. The intensity of this rapidly varying component of the diffraction pattern is estimated as a function of the angle of scattering by visual examination of the photographs, whereby the observer, consciously aiding the contrast-sensitive properties of his eye, separates this component of the total intensity from the rest. The observations are interpreted in accordance with the appearance of the photographs and in a manner such that the resultant "visual curve" will prove useful in comparing the experimental data with theoretical calculations made in accordance with the reduced intensity function,

$$I(q) = \frac{K}{\sum_i (Z_i - f_i)^2} \sum_i \sum_{i \neq j} \frac{(Z_i - f_i)(Z_j - f_j)}{r_{ij}} \sin\left(\frac{\pi r q}{10}\right), \qquad (1)$$

where $r_{ij}$ is the value assigned to the distance between the $i^{\underline{th}}$ and $j^{\underline{th}}$ atoms in the molecule, K is a constant, $Z_i$ is the atomic number and $f_i$ the x-ray form factor of the $i^{\underline{th}}$ atom, and $q = 40/\lambda \sin \theta/2$ (where $\theta/2$ is the angle of diffraction and $\lambda$ is the wave length of the electrons.)

In the interpretation of the experimental data, it is customary to use the radial distribution method[2,3] in order to obtain a probability distribution of the distances in the molecules. The radial distribution integral, approximated by a summation, provides a direct method for determining the frequency of the terms contributing to the intensity pattern described by equation (1); from the frequency of these terms, the interatomic distances occurring in the molecule may be deduced. The radial distribution function (RDI) is calculated from the equation,

$$rD(r) = \sum_{q=1}^{q_{max}} I_o(q)\, e^{-aq^2} \sin \frac{\pi rq}{10} , \qquad (2)$$

where $I_o(q)$ is an intensity function taken from the visual curve; a is usually so adjusted that $e^{-aq^2} = 0.1$ at $q = q_{max}$. The unobservable first maximum in the visual curve is first estimated roughly and is finally drawn to agree approximately with that of the theoretical intensity curves. Generally, models of the molecule in which the interatomic distances disagree with the information obtained from the RDI may be regarded immediately as representing incorrect structures.

For a final determination of the molecular structure and for an estimation of the probable limits of error, the correlation method is used.[4] Theoretical intensity functions, I(q), are calculated from equation (1) or (for molecules in which the atoms do not differ widely in atomic number) from the simplified theoretical scattering formula,

$$I(q) = K \sum_{i} \sum_{j}' \frac{Z_i Z_j}{r_{ij}} e^{-b_{ij}q^2} \sin \left(\frac{\pi rq}{10}\right) , \qquad (3)$$

where the symbols are those defined in the preceding discussion, except that the value assigned for the atomic number of hydrogen is 1.25. This value is required for $q < 15$ because of the substitution of $Z_i Z_j$ for $(Z_i - f_i)(Z_j - f_j)/\overline{(Z_i - f_j)^2}$ and is tolerable otherwise because of the temperature factor, $e^{-b_{ij}q^2}$, which is active in the terms of the summation corresponding to X. . .H distances. The temperature factor is applied to account for thermal vibrations which vary the interatomic distances somewhat about their mean value. The value given to b is usually 0.00016 for bonded X–H terms, 0.0003 for X—H terms through one angle, and in cyclic compounds,

zero for all other terms. X. . .H terms through more than one angle and H. . .H terms are usually omitted from the summation. Calculations involving the use of equations (1), (2) and (3) are made with punched cards on International Business Machines.[5]

The theoretical intensity curves calculated by equations (1) and (3) are compared with the visual curve; those which in the opinion of the observer are an acceptable representation of the appearance of the photographs usually fall within an ellipsoidal or hyperellipsoidal volume in parameter space if the structure can be determined uniquely. From this region of acceptability, the observer estimates the limits of error for each parameter and chooses the model which he believes to represent best the structure of the molecule. If the structure cannot be determined uniquely by the electron diffraction method, it is necessary to deal with two or more ellipsoidal volumes in parameter space. The estimation of the best model and of the limits of error completes the determination.

a) Some Cyclic Derivatives of Ethylene Glycol

A number of new compounds, involving hitherto unknown ring systems, were synthesized by Majima and Simanuki and by Lucas, Mitchell and Scully. Among these are ethylene glycol sulfite ester (I),[6] ethylene glycol chlorophosphite ester (II)[7,8] and ethylene glycol acetal (III).[9]

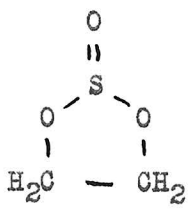

(I)

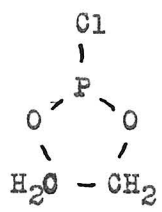

(II)

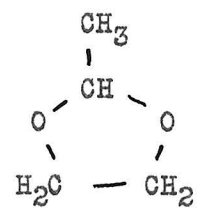

(III)

The interest in the molecular structure of these compounds centers about several points. They present new ring systems for investigation with respect to the planarity of the atoms and in addition offer an opportunity to the structural chemist for measuring some interatomic distances (e.g., single-bond sulfur-oxygen) which are not commonly found in molecules. To the organic chemist, the spatial configuration of the molecules (I), (II), and (III) is of interest with respect to the possibility of preparing geometric isomers of homologous derivatives. Compounds of the type (IV), for example should form geometrical isomers if atom X or atom Y is not coplanar with the remaining atoms in the ring.

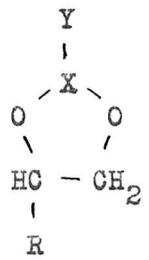

(IV)

R = any group other than H

In this investigation, some assumptions were made in calculating theoretical intensity curves for correlation with the visual curve. The general assumptions are described here and any special ones are presented below in connection with the compounds to which they apply. The bonded C-H distance was taken to be 1.09 Å. with a temperature factor applied as described previously. The plane of H-C-H was taken to be normal to that of C-C-O and to bisect the angle. Unless specific evidence could be obtained from the data, the angle C-C-H was adjusted by the method of least strain in which the deviation from $109^{\circ}28'$ is held constant for all angles about a particular carbon atom.

With the assumption that a plane of symmetry exists in the molecules, the structure of each may be completely described by the specification of three bond angles and four bond distances. Of the four bond distances, only three (expressed as ratios to the fourth) need be considered as parameters in determining the shape of the molecule. The fourth distance (the size parameter) is determined at the very last by a comparison of the positions of the main features in the visual curve with those in the best theoretical curve. Although the number of parameters is reduced to six, a complete determination of the limits of error by the correlation method still involves an almost impossibly long procedure. Consequently, in order to reduce further the number of necessary calculations, maximum use was made of the information to be obtained from the radial distribution function, and of some rational assumptions which were compatible with experience in the study of molecular structure. In the geometrical models considered, the bonded carbon-carbon and carbon-oxygen distances were arbitrarily assigned the value which was indicated in the respective RDI, and the group $O_{C-C}^{O}$ was taken to be coplanar. Other assumptions were made in the individual cases. Models were considered in which the remaining parameters were subjected to a systematic variation about the values obtained from the RDI. Theoretical intensity functions were calculated on the basis of these models, a "best fit" to the visual curve was obtained and a tentative set of the limits of acceptable variation of each of the parameters was determined on the basis of a qualitative comparison of the calculated curves with the visual curve. It was desired, furthermore, to extend these limits to include some measure of the possible errors incurred in arbitrarily fixing some of the shape parameters. Consequently, each

previously fixed parameter was assigned a "working deviation" from the fixed value; each was varied in turn by approximately this amount in a model having the other distances corresponding to those in the best curve obtained in the previous correlation procedure. The effects of these variations on the chosen calculated curve were noted and the tentative limits assigned previously to the determined parameters were revised to include the sum of these effects and to include an estimate of the experimental and random errors inherent in the method. Hence, the final statement of the limits of acceptable variation are to be interpreted as follows: if the arbitrarily fixed parameters are correct within the assigned working deviation, the limits of error of the determined parameters are as reported in the investigation. Thus the conclusions as to the limits of error of the structural parameters which were measured have been arrived at with a consideration of the validity of the assumptions which were made in their determination.

## EXPERIMENTS AND RESULTS

### i - Ethylene Glycol Sulfite Ester

The sample of ethylene glycol sulfite ester used in this investigation was prepared by Mrs. G. Guthrie by the action of thionyl chloride on ethylene glycol in methylene chloride solution.[6,9] The compound hydrolyzes rapidly in water and boils at 169-172°C. Purification was effected by vacuum distillation, and the fraction boiling at 61.2-61.8°C./12 mm. (uncorr.) was used in the electron diffraction experiments. The sample was admitted to the diffraction chamber through the standard high temperature nozzle which was maintained at approximately 100°C. The jet-to-film distance was 11.00 cm. The wave length of electrons in the present work was 0.06085 Å., determined against zinc oxide smoke.[10] The photographs showed features extending to q values of about 100.

The radial distribution function R of Figure 1 has strong maxima at 1.08, 1.42, 1.63, 2.46, and 2.95 Å. These distances are in complete agreement with a model of ethylene glycol sulfite ester in which the angle O-C-C is 111°, the ring oxygens and carbons are coplanar and the bond distances are as follows:

| | | |
|---|---|---|
| S - O | 1.64 Å. | (Single bond) |
| S = O | 1.42 | (Double bond) |
| C - O | 1.42 | |
| C - C | 1.52 | |
| C - H | 1.09 | |

However, the position of the sulfur atom relative to the assumed $^{O}\!\diagdown_{C - C}\!\diagup^{O}$

plane is not located definitely by the RDI. The peak at 2.95 Å. may correspond either to the sulfur-hydrogen distance in a model in which the ring system is entirely coplanar (B of Figure 1) or to the oxygen-carbon distance (through two angles) in a model in which the plane of O-S-O makes an angle of about 30° with that of O-C-C-O (C of Figure 1). The two theoretical intensity curves (B and C) were distinguishable only by an incipient doubling in the last maximum of curve A, the absence of which was felt to be confirmed upon reexamination of the photographs. The ring was assumed to be planar,* the C-H and S-H distances were fixed at 1.09 and 2.95 Å., respectively, and the ratios $\frac{C-C}{S=O}$ and $\frac{C-O}{S=O}$ were assumed to be $\frac{1.52}{1.42}$ and $\frac{1.42}{1.42}$, values which were in good agreement with the RDI peaks and with the results obtained for similar distances in other molecules.** The parameters S-O, ∠ C-C-O, and ∠ O-S=O were subjected to a systematic variation about the values indicated for them in the RDI. Some

---

* The author feels that this conclusion is somewhat uncertain since the region in which the difference occurs is low in intensity and difficult to interpret. In addition, there could probably be found a small change in some other parameter of the non-planar model which would bring the last feature back to coincidence with the visual curve without materially altering the rest of the curve. If non-planarity of the ring were proved, however, other results which are reported more definitely in this paper would not necessarily be invalidated, as the effect (on the other curves) of moving the sulfur atom out of the plane would undoubtedly be equally small.

** The value of 1.52 Å. is somewhat shorter than that usually accepted for the carbon-carbon bond distance. In order to account for the strength of the peak at 1.42 Å. in the RDI (compared to that at 1.63 Å.), it was necessary to take equal values for the S=O and C-O distances at 1.42 A., and to take a shorter distance for C-C than is usually found. It is of interest that in similar oxygen-containing compounds, the C-C distance may also be slightly short; viz., 1.51 ± 0.02 A. in diethyl ether,[11] 1.51 ± 0.03 A. in dioxane,[11] and 1.52 ± 0.02 A. in ethylene glycol.[12]

theoretical intensity functions are shown in Figure 1. Those based upon models in which ∠ O-C-C is 108° are characterized by too low an intensity in the region between q = 30 and q = 60 (D and E), whereas those based on models with ∠ O-C-C = 114° (I and J) are likewise unsatisfactory because of a common lack of prominence of the fourth maximum and also because of a doubled ninth minimum in place of the pronounced shelf which lies between the seventh maximum and the ninth minimum in the visual curve. A good fit to the visual curve is afforded by curve G, which corresponds to a model with S-O = 1.64 Å., ∠ C-C-O = 111°, and ∠ O-S=O = 106°.

In models corresponding to G, the previously fixed parameters were varied in turn by a small amount as described in the introduction to this section. The resultant curves are exemplified by K in which the C-C distance is increased by 0.01 Å. No material change may be noted. However, combined changes in these previously fixed parameters bring about variations in the theoretical intensity curves similar to those which occur as a result of changing the angle O-S=O, and to a lesser extent of changing the S-O distance. Consequently, upward revision of the error limits for these determined parameters was required.

An attempt was made to establish the rigidity of the O-S=O angles by assuming an entirely coplanar average structure in which the oxygen atom outside the ring vibrates symmetrically above and below the plane. This effect was simulated by applying appropriate temperature factors to the terms corresponding to distances which would be affected by such a vibration. It was concluded that though showing improvement in the relative width of the ninth and tenth maxima, these models are

outside the region of acceptability because of the incipient doubling of the eighth maximum in comparison with the seventh maximum and because of the shift in position of several of the main features. Similarly, models were calculated (A) in which the oxygen atom outside of the ring vibrates about the mean position assigned in Model G, in which the S=O bond makes an angle of 67° with its projection on the plane of the ring. Curve A is considered acceptable despite the disagreement with the visual curve in the last maximum; this discrepancy is not considered sufficient to rule out models of this type (see footnote page 74).

The values assigned to the structural parameters of ethylene glycol sulfite ester on the basis of this investigation and the probable limits of error are as follows:

| | | |
|---|---|---|
| C-H | 1.09 Å. | (assumed) |
| S-H* | 2.95 | |
| C-C* | 1.52 | (± 0.03 Å.) |
| C-O* | 1.42 | (± 0.02 Å.) |
| S=O* | 1.42 | (± 0.02 Å.) |
| S-O | 1.64 ± 0.05 Å. | |
| ∠ C-C-O | 111 ± 2° | |
| ∠ O-S O | 106 ± 3° | |

* These are the parameters fixed in the correlation procedure, the values for which are taken from the RDI. The quantities in parentheses are the variations of these distances within which the stated limits of error of the determined parameters hold.

The agreement between the intensity function for this model (which is based on a planar configuration of the ring) and the visual curve is shown (Table I) by a comparison of the positions of the main features. A non-planar ring structure is not definitely excluded.

Table I

Ethylene Glycol Sulfite Ester

| Min | Max | $q_{obs}$ | $q_G$ | $q_G/q_{obs}$ |
|---|---|---|---|---|
| 1 | | 7.77 | 7.3 | 0.940* |
| | 1 | 10.46 | 9.5 | 0.908* |
| 2 | | 13.59 | 12.0 | 0.883* |
| | 2 | 17.90 | 17.6 | 0.983 |
| 3 | | 22.96 | 22.8 | 0.993 |
| | 3 | 26.82 | 27.1 | 1.011 |
| 4 | | 31.40 | 31.3 | 0.997 |
| | 4 | 34.66 | 34.2 | 0.987 |
| 5 | | 38.50 | 38.4 | 0.997 |
| | 5 | 42.75 | 42.8 | 1.001 |
| 6 | | 46.92 | 46.9 | 1.000 |
| | 6 | 50.42 | 50.5 | 1.001 |
| 7 | | 54.50 | 54.7 | 1.004 |
| | 7 | 59.18 | 59.8 | 1.010 |
| 8 | | 66.49 | 66.8 | 1.005 |
| | 8 | ----- | ---- | ----- |
| 9 | | 69.76 | 70.6 | 1.012 |
| | 9 | 75.54 | 75.3 | 0.996 |
| 10 | | 82.26 | 80.8 | 0.981 |
| | 10 | 88.68 | 88.8 | 1.001 |
| 11 | | 95.44 | 95.3 | 0.998 |
| | | | Average (17 features) | 0.999 |
| | | | Average deviation | 0.007 |

* Not included in average

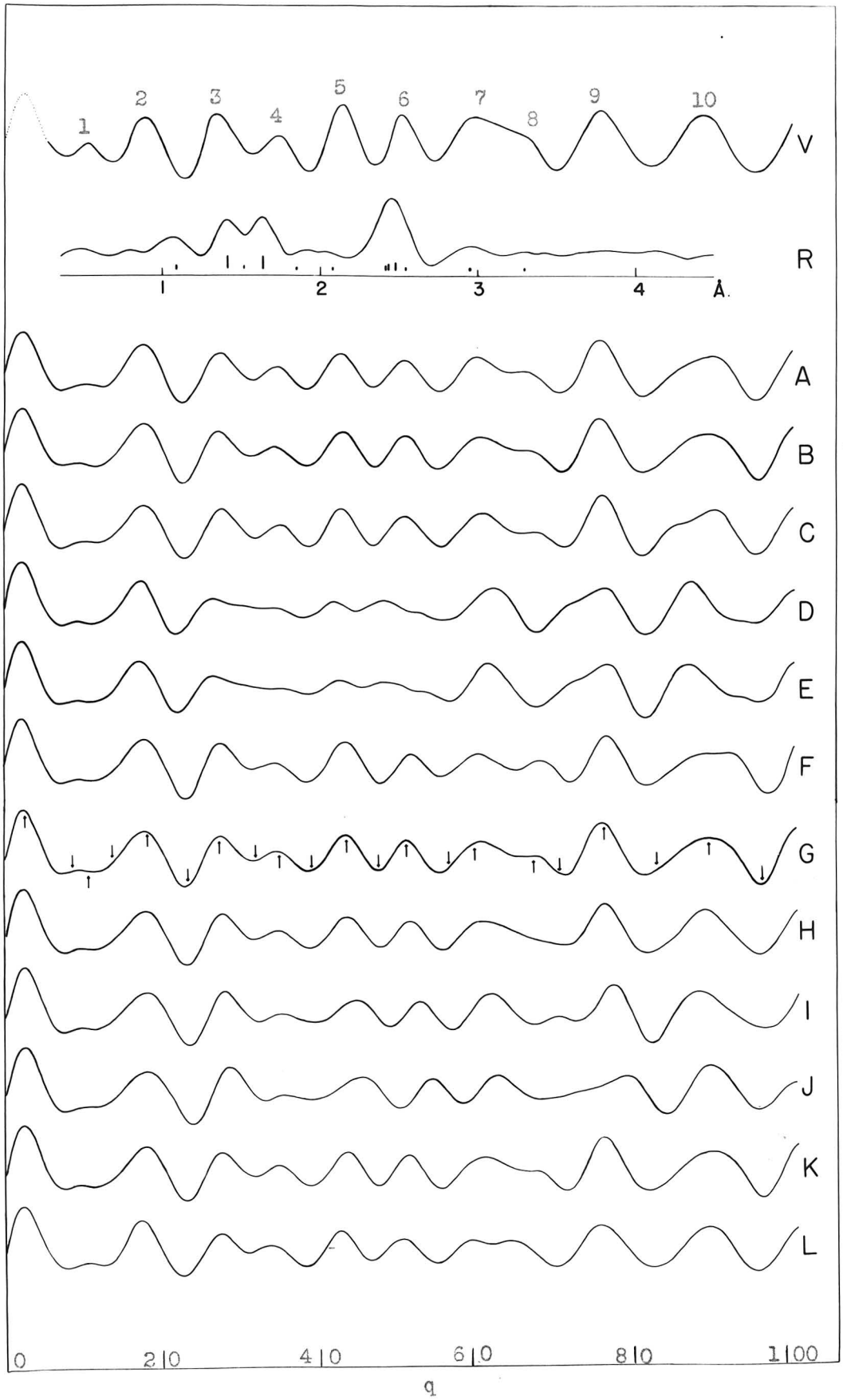


Figure 1: Electron Diffraction Curves for Ethylene Glycol Sulfite Ester

Table of Parameters (Figure 1)

Ethylene Glycol Sulfite Ester

| Model | S=O | S–O | C–C | ∠ C–C–O | ∠ O–S=O | ∠ C–O–S |
|---|---|---|---|---|---|---|
| | | Å. | | | | |
| A* | 1.41 | 1.64 | 1.52 | 111° | 106° | 108°30' |
| B | 1.41 | 1.64 | 1.52 | 111 | 106 | 108°30' |
| C | 1.41 | 1.64 | 1.52 | 108 | 106 | 102° |
| D | 1.42 | 1.67 | 1.52 | 108 | 103 | 108°30' |
| E | 1.42 | 1.67 | 1.52 | 108 | 106 | 108°30' |
| F | 1.42 | 1.61 | 1.52 | 111 | 106 | 108°30' |
| G | 1.42 | 1.64 | 1.52 | 111 | 106 | 108°30' |
| H | 1.42 | 1.64 | 1.52 | 111 | 109 | 108°30' |
| I | 1.42 | 1.64 | 1.52 | 114 | 106 | 108°30' |
| J | 1.42 | 1.61 | 1.52 | 114 | 109 | 108°30' |
| K | 1.42 | 1.64 | 1.53 | 111 | 106 | 108°30' |
| L | 1.42 | 1.64 | 1.52 | 111 | 106 | 129°30'** |

* Term in summation corresponding to non-bonded C---O distance at 3.28 Å. omitted.

** This is the mean position. The temperature factor $e^{-aq^2}$ with a 0.0003 was applied to the C---O distance at 3.86 Å.

All models

| | | |
|---|---|---|
| S=O | 1.42 Å. | (except A, B, and C) |
| C–O | 1.42 | |
| C–H | 1.09 | |
| S–H | 2.95 | |

ii - Ethylene Glycol Chlorophosphite Ester

The sample of ethylene glycol chlorophosphite ester used in this investigation was prepared by Mr. C. N. Scully by the action of phosphorus trichloride on ethylene glycol in methylene chloride solution.[7,8] The compound was purified by vacuum distillation and the fraction boiling at 42-43°/12 mm. was used in preparing electron diffraction photographs. The compound is of special interest because of the extremely high chemical activity of the chlorine atom. Hydrolysis occurs rapidly in water or in moist air with the evolution of hydrochloric acid; extensive decomposition of the pure material with the formation of a bright orange precipitate (probably phosphorus) was observable a few days after purification.

Diffraction photographs were taken at temperatures ranging from 20°C. to 100°C. with the use of a heated, glass nozzle designed by Dr. S. Claesson for high temperature work. In obtaining dense photographs, a beam-stop, designed by Mr. H. G. Pfeiffer, was placed between the jet and the film to reduce the background scattering. The jet-to-film distance was 10.93 cm. Features were observed at q values extending to about 105. The photographs were examined independently by this author and by four other investigators* and a visual curve (V of Figure 2) was drawn to represent the final compromise among these workers with respect to the interpretation of the diffraction pattern. The general agreement was good but some differences in the interpretation of fine structure in the pattern were registered by the various observers; e.g., in the prominence of the second and fifth maxima and in the extent of

---

* Dr. V. Schomaker, Dr. K. W. Hedberg, Mr. G. Guthrie, and Mr. H. G. Pfeiffer.

doubling in the ninth and eleventh maxima. In the assignment of limits of error by the correlation method, liberal allowance was made for these differences in interpretation. The finally chosen theoretical intensity curve satisfies all observers in that each of the features in contention is an acceptable compromise among the various observations.

The radial distribution function, R, is shown in Figure 2. Peaks are observed at 1.55, 2.11, 2.43 (diffuse), 2.85 and 3.20 Å. It is immediately striking that no maximum is observed at 1.76 Å., a position corresponding to the sum of the covalent bond radii of the atoms, for the P-O single-bond distance. The absence of this peak, coupled with the strength of the maximum at 1.54 Å., led to the conclusion that the P-O distance in the molecule is considerably shorter than might be predicted. An analysis of the first peak in the radial distribution curve (as a sum of Gaussian peaks of suitable area) indicated the following most probable interatomic distances in the molecule: C-O = 1.41 Å., C-C = 1.52 Å., P-O = 1.58 Å. The maximum at 2.11 Å. corresponds to the bonded P-Cl distance, which is considerably greater than 2.00-2.05 Å., observed for the P-Cl distance in $POCl_3$, $POF_2Cl$, $PSCl_3$, $PFCl_2$ and similar compounds. The diffuse peak at 2.43 Å. corresponds to the cross-ring distances (through one angle), P---C, O---O, and O---C, and the peaks at 2.85 and 3.20 Å. correspond respectively to the Cl---O and Cl----C distances. No geometrical model containing the indicated bond distances and a planar ring can be formulated which will satisfy the last three peaks in the RDI. For example, such a model with $\angle$ O-C-C = 107° gives reasonable agreement with the peak at 2.43 Å., but if the Cl---O distance be fixed at 2.85 Å., the Cl----C distance is found to be 3.67 Å., in severe disagreement with

3.20 Å. indicated in the RDI. The theoretical intensity function for this planar model, curve A, is shown in Figure 2. The general shape of the region comprising the first, second, and third maxima and minima is in severe disagreement with the visual curve.

An excellent fit to the RDI was afforded by a model in which the group $O_{C-C}^{O}$ was assumed planar with $\angle$ O-C-C = 107°. The position of the chlorine atom was fixed at a distance of 2.85 Å. from each oxygen and 3.20 Å., from each carbon. With the bond distances P-O = 1.58 Å. and P-Cl = 2.11 Å., the phosphorus is fixed in a position such that the plane of O-P-O makes an angle of about 30° with that of $O_{C-C}^{O}$.

For the correlation procedure, a number of assumptions were made: the ratios $\frac{C-C}{P-Cl}$ and $\frac{C-O}{P-Cl}$ were fixed at $\frac{1.52}{2.11}$ and $\frac{1.41}{2.11}$; the O-C-C angle was tentatively assigned a value of 107°. It is not to be inferred that the weak contribution of the C-C distance to the theoretical intensity curves is well-defined by the RDI, but since this term was of little significance in the summation and since the distance, 1.52 Å., in combination with the other bond distances as stated, resulted in the best fit to the first main peak in the RDI, this value was assumed to be best.

The remaining parameters were systematically varied as follows: $\angle$ C-O-P from 109 to 113°, $\angle$ O-P-Cl from 99 to 103°, and P-O from 1.55 to 1.64 Å. Equation (3) was used in all calculations except that resulting in curve JA. The non-bonded X. . .H distances were omitted in all except the finally accepted curve. Some representative theoretical intensity curves are shown in Figure 2. The effect on the curves of a variation in the P-O distance is shown by curves B, C, and D. In increasing the P-O distance, the main effects throughout are to strengthen the second maximum, to weaken the fifth maximum, to strengthen the feature which in

these curves occurs between the eighth and ninth maximum (but which in more acceptable curves occurs on the outside of the ninth maximum) and to decrease the doubling in the eleventh maximum. Curves with P-O as short as 1.55 Å. (B) invariably show an inacceptable reversal of the relative strength of the seventh and eighth maxima and of the corresponding minima. These discrepancies are corrected in curves with P-O = 1.58 Å. or somewhat greater. The sequence, curves C,E, and F exemplifies the effect of increasing the angle C-O-P from 109 to 111°. The result, in general, is to weaken the second maximum, to strengthen the fifth maximum, to move the doubling from the ninth minimum toward the ninth maximum, and from the eleventh maximum toward the eleventh minimum. The general effect of an increase in the angle O-P-Cl is exemplified by the sequence, curves G,H, and E. The second maximum is weakened, the fifth maximum becomes more prominent, and the feature which in curve G occurs as an asymmetry on the outside of the ninth maximum moves to the inside of the ninth minimum in curve E. The nature and the position of the eleventh maximum, which is strongly doubled in these curves, is altered somewhat by this variation, but apparently is not improved in comparison with the visual curve.

The theoretical intensity function which best combines the features of the curves described above corresponds to a model in which the P-O distance is 1.60 Å., and the angles C-O-P and O-P-Cl are 110° and 100°, respectively. This curve, I of Figure 2, compares well with the visual curve in many features. The nature of the region comprising the fifth and sixth maxima and minima is quite acceptable and the character

of the region between the sixth maximum and the eleventh minimum is very good in that the envelope covering the maxima and that covering the minima show respectively the concave upward and concave downward curvature which was finally agreed upon by all observers. A number of discrepancies, however, in comparison with the visual curve may still be noted. The second maximum appears to be too strong in comparison with the third, the seventh maximum is a trifle too strong compared to the sixth, the ninth maximum is too strongly doubled and the eleventh maximum appears to be too sharp. Definite improvement in all of these features is noted with the application of a temperature factor, $e^{-aq^2}$, to the term corresponding to the Cl-C distance (curve J). The value assigned to $\underline{a}$ is 0.0003 which corresponds to a distribution of distances about the mean in the form of a Gaussian curve with half-width equal to approximately 0.1 Å. An appreciably smaller value for $\underline{a}$ results in more doubling of the ninth maximum than we are willing to accept, whereas a larger value has no further noticeable effect on the curve.

The agreement of curve J with the visual curve is considered to be excellent. The ninth maximum was held to be a weak and indistinct feature, quite broad with perhaps a slight tendency toward doubling. The eleventh maximum was first drawn by this author to be strongly doubled much as shown in curve H, but after examination of three heavy pictures piled atop one another, it appears very likely that no such strong doubling exists, and that the eleventh maximum in curve J is an excellent representation of this feature. Other observers did not make a similar mistake in the interpretation of this feature. The second maximum in curve J is somewhat stronger in comparison with the first and third than had been drawn in the visual curve. Some improvement is noted in curve

JA in which the reduced intensity function, equation (1) was used instead of equation (3) to calculate the initial portion of the curve. Equation (1) is a closer approximation to the appearance of the photographs, especially in molecules containing atoms of widely differing atomic number. The shift in the second minimum in going from curve J to JA may be attributable to the use of a step function in approximating the dependence of f on q. The second maximum in curve JA is still somewhat stronger than is desirable but is acceptable for this difficultly interpretable region of the film.

During the course of the investigation, the effect of variations in the fixed parameters was investigated. Of the variations investigated, $\Delta(C\text{-}C) = 0.02$ Å., $\Delta(C\text{-}O) = 0.03$ Å. and $\Delta(\angle\ O\text{-}C\text{-}C) = 2^{\circ}$, the largest effect was shown by the last-named. Curve K corresponds to a model similar to that for curve G, but with the angle $O\text{-}C\text{-}C = 109^{\circ}$. Changes in these fixed parameters by the amounts indicated appear to be similar in effect on the curves to changes in the angles O-P-Cl and C-O-P of about $1/2^{\circ}$, and would appear to add this uncertainty to the determination of these parameters.

In the determination of the error limits, a good deal of weight was attached to the appearance of single features. The nature of the eleventh maximum is affected quite strongly by variations in the P-O distance, but not so strongly by changes in the angle parameters. Thus, from the correlation procedure alone, a limit of error of 0.02 Å. was assigned to the P-O distance. The eleventh maximum is certainly not so broad and doubled as is shown in curves with P-O = 1.58 Å., nor so sharp as is shown by curves with P-O = 1.64 Å. (L). Temperature factors improve this feature very little in these curves. A variation in the angles C-O-P and O-P-Cl have marked effects on several features: the fifth maximum,

the relative height of the seventh, eighth and ninth maxima, the shape of the ninth maximum, etc. A consideration of the relative changes brought about in these features have led to a limit of error of $2^{\circ}$ for each of the angle parameters C-O-P and O-P-Cl from the correlation procedure alone. A consideration of the average deviation of observed q values from those calculated and of the errors introduced by variations in the fixed parameters, led to the following structural parameters for ethylene glycol chlorophosphite ester:

| | |
|---|---|
| C-H | 1.09 Å. (assumed) |
| C-C | 1.52 ($\pm$ 0.02) Å.* |
| C-O | 1.41 ($\pm$ 0.03) Å.* |
| P-Cl | 2.11 ($\pm$ 0.02) Å.* |
| $\angle$ O-C-C | 107 ($\pm$ 2)$^{\circ}$ |
| P-O | 1.60 $\pm$ 0.04 Å. |
| $\angle$ C-O-P | 110 $\pm$ 2.5$^{\circ}$ |
| $\angle$ O-P-Cl | 100 $\pm$ 2.5$^{\circ}$** |

* These are the parameters fixed in the correlation procedure, the values for which are taken from the RDI. The quantities in parenthesis are the variations of these distances within which the stated limits of error of the determined parameters hold.

** The chlorine atom vibrates about this mean position such that the distribution of Cl-C distances is in the form of a Gaussian curve of half-width = 0.1 Å.

The positions of the main features of the visual curve are compared in Table II with those of curve J. There is good agreement with an average deviation of less than one percent.

Table II

Ethylene Glycol Chlorophosphite Ester

| Min | Max | $q_o$ | $q_J$ | $q_J/q_o$ | |
|---|---|---|---|---|---|
| 1 | | 6.47 | 6.4 | 0.989* | |
| | 1 | 9.48 | 9.5 | 1.002* | |
| 2 | | 11.58 | 11.7 | 1.010* | |
| | 2 | 15.04 | 15.4 | 1.024 | |
| 3 | | 17.15 | 17.5 | 1.020 | |
| | 3 | 19.67 | 20.0 | 1.017 | |
| 4 | | 24.16 | 24.2 | 1.002 | |
| | 4 | 29.39 | 29.1 | 0.990 | |
| 5 | | 35.34 | 34.9 | 0.988 | |
| | 5 | 37.72 | 37.5 | 0.994 | |
| 6 | | 40.21 | 39.9 | 0.992 | |
| | 6 | 43.05 | 42.5 | 0.987 | |
| 7 | | 47.31 | 47.2 | 0.998 | |
| | 7 | 50.98 | 51.1 | 1.002 | |
| 8 | | 54.98 | 55.0 | 1.000 | |
| | 8 | 58.56 | 58.6 | 1.001 | |
| 9 | | 62.75 | 62.4 | 0.994 | |
| | 9 | 66.64 | 66.1 | 0.992 | |
| 10 | | 73.84 | 73.8 | 0.999 | |
| | 10 | 78.11 | 78.1 | 1.000 | |
| 11 | | 83.21 | 82.9 | 0.996 | |
| | 11 | 88.97 | 89.3 | 1.004 | (center of gravity) |
| 12 | | 95.64 | 95.7 | 1.001 | |
| | 12 | 99.26 | 99.4 | 1.001 | |
| 13 | | 103.12 | 102.2 | 0.991 | |
| | 13 | 105.97 | 106.0 | 1.000 | |
| | | | Average (23 features) | 0.999 | |
| | | | Average deviation | 0.007 | |

* Not included in the average

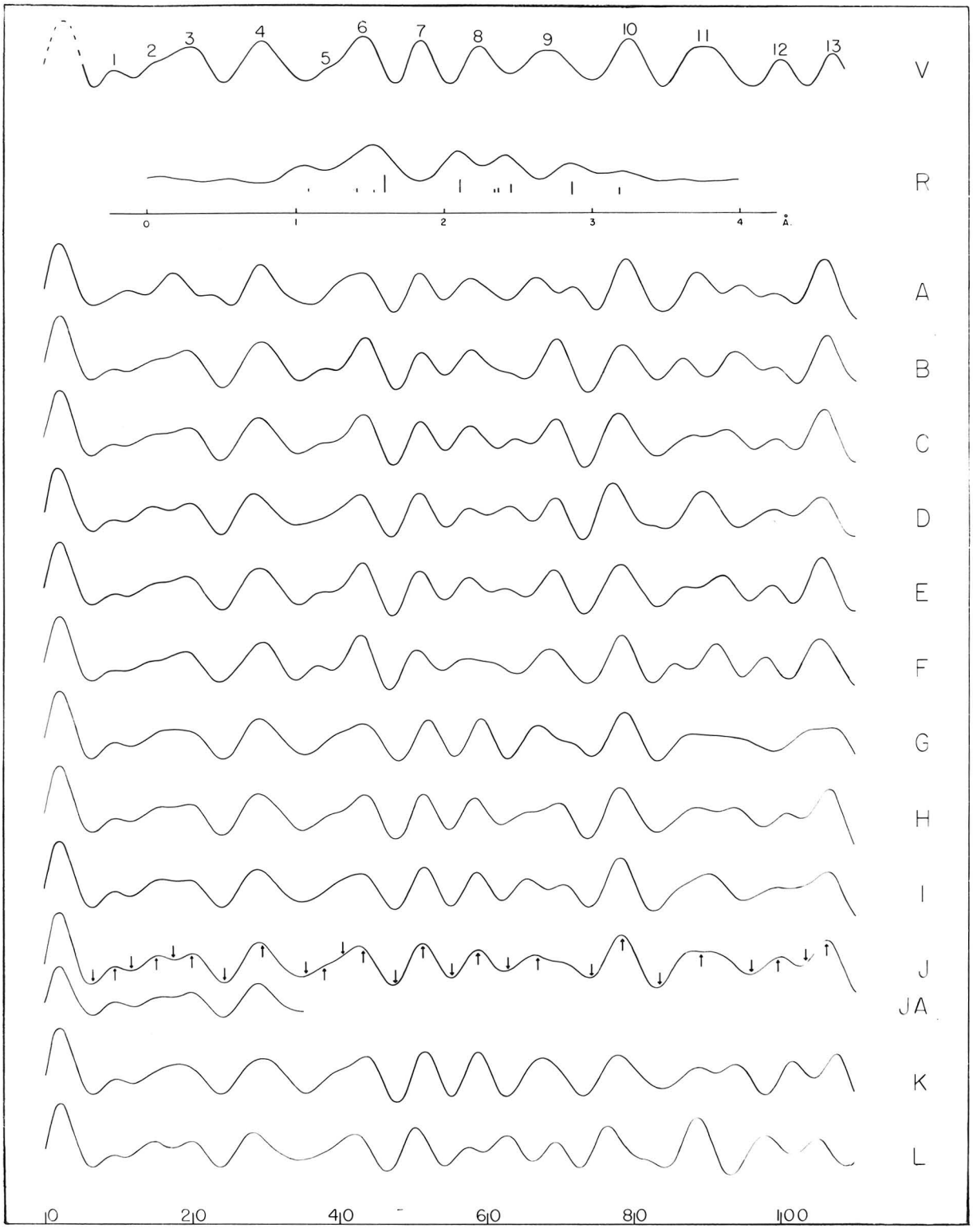


Figure 2: Electron Diffraction Curves for Ethylene Glycol Chlorophosphite Ester

Table of Parameters (Figure 2)

Ethylene Glycol Chlorophosphite Ester

| Model | P-O | ∠ O-P-Cl | ∠ C-O-P |
|---|---|---|---|
| A | 1.58 | 101° | 116° |
| B | 1.55 | 103 | 109 |
| C | 1.58 | 103 | 109 |
| D | 1.61 | 103 | 109 |
| E | 1.58 | 103 | 110 |
| F | 1.58 | 103 | 111 |
| G | 1.58 | 99 | 110 |
| H | 1.58 | 101 | 110 |
| I | 1.60 | 100 | 110 |
| J*† | 1.60 | 100 | 110 |
| JA*‡ | 1.60 | 100 | 110 |
| K | 1.58 | 99 | 110 |
| L | 1.64 | 103 | 110 |

All models

| | | |
|---|---|---|
| C-C | 1.52 Å. | |
| C-O | 1.41 | |
| P-Cl | 2.11 | (except model K in which P-Cl = 2.13 Å.) |
| ∠ C-C-O | 107° | |
| C-H | 109 | |

* The non-bonded hydrogen distances have been omitted from all theoretical intensity calculations except J and JA

† Temperature factor, $e^{-aq^2}$, applied to Cl-C distance (a = 0.0003)

‡ Model JA is similar to J except that the theoretical intensity function is calculated according to equation (1).

iii - Ethylene Glycol Acetal

The sample of ethylene glycol acetal used in this investigation was prepared by Mrs. G. Guthrie in an original two-step synthesis.[9] Di-n-amyl acetal was first prepared by the action of n-amyl alcohol on paraldehyde in the presence of dry hydrogen chloride gas. After purification, the di-n-amyl acetal was treated with ethylene glycol in the presence of p-toluenesulfonic acid. An exchange of the alkyl groups resulted with the formation of ethylene glycol acetal (b.p. = 82.5°C.) and the regeneration of amyl alcohol.

Electron diffraction photographs were taken at room temperature. The gas was admitted to the chamber through the standard low-temperature nozzle which, in one series of experiments, was equipped with a beam-stop. The jet-to-film distance was 10.95 cm. Features were observed on the photographs at q values extending to about 100. The visual curve, V, is shown in Figure 3.

Ethylene glycol acetal is a homologue of ethylenemethylene dioxide, the structure of which was determined by Dr. W. Shand.[11] He chose, as the best structure for his compound, a model in which the ratio $\frac{C-O}{C-C}$ is $\frac{1.42}{1.54}$ and the ring is coplanar with the angle O-C-C = 105°37'. However, the theoretical intensity curve corresponding to this model deviates markedly from his visual curve in two important features. I believe that this model is not the correct one for the structure of ethylenemethylene dioxide.

The estimated visual curves of ethylenemethylene dioxide and of ethylene glycol acetal show a great similarity which is borne out by a comparison of the diffraction photographs of the two compounds. The

region comprising the sixth and seventh maxima is broad and somewhat doubled and appears to be definitely weaker than the following eighth maximum as drawn by this author and by Dr. Shand. The general aspect of this region is denied by the model chosen by Shand.

The visual curve, V, and the radial distribution integral, R, of ethylene glycol acetal are shown in Figure 3. In the RDI, peaks were observed at 1.13, 1.44, 2.03, 2.30, 2.80, 3.18, and 3.60 Å., the last being quite diffuse. A good approximation to the maximum at 1.44 Å. was calculated from Gaussian curves representing C-O and C-C distances of 1.43 and 1.53 Å. respectively. The peak at 2.30 Å. is sharp, symmetrical, and of theoretical half-width, from which it may be inferred that the C--C, O--O, and O--C distances through one angle are all very close to this value.

An examination of the peak at 1.44 Å. in the RDI and a consideration of the structure determination of ethylenemethylene dioxide led to the conclusion that an attempt to resolve the two C-C or the two C-O distances would be futile. In the correlation procedure, it was deemed more profitable to determine the bond angles in the molecule than to attempt a redetermination of C-C and C-O distances for which the values indicated are in good agreement with those found by Shand[11] in similar compounds.* The

---

* Ethylenemethylene dioxide: C-C = 1.54 ± 0.05 Å.; C-O = 1.42 ± 0.03 Å.; all angles = 108°; probably planar.

Trimethylene oxide: C-C = 1.54 ± 0.03 Å.; C-O = 1.46 ± 0.03 Å.; ∠ C-C-C = ∠ C-C-O = 88.5 ± 3°; ∠ C-O-C = 94.5 ± 3°; probably planar within 15-20°.

1,4-Dioxane: C-C = 1.51 ± 0.04 Å.; C-O = 1.44 ± 0.03 Å.; ∠ C-O-C = 112 ± 5°; ∠ O-C-C = 109½ ± 5°; "chair" form.

1,3,5-Trioxane: C-O = 1.42 ± 0.03 Å.; ∠ C-O-C = ∠ O-C-O = 112 ± 3°; "chair" form.

ratio $\frac{C-C}{C-O}$ was held constant at $\frac{1.53}{1.43}$. The angle O-C-C in the ring was varied from 104° to 108°, the angle C-O-C from 105° to 109°, and the angle O-C-C' (C' is the carbon atom not contained in the ring) from 100 to 104°. Within the region of variation is found a smaller region of geometrically impossible models which, of course, could not be calculated. The calculation of theoretical intensity curves was carried out with the use of equation (3). A number of representative theoretical intensity curves are shown in Figure 3. In all except the finally accepted curve, non-bonded X. . .H terms were omitted from the summation. Curves A, B, and C correspond to models in which the five-membered ring is planar, with the ring angle, O-C-C, equal to 104, 106, and 108° respectively. Of these, only B, which is similar to Shand's chosen model of ethylenemethylene dioxide, is considered acceptable. A and C are inacceptable beyond q = 50. Of the models containing a non-planar five-membered ring, three types may be considered depending on the position of the carbon atom, C', relative to the two glycol carbon atoms in the ring. Curve D represents the "chair" form, and curve E the "cradle" form, in each of which the group $O_{C-C}^{O}$ is planar; curve F represents the "staggered ring" form, in which one of the glycol carbon atoms is above, and the other is below, the plane of O-C-O, and the projection of the C-C' bond bisects the angle O-C-O. The distances in each of these models are in reasonable agreement with the RDI. Curve E, corresponding to the "cradle" form, is in excellent qualitative agreement with the visual curve. The curves D and F are considered to be unacceptable because of the strong doubling of the sixth and seventh maxima. It is highly probable, however,

that acceptable models of the "chair" and staggered ring" form could be found. In the remainder of the correlation procedure, only models corresponding to the "cradle form" were considered. A number of these are shown (G, H, I, J, K). The acceptability of these curves, in general, had to be decided by the nature of the region comprising the sixth, seventh, and eighth maxima and minima.

An attempt to resolve the two different C-O distances in the molecule served to justify the original assumption that a definite result could not be obtained. The average of the C-O distances was determined to be 1.43 ± 0.03 Å., but a change of 0.05 Å. in the individual distances (holding the average constant) resulted in curves which were considered still acceptable. The application of a temperature factor to the term corresponding to the C---C distance at 2.84 Å., apparently does not change curve E by an appreciable amount in any feature. This may be inferred from curve M in which this term is omitted completely. The sixth and seventh maxima remain acceptable and the ninth maximum is weakened such that it approximates more closely the visual curve; this, however, occurs in a difficultly interpretable region of the film and is not considered significant.

A comparison of the positions of the main features in the visual curves with those in curve E is made in Table III. The structural parameters for ethylene glycol acetal are as follows:

| | |
|---|---|
| C-H | 1.09 Å. (assumed) |
| C-C (individual) | 1.53 (assumed) |
| C-O (individual) | 1.43 ± 0.05 A. |
| C-O (average) | 1.43 ± 0.03 A. |
| ∠ C-C-O | 106 ± 4° |
| ∠ C'-C-O | 101.5 ± 4° |
| ∠ C-O-C | 106.5 ± 4° |

Table III

Ethylene Glycol Acetal

| Min | Max | $q_o$ | $q_E$ | $q_E/q_o$ |
|---|---|---|---|---|
| 1 | | 8.26 | 7.5 | 0.908* |
| | 1 | 11.71 | 11.0 | 0.939* |
| 2 | | 14.83 | 14.1 | 0.951* |
| | 2 | 19.17 | 19.2 | 1.002 |
| 3 | | 24.55 | 24.4 | 0.994 |
| | 3 | 28.94 | 29.1 | 1.006 |
| 4 | | 32.87 | 33.9 | 1.031** |
| | 4 | 36.58 | 36.8 | 1.006 |
| 5 | | 40.86 | 40.3 | 0.986** |
| | 5 | 45.42 | 44.9 | 0.989 |
| 6 | | 49.75 | 50.1 | 1.007 |
| | 6 | 54.19 | 55.0 | 1.015** |
| 7 | | 58.41 | 57.8 | 0.990 |
| | 7 | 62.01 | 61.6 | 0.993** |
| 8 | | 66.89 | 66.9 | 1.000 |
| | 8 | 71.88 | 71.7 | 0.997 |
| 9 | | 76.80 | 76.2 | 0.992 |
| | 9 | 80.43 | 79.9 | 0.993 |
| 10 | | 84.02 | 83.4 | 0.993 |
| | 10 | 88.40 | 88.0 | 0.995 |
| 11 | | 93.62 | 93.3 | 0.997 |
| | 11 | 99.05 | 98.2 | 0.991 |
| | | | Average (19 features) | 0.998 |
| | | | Average deviation | 0.007 |

* Not included in the average

** In computing the average and average deviation, these quantities were given half weight since the measurements of $q_o$ were subject to errors introduced by the St. John effect.

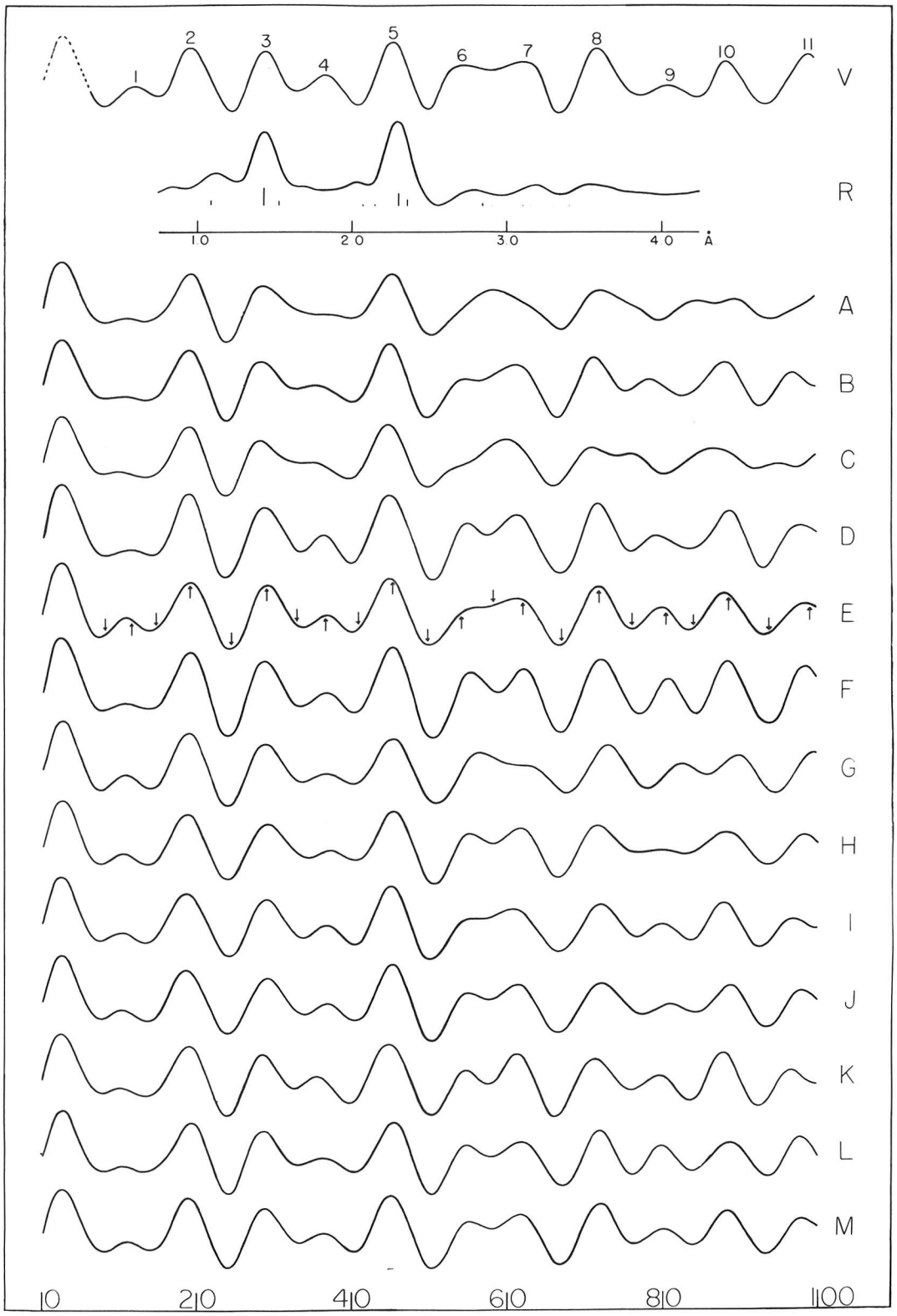


Figure 3: Electron Diffraction Curves for Ethylene Glycol Acetal

Table of Parameters (Figure 3)

Ethylene Glycol Acetal

| Model* | ∠ O-C-C | ∠ O-C-C' | ∠ C-O-C |
|---|---|---|---|
| A | 104° | 115° | 100° |
| B | 106 | 110 | 102 |
| C | 108 | 104 | 104 |
| D | 105°37' | 101°44' | 106°52' |
| E | 105°37' | 101°44' | 106°52' |
| F | 105°37' | 101°44' | 106°52' |
| G | 104 | 100 | 105 |
| H | 104 | 104 | 107 |
| I | 104 | 104 | 109 |
| J | 106 | 100 | 107 |
| K | 106 | 104 | 109 |
| L | 106 | 102 | 107 |
| M | 105°37' | 101°44' | 106°52' |

All models

| | | |
|---|---|---|
| C-O | 1.43 Å. | (except model M)** |
| C-C | 1.53 | |
| C-H | 1.09 | |

* The non-bonded hydrogen terms are omitted from all models except model E, in which all terms are included, calculated and temperature-factored as described in the introduction.

** In model M, the bonded C-O distances in the group $O_{C-C}^{O}$ are 1.40 Å., and in the group $O^{C}_{O}$ are 1.46 Å.

## DISCUSSION

The molecules of ethylene glycol sulfite ester, ethylene glycol chlorophosphite ester and ethylene glycol acetal have been found to contain several interatomic distances which are appreciably different from those which might have been predicted from a consideration of the covalent radii of the atoms. The most striking discrepancies are observed in the structure of the chlorophosphite ester. The value for the P-O bond distance, obtained in the present work, is 1.60 Å., considerably shorter than the theoretical distance for a normal covalent single-bond, calculated either from the covalent radii suggested by Pauling[13,14] (1.76 Å) or from the Schomaker-Stevenson relationship[15] (1.71 Å.). Indeed, the value 1.60 Å. just corresponds to one-half covalent double-bond character for each P-O distance, calculated from the Pauling radii and the Pauling formula for percent double-bond character. In addition, the P-Cl bond distance, 2.11 Å., in this molecule is significantly greater than that which is predicted from the same sources (2.09 Å. and 2.01 Å., respectively). According to theories of resonance, after Pauling,[16] the interpretation of these apparent anomalies may be made in terms of ionic or double-bonded structures which, in contributing to the state of the molecule, would be expected to affect the distances in a way indicated by the experimental results. Several possible structures are written below. In each of these, the adjacent charge rule and the octet rule for first row elements are satisfied. Structure (I) is a classical representation of a molecule in which normal covalent single-bond distances would be exhibited. If a structure of the type (II),

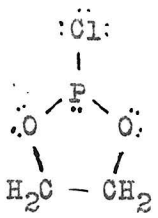

(I)

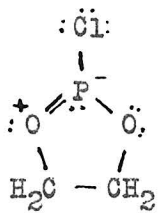

(II)

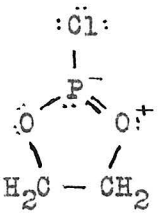

(IIa)

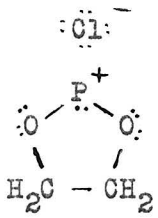

(III)

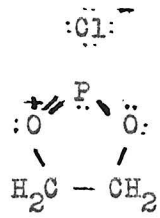

(IV)

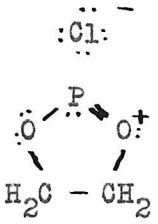

(IVa)

resonating with its equivalent, (IIa), completely described the state of the molecule, the P-O bond would have one-half double-bond character but the P-Cl bond would only be lengthened by about 0.05 Å. from the normal covalent distance.[15] This could not completely account for the discrepancies, especially since the unfavorable distribution of charge between the phosphorus and the oxygen atoms makes it unlikely that this structure would contribute to so great an extent to the state of the molecule. (III) would be expected to shorten the P-O bond distance by only 0.03 Å. Structure (IV), resonating with (IVa), might reasonably account for the observed structure of the molecule. In (IV) and (IVa), the coulomb attraction of unlike charges would be expected to be very weak in contrast to a normal $X\ Y^-$ ionic bond; in addition, since the

electronic configuration about the phosphorus in (IV) is different from that in (I), an extra van der Waals' repulsion between the electrons of $Cl^-$ and the unshared pair on the phosphorus may well account for the increase in the interatomic distance. The postulation of ionic character for the chlorine atom is in line with the high chemical activity observed in the molecule. Furthermore, if the molar refractivity of the chlorophosphite ester by compared with that of, say, the methoxyphosphite ester, 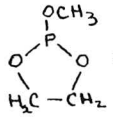 , which might be expected to exhibit a normal covalent structure analogous to (I), one observes an exaltation of refractivity in the chlorophosphite ester corresponding to approximately one-third of a double-bond.* This may or may not constitute evidence in favor of structures (IV) and (IVa) since the validity of the additivity rule for second row elements has not definitely been shown. However, Mitchell[7] has shown that, for phosphorus in a large number of compounds of the type discussed here, the additivity rule is quite reliable.

It may also be pointed out that an effect analogous to that reported here has been observed in nitrosyl chloride. In this compound, the N-O and N-Cl distances are 1.12 and 1.98 Å., respectively, instead of the calculated values 1.21 and 1.69 Å. This has been explained[18] by

---

* Mitchell[7] has carried out this calculation as follows: Assuming the average values for the atomic refractivity of carbon, hydrogen, and oxygen[17] and assuming the additivity of the atomic refractivity to yield the molar refractivity, values of the atomic refractivity of phosphorus were calculated from the experimental value for the methoxyphosphite ester and several of its homologues. Using an average of these values for phosphorus (the deviations being small), and using an average value for chlorine,[17] the molar refractivity of the chlorophosphite ester was calculated. The observed value deviated from the calculated value as indicated in the text.

resonance between the normal covalent structure, $:\ddot{\underset{\cdot\cdot}{Cl}}-\ddot{N}=\ddot{O}:$, and the ionic structure $:\ddot{\underset{\cdot\cdot}{Cl}}:^{-}\ :N\equiv O:^{+}$. The situation is similar in nitrosyl bromide.

The major difficulty in the proposal of structures (IV) and (IVa) is that the experimental results require that these contibute almost completely to the state of the molecule to the exclusion of any appreciable quantity of (I), which should represent a state of energy equal to or lower than that of (IV). One might be tempted to formulate structures which show two double-bonds or a triple-bond in the ring; these, however, are extremely unsatisfactory with respect to the distribution of charge. Consequently, for an interpretation of the results in terms of multiple and/or ionic bonds, one is forced to accept resonance between (IV) and (IVa) with perhaps a small contribution from (I) as representing the structure of the molecule. It may, of course, be that, as set forth by Pitzer[19] in a recent article and by others, the postulation of multiple bonds for other than first row elements is unjustified, but this language does present a plausible basis for the interpretation of many apparently anomalous results.

It should perhaps be pointed out that a number of anomalous P-O and P-Cl distances have previously been reported. In $P_4O_6$,[20] $P_4O_{10}$,[20] and $P_4O_6S_4$,[21] the "single-bond" P-O distances have the values 1.65, 1.62, and 1.61 Å., respectively. These correspond to something less than 50% double-bond character in the bond but, contrary to the statement of Hampson and Stosick, the distances cannot be satisfactorily explained on the basis of ionic or multiple-bond structures. In $PCl_5$, which has the form of a trigonal bipyramid, the two P-Cl bonds which are directed along

the three-fold axis of the molecule are 2.12 Å. in length. However, it is very probable that this is not analogous to the present work, since in $PCl_5$, the chlorine atoms suffer severe steric interactions, with those farthest from the central phosphorus atoms having the greater number of close Cl. . .Cl interactions. In ethylene glycol sulfite ester, the single-bond S-O distance has been determined to be 1.64 Å., significantly shorter than that predicted from the Pauling covalent radii or from the Schomaker-Stevenson modification (1.70 and 1.69 Å., respectively). In terms of multiple bonds the discrepancy corresponds to approximately 12 percent double-bond character in each S-O bond. No anomaly is necessarily indicated here, since structures of the type (V), resonating with (Va) may reasonably be written. Contributions from these will satisfactorily

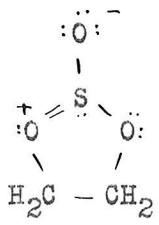

(V)

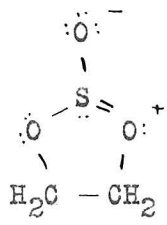

(Va)

account for the observations. The only value for a single-bond S-O distance that has previously been reported is that found by Westrink and MacGillavry[22] for the $\gamma$-modification of $(SO_3)_3$. Their value of 1.60 Å. is in more serious disagreement with predicted values than is the present work. However, no great precision is claimed for the atomic positions.

It is of interest that the C-C distance in each of the molecules appears to be slightly shorter than that usually found. This is in agreement with values for this distance in ethylene glycol, diethyl ether, and dioxane (see footnote, p. 92). These discrepancies found in the present work cannot, however, be considered significant since the limits of error of these distances have been assumed rather than determined.

## SUMMARY

A determination of the molecular structure of three compounds, ethylene glycol sulfite ester, ethylene glycol chlorophosphite ester, and ethylene glycol acetal has been carried out. In each compound, the minimum symmetry $C_s$-m and a planar configuration of the group $O_{C-C}^{O}$ was assumed. In the sulfite ester, the assumption of a planar ring led to a reasonable structure in good agreement with the data, although non-planar structures could not be excluded. The symmetry $C_{2v}$-Pmm was ruled out, but vibration of the O-S=O angle about the position finally assigned could not be proved or disproved. In the chlorophosphite ester, the ring is definitely non-planar; the plane of $O^{P}O$ makes an angle of about 30° with that of $O_{C-C}^{O}$. In the acetal, the favored structure contained a non-planar ring, but a range of planar ring models falls within the region of acceptability. In the three molecules, a number of anomalous distances are found and an interpretation of these apparent anomalies is discussed in terms of multiple and ionic bonds. The structural parameters of the three molecules are as follows:

Ethylene glycol sulfite ester

| | |
|---|---|
| C-H | 1.09 Å. (assumed) |
| S-H | 2.95 * |
| C-C | 1.52 ( ± 0.03) Å.* |
| C-O | 1.42 ( ± 0.02) * |
| S=O | 1.42 ( ± 0.02) * |
| S-O | 1.64 ± 0.05 Å. |
| ∠ C-C-O | 111 ± 3° |
| ∠ O-S O | 106 ± 3° |

Ethylene glycol chlorophosphite ester

| | |
|---|---|
| C-H | 1.09 Å. (assumed) |
| C-C | 1.52 ( ± 0.02) Å.* |
| C-O | 1.41 ( ± 0.03) * |
| P-Cl | 2.11 ( ± 0.02) * |
| ∠ O-C-C | 107 ( ± 2)° * |
| P-O | 1.60 ± 0.04 Å. |
| ∠ C-O-P | 110 ± 2.5° |
| ∠ O-P-Cl | 100 ± 2.5° |

The chlorine atom vibrates about its mean position such that the distribution of Cl---C distance is in the form of a Gaussian curve of half-width = 0.1 Å.

Ethylene glycol acetal

| | |
|---|---|
| C-H | 1.09 Å. (assumed) |
| C-C (individual) | 1.53 (assumed) |
| C-O (individual) | 1.43 ± 0.05 Å. |
| C-O (average) | 1.43 ± 0.05 |
| ∠ C-C-O | 106 ± 4° |
| ∠ C'-C-O | 101.5 ± 4° |
| ∠ C-O-C | 106.5 ± 4° |

C' is the carbon atom outside of the ring

* In these structure determinations, an attempt was made to estimate the additional errors brought into the investigation by the assumption of certain parameters in the molecules. The starred parameters are those fixed in the correlation procedure; the values were taken from the RDI. The quantities in parentheses are the variations of these distances within which the stated limits of error of the determined parameters hold.

ii Naphthalene and Anthracene

The stability and the characteristic aromatic properties of both naphthalene and anthracene have suggested the formulation of resonating structures for these compounds similar to those proposed by Kekulé for benzene. In benzene, the contribution of equivalent structures, whether they be of the Kekulé, the Dewar or the Claus-Armstrong-Baeyer type, results in complete six-fold symmetry in the molecule. In naphthalene, however, resonance between the nearly equivalent structures of lowest energy, (VI), (VII), (VIII), should result in a molecule in which the bonds have differing amounts of double-bond character (IX). The length of a C-C bond with 1/3 double-bond character should be, after Pauling,[18] 1.42 Å.; that of a bond with 2/3 double-bond character should be 1.37 Å. Similarly, in anthracene, resonance among the structures

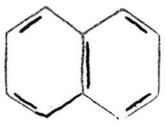

(VI)

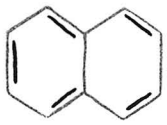

(VII)

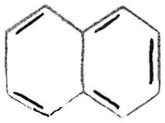

(VIII)

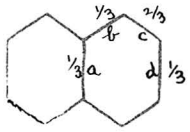


(IX)

(X), (XI), (XII) and (XIII), which are nearly equivalent and lowest in energy, should result in bonds with double-bond character as in (XIV).

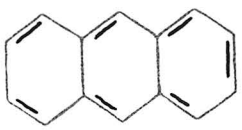

(X)

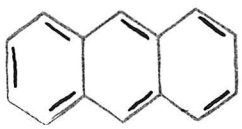

(XI)

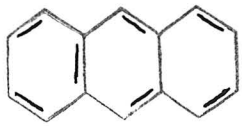

(XII)

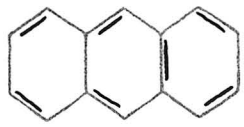

(XIII)

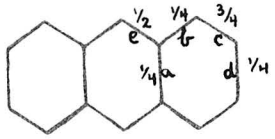


(XIV)

The lengths of C-C bonds with 1/4, 1/2, and 3/4 double-bond character should be 1.44, 1.39, and 1.355 Å. respectively.

A number of other treatments, inspired by quantum mechanics, have been given to the structure of naphthalene. In addition to the calculation by Pauling, which is outlined above, predictions of interatomic bond distances have been made by Lennard-Jones and Turkevich,[23] by Coulson,[24] by Penney[25] and by Brockway, Beach and Pauling.[26] The results of these calculations are summarized in Table IV. The bonds are designated a, b, c, and d as depicted in (IX) above.

Table IV

Theoretical Bond Lengths in Naphthalene

| | a | b | c | d | reference |
|---|---|---|---|---|---|
| $P_1$ [i] | 1.42 | 1.42 | 1.39 | 1.42 | 20 |
| $P_2$ [ii] | 1.40 | 1.44 | 1.39 | 1.42 | 26 |
| $C_1$ [iii] | 1.44 | 1.40 | 1.39 | 1.40 | 24 |
| $C_2$ [iv] | 1.42 | 1.41 | 1.38 | 1.40 | 24 |
| L-J [v] | 1.37 | 1.39 | 1.37 | 1.39 | 23 |
| Py [vi] | 1.42 | 1.40 | 1.38 | 1.40 | 25 |

i From consideration of double-bond character in each bond for equal contributions of (VI), (VII), and (VIII) (Pauling)

ii From Sherman's wave function[27] considering contributions of 42 possible structures (Brockway, Beach and Pauling)

iii From empirical consideration of bond interaction (Coulson)

iv From a valence-bond treatment of resonance (Coulson)

v From a molecular-orbital treatment (Lennard-Jones and Turkevich)

vi From a valence-bond treatment of resonance (Penney)

Theoretical treatments of the anthracene molecule have not been as numerous nor, in general, have the results been as precisely stated as was the case for naphthalene. The results of numerical calculations by Pauling and coworkers[18,26] and by Michailov[28] are summarized in Table V. The bonds are designated a, b, c, d, and e as depicted in (XIV) above.

Table V

Theoretical Bond Lengths in Anthracene

| | a | b | c | d | e | reference |
|---|---|---|---|---|---|---|
| $P_1$[i] | 1.44 | 1.44 | 1.355 | 1.44 | 1.39 | 18 |
| $P_2$[ii] | 1.474 | 1.453 | 1.395 | 1.446 | 1.425 | 26 |
| M[iii] | 1.44 | 1.416 | 1.375 | 1.41 | 1.396 | 28 |

i From consideration of double-bond character in each bond for equal contributions of (X), (XI), (XII), and (XIII) (Pauling)

ii From Sherman's wave function[27] (Brockway, Beach and Pauling) (by Michailov)

iii From a valence-bond treatment of resonance, after Penney[25] (Michailov)

Determinations of the structures of crystalline naphthalene[29] and anthracene[30] have been made by Robertson. The molecules were reported to be planar, with atoms at the corners of regular hexagons. The C-C bond distances were reported to be equal and, in each molecule, to have the length 1.41 Å. Pauling[26] has noted small deviations from regularity in Robertson's Fourier projection of the naphthalene molecule and has interpreted these to indicate that the carbon-carbon distances are not truly equal.

An electron diffraction investigation of the structure of naphthalene was carried out by Specchia,[31] but only an average value, 1.397 Å. was arrived at for the C-C bond distances.

The present work, a determination of the structures of naphthalene and anthracene in the gas phase, is a completion of an investigation begun in 1941 by Dr. Jurg Waser, who prepared electron diffraction photographs of the two compounds and calculated a number of theoretical curves for naphthalene. The large number of parameters which were to be determined in each molecule necessitated a procedure somewhat different from that which is usually followed in electron diffraction investigations. The distances reported by Robertson in naphthalene and anthracene were, for each case, in reasonable agreement with the peaks in the radial distribution function. Theoretical intensity functions which were calculated from these models, however, were not in full agreement with the visual curve. The parameters of the $D_{2h}$ model were varied individually about the values assigned in the Robertson model, which was used as a standard for comparison. From a consideration of the effects of each of these parameter variations on the theoretical intensity curves, it was possible to suggest a model, the intensity function for which would be in best agreement (in the range investigated) with experimental observations.

The estimation of limits of error for the individual parameters in naphthalene and anthracene is almost impossibly difficult, since the treatment of each problem by a systematic correlation procedure is not feasible. Consequently, I have attempted only to estimate the limits of error for the average bond distance, to determine the model which, in the

region of parameter space considered, appears to result in the best possible agreement with experimental observations, and to indicate the parameter variations to which the theoretical intensity functions are most sensitive.

In the parameter range investigated, the variations in the qualitative aspect of the theoretical curves are quite small; as a result, much of the comparison of these curves with the visual observations was made on the basis of the relative positions of the features. Indeed, the final choice of a favored model was based upon these considerations.

i Naphthalene

The electron diffraction photographs were taken by Dr. Waser with the use of the standard high-temperature nozzle. The jet-to-film distance was 10.91 cm. Features were observed at q values extending to about 100.

The visual curve, V, for naphthalene and the radial distribution function, R, are shown in Figure 4. Peaks are observed at 1.39, 2.20, 2.43, 2.78, 3.08, 3.73, and 4.20 Å. These distances are in reasonable agreement with the Robertson model. Some theoretical intensity functions for molecular models of symmetry $D_{2h}$ are also shown in Figure 4. The Robertson model (Curve A) is seen to be acceptable within the limits of experimental error. Similar models, with angles different from 120° become unsatisfactory (B and C) in the region of the tenth and eleventh maxima and also in the relative positions of many of the main features. The shift in these positions is much larger than that brought about by a change of 0.03 Å. in any bond distance. No combination of such changes

has been found which brings curves B and C back to coincidence with the observations. Consequently, it may be that the allowable variation in the angle is as little as $2^{\circ}$, although a precise statement cannot be made from this examination of a comparatively small number of curves.

A comparison of the relative positions of the main features in curves B-E and G-L with the visual curve led to the suggestion of a model, corresponding to curve F, which, in the range of parameters considered, best represents the appearance of the photographs. Curve F, after adjustment of the size parameter, corresponds to the following model:

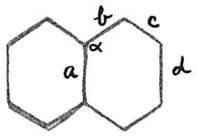


a $1.42_4$ Å.
b $1.40_4$
c $1.38_4$
d $1.40_4$
$\angle \alpha$ $120^{\circ}$

A conclusion concerning the average bond distance in naphthalene was reached in the following manner: for each of a large number of models (in the region of parameter space under consideration), the average bond distance was multiplied by the $\overline{q/q_o}$ for the corresponding theoretical intensity curve. The mean of the resultant set of numbers was taken as the average bond distance. The maximum deviation from the mean was taken as the probable limit of error. The value finally arrived at was $1.39_7 \pm 0.02$ Å.

Of the individual parameters, the angle $\alpha$ appears to be most precisely determinable by the electron diffraction method. The precision

in the individual bond distances, as might have been predicted from the relative effect of displacing the various atoms in the molecule, appears to be in the order b > c > d > a.

A number of errors in the interpretation of the photographs appear to have been made. The height of the fifth maximum was thought to be greater than that of the sixth, and the strength of the tenth maximum was overestimated. From reexamination of the photographs with particular reference to these features, it was estimated that curve F is a better representation of the photographs in these regions than is the visual curve. These errors are probably not serious since all theoretical intensity curves which were considered are similar in the particular aspects which were misinterpreted.

A comparison between the positions of the main features in the selected model, which is just Penney's (see Table IV, Py), it happens, and in Robertson's model with those in the visual curve is made in Table VI.

Table VI

Naphthalene

| Min | Max | $q_o$ | $q_F$ | $q_F/q_o$ | $q_A$ | $q_A/q_o$ |
|---|---|---|---|---|---|---|
| 1 | | 7.67 | 7.68 | (1.001)* | 7.60 | (0.990)* |
| | 1 | 10.08 | 10.04 | (0.996)* | 10.08 | (1.000)* |
| 2 | | 13.98 | 13.84 | 0.990 | 13.92 | 0.995 |
| | 2 | 17.70 | 18.12 | 1.023 | 17.84 | 1.008 |
| 3 | | 23.74 | 23.76 | 1.001 | 23.44 | 0.987 |
| | 3 | ----- | ----- | ----- | ----- | ----- |
| 4 | | ----- | ----- | ----- | ----- | ----- |
| | 4 | 28.96 | 29.60 | 1.022 | 29.44 | 1.017 |
| 5 | | 31.34 | 31.60 | 1.008 | 31.20 | 0.995 |
| | 5 | 33.92 | 34.12 | 1.006 | 34.24 | 1.009 |
| 6 | | 41.04 | 40.92 | 0.997 | 40.00 | 0.975 |
| | 6 | 44.12 | 44.40 | 1.006 | 44.40 | 1.006 |
| 7 | | 47.40 | 47.40 | 1.000 | 47.68 | 1.006 |
| | 7 | 49.24 | 49.96 | 1.015 | 50.40 | 1.024 |
| 8 | | 51.30 | 51.50 | 1.004 | 51.45 | 1.003 |
| | 8 | 53.63 | 53.96 | 1.006 | 53.73 | 1.002 |
| 9 | | 56.00 | 55.44 | 0.990 | 55.28 | 0.987 |
| | 9 | 59.52 | 60.04 | 1.009 | 59.84 | 1.005 |
| 10 | | 63.84 | 64.48 | 1.010 | 64.56 | 1.011 |
| | 10 | 66.72 | 67.36 | 1.010 | 67.28 | 1.008 |
| 11 | | 70.08 | 70.12 | 1.001 | 69.84 | 0.997 |
| | 11 | 72.88 | 72.80 | 0.999 | 72.48 | 0.995 |
| 12 | | 74.45 | 74.60 | 1.003 | 73.76 | 0.992 |
| | 12 | 75.76 | 76.44 | 1.009 | 76.32 | 1.007 |
| 13 | | 80.32 | 80.76 | 1.005 | 80.80 | 1.006 |
| | 13 | 82.80 | 82.40 | 0.995 | 83.44 | 1.008 |
| 14 | | 84.80 | 85.08 | 1.003 | 84.64 | 0.998 |
| | 14 | 87.84 | 87.88 | 1.000 | 87.72 | 0.996 |
| 15 | | 90.56 | 90.28 | 0.997 | 90.08 | 0.993 |
| | 15 | 93.60 | 92.92 | 0.993 | 92.32 | 0.986 |
| | | Average | | 1.004 | | 1.000 |
| | | Average deviation | | 0.008 | | 0.009 |

* Not included in the average

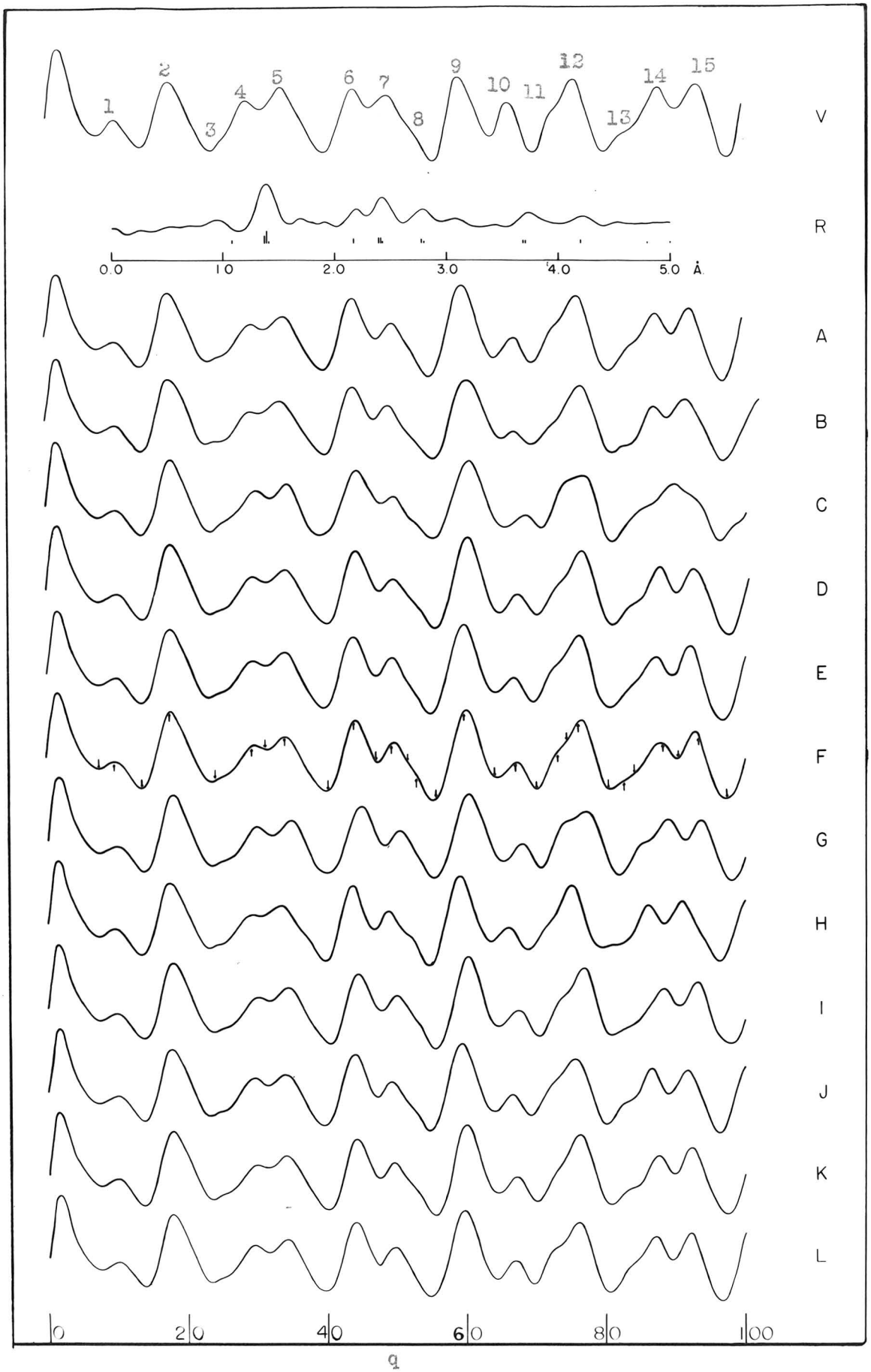


Figure 4: Electron Diffraction Curves for Naphthalene

Table of Parameters (Figure 4)

Naphthalene

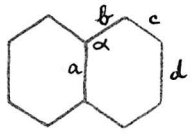


| Model | a | b | c | d | ∠α |
|---|---|---|---|---|---|
| A | 1.40 | 1.40 | 1.40 | 1.40 | 120 |
| B | 1.40 | 1.40 | 1.40 | 1.40 | 118 |
| C | 1.40 | 1.40 | 1.40 | 1.40 | 122 |
| D | 1.36 | 1.40 | 1.40 | 1.40 | 120 |
| E | 1.44 | 1.40 | 1.40 | 1.40 | 120 |
| F | 1.42 | 1.40 | 1.38 | 1.40 | 120 |
| G | 1.40 | 1.44 | 1.40 | 1.40 | 120 |
| H | 1.40 | 1.40 | 1.36 | 1.40 | 120 |
| I | 1.40 | 1.40 | 1.44 | 1.40 | 120 |
| J | 1.40 | 1.40 | 1.40 | 1.36 | 120 |
| K | 1.40 | 1.40 | 1.40 | 1.44 | 120 |
| L | 1.40 | 1.36 | 1.40 | 1.40 | 120 |

All models planar with symmetry $D_{2h}$

ii Anthracene

The electron diffraction photographs were taken by Dr. Waser under conditions similar to those in which pictures of naphthalene were prepared. The jet-to-film distances were 10.91 cm. and 20.25 cm.; pictures at the longer camera distance were taken to aid in the estimation of fine structure in the intensity pattern at small q values.

The visual curve, V, is shown in Figure 5. Peaks in the radial distribution function, R, are observed at 1.09, 1.41, 2.17, 2.42, 2.83, 3.37, 3.70, 4.19, and 4.98 Å. Beyond 5.5 Å., no significant peaks appeared in the RDI. The procedure followed in applying the correlation method was similar to that outlined in the introduction to part III b and to that used in determining the structure of naphthalene. The parameters of the $D_{2h}$ model, a, b, c, d, e, $\alpha$ and $\beta$ (as shown below), were varied individually about the values assigned in the Robertson model, A of Figure 5, which was used as a standard for comparison.

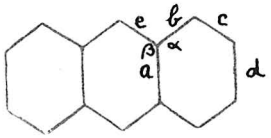


The attempt to determine individual bond distances in anthracene was of no avail. The differences in the theoretical intensity curves shown in Figure 5 are, for the most part, too small to permit one model to be chosen over other models on the basis of qualitative comparison. The best model was chosen on the basis of a comparison of the positions of the main features with those in the visual curve. Variations in the distances a or d (curve H, I, J, K) bring about such small changes in the intensity functions that extremely wide limits of error must be assigned to these

distances. On the other hand, an increase in either the distance b or e (curves G and O) brings about similar variations in the positions of the main features so that only an average of these two distances may be stated.

The Pauling model of anthracene (curve P), described in the introduction to this section, is considered to be within the acceptable region. The diffuse nature of the next-to-last maximum, the reversed asymmetry in the last minimum and the general disagreement in the positions of these features occur in a region in which the visual curve must be considered uncertain. Consequently, in the absence of more serious disagreement, curve P is considered acceptable. By comparison with the visual curve, G is best in agreement with observed data, the average deviation of $q_{calc}/q_{obs}$ being 0.007. Average deviations of $q_{calc}/q_{obs}$ for curves A, M, and O are 0.009, 0.009, and 0.010 respectively. Curve G, after adjustment of the size parameter, corresponds to the following model:

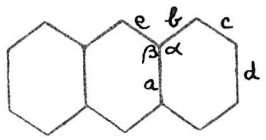


a $1.41_7$ Å.

b $1.43_7$

c $1.41_7$

d $1.41_7$

e $1.43_7$

$\angle\alpha$ 120°

$\angle\beta$ 120°

The average bond distance, determined as in naphthalene from a consideration of the $\overline{q/q_o}$ for each of a large number of curves, was found to be $1.41_9 \pm 0.02$ Å.

The most precisely determinable parameters in anthracene appear to be the angles $\alpha$ and $\beta$ ; these, however, can probably not be estimated with as much certainty as can the angle in naphthalene. The statement of the bond distances b, c, and e, is probably more precise than that of a and d, but less so than that of the angles $\alpha$ and $\beta$ . The quantitative changes in theoretical intensity curves brought about by variations in the distances b and e are such that their average is probably more precisely determinable than are the individual distances.

It should be pointed out that several distances in model G are in disagreement with their respective peaks in the RDI, although curve G is in good agreement with the visual curve. No explanation for the anomaly is offered.

A comparison of the positions of the main features in curve G with those in the visual curve is shown in Table VII.

Table VII

Anthracene

| Min | Max | $q_o$ | $q_G$ | $q_G/q_o$ |
|---|---|---|---|---|
| 1 | | 7.91 | 7.65 | 0.967 |
| | 1 | 10.30 | 10.20 | 0.990 |
| 2 | | 14.00 | 14.00 | 0.998 |
| | 2 | 16.85 | 17.30 | 1.027 |
| 3 | | 23.60 | 23.70 | 1.004 |
| | 3 | ----- | ----- | ----- |
| 4 | | ----- | ----- | ----- |
| | 4 | 28.72 | 28.60 | 0.996 |
| 5 | | 31.38 | 30.75 | 0.980 |
| | 5 | 34.34 | 33.25 | 0.968 |
| 6 | | 40.32 | 39.70 | 0.985 |
| | 6 | 43.44 | 43.40 | 0.999 |
| 7 | | 46.94 | 47.05 | 1.002 |
| | 7 | 49.73 | 49.40 | 0.993 |
| 8 | | 51.61 | 51.25 | 0.993 |
| | 8 | 53.63 | 53.25 | 0.993 |
| 9 | | 54.96 | 54.25 | 0.996 |
| | 9 | 59.13 | 58.95 | 0.997 |
| 10 | | 63.43 | 63.45 | 1.000 |
| | 10 | 65.54 | 65.60 | 1.001 |
| 11 | | 68.30 | 68.65 | 1.005 |
| | 11 | 71.39 | 71.00 | 0.995 |
| 12 | | 73.22 | 72.60 | 0.992 |
| | 12 | 75.42 | 74.60 | 0.989 |
| 13 | | 78.97 | 79.30 | 1.004 |
| | 13 | 82.04 | 81.60 | 0.995 |
| 14 | | 83.70 | 82.85 | 0.990 |
| | 14 | 85.08 | 85.80 | 1.008 |
| 15 | | 88.38 | 88.00 | 0.996 |
| | 15 | 90.74 | 90.30 | 0.995 |
| 16 | | 96.41 | 95.90 | 0.995 |

| | |
|---|---|
| Average | 0.995 |
| Average deviation | 0.007 |

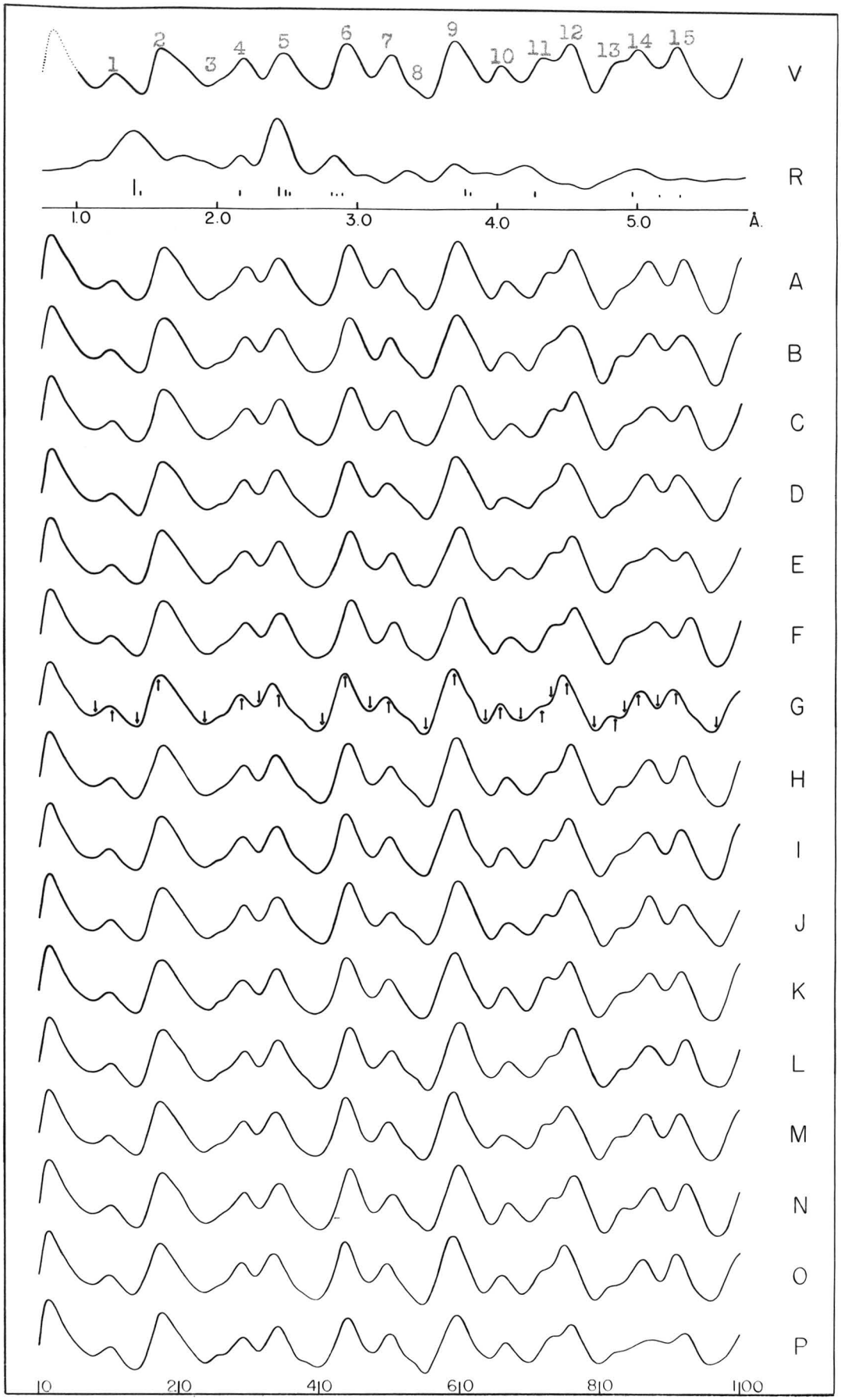


Figure 5: Electron Diffraction Curves for Anthracene

Table of Parameters (Figure 5)

Anthracene

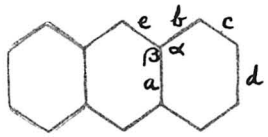


| Model | a | b | c | d | e | ∠α | ∠β |
|---|---|---|---|---|---|---|---|
| A | 1.41 | 1.41 | 1.41 | 1.41 | 1.41 | 120 | 120 |
| B | 1.41 | 1.41 | 1.41 | 1.41 | 1.41 | 120 | 118 |
| C | 1.41 | 1.41 | 1.41 | 1.41 | 1.41 | 120 | 122 |
| D | 1.41 | 1.41 | 1.41 | 1.41 | 1.41 | 118 | 120 |
| E | 1.41 | 1.41 | 1.41 | 1.41 | 1.41 | 122 | 120 |
| F | 1.41 | 1.41 | 1.41 | 1.41 | 1.37 | 120 | 120 |
| G | 1.41 | 1.41 | 1.41 | 1.41 | 1.45 | 120 | 120 |
| H | 1.41 | 1.41 | 1.41 | 1.37 | 1.41 | 120 | 120 |
| I | 1.41 | 1.41 | 1.41 | 1.45 | 1.41 | 120 | 120 |
| J | 1.37 | 1.41 | 1.41 | 1.41 | 1.41 | 120 | 120 |
| K | 1.45 | 1.41 | 1.41 | 1.41 | 1.41 | 120 | 120 |
| L | 1.41 | 1.41 | 1.37 | 1.41 | 1.41 | 120 | 120 |
| M | 1.41 | 1.41 | 1.45 | 1.41 | 1.41 | 120 | 120 |
| N | 1.41 | 1.37 | 1.41 | 1.41 | 1.41 | 120 | 120 |
| O | 1.41 | 1.45 | 1.41 | 1.41 | 1.41 | 120 | 120 |
| P | 1.44 | 1.44 | 1.355 | 1.44 | 1.39 | 120 | 120 |

All models planar with symmetry $D_{2h}$

## SUMMARY

The molecular structures of naphthalene and of anthracene have been determined by the electron diffraction method. The assumption of a planar structure with a molecular symmetry $D_{2h}$ leads to models in excellent agreement with the observed intensity function. The individual C-C bond distances could not be determined with a desirable degree of accuracy, but the average bond distance was determined within very narrow limits. The models which, in the regions investigated, were favored as being in best agreement with the visual observations were as follows:

Naphthalene

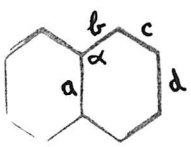


a $1.42_4$ Å.

b $1.40_4$

c $1.38_4$

d $1.40_4$

$\angle \alpha$ 120°

Average bond distance $1.39_7 \pm 0.02$ Å.

Anthracene

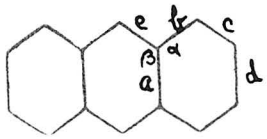


a $1.41_7$ Å.

b $1.43_7$

c $1.41_7$

d $1.41_7$

e $1.43_7$

$\angle \alpha$ 120°

$\angle \beta$ 120°

Average bond distance $1.41_9 \pm 0.02$ Å.

## REFERENCES


1. L. O. Brockway, Rev. Mod. Phys. 8, 231 (1936)
2. L. Pauling and L. O. Brockway, J.A.C.S. 59, 2181 (1937)
3. R. Spurr and V. Schomaker, J.A.C.S. 64, 2693 (1942)
4. L. Pauling and L. O. Brockway, J. Ch. Phys. 2, 867 (1934)
5. P. A. Shaffer, Jr., V. Schomaker and L. Pauling, J. Ch. Phys. 14, 659 (1946)
6. R. Majima and H. Simanuki, Prco. Imp. Acad. (Japan) 2, 544 (1926)
7. H. J. Lucas, F. W. Mitchell and C. N. Scully (to be published)
8. C. N. Scully, M. S. Thesis, Calif. Inst. of Tech. (1947)
9. M. Guthrie, B. A. Thesis, Reed College (1948)
10. C. S. Lu and E. W. Malmberg, Rev. Sci. Instr. 14, 271 (1943)
11. W. Shand, Jr., Ph.D. Thesis, Calif. Inst. of Tech. (1947)
12. J. Donohue, Ph.D. Thesis, Calif. Inst. of Tech. (1947)
13. L. Pauling and M. L. Huggins, Z. Krist. 87, 205 (1935)
14. L. Pauling and L. O. Brockway, J.A.C.S. 59, 1223 (1937)
15. V. Schomaker and D. P. Stevenson, J.A.C.S. 63, 37 (1941)
16. L. Pauling, The Nature of the Chemical Bond, Second Edition, Cornell University Press, Ithaca, N.Y. (1940), Chap. V.
17. Smiles, The Relation Between Chemical Constitution and Some Physical Properties, Longman, Green and Co., London (1910)
18. Reference 16, Chap. VIII
19. K. S. Pitzer, J.A.C.S. 70, 2140 (1948)
20. G. C. Hampson and A. J. Stosick, J.A.C.S. 60, 1814 (1938)
21. A. J. Stosick, J.A.C.S. 61, 1130 (1939)
22. Westrink and MacGillavry, Rec. trav. chim. 60, 794 (1941)
23. J. E. Lennard-Jones and J. Turkevich, Prov. Roy. Soc. (London) A158, 280 (1937)

24. C. A. Coulson, J. Ch. Phys. 7, 1069 (1939)

25. W. G. Penney, Proc. Roy. Soc. (London) A158, 306 (1937)

26. L. O. Brockway, J. Y. Beach and L. Pauling, J.A.C.S. 57, 2705 (1935)

27. J. Sherman, J. Ch. Phys. 2, 488 (1934)

28. B. Michailov, Acta Physicochimica U.R.S.S. XXI, 387 (1946)

29. J. M. Robertson, Proc. Roy. Soc. (London) A125, 542 (1929)

30. J. M. Robertson, Proc. Roy. Soc. (London) A140, 79 (1938)

31. G. Specchia, Nuovo Cimento XVIII, 102 (1941)

Propositions Submitted by Bertram Keilin

Ph.D. Oral Examination, November 23, 1949, 1:00 P.M., Crellin Conference Room

Committee: Professors V. Schomaker (Chairman), C. D. Anderson, R. M. Badger, S. J. Bates, C. Niemann, J. G. Kirkwood, and L. Pauling

1. a) The molecular structure of selenium tetrachloride in the gas phase has been reported by Lister and Sutton.[1] Prof. V. Schomaker has pointed out that at equilibrium selenium tetrachloride vapor is completely dissociated into $SeCl_2$ and $Cl_2$,[2] that the diffraction photographs obtained by Lister and Sutton may have been of such a mixture, and that their reported data, indeed, agree more fully with a $SeCl_2 + Cl_2$ model than with any of their $SeCl_4$ models. It would be interesting to compare photographs taken of an equilibrium mixture of gas with those taken of a flowing gas. The former would be obtained in the usual way from an equilibrium gas mixture, the latter, which might possibly be characteristic of a transient $SeCl_4$ gas species, would be obtained by allowing the vapor from $SeCl_4$ crystals to pass continuously across the path of the electron beam. The excess gas in the chamber should not prove troublesome in causing secondary scattering of the electrons since it will be expected to condense rapidly on the walls.

b) The structure of $SeCl_2$ may be determined in a diffraction experiment from the vapor over $Se_2Cl_2$.[3]

1. Lister and Sutton, Trans. Far. Soc., 37, 393 (1941)
2. Yost and Kircher, J.A.C.S., 52, 4680 (1930)
3. Wehrli, Helv. Phys. Acta, 9, 329 (1936)

2. The planar model favored by Shand[4] as representing the structure of ethylene-methylene dioxide results in a theoretical intensity curve which is in severe disagreement with his data (obtained from electron diffraction

TABLE OF CONTENTS

ACKNOWLEDGEMENT

I wish to express my sincere and warm appreciation for the aid, the guidance and the encouragement afforded to me by Professor Verner Schomaker in all phases of the work described in this thesis.

I wish also to thank Professor Linus Pauling and Dr. Robert B. Corey for their direction of this work in the absence of Professor Schomaker.

I am indebted to Mrs. G. Guthrie, Mr. C.N. Scully and Mr. H. Garner for the preparation and purification of the various derivatives of ethylene glycol which were investigated in Part III of this thesis.

I am grateful to my colleagues Mr. G. Guthrie, Mr. K. Hedberg, and Mr. H.G. Pfeiffer for their aid in preparing photographs and for many helpful discussions in the field of electron diffraction.

The work described in Part II of this thesis was carried out with the collaboration of Dr. John W. Otvos, who has never failed to afford me good advice and good friendship.

## ABSTRACT

Part I. The Adsorption of Capillary-Active Materials at the Dropping Mercury Electrode

It has been found that the addition of a capillary-active substance to a solution which is to be analyzed at the dropping mercury electrode brings about a decrease in the diffusion current which passes as a result of the discharge of the reducible ion. Molecules of the capillary-active compound, adsorbed on the surface of the growing drop, appear to deactivate a portion of this electrode surface. As a result, some of the reducible ions or molecules which reach the electrode vicinity by diffusion do not actually reach the electrode surface, and the current which passes as a result of the reduction is consequently decreased. As the concentration of capillary-active material is increased, the diffusion current decreases to a limiting value which is apparently dependent upon the amount of surface still left free on the electrode after a monomolecular layer of material has been adsorbed. Experimental verification and theoretical consequences of the foregoing are described in Part I of this thesis.

Part II. The Polarographic Analysis of Nitrite and of Nitrite-Nitrate Mixtures

It has been found that a solution containing both nitrate and nitrite ions can be analyzed for both constituents in two polarographic experiments. With one aliquot part, the diffusion current due to the two constituents in the original solution is measured. In another aliquot part, the nitrite present is quantitatively oxidized to nitrate and the diffusion current of the resulting solution is measured as before. The two experiments provide sufficient data for determining the quantity of each ion in the solution. The oxidation of nitrite is conveniently carried out with hydrogen peroxide in acid solution and the excess peroxide is destroyed catalytically by manganese dioxide in basic solution.

Part III. An Electron Diffraction Investigation of the Structure of Some Organic Molecules

a) Some Cyclic Derivatives of Ethylene Glycol

The results of an electron diffraction investigation of some cyclic derivatives of ethylene glycol (chlorophosphite ester, sulfite ester, and acetal) confirm the configuration assigned by the organic chemist to these molecules. Non-planarity of the five-membered ring may be demonstrated only in the chlorophosphite ester, in which also there is found an abnormally long phosphorus-to-chlorine bond distance and a subnormally short phosphorus-to-oxygen bond distance. The covalent bond distances in the other molecules were shown to be normal but no conclusion could be drawn concerning the planarity or non-planarity of the ring systems.

b) Naphthalene and Anthracene

In an electron diffraction investigation of naphthalene, the average carbon-to-carbon bond distance has been found to be $1.39_7 \pm 0.02$ Å. The limits of error cannot be narrowed sufficiently to permit a definite choice to be made among the theoretical models proposed by various workers, but the configuration suggested by Penney and Coulson appears to be in best agreement with the observations.

In anthracene, the mean carbon-to-carbon bond distance has been found to be $1.41_9 \pm 0.02$ Å. Although no statement of the limits of error for the individual distances could be made, it was concluded that

the best model in the region investigated is different than that proposed by Robertson, in which the atoms lie at the corners of regular hexagons.

# PART I

## The Adsorption of Capillary-Active Substances at the Dropping Mercury Electrode

# THE ADSORPTION OF CAPILLARY-ACTIVE SUBSTANCES AT THE DROPPING MERCURY ELECTRODE

The polarographic method of analysis was invented by Jaroslav Heyrovsky[1] in 1922, when, at the suggestion of Professor G. Kucera, he attempted to explain some anomalous inflections in the electrocapillary curve of mercury in electrolyte solutions containing reducible substances. The method of analysis is based upon the interpretation of the current-voltage (c.-v.) curve which is obtained when a dilute solution of a reducible or an oxidizable substance is electrolyzed in a cell in which one electrode consists of mercury falling dropwise from a fine-bore capillary tube. The value of the polarographic method lies in its suitability for a simultaneous qualitative and quantitative analysis of very dilute solutions ($10^{-6}$ to $10^{-2}$ molar).

As the potential applied to a dropping mercury electrode dipped into a solution of a reducible substance is made more negative, a sharp rise in the current passing between the electrodes is observed at a voltage approximately corresponding to the equilibrium reduction potential of the material in solution. The current gradually approaches a limiting value, and finally becomes constant and almost independent of further increase in the applied electromotive force. In the presence of a comparatively large concentration of a non-reducible electrolyte (which is used to render negligible the transference number of a reducible ion) and with all other factors constant, the limiting current is a function

of the concentration of the electroreducible substance. The limiting current is due to a virtually complete state of concentration polarization at the dropping electrode. The reaction which takes place at the electrode surface brings about a decrease in the concentration of the reducible substance in the immediate vicinity, and a radial concentration gradient is set up between the electrode and the body of the solution. Diffusion of the reducible substance to the electrode is controlled by this gradient and reaches a limit when the concentration at the electrode surface is effectively zero at all times. With an excess of some indifferent salt (a "supporting electrolyte") present in the solution, the effect of migration (induced by the electric field gradient in the solution) in aiding the approach of the reducible substance to the electrode is negligible and the limiting current is determined almost entirely by the rate of diffusion; hence, it is called a "diffusion current." The potential of the dropping electrode (with respect to an external reference electrode) at that point in the c.-v. curve at which the diffusion current is one-half of its limiting value is characteristic, for reversible electrode reactions, of the particular substance which is being reduced, and is independent of the concentration. This voltage is termed the "half-wave potential."

A quantitative description of diffusion to a growing spherical electrode was first given by Ilkovic[2] in 1934. MacGillavry and Rideal[3] later succeeded in carrying out a more rigorous derivation of the Ilkovic equation, but with an identical result. The fundamental equation relating the average diffusion current, $i_d$, (observed at the

dropping mercury electrode) to the concentration, C, of the reducible substance is

$$i_d = KnD^{1/2}Cm^{2/3}t^{1/6}, \qquad (1)$$

where K is a dimensional constant depending on the units employed in the description of the various quantities, n is the number of faradays of electricity required per mole of the electrode reaction, D is the diffusion coefficient of the reducible substance in the given medium, m is the rate of flow of mercury from the dropping electrode and t is the drop time. The proportionality, under a given set of conditions, between the diffusion current and the concentration of a reducible substance is valid only up to concentrations of the order of $10^{-2}$M. In less dilute solutions, the current which passes is limited by the saturation of the electrode surface; that is, the electrode surface is not large enough to accommodate all of the reducible material which may approach it by diffusion.

The shape of the polarographic wave (c.-v. curve) is determined by the nature of the reaction which takes place at the electrode. For a reversible electrode reaction in an efficiently buffered solution, in which the concentration of the products is effectively zero at all times, the relation between the instantaneous current and the applied voltage is given by

$$E_{d.e.} = E_{1/2} - \frac{0.059}{n} \log \frac{i}{i_d - i}, \qquad (2)$$

where i is the instantaneous current passing to the electrode under the applied potential, $E_{d.e.}$, $i_d$ is the limiting diffusion current and $E_{1/2}$

is the half-wave potential.[4]

The current-voltage curves do not always exhibit the ideal shape described above. In the polarographic analysis of certain molecules or ions, one of the general characteristics of the c.-v. curve is the pronounced maximum which occurs unless special measures are taken to suppress it. The maximum is perfectly reproducible[5] and usually independent of the direction in which the applied electromotive force is changed. As the applied voltage is increased, this feature of the curve always begins at a point approximately corresponding to the toe of the normal c.-v. curve and is characterized by a linear increase in current until a maximum is reached. The shape of the maximum may vary, for different substances, from a sharp, almost discontinuous peak, to a well-rounded hump followed by a more or less rapid decrease to approximately the expected value of the diffusion current, as predicted from the Ilkovic equation.

Many attempts have been made to explain the nature and the origin of the polarographic maximum. Heyrovsky[6] and Ilkovic[7] attributed the phenomenon to the adsorption of the reducible substance at the surface of the drop, whereby the concentration of reducible substance in the immediate electrode area is increased above that in the body of the solution and normal concentration polarization is prevented. This theory has been strongly opposed by Antweiler and von Stackelberg[8,9] who interpret maxima as an electrokinetic effect. These workers, and also Frumkin and his coworkers,[10,11,12] have shown conclusively that there is a pronounced streaming of the liquid around the mercury drop

at that stage in the reduction at which a maximum occurs in the c.-v. curve. Although many attempts have been made to explain the polarographic maximum, none of them has thus far been accepted as a completely satisfactory explanation of the phenomenon; all, including the two mentioned above, appear to meet with serious theoretical difficulties.

Early in the development of the polarographic method of analysis, it was discovered that maxima could be suppressed by the addition to the solution of small traces of certain capillary-active ions (or molecules) or of various non-capillary-active ions or charged colloids. According to Heyrovsky,[5] the Hardy-Schultze rule, with some exceptions, has been found to hold for the suppression of maxima by non-capillary-active substances. For the most part, investigators, interested mainly in practical polarographic analysis, have treated the phenomenon as a nuisance, to be eliminated in whatever way possible. The small effect on the limiting current which sometimes occurred as a result of the addition of capillary-active substances to the solution was ignored, especially since incomplete data on diffusion coefficients often render predictions of the diffusion currents from the Ilkovic equation uncertain, and accurate polarographic analysis is, for the most part, empirical. In the few cases in which the effect was large, attempted explanations were short, scanty, and highly unsatisfactory.

Although the phenomenon of maximum suppression was early associated with the adsorption of molecules at the dropping electrode, the steric hindrance and concomitant deactivation of portions of the electrode surface which one should expect as a result of the adsorption has

apparently not been considered or discussed. It will be shown here that the adsorption of a protein at the dropping mercury electrode may have a large effect in decreasing the limiting current of a reducible substance, that the decrease is a function of the protein concentration, and that there is a limiting concentration of protein above which no further decrease in the diffusion current is observed.

## EXPERIMENTAL PROCEDURES AND RESULTS

### a) Preparation of Solutions and Recording of Polarograms

Polarograms were recorded at 25°C. (±1°) on a Heyrovsky Polarograph, Type XII, manufactured by E. H. Sargent and Co., Chicago, Illinois. Oxygen was removed by bubbling nitrogen through the solution, since it was found to have a large effect on the properties of the c.-v. curves. Potentials were measured with respect to a saturated calomel electrode (S.C.E.) which acted as a standard. The polarograms were analyzed according to the graphical method, a correction being made as usual for the residual current.

Experiments were carried out with the dye p-hydroxyphenyl-azophenylarsonic acid (HPA),

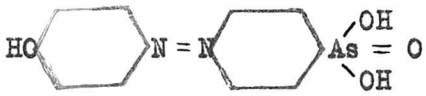


or with cystine, $(HOOC - CH(NH_2) - CH_2S -)_2$, as the reducible substance. Sodium chloride, 0.15 M., was used as the supporting electrolyte and the solutions were buffered at pH 8 with 0.02 M. veronal, the monosodium salt of diethyl barbituric acid,

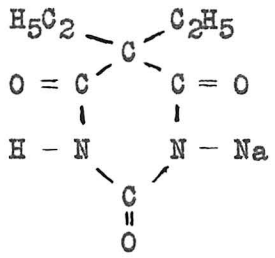


. In solutions of the reducible azo dye, no maximum suppressor is needed in the range of concentrations which were of interest, although a pronounced

maximum occurs in the c.-v. curve at concentrations above $10^{-3}$M. In the reduction of cystine, thymol was used as a maximum suppressor.[13]

A variety of protein substances were used. Quantitative observations were made on solutions containing purified horse albumin (prepared by Dr. G. Wright at this laboratory) or crystallized human albumin (supplied by the Harvard Medical School). The protein content of these preparations was determined by an estimation of the amino nitrogen with Nessler's reagent (analyses by Mr. D. Rice). The results in similar experiments were identical in the two cases. Qualitative comparisons were made with normal rabbit serum, normal sheep serum, purified rabbit globulin, azo albumin (diazo-p-arsanilic acid coupled to purified albumin), and anti-$R_p$ serum (rabbit serum which contains antibodies for the haptenic p-azophenylarsonic acid group).

b) Diffusion Current Constant of p-Hydroxyphenylazophenylarsonic Acid

A test of the accuracy of the Ilkovic equation (1) and a determination of the ratio (known as the "diffusion current constant") between the diffusion current and the concentration of HPA was first carried out. The results of this series of experiments are tabulated in Table I, and are illustrated in Figure 1, wherein the diffusion current is plotted directly against the concentration. A typical polarogram is reproduced in Figure 2.

Table I

p-Hydroxyphenylazophenylarsonic Acid

The Ratio of the Diffusion Current to the Concentration of Azo Dye

All solutions 0.15 M. in NaCl, 0.02 M. in Veronal; pH 8;

temp. 25°C.; $m^{2/3}t^{1/6} = 1.503$ mg.$^{2/3}$-sec.$^{-1/2}$.

| Conc. of Azo Dye, C (millimoles/liter, mm./l.) | Diffusion Current, $i_d$ (microamperes, $\mu$a.) | Diffusion Current Constant, $K' = \frac{i_d}{Cm^{2/3}t^{1/6}}$)* | Half-Wave Potential, $E_{1/2}$** (volts vs. S.C.E.) |
|---|---|---|---|
| 0.986 | 3.72 | 2.50 | -0.419 |
| .906 | 3.38 | 2.48 | .418 |
| .725 | 2.76 | 2.53 | .419 |
| .362 | 1.36 | 2.50 | .416 |
| .181 | 0.69 | 2.55 | .416 |
| .136 | .51 | 2.49 | .417 |
| .0906 | .34 | 2.46 | .422 |
| .0453 | .18 | 2.60 | .421 |
| .0181 | .07 | 2.53 | .420 |
| | Average | 2.52 | -0.419 |
| | Average Deviation | 0.03 | 0.002 |

* Units of K' are $\mu$a.-l.-mm.$^{-1}$-mg.$^{-2/3}$-sec.$^{1/2}$

** The last figure is considered to be unreliable

It may be seen from Table I and from Figure 1 that with all other factors held constant, there is strict linearity between the diffusion current and the concentration of the azo dye in the concentration range investigated. The average diffusion current constant, K', is 2.52 microamperes-liters-millimoles$^{-1}$-milligrams$^{-2/3}$-seconds$^{1/2}$, with an average deviation of 1.3% and a maximum deviation of 3.2%, well within the limits of experimental error. The half-wave potential was found to remain constant (within the limits of error of measurement) at -0.42 volts with respect to a saturated calomel electrode.

From the studies of Shikata and Tachi[14,15] and of Nga,[16] it appears that two electrons are involved in the reduction of the azo group at the dropping mercury electrode and that hydrazo compounds are the reduction products:

$$R - N = N - R + 2H^{+} + 2e^{-} \longrightarrow R - NH - NH - R. \qquad (3)$$

If the Ilkovic equation (1) is written in the form

$$K' = KnD^{1/2} = \frac{i_d}{Cm^{2/3}t^{1/6}}, \qquad (4)$$

then, with K' in the units employed in Table I and D in cm.$^2$/sec., the dimensional constant K has the value 605 $\mu$a.-sec.-cm.-mg.$^{-2/3}$-$\ell$.-mm.$^{-1}$-$F_y^{-1}$, where $F_y$ is the faraday. Substituting in equation (4) the average value of K' (from Table I) and setting n equal to 2, the value for the diffusion coefficient of the azo dye is seen to be

$$D = 4.53 \times 10^{-6} cm^2/sec.$$

This value is in reasonably good agreement with the value

$$D = 5.55 \times 10^{-6} cm.^2 /sec.$$

which is calculated from the Stokes-Einstein relation between the diffusion coefficient and the molecular weight of a spherical molecule.* This result serves to confirm the conclusion of Shikata and Tachi and of Nga (loc. cit.) with respect to the end-product which is formed as a result of the reduction. It is evident then that the concentration of hydrogen ion will affect the position of the wave and that the solutions must be efficiently buffered to insure reproducible results.

Analysis of a typical c.-v. curve of HPA gives a result which throws question upon the general conclusion of Conant and Pratt[17] and of Tachi[18] that the azo-hydrazo systems are reversible. According to equation (2), a plot of the applied potential against log $(\frac{i_d}{i_d - i})$ should result in a straight line with a slope of 0.0295 for a reversible

---

* The assumption of a spherical molecule in this case is a poor one and accounts partly for the disagreement between the calculated and the observed values of the diffusion coefficient. This azo dye molecule undoubtedly has an elongated ellipsoidal shape rather than a spherical one.

The Stokes-Einstein relation is given by

$$D = \frac{RT}{6\pi\eta N (\frac{3M}{4\pi\rho N})^{1/3}}$$

where R is the gas constant, T is the absolute temperature, $\eta$ is the viscosity of the medium, N is Avogadro's number, M is the molecular weight of the dye, and $\rho$ is the density of the dye. The value 0.00895 poises (dyne-sec.-cm.$^{-2}$) was used for the viscosity of the saline solution (I.C.T.), and the density of the dye was found by Dr. Arthur B. Pardee to be 1.5 gms./cc.

two-electron reduction. The results of such an analysis are given in Table II and are plotted in Figure 3.

Table II

p-Hydroxyphenylazophenylarsonic Acid

Reversibility of the Electrode Reaction

| $E_{d.e.}$ (volts vs. S.C.E.) | $\frac{i}{(i_d - i)}$ |
|---|---|
| -0.380 | 0.148 |
| .390 | .239 |
| .400 | .474 |
| .410 | .866 |
| .420 | 1.640 |
| .430 | 2.781 |
| .440 | 4.602 |
| .450 | 8.340 |

These data correspond to 1.50 electrons per molecule for a reversible reduction. The reproducibility of this result in curves obtained from solutions of different dye concentrations makes it improbable that the deviation from the value of 2 for the number of electrons involved in the overall reduction is attributable to an error in measurement. It may well be that the electrode reaction takes place in two stages, one being reversible, the other irreversible. In any case, it must be concluded that the overall electrode reaction is irreversible.

c) Effect of Protein on the Diffusion Current of p-Hydroxyphenylazophenylarsonic Acid

The characteristics of what might be called the normal polarographic reduction of the azo dye having been determined, it is now possible to consider the effect on the diffusion current of the addition of protein to the solutions. A series of solutions were prepared containing constant concentrations of dye, sodium chloride, and veronal, but various concentrations of purified horse albumin. A similar series was prepared with crystallized human albumin. The hydrogen ion concentration was carefully adjusted to pH 8, and a polarogram was recorded for each of the solutions. The composition of the solutions and the results obtained from the polarograms are tabulated in Tables III and IV.

Table III

p-Hydroxyphenylazophenylarsonic Acid

Diffusion Current of Dye in the Presence of Horse Albumin

All solutions $9.86 \times 10^{-4}$ M. in dye, 0.15 M. in NaCl, 0.02 M. in Veronal; pH 8; temp. 25°C., $m^{2/3}t^{1/6} = 1.503$ mg.$^{2/3}$sec.$^{-1/2}$.

| Conc. of Horse Albumin (moles/ℓ. x $10^7$) | Diffusion Current (μa.) | Half-Wave Potential (volts vs. S.C.E.)* |
|---|---|---|
| 228 | 0.94 | -0.515 |
| 114 | 1.01 | .513 |
| 79.9 | 1.17 | .512 |
| 68.5 | 1.26 | .514 |
| 57.1 | 1.48 | .510 |
| 45.7 | 1.76 | .508 |
| 40.0 | 1.84 | .503 |
| 28.6 | 2.28 | .475 |
| 22.8 | 2.74 | .448 |
| 11.4 | 3.30 | .431 |
| 7.99 | 3.48 | .426 |
| 6.85 | 3.55 | .420 |
| 5.71 | 3.75 | .419 |
| 4.57 | 3.68 | .418 |
| 1.14 | 3.79 | .416 |
| 0.114 | 3.71 | .412 |

* The last figure is considered to be unreliable.

Table IV

p-Hydroxyphenylazophenylarsonic Acid

Diffusion Current of Dye in the Presence of Human Albumin

All solutions $9.86 \times 10^{-4}$ M. in dye, 0.15 M. in NaCl, 0.02 M. in Veronal; pH 8; temp. 25°C.; $m^{2/3}t^{1/6} = 1.503$ mg.$^{2/3}$-sec.$^{-1/2}$.

| Conc. of Human Albumin (moles/ℓ. x $10^7$) | Diffusion Current ($\mu$a.) | Half-Wave Potential (volts vs. S.C.E.)* |
|---|---|---|
| 228 | 0.94 | -0.517 |
| 114 | 1.01 | .514 |
| 79.9 | 1.19 | .512 |
| 68.5 | 1.24 | .511 |
| 57.1 | 1.45 | .510 |
| 45.7 | 1.75 | .506 |
| 40.0 | 1.84 | .502 |
| 28.6 | 2.30 | .472 |
| 22.8 | 2.76 | .453 |
| 11.4 | 3.31 | .430 |
| 7.99 | 3.52 | .427 |
| 6.85 | 3.59 | .420 |
| 5.71 | 3.68 | .418 |
| 4.57 | 3.70 | .418 |
| 1.14 | 3.73 | .415 |
| 0.114 | 3.74 | .414 |

* The last figure is considered to be unreliable.

The similarity of the results recorded in Table III to those in Table IV is immediately striking. It is apparent that horse albumin and human albumin have the same effect on the diffusion current of the azo dye. A comparison of a typical current-voltage curve obtained from a dye solution containing protein with that from a slightly less concentrated dye solution containing no protein is made in Figure 6. The diffusion current of the former has been suppressed far below its normal value. Control solutions containing protein, salt, and buffer at pH 8, but no reducible ion, exhibit no diffusion current. In such solutions, the slowly increasing residual current shows a sharp change in slope in the neighborhood of the electrocapillary zero, indicating a change in the cell resistance, due perhaps to the beginning of desorption of the protein from the mercury surface. It should be noted (Figure 6) that the diffusion current of a dye solution containing protein does not reach a true limiting value, but that after leveling off, it begins to increase sharply again in the neighborhood of the electrocapillary zero, almost reaching its normal value before the discharge of hydrogen ion. It seems likely that the decrease in the diffusion current of the dye which is brought about by the addition of albumin to the solution may be attributed to a decrease in the electrode surface available for reduction. The protein molecules which are adsorbed at the interface may constitute a real barrier to the approach of dye molecules to the electrode, and thus prevent a portion of those which reach the electrode vicinity by diffusion from undergoing reduction. The adsorption of protein at the

mercury surface may also be expected to be diffusion-controlled; if so, the average fraction of surface covered by protein during the life of the drop should increase with increasing concentration in the solution to a limiting value which corresponds to a monomolecular layer being effectively maintained over the surface. The diffusion current is found to decrease to a limiting value which, however, is not zero. It may well be that the interstices in a monomolecular layer of protein are of such a size that a portion of the dye molecules may still reach the electrode surface although no further protein can be absorbed. The abrupt increase in current which is observed after the initial attainment of the diffusion current occurs in the neighborhood of the electrocapillary zero, and may be due to desorption of the protein from the electrode surface. The initiation of the desorption process is perhaps attributable to the change in the sign of the charge on the mercury drop as the applied potential becomes more negative than that corresponding to the electrocapillary zero. The electrostatic repulsion of the negatively charged electrode for the similarly charged protein molecules (at pH 8) may then begin to overcome the adsorptive attraction of the mercury surface, and desorption occurs with a resultant increase in diffusion current.

The shift in the half-wave potential brought about by increasing the protein concentration in the solution should be pointed out here. This result is not necessarily indicated by the foregoing hypotheses. The character of the initial wave appears to change in the presence of protein, with the current increase becoming more diffuse so that at large concentrations of protein, the attainment of the pseudo-limiting current

is almost coincident with the initiation of the desorption process; however, at low protein concentrations, a half-wave shift in the initial wave is observed although the resolution of the two waves is complete (See Figure 6, curve B). It must be noted that the composition of the solutions and the cell characteristics are changed by the addition of protein, the effects of which are not easy to predict in this irreversible system. It is well known that changes in the concentration or in the nature of a supporting electrolyte may bring about unexplained changes in the half-wave potential of a reducible ion, even in a reversible system. In this light, it is difficult to determine whether the half-wave shift in the present work is significant or important. Similar data for some reversible redox systems would be desirable and enlightening for the resolution of this difficulty.

The data in Tables III and IV are plotted in Figure 4, from which it may be shown that an empirical equation which describes the experimental data extremely well is of the form

$$\ln k(i_d - i_d^l) = -k'C_p, \qquad (5)$$

where $i_d$ is the diffusion current observed in a solution of azo dye with albumin concentration $C_p$, and $i_d^l$ is the minimum diffusion current observed in similar solutions containing increasingly larger concentrations of the protein. The validity of this relation is illustrated in Figure 5, in which a plot of log $(i_d - i_d^l)$ against the protein concentration, $C_p$, results in a straight line. An explanation of these phenomena is pre-

sented later in this thesis and a theoretical expression which is in reasonable agreement with the experimental data, but which is not of the form of equation (5) is deduced. It appears that either the validity of equation (5) in this form is coincidental, or the assumptions made in the development of the equations later in this thesis are not adequate.

d) Saturation Current at the Dropping Mercury Electrode

In a previous section of this thesis, it has been mentioned that the ratio of the diffusion current of a reducible substance to its concentration in solution is constant only over a limited range of concentration. As the concentration is increased, the limited amount of electrode surface available for reduction becomes important in determining the current density; that is, above some limiting concentration, the electrode can no longer reduce all of the molecules or ions which would reach its surface if complete concentration polarization were to occur. Consequently, there is a concentration of dye above which the polarization is incomplete and the diffusion current attains a maximum value. If, as postulated in the preceding section, a protein molecule adsorbed at the mercury-solution interface immobilizes a portion of the electrode for use in reduction, it would be expected that in the presence of protein, the saturation current will be decreased accordingly. The dropping electrode, in a solution containing protein, should act toward a reducible ion as if its surface area were smaller than that calculated from the capillary constants, and at a given protein concentration, the fractional decrease of the diffusion current should be independent of the dye concentration. In order to

examine the effect of protein on the maximum diffusion current, an experiment was carried out in which the diffusion current was measured in solutions having a constant protein concentration but various concentrations of dye. The results are tabulated in Table V.

Table V

p-Hydroxyphenylazophenylarsonic Acid

Variation of the Diffusion Current with Concentration in the Presence and in the Absence of Proteins

All solutions 0.15 M. in NaCl; 0.02 M. in Veronal, pH 8; temp. 25°C.; $m^{2/3}t^{1/6} = 1.503$ mg.$^{2/3}$-sec.$^{-1/2}$.

| Conc. of dye (millimoles/ℓ.) | Diffusion Current, $i_d'$, in presence of protein* (microamperes) | Diffusion Current in absence of protein, $i_d$ (microamperes) | $\frac{i_d'}{i_d}$ |
|---|---|---|---|
| 0.181 | 0.25 | 0.69 | 0.36 |
| 0.362 | 0.50 | 1.36 | .37 |
| 0.725 | 0.99 | 2.76 | .36 |
| 0.906 | 1.21 | 3.38 | .36 |
| 0.986 | 1.36 | 3.72 | .37 |
| 1.36 | 1.80 | 5.09 | .35 |
| 1.81 | 2.04 | 5.82 | .35 |
| 2.27 | 2.13 | 6.03 | .35 |
| 2.72 | 2.11 | 5.98 | .35 |

* These solutions were $6.1 \times 10^{-6}$M. in crystallized human albumin.

It may be noted in Figure 7 that the maximum current, both in the presence and in the absence of proteins is reached at almost exactly the same dye concentration, although the current density is greatly decreased in the former case, and that the ratio $i'_d/i_d$ remains constant over the entire range investigated. The results of this series of experiments appear to support very strongly the hypothesis of reduced electrode surface.

e) Effect of Other Proteins on the Diffusion Current of Azo Dye

Qualitative observations have indicated that other proteins have an effect similar to that of albumin on the diffusion current of HPA. Lack of pure materials, however, rendered quantitative studies unattractive. The addition, to buffered saline solutions of HPA, of any of the following materials was found to suppress the diffusion current of the azo dye appreciably:*

Normal Rabbit Serum

Normal Sheep Serum

Purified Rabbit Globulin

Azoalbumin (diazo-p-arsanilic acid coupled to albumin)

Anti-$R_p$ Serum (rabbit serum containing antibodies for the haptenic p-azophenylarsonic acid group)

No protein-containing substances were found which did not materially affect the diffusion current of HPA. Control solutions of the above

---

* In preliminary experiments, a similar qualitative effect was observed in the reduction of cadmium ions in the presence of gelatin, but this result may be due largely to a change in the viscosity of the solution, which would affect the diffusion coefficient of the cadmium ions.

proteins ( in the absence of a reducible substance) characteristically exhibited no diffusion wave, but there was evident, in each polarogram, a sharp change in the slope of the residual current line at applied potentials in the neighborhood of that corresponding to the electrocapillary zero.

### f) Effect of Thymol on the Reduction of Cystine

A survey of the literature revealed an example in which a decrease in the diffusion current from solutions of a reducible substance was attributed to the effect of maximum suppressors. Kolthoff and Barnum[13] investigated extensively the effects of gelatin, phenol, resorcinol, thymol, methylene blue, methyl red and camphor in suppressing the maximum in the reduction wave of cystine. They observed current suppressions, half-wave shifts and changes in the shape of the wave. These authors propose that "cystine must be oriented in a favorable position at the surface of the electrode before it can be reduced" and that "the capillary-active substances inhibit this orientation." This picture seems rather unclear and it is difficult to say whether the authors had in mind an explanation similar to the present one, or whether they intended to imply only that the effect was due to the capillary-active substance in a way which they did not clearly understand.

A brief and very incomplete confirmation of the results of Kolthoff and Barnum is reported in this section. A series of solutions was prepared in which the concentration of cystine was held constant as the concentration of thymol was varied. The composition of these solutions is given in Table VI.

Table VI

Composition of Cystine Solutions

All solutions 0.001 M. in cystine, 0.15 M. in NaCl; pH 1; temp. 25°C.;
$m^{2/3}t^{1/6} = 1.503$ mg.$^{2/3}$-sec.$^{-1/2}$

| Solution Number | Concentration of Thymol (moles/ℓ. x $10^5$) |
|---|---|
| 1 | 0.00 |
| 2 | 1.00 |
| 3 | 3.00 |
| 4 | 9.00 |
| 5 | 10.0 |
| 6 | 15.0 |
| 7 | 20.0 |

The polarograms of these solutions are reproduced in Figure 8. The trend is clearly indicated. As the concentration of thymol is increased, the reduction wave of cystine is shifted to more negative potentials. From these curves, it appears that the adsorption of a monomolecular layer of thymol completely suppresses the reduction wave of cystine, which is observed only after desorption has begun. At low concentrations of thymol, the desorption from the electrode appears to occur at a potential which is only slightly greater than that corresponding to the beginning of the reduction of cystine. However, as the concentration of thymol is increased, there is observed a decrease in the slope of the initial portion of the reduction wave and an increase in the slope of the final portion which are analogous respectively to the small diffusion current observed for HPA in the presence of proteins, and the increase

in current observed as the desorption of protein occurs. The shift in the half-wave potential is probably due to the increasing difficulty with which thymol is desorbed as its concentration increases. Further discussion of the curves is given later.

g) Effect of Adsorbed Protein Molecules on the Mercury Droplet

The polarographic experiments carried out with solutions of azo dye in the presence of proteins were characterized by a reluctance of the mercury drops to coalesce at the bottom of the electrolysis vessel. The droplets remained separate and failed to coalesce even after violent shaking or profuse washing. In order to study the adsorption more directly, a cell was devised in which the mercury droplets formed at the electrode just above a liquid boundary between a solution which was $2.2 \times 10^{-5}$M. in horse albumin, 0.02 M. in veronal, and 0.15 M. in NaCl at pH 8, and another solution which was simply 0.75 M. in NaCl. In this way, an attempt was made to preclude the adsorption of protein on the droplet after it had detached itself from the capillary. When the droplets were allowed to form at an applied voltage less negative than -2.2 volts (vs. S.C.E.), the drops did not coalesce. When the applied potential was more negative than -2.2 volts, however, the drops coalesced immediately. Moreover, when the drops were allowed to fall, at -2.2 volts or greater into a previously collected pool of individual droplets, the entire pool slowly fused, a few drops at a time, as each fresh spherule joined the group. A collection of discrete globules of mercury could also be made to coalesce by passing a platinum electrode, at a potential more negative than -0.7 volts, through the array. The speed of fusion increased as the voltage was increased, being extremely slow up to -1.1 volts and extremely rapid in the neighborhood of -2.0 volts.

It seems likely that the apparent discrepancy between -0.7 volts for coalescence of the mercury droplet pool by a platinum electrode and -2.2 volts for immediate coalescence upon leaving the capillary may be explained as follows: desorption of the albumin from the mercury surface occurs at any applied voltage more negative than -0.7 volts (vs. S.C.E.). However, between -0.7 and -2.2 volts, the charge on the drop, after it leaves the electrode, is rapidly dissipated and, despite the precautions taken, albumin is adsorbed on the surface before the drop leaves the protein medium. When the applied voltage is more negative than -2.2 volts, it is to be expected that during the growth of the drop, sodium ions from the solutions are reduced; consequently, the surface of the falling drop consists of a dilute sodium amalgam. The discharge of sodium from this amalgam, as the drop falls through the solution, may maintain a potential sufficient to preclude the adsorption of protein.

These experiments, supporting very strongly the adsorption hypothesis, lend added credibility to the explanations presented in the preceding sections which are more fully developed in the following discussion.

## DISCUSSION

It seems likely from the results of the experiments described that the large effect which proteins have on the polarographic properties of a solution of a reducible substance may be attributed to adsorption of the protein molecules on the surface of the dropping mercury electrode. That such adsorption does occur was recognized early in the history of polarography and is further borne out in the present work by the reluctance of the individual mercury droplets to fuse with one another after departing from the end of the capillary.

In general, the number of solute molecules adsorbed from any solution onto a surface increases with increasing concentration, but reaches a limit when the concentration is such that a monomolecular layer of adsorbed molecules is maintained over the surface. It will be assumed, in the following discussion, that these considerations apply to the adsorption of proteins at the dropping electrode, and inferences will be drawn to explain the observed phenomena.

That the presence of adsorbed molecules may impede the approach of other particles to the electrode and thus by a steric effect hinder the reduction has not heretofore been considered. The diffusion current which passes in a polarographic experiment is dependent upon the number of particles which reach the electrode for reduction. If a particle is unable to undergo immediate reduction because that portion of the electrode toward which it is approaching is covered by a protein molecule, it may be deflected back toward the body of the solution. Of those molecules which

enter the electrode vicinity at a given time the fraction which cannot make contact with the reducing surface and are consequently deflected should be just equal to the fraction of the surface which is covered by the adsorbed material. Complete concentration polarization would hence not be achieved, the concentration gradient between the electrode surface and the body of the solution would be less than predicted and a decrease from the normal diffusion current would be observed.

It seems likely that at any given instant in the life of the drop the fraction of electrode surface which is covered by protein molecules increases with the protein concentration in the solution to a limiting value which corresponds to the adsorption of a monomolecular layer. Such a monomolecular layer, however, need not completely inactivate the entire surface of the electrode. If it be assumed that for secondary layers of protein molecules the adsorptive forces are weak or absent, as will be true for a soluble protein, except possibly at the isoelectric point, the adsorbed film, consisting of a single layer of large ellipsoidal particles, may, even in closest packing, have holes of a size large enough to permit some of the reducible material, usually smaller in size, to reach the electrode and undergo reduction. On the other hand, the holes in the adsorbed film would be too small to allow other protein molecules to fit among those which are adsorbed in the primary layer. Thus in increasing the concentration of albumin the effect would be to decrease the diffusion current of an azo dye to a limiting value which would <u>not necessarily</u> be zero (Figure 4). In this case, the diffusion current is suppressed by protein adsorption to about twenty-five percent of its normal value. For

comparison, it may be noted that a layer of ellipsoids in closest packing projected onto a flat surface leave interstices which total about 9.1 percent of the area. The percentage of voids in simple rectangular packing of ellipses is about 21.5 percent. In view of the present hypotheses, the monomolecular layer of protein molecules apparently does not arrange itself into a closest packed array.

Further evidence in support of the present hypotheses is afforded by an examination of the characteristic effects of saturation of the electrode. It has been shown, for example, that the capacity of a mercury electrode in saturated solutions of capillary-active organic substances depends inversely upon the chain length of the molecule.[19] In Figure 7, the variation of the diffusion current with concentration of azo dye in the presence of a constant concentration of protein is compared with that in the absence of protein. It is striking that the fractional decrease in current brought about by a given amount of protein is constant. It may be inferred that the average fraction of surface covered during the life of the mercury drop remains constant in the presence of a given concentration of protein, and that the diffusion current is affected accordingly. It must be pointed out that the effects which are discussed here are average ones, over the surface of the drop, since with portions of the electrode surface inactivated, the spherical symmetry of the diffusion layer would be destroyed.

Since the adsorption process at the electrode surface would also be diffusion dependent, it may be asked whether, at a protein concentration at which the limiting suppression is achieved, it is possible for enough protein molecules to reach the electrode to maintain a monomolecular layer over the surface. Such a calculation must of needs be idealized since in

the actual case such factors as the electrostatic forces between the electrode and the protein molecules and the competition between dye and albumin molecules for the electrode surface must be considered as well as the fact that the spherical symmetry of the concentration gradients is destroyed by molecules which are neither adsorbed nor reduced at the mercury surface, even though they reach the electrode vicinity.

Let it be assumed, for simplicity, that the diffusion of protein to the mercury drop may be described by the Ilkovic equation (1); that is to say, that all protein molecules which reach the electrode vicinity are immediately adsorbed on the surface and are thus effectively removed from the solution. The Ilkovic equation (1) may be alternately written

$$N = 0.63\ C m^{2/3} t_{max}^{1/6}\ D^{1/2}\ , \qquad (6)$$

where N is the number of moles of diffusing substance reaching the electrode during the life of the drop, $t_{max}$ (secs.); D is the diffusion coefficient ($cm.^2/sec.$); C is the concentration (moles/cc.); and m is the dropping rate of mercury (mg./sec.).

In the present experiments, m = 1.22 mg./sec. and $t_{max}$ = 5.33 secs. at approximately the reduction potential of the dye: The diffusion coefficient of horse albumin is approximately $6 \times 10^{-7} cm^2/sec.$ Consequently,

$$N = 3.9 \times 10^{-5} C, \qquad (7)$$

Since the concentration of albumin at which the diffusion current of azo dye reaches its minimum value is approximately $1 \times 10^{-8}$ moles per cubic centimeter, it is seen that $3.9 \times 10^{-13}$ moles of protein may reach the electrode under the stated conditions. Assuming again, for simplicity, a spherical albumin molecule with a density of 1 gm./cc., and a molecular

weight of 70000, the radius of each molecule is calculated to be 3.03 x $10^{-7}$cm. The projected area of a sphere of this radius onto a flat surface is then 2.88 x $10^{-13}$sq. cm., and the projected area for all molecules which may reach the electrode during the life of a drop is 0.0676 sq. cm. From the known weight of each droplet, 6.6 mg., the maximum area of the surface is calculated to be 0.0264 sq. cm. Thus, under the ideal conditions set forth, approximately two and a half times as much protein may diffuse to the electrode during the life of the drop as is actually needed to cover the maximum surface attained. The agreement in order of magnitude is good.

An approximate expression for the reduction of azo dye under conditions similar to those specified in the preceding calculation may be derived. Let us assume the Ilkovic equation (1) for the flux of diffusing molecules to a growing surface to hold, both for protein and for reducible substance, with the exceptions only that the instantaneous reduction current is diminished by a fraction equal to the fraction of the electrode surface which has become covered by protein and that the rate of deposition of protein molecules is similarly decreased but with a different proportionality constant. The assumption (which would appear to become increasingly inadequate as the protein concentration is increased) is that in effect the molecules which are not permitted to reach the electrode surface simply cease to exist insofar as the diffusion problem is concerned. Let us denote by X the area of the electrode per unit area covered by protein at a given time, t, in the life of the drop. The amount of protein on the electrode in units of (area excluded to other protein molecules) per unit area is then $k_1$ X, where $k_1$ may be described as the protein-protein blocking factor,

introduced to express the hypothesis that the inactivation of the surface with respect to the adsorption of more protein is greater than the area actually covered by the previously adsorbed albumin molecules. Let us then write

$$i = i_o(1 - X), \tag{8}$$

where i is the instantaneous reduction current at time, t, in the presence of a concentration, $C_p$, of protein and $i_o$ is the corresponding instantaneous current in the absence of protein. Let us denote by T the amount of protein on the drop in the units of area covered. Then

$$T = S_o X = 4\pi^{1/3}\left(\frac{3m}{d}\right)^{2/3} t^{2/3} X = pt^{2/3}X, \tag{9}$$

where $S_o$ is the surface area of the drop at time, t; m is the dropping rate of mercury and d is the density of mercury. Let us now write

$$\frac{dT}{dt} = \left(\frac{dT}{dt}\right)_o (1 - k_1 X), \tag{10}$$

where $\left(\frac{dT}{dt}\right)_o$ is the rate at which protein diffuses toward the drop which, under our assumptions, is given by the Ilkovic equation. Hence,

$$\left(\frac{dT}{dt}\right)_o = \frac{0.73}{k_2} D^{1/2} C_p m^{2/3} t^{1/6}, \tag{11}$$

where D is the diffusion coefficient of the protein and $k_2$ is introduced to convert to units of area. $k_2$ is then the number of moles of protein which cover unit surface area of the drop. From equation (10) and (11), then,

$$\frac{dT}{dt} = at^{1/6} - \frac{bT}{t^{1/2}}, \tag{12}$$

where $a = \frac{0.73}{k_2} D^{1/2} C_p m^{2/3}$, and $b = \frac{ak_1}{p}$. Equation (12) is a linear differential equation, the solution of which may be found in any elementary

treatise on differential equations. For this particular equation, a solution in terms of a useful, convergent, infinite series is:

$$T = 6/7\ at^{7/6} - 6/7\ 6/10\ abt^{10/6} + 6/7\ 6/10\ 6/13\ ab^2t^{13/6} - + \text{---}. \quad (13)$$

From equation (9), then,

$$X = \frac{T}{pt^{2/3}} = 6/7\ a/p\ t^{1/2} - 6/7\ 6/10\ \frac{ab}{p}\ t + 6/7\ 6/10\ 6/13\ \frac{ab^2}{p}t^{3/2} \text{--}, \quad (14)$$

and from equation (8),

$$i = i_o(1 - X) = At^{1/6}\left(1 - \frac{6}{7}\frac{a}{p}\ t^{1/2} + \frac{6}{7}\frac{6\,ab}{10\ p}\ t - \frac{6}{7}\frac{6\ 6}{10\ 13}\frac{ab^2}{p}\ t^{3/2} + \text{--}\right), \quad (15)$$

where $i_o = At^{1/6}$ is given by the Ilkovic equation. The average current, which is measured experimentally, is then given by

$$\bar{i} = \frac{1}{\tau}\int_o^\tau i\,dt = 6/7\ A\tau^{1/6} - 6/7\ 6/10\ \frac{Aa}{p}\tau^{4/6} + 6/7\ 6/10\ 6/13\ \frac{Aab}{p}\tau^{7/6} - + \text{--} \quad (16)$$

where $\tau$ is the drop time. But

$$\bar{i}_o = \frac{1}{\tau}\int_o^\tau i_o\,dt = \frac{1}{\tau}\int_o^\tau At^{1/6}dt = 6/7\ At^{7/6}$$

$$\therefore\ \bar{i} \quad \bar{i}_o - \bar{i}_o\left(6/10\ \frac{a}{p}\tau^{1/2} - 6/10\ 6/13\ \frac{ab}{p}\tau + 6/10\ 6/13\ 6/16\ \frac{ab^2}{p}\tau^{3/2} \text{--}\right). \quad (17)$$

Let $\bar{i}_o - \bar{i} = \delta\bar{i}$, and let $u = 6b\tau^{1/2}$. Then, from equation (17), since

$a/b = p/k_1$ ,

$$\frac{k_1\,\delta\bar{i}}{\bar{i}_o} = (u/10 - u^2/10\cdot13 + u^3/10\cdot13\cdot16 - + \text{----}), \quad (18)$$

or $$\frac{k_1 \overline{\delta i}}{\overline{i}_o} = f(u), \tag{19}$$

when $$f(u) = u/10 - \frac{u^2}{10.13} + \frac{u^3}{10.13.16} - + - - -. \tag{20}$$

It may be shown that $f(u)$ is a convergent series which approaches unity as $u$ becomes large. The expression $f(u)$ has been evaluated as a function of $u$. A number of values are given in Table VII and a plot of $f(u)$ against $u$ is made in Figure 9.

Table VII

Evaluation of $f(u)$ as a Function of $u$

| u | f(u) |
|---|---|
| 0 | 0.000 |
| 1 | .093 |
| 2 | .172 |
| 3 | .242 |
| 5 | .355 |
| 7 | .442 |
| 10 | .540 |
| 14 | .630 |
| 15 | .648 |
| 20 | .716 |
| 30 | .797 |
| 50 | .871 |
| 70 | .900 |

From equation (12),

$$u = 6bT^{1/2} = 6\left(\frac{0.73K_1}{K_2 P} D^{1/2} C_p m^{2/3}\right) T^{1/2}, \qquad (21)$$

or from equation (9),

$$u = \frac{4.38 D^{1/2} C_p K_1 T^{1/2} d^{2/3}}{K_2 (4\pi)^{1/3} (3)^{2/3}} \qquad (22)$$

In the present experiments, $T$ = 5.33 secs.; from the known values $D_{albumin} = 6 \times 10^{-7}$ cm.$^2$/sec. and $d_{Hg}$ = 13.55 gms./cc., it may be shown that

$$u = 0.925 \frac{k_1 C_p}{k_2}. \qquad (23)$$

Assuming a spherical albumin molecule with a molecular weight of 70000 and a density of 1, it may be shown that $k_2$, the number of moles of albumin which, projected, may cover unit area of surface, is $5.76 \times 10^{-12}$ moles/cc. Since the asymptotic value of the reduction current in the present experiments is about 25 percent of the "true" value, it may be inferred that $k_1$, the protein-protein blocking factor, is approximately 1.33. Hence,

$$u = 0.214 \times 10^{10} C_p. \qquad (24)$$

The reduction current to be expected under the stated conditions may now be calculated. In Table VIII and in Figure 10, the calculated values are compared with those observed. In each calculation, $u(C_p)$ was obtained from equation (24). The corresponding value for $f(u) = \frac{K_1 \delta i}{\bar{i}_o}$ was read from Figure 9; from this, $\bar{i}_{calc.}$ was obtained.

Table VIII

p-Hydroxyphenylazophenylarsonic Acid

Comparison of $\bar{i}_{calc.}$ with $\bar{i}_{obs.}$

| $C_p$ (moles/cc. x $10^{10}$) | u | f(u) | $\bar{i}_{calc.}$ | $\bar{i}_{obs.}$ |
|---|---|---|---|---|
| 228 | 48.70 | 0.87 | 1.29 | 0.94 |
| 114 | 24.35 | .76 | 1.60 | 1.01 |
| 79.9 | 17.08 | .68 | 1.82 | 1.17 |
| 68.5 | 14.65 | .64 | 1.93 | 1.26 |
| 57.1 | 12.21 | .59 | 2.07 | 1.48 |
| 45.7 | 9.75 | .53 | 2.24 | 1.76 |
| 40.0 | 8.55 | .49 | 2.35 | 1.84 |
| 28.6 | 6.10 | .40 | 2.60 | 2.28 |
| 22.8 | 4.87 | .35 | 2.74 | 2.74 |
| 11.4 | 2.44 | .21 | 3.13 | 3.30 |
| 7.99 | 1.71 | .16 | 3.27 | 3.48 |
| 6.85 | 1.47 | .14 | 3.33 | 3.55 |
| 5.71 | 1.22 | .12 | 3.38 | 3.68 |
| 4.57 | 0.98 | .09 | 3.47 | 3.70 |
| 1.14 | 0.24 | .02 | 3.66 | 3.73 |
| 0.114 | 0.02 | .00 | 3.72 | 3.74 |

The agreement between the experimental and the calculated curves is reasonably good in the light of the assumptions made. It is

possible to bring about somewhat better agreement by a suitable variation of the constant, $k_2$, or at the expense of adding another parameter; however, these modifications would be of an empirical nature, and although there is much justification for them, they would seem to contribute little to our knowledge of the system. The agreement afforded by the present treatment appears to be at least as instructive as the better agreement that could be obtained by the addition of further constants.

A reasonable theoretical background having been established for the hypotheses herein presented, it is possible to inquire further into the nature of the phenomena at the electrode. The effects of electrostatic forces between the electrode and the protein molecule should be considered. At pH 8, the albumin molecule has an overall negative charge, and should be attracted to an electrode which is positively charged, a situation which obtains when the applied voltage is more positive than that corresponding to the electrocapillary zero ( which varies from solution to solution in the neighborhood of -0.6 volts vs. S.C.E.). On the other hand, as the applied voltage becomes more negative than the potential corresponding to zero charge, the electrostatic repulsion between the electrode and the protein molecule would be expected to counterbalance and finally overcome the adsorptive forces, eventually effecting a desorption from the electrode surface. The experiments described in section (g) bear out these contentions, since it was shown that a platinum electrode at a potential more negative than -0.7 volts, when passed through a collection of individual mercury droplets formed in a protein solution, brings about their fusion, and that the rate of fusion increases with increasing voltage.

The difference in appearance between the current-voltage curve obtained from an azo dye solution in the absence of protein and that from a similar solution containing a comparatively large concentration of protein (Figure 6) may easily be explained. In the former case, the diffusion current reaches a limiting value and remains practically constant thereafter, whereas in the presence of protein, the diffusion current flattens, but in the region corresponding to the electrocapillary zero, takes a sharp turn upward and increases with voltage, finally approaching the normal limiting current as the hydrogen-ion discharge begins. This is attributed to the gradual desorption of albumin from the electrode with a concomitant increase of available space at which the dye may be reduced.

The results, summarized in Figure 8, of adding thymol to solutions of cystine may be similarly explained. Apparently, adsorption of the thymol molecule (which is smaller than the albumin molecule and consequently leaves only very small holes in the adsorption layer) almost completely suppresses the reduction of cystine. As desorption occurs at more negative voltages, reduction may take place. Since the desorption may be expected to become more difficult as the thymol concentration is increased, there is observed an apparent shift in the half-wave potential of cystine. These results confirm the experimental observations of Kolthoff and Barnum (loc. cit.)

The explanation for the desorption of thymol is probably not based on a simple electrostatic repulsion in this case for at pH 1, thymol would be expected to exist almost completely as a neutral molecule. How-

ever, Tachi[18] and Kolthoff and Barnum[13] have shown that camphor is desorbed from the electrode at increasing negative potentials, and that the desorption is complete at -1.24 volts (vs. S.C.E.). It seems probable that thymol is similarly desorbed at high negative potentials and that the desorption is due rather to the preferential adsorption of cystine or of water molecules than to electrostatic repulsion.

In part (e) of the experimental section, it was mentioned that in polarograms of control solutions containing various protein mixtures (but no reducible substance), no diffusion current is observed, and that in each case, a sharp change in the slope of the residual current line occurs at applied potentials which are in the region of the electrocapillary zero of potential. Although no diffusion layer is to be expected in such solutions, the desorption of proteins from the electrode surface would bring about a change in the electrokinetic potential at the interface and would disrupt the linearity of the residual current line usually observed in such solutions.

The shift in the half-wave potential brought about by the addition of proteins to a solution of HPA is not yet understood. We are not at all positive that the shift is related to the present phenomena. It is often true in polarographic analysis that a shift in half-wave occurs as a result of changing certain constituents in the solution. On the other hand, it may be that there is a very definite relationship between the shift in the half-wave potential and the decrease in diffusion current. We have not yet arrived at a satisfactory explanation for the observed shift and we feel that this may constitute a serious flaw in our proposed explanation. In the absence of further experimental evidence, however, we are forced to leave

this point unexplained.

In reference to the half-wave potential of a reducible ion in the presence of capillary-active substances, it must be recognized that adsorption at an electrode is dependent on the applied voltage. The desorption potential of a surface active material is a characteristic of the molecule or ion and is probably dependent upon the strength of adsorption and on the relative charge of the mercury and the adsorbate. We may then recognize three possible effects on the half-wave potential. If the desorption takes place at a more positive potential than that corresponding to the beginning of discharge of the reducible ion, there should be no effect on the diffusion current or on the half-wave potential. Secondly, if desorption takes place at a much greater negative potential than that at which the ion reduces, two waves should result. The first will correspond to the normal polarographic wave, but will be suppressed by the immobilization of electrode surface and will reach a limiting value which may or may not be zero. The second wave will occur when desorption suddenly increases the available electrode surface for reduction of the ion in question. Such a situation apparently obtains in the reduction of HPA in the presence of albumin, in the reductions of methylene blue and of riboflavin which are cited below, and in the reduction of cystine in the presence of high concentrations of thymol, where the wave is completely suppressed. In this last case, the wave is sharpened considerably because of the sudden desorption at a higher negative potential than that at which the normal reduction occurs. Thirdly, the desorption may occur in the region of the normal reduction wave. The potential of the inception of reduction will be unaffected, but as the current is building up to its limiting value, desorption

may begin, and the current will continue to increase until the surface is completely free of adsorbed material. The effect will be to spread out the wave and give an apparent shift in half-wave potential to more negative voltages. Apparently, one observes this in the reduction of cystine at low concentrations of thymol. Depending upon how small is the difference between the reduction potential and the desorption potential and upon how sharply the desorption occurs, the wave may simply be a very diffuse one, or it may involve a more or less sharp break in the current-voltage curve.

In addition to the work of Kolthoff and Barnum, a few examples of phenomena similar to those reported herein have been noted. For example, Salac[20] reports that substances, including albumin, possessing high surface activity interfere with the polarographic determination of saccharin in beer, decreasing the observed diffusion currents. The original paper is unavailable at this writing, and no detailed consideration can be given to the work.

Brdicka[21] reports that in the polarographic reduction of methylene blue and of riboflavin, a small anomalous wave, independent of concentration when the concentration of reducible ion is above a given value, precedes the large reduction wave. He suggests that this may be due to the adsorption of reduction products and he suggests that the so-called anomalous wave corresponds to the beginning of reduction, which is suppressed by the adsorption of reduction products. The second wave, representing the true diffusion current, occurs at a more negative potential where the products are desorbed from the electrode. This explanation fits well with the present work and is apparently a satisfactory explanation of the observations.

The effect of protein in reducing the diffusion current of the dye is so large that the possibility of attributing the results to an inter-

action between dye and protein molecules in solution is immediately excluded. If it is assumed that the decrease in current is due to compound formation with the concomitant decrease in diffusion coefficient, and if the data are then treated in a manner analogous to that of Klotz, Walker and Pivan[22] according to their derived equation,

$$\frac{1}{r} = \frac{K}{n[A]} + \frac{1}{n},$$

where r is the ratio of molecules of bound dye to total moles of protein, $[A]$ is the concentration of free dye, and n is the maximum number of dye molecules which may be bound to a single protein molecule, it may then be shown that n is of the order of 1000. Spatially, this result is, of course, impossibly large, especially since Klotz has shown that, for calcium ion, which is much smaller than the protein molecule, n is 22. In addition, the data of Figure 7, from which it may be seen that a given concentration of protein decreases the diffusion current by a constant fraction, independent of the dye concentration, is in disagreement with the hypothesis that an equilibrium between dye, protein, and combined dye-protein is of importance here. It is not improbable that there is some small effect of interaction, but of the total decrease in current observed, this can be, at most, of the order of a few percent.

The confused state of present theories of polarographic maxima makes it a difficult task to present an accurate picture of the role of capillary-active substances in maximum suppression. However, it seems very likely that the suppression of maxima is closely related to adsorption on the electrode surface. We may, as a result of the present work, attempt to place the use of maximum suppressors upon a less empirical basis. It seems likely that a capillary-active substance which is desorbed from the

electrode at a more positive potential than that at which reduction of the substance in question occurs will be inactive as a maximum suppressor. A maximum suppressor should be used in accurate polarographic work only when absolutely required, and then in a minimal concentration. The choice should probably be such that desorption of the capillary-active material occurs rather sharply at a potential just slightly more negative than that at which the maximum in the c.-v. curve is reached. (We cannot, of course, state just what the optimum criterion will prove to be.) The measurement of the current should be made just beyond this desorption point. A systematic tabulation of the desorption characteristics of the commonly used maximum suppressors would be very convenient for these purposes.

The relation of the present work to the phenomenon of maxima and their suppression should be explored briefly. Antweiler and von Stackelberg[8,9] have shown conclusively that a pronounced streaming occurs about the electrode during the stage in the reduction at which a maximum is observed in the c.-v. curve. There appears to be no diffusion layer, the reducible substance reaching the electrode by the streaming process. Antweiler points out that the tip of the capillary exerts a screening effect and prevents the free diffusion of reducible material at this point with the result that the current density at the bottom is greater than at the top; there remains in the solution an unequal distribution of the indifferent ions between the bottom and the top of the drop and consequently, a tangential potential gradient exists in the solution about the drop. The double layer migrates along this gradient, inducing a streaming of the solution. This flow brings more reducible ions to the incipient "hot spot,"

bringing about a further inequality in the distribution of indifferent ions,* and thus the cycle continues. It seems almost certain that the adsorption of capillary-active substances on these centers of high current density with consequent immobilization of the given area as an electrode surface is the mode of action of such substances as maximum suppressors. The incipient center being deactivated, the whole mechanism for production of the anomalous current loses its driving force. The concentration of capillary-active substance, according to this interpretation, need not be so high as to produce a notable effect on the normal diffusion current because at any incipient center, the suppressor will be brought to the electrode by flow as well as by diffusion and because the whole phenomenon obviously represents a rather narrow choice between the two types of behavior which may depend quite sensitively on very small changes in a considerable number of factors including the reactivity of the electrode surface which we have been discussing.

---

* This explanation is set forth by Antweiler, but it has been pointed out by Kolthoff and Lingane[4] that no consistent picture of the charge distribution about the drop can be drawn for the general case. In addition, the specific effects observed in the study of maxima are unexplained.

## SUMMARY

A search of the literature reveals that although adsorption of capillary-active materials at the dropping mercury electrode was considered important in polarographic work almost from its inception, consideration has never been given to the actual inhibiting effect an adsorbed ion might have on the reduction of other ions. It has been shown in this paper that under certain conditions, the effect may be extremely large although only a small trace of the capillary-active substance is present.

Polarograms prepared from solutions which contained various concentrations of serum albumin (either human or horse) buffered at pH 8 with veronal and which, in each case, contained the same concentration of a dye (p-hydroxyphenylazophenylarsonic acid) and of sodium chloride indicated that the diffusion current was suppressed to approximately 90% of its true value at a protein concentration of $1 \times 10^{-6}$M. and to an asymptotic value of about 25% at $1 \times 10^{-5}$M.

It seems likely that the albumin, a capillary-active substance, is adsorbed on the growing mercury drops, decreasing the surface available for reaction with the reducible molecules or ions, and thus decreasing the diffusion current. The fraction of inactivated surface and the consequent reduction of the instantaneous diffusion current is, at any stage in the life of the drop, proportional to the diffusion rate of the protein or accordingly, its concentration. At moderately high concen-

trations of protein, however, a monomolecular layer would be formed and an asymptotic diffusion current would be attained which may or may not be zero, for a monomolecular layer of adsorbed molecules may well have interstices large enough so that some of the reducible material can reach the electrode. The hypothesis of reduced electrode surface is supported by the observation that at a given concentration of protein, the fractional decrease in the diffusion current is constant, independent of the concentration of reducible material.

Such considerations clarify, in part, the decrease in diffusion current which is observed in this and a number of other cases upon the addition to the solution of capillary-active molecules or ions.

## ADDENDUM

In a paper published in 1945, S. Fiala[23] reported that the reduction potential of oxygen at the dropping mercury electrode is shifted to more negative values when dyes of the eosine group are present in the solution. At low concentrations of the dye, only part of the oxygen wave is shifted. With increasing dye concentration, the shifted wave increases at the expense of the original wave until finally, a single wave occurs at the more negative potential. Fiala attributed this to the combination of molecular oxygen with the dye.

K. Wiesner in a recent paper[24] has pointed out that, according to Henry's Law, unbound molecular oxygen could not be absent from a solution open to the atmosphere and that one should expect the normal oxygen wave to appear in all the polarograms even if some oxygen were bound to the dye. Wiesner investigated more thoroughly the role of eosine and its derivatives in the polarographic depolarization process with a study of some reversible redox systems, such as quinone, hydroquinone, and a number of quinone derivatives. He concluded that the observations could be attributed to the adsorption of dye on the electrode with a concomitant suppression of the diffusion current. Furthermore, the effect was observed only when the dye concentration was above a minimum value. Wiesner concentrated his attention on this last observation. He concluded that the dye, when first adsorbed, behaves as a two-dimensional gas (after Langmuir[25] and Volmer[26]) which cannot inhibit the approach of reducible ions or molecules, but that after a time (the length of which is dependent

on the dye concentration), the adsorbate crystallizes, acquiring a definite structure, and then hinders the reduction process. At low concentrations of dye, the incubation period (during which the adsorbate acts as a two-dimensional gas) is longer than the drop time, and no effect is observed. At higher concentrations, the crystallization occurs during the life of the drop, and a suppression of the current may be observed. Wiesner supported his conclusions with oscillographic current-time curves.

As the eosine concentration was increased in solutions containing a constant concentration of a reducible dye, the current was suppressed in a manner similar to that recorded in Figure 4 of this thesis. The curve analogous to Figure 4 was shifted, however, being preceded by a flat portion, the length of which varied with the drop time. It appears that the phenomenon is very similar to that observed in the HPA-albumin system, except that here no evidence of an incubation period is observed. The work and the conclusions of Wiesner are in good agreement with the observations reported in the preceding sections.

## REFERENCES


1. J. Heyrovsky, Chem. Listy. 16, 256 (1922); Phil. Mag. 45, 303 (1923)

2. D. Ilkovic, Collection Czechoslov. Chem. Commun. 6, 498 (1934); J. chim. phys. 35, 129 (1938)

3. D. MacGillavry and E. K. Rideal, Rec. trav. chim. 56, 1013 (1937)

4. I. M. Kolthoff and J. J. Lingane, "Polarography," Interscience Publishers, New York, N.Y. (1941), p. 168

5. J. Heyrovsky and E. Vascantzann, Collection Czechoslov. Chem. Commun. 3, 418 (1931)

6. J. Heyrovsky, Actualities scientifiques et industrielles, No. 90, Paris, 1934

7. D. Ilkovic, Collection Czechoslov. Chem. Commun. 8, 13 (1936)

8. H. J. Antweiler, Z. Electrochemie, 43, 896 (1937); 44, 719, 813, 888 (1938)

9. M. Von Stackelberg, H. J. Antweiler, and Keisenbach, Z. Electrochemie 44, 663 (1938)

10. A. Frumkin and B. Bruns, Acta physicochim., U.R.S.S. 1, 232 (1934)

11. B. Bruns, A Frumkin, S. Jofa, L. Vanjukova and S. Zolotarevskaja, Acta physicochim., U.R.S.S. 9, 359 (1938)

12. S. Jofa and A. Frumkin, Compt. rend. acad. sciences, U.R.S.S. 20, 293 (1938)

13. I. M. Kolthoff and C. Barnum, J.A.C.S. 63, 520 (1941)

14. M. Shikata and I. Tachi, Mem. Coll. Agr. Kyoto Imp. Univ. 17, 45 (1931)

15. I. Tachi, Mem. Coll. Agr. Kyoto Imp. Univ. 40, 1, 11 (1937); 42, 1 (1938)

16. N. T. Nga, J. chim. phys. 35, 345 (1938)

17. J. B. Conant and M. F. Pratt, J.A.C.S. 48, 2468 (1926)

18. I. Tachi, Mem. Coll. Agr. Kyoto Imp. Univ., 42, 36 (1938)

19. A. Ksenofontov, M. Proskurnin, A. Gorodetzkaya, J. Phys. Chem., U.S.S.R. 12, 408 (1938)

20. Salac, Kvas 64, 383 (1936)

21. R. Brdicka, Z. Electrochemie 47, 721 (1941); 48, 278, 686 (1942)

22. I. M. Klotz, F. M. Walker, and R. B. Pivan, J.A.C.S. 68, 1486 (1946)

23. S. Fiala, Chem. listy 39, 14 (1945)

24. K. Wiesner, Collection Czechoslov. Chem. Commun. 12, 594 (1947)

25. I. Langmuir, Chem. Reviews 13, 147 (1933)

26. M. Volmer, Z. phys. chem. 119, 46 (1925)

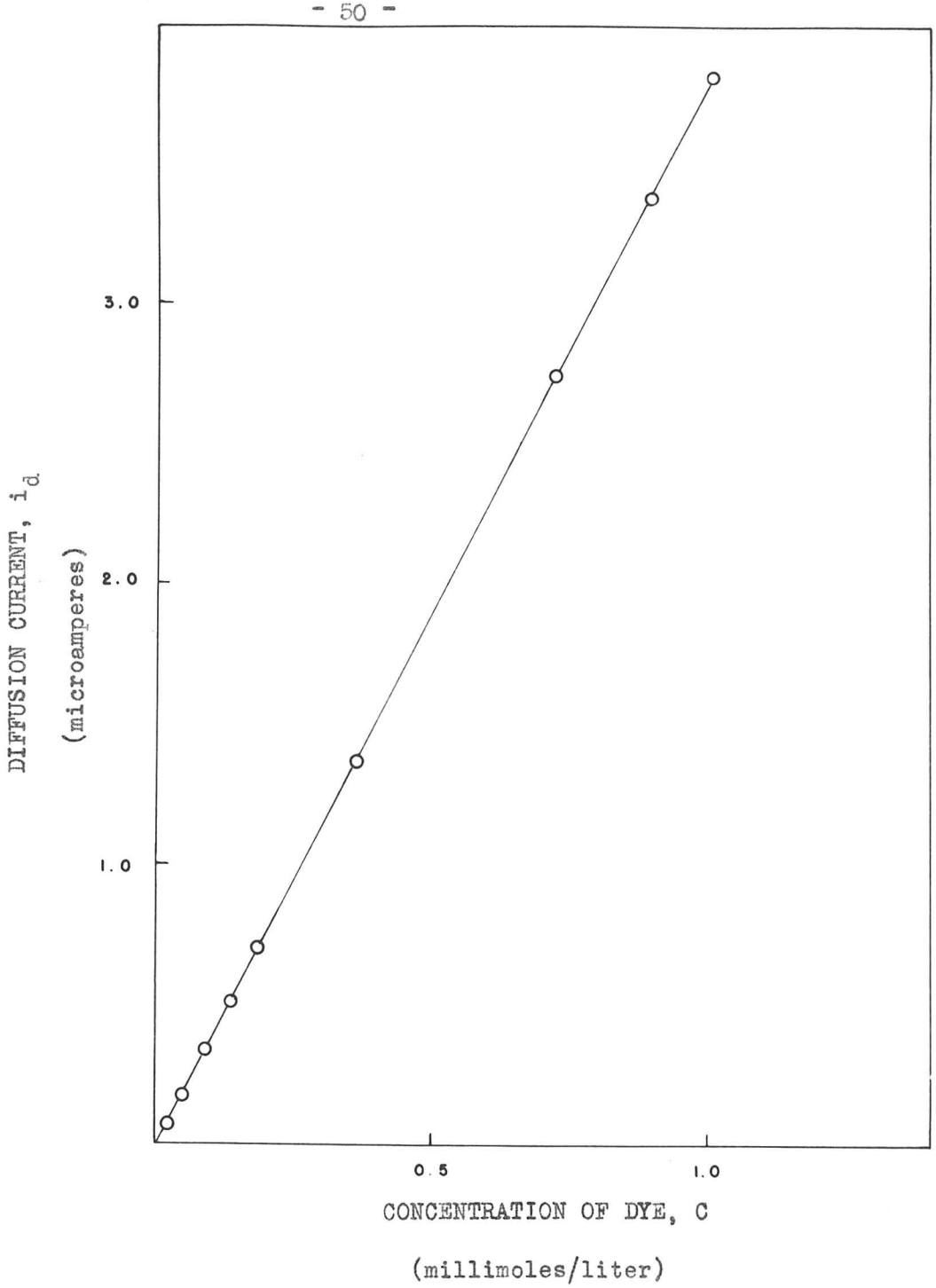


Figure 1: p-Hydroxyphenylazophenylarsonic Acid. A Test of the Ilkovic Equation.(See Table I) All solutions 0.15 M. in NaCl, 0.02 M. in veronal; pH 8

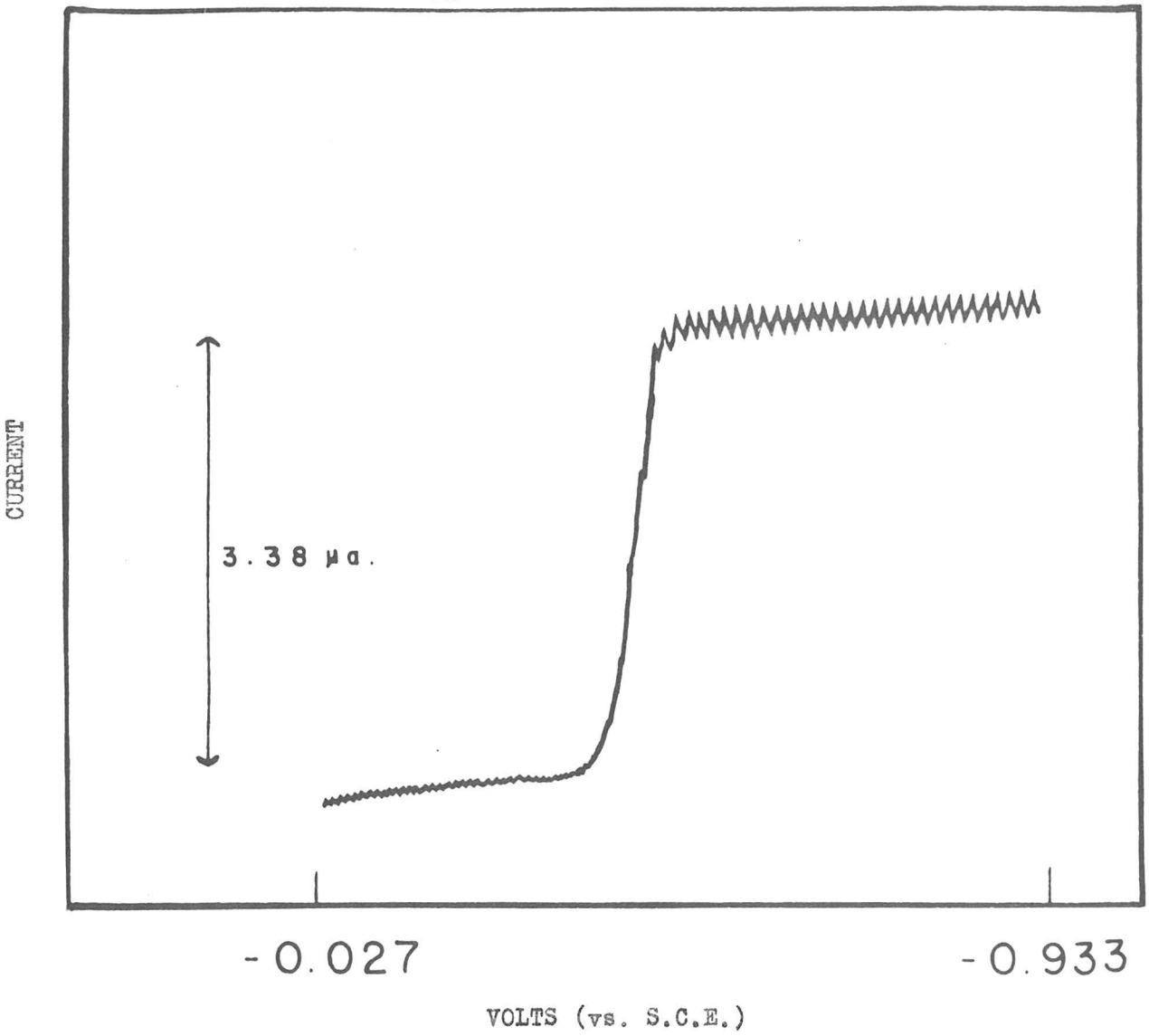


Figure 2: A Typical Polarogram of p-Hydroxyphenylazophenylarsonic Acid. The solution is 9.06 X $10^{-4}$ M. in dye, 0.15 M. in NaCl, 0.02 M. in veronal; pH 8

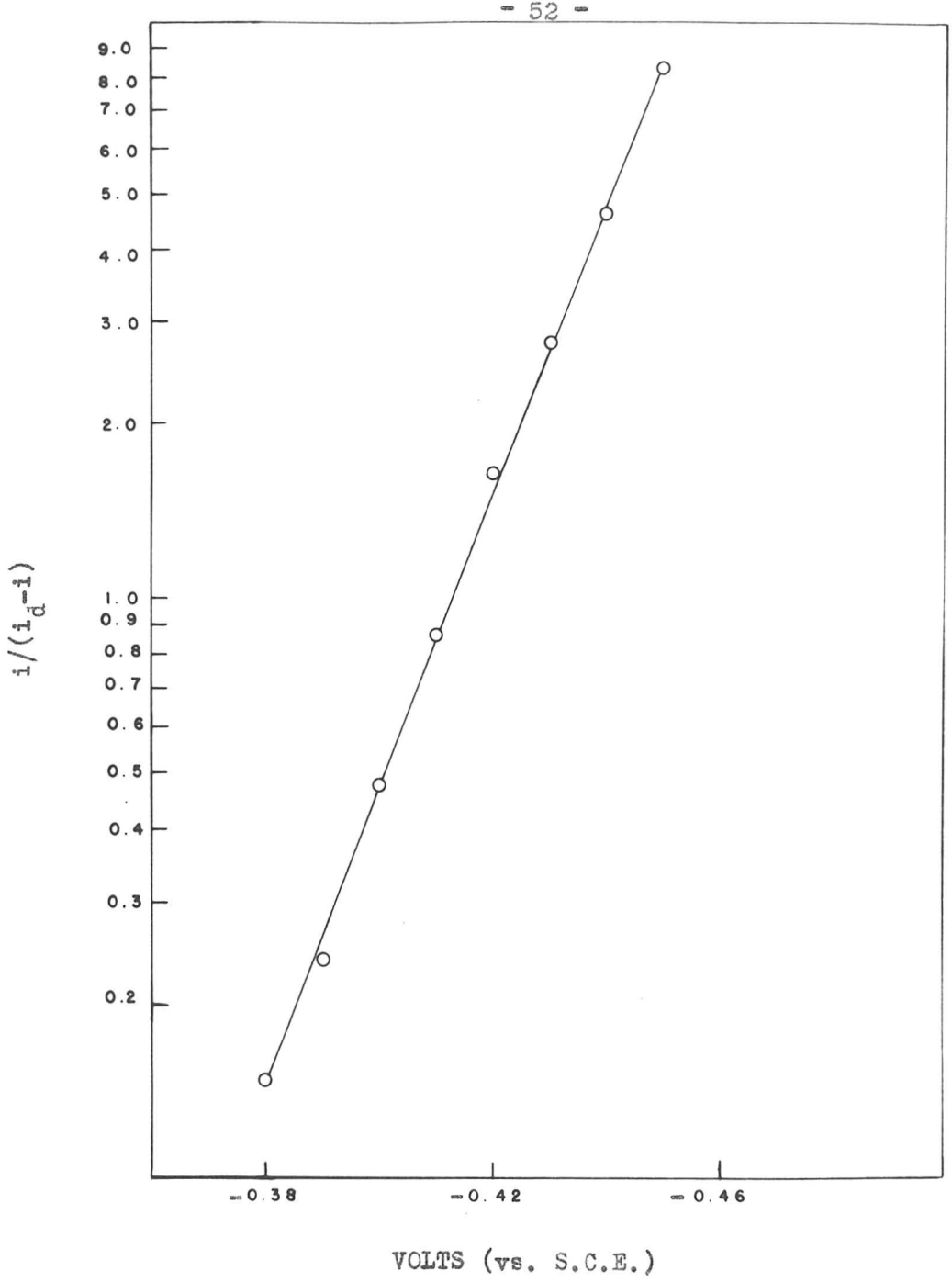


Figure 3: p-Hydroxyphenylazophenylarsonic Acid. A Test of the Reversibility of the Electrode Reaction (See Table II). The solution is 5 X $10^{-4}$ M. in dye, 0.15 M. in NaCl, 0.02 M. in veronal; pH 8

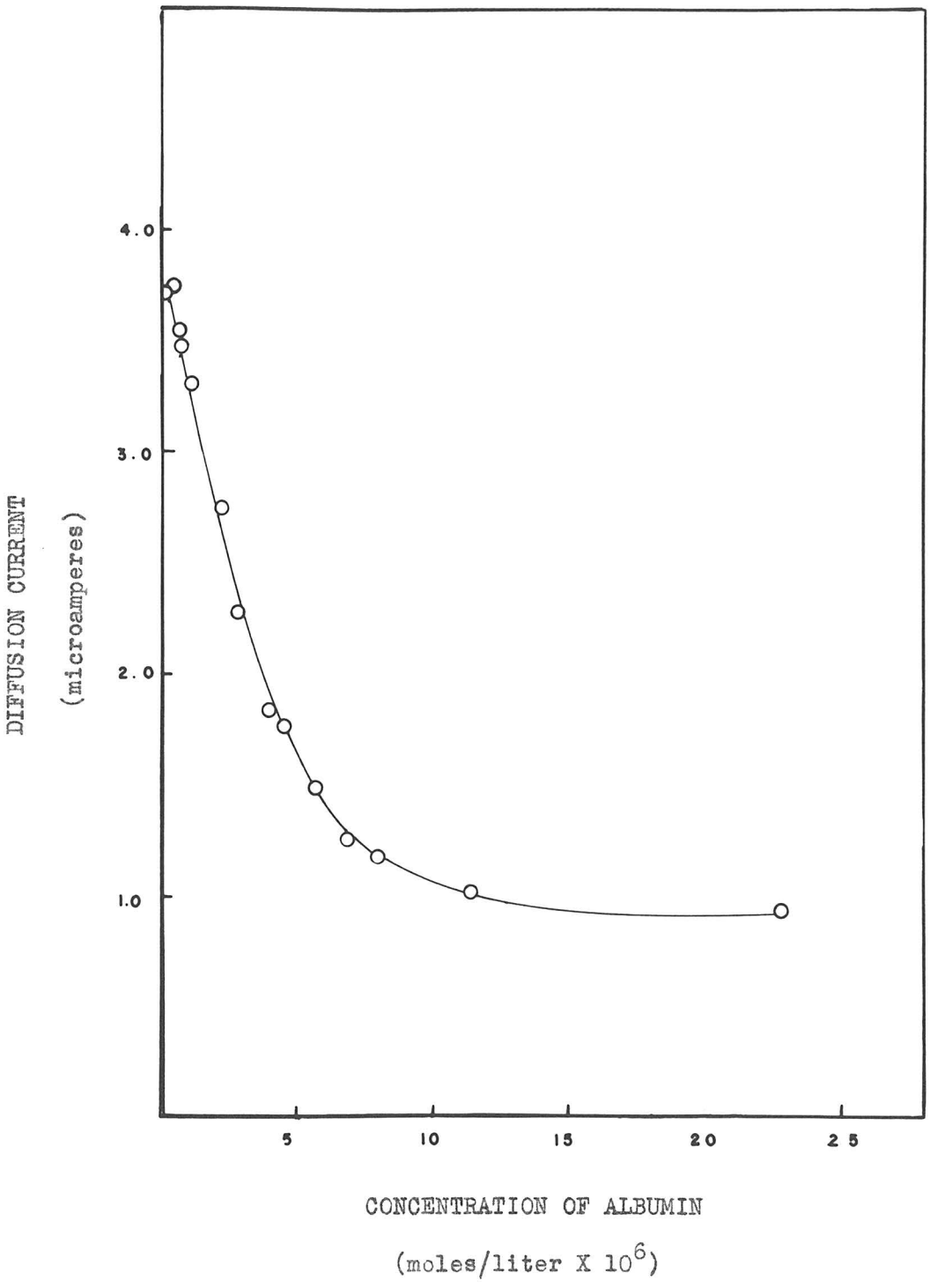


Figure 4: p-Hydroxyphenylazophenylarsonic Acid. The Effect of Increasing Albumin Concentration on the Diffusion Current of the Dye (See Tables III and IV). All solutions are 9.86 X $10^{-4}$ M. in dye, 0.15 M. in NaCl, 0.02 M. in veronal; pH 8

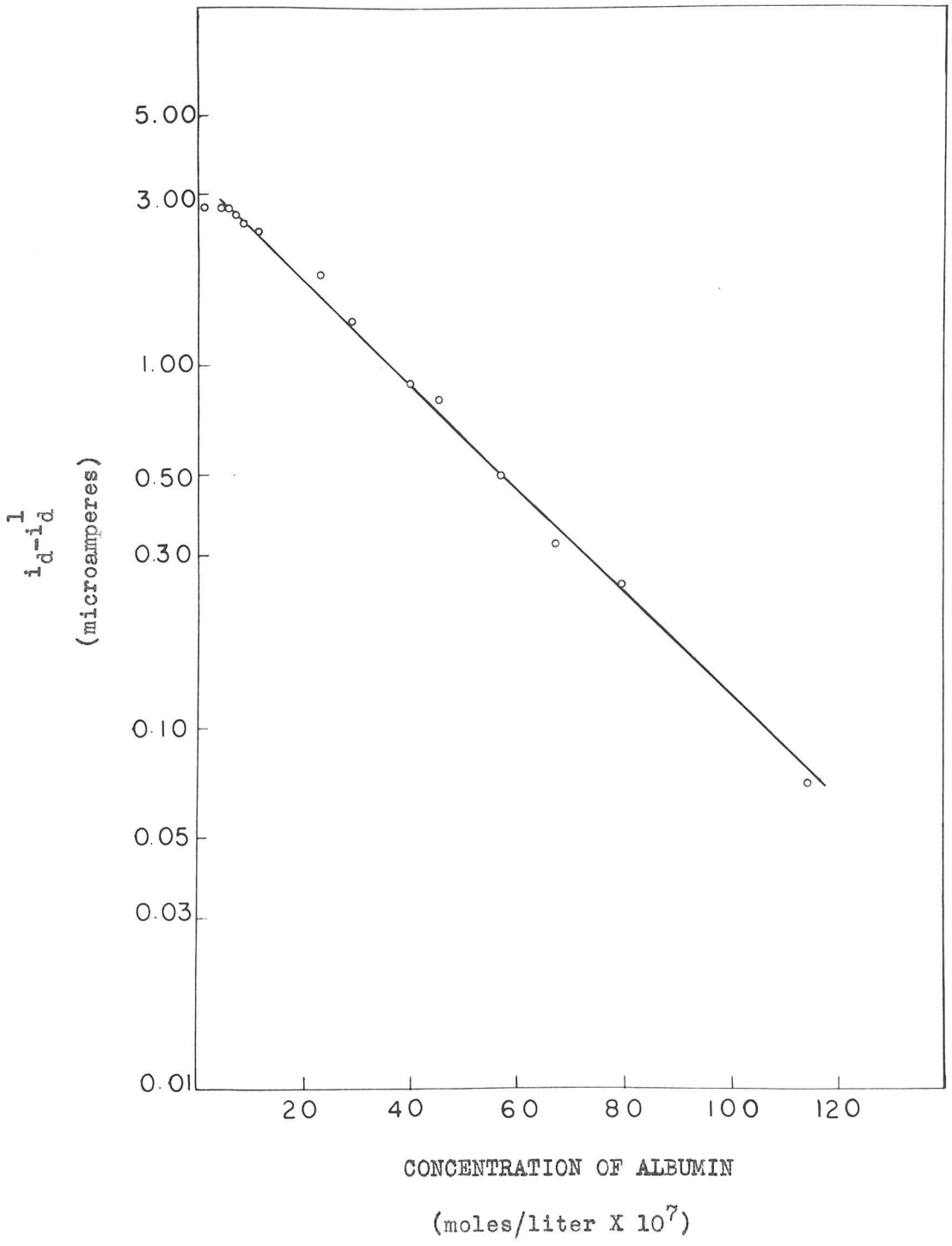


Figure 5: p-Hydroxyphenylazophenylarsonic Acid. The Linear Relationship Between log $(i_d - i_d^1)$ and the Concentration of Protein. All solutions are 9.86 X $10^{-4}$ M. in dye, 0.15 M. in NaCl, 0.02 M. in veronal; pH 8

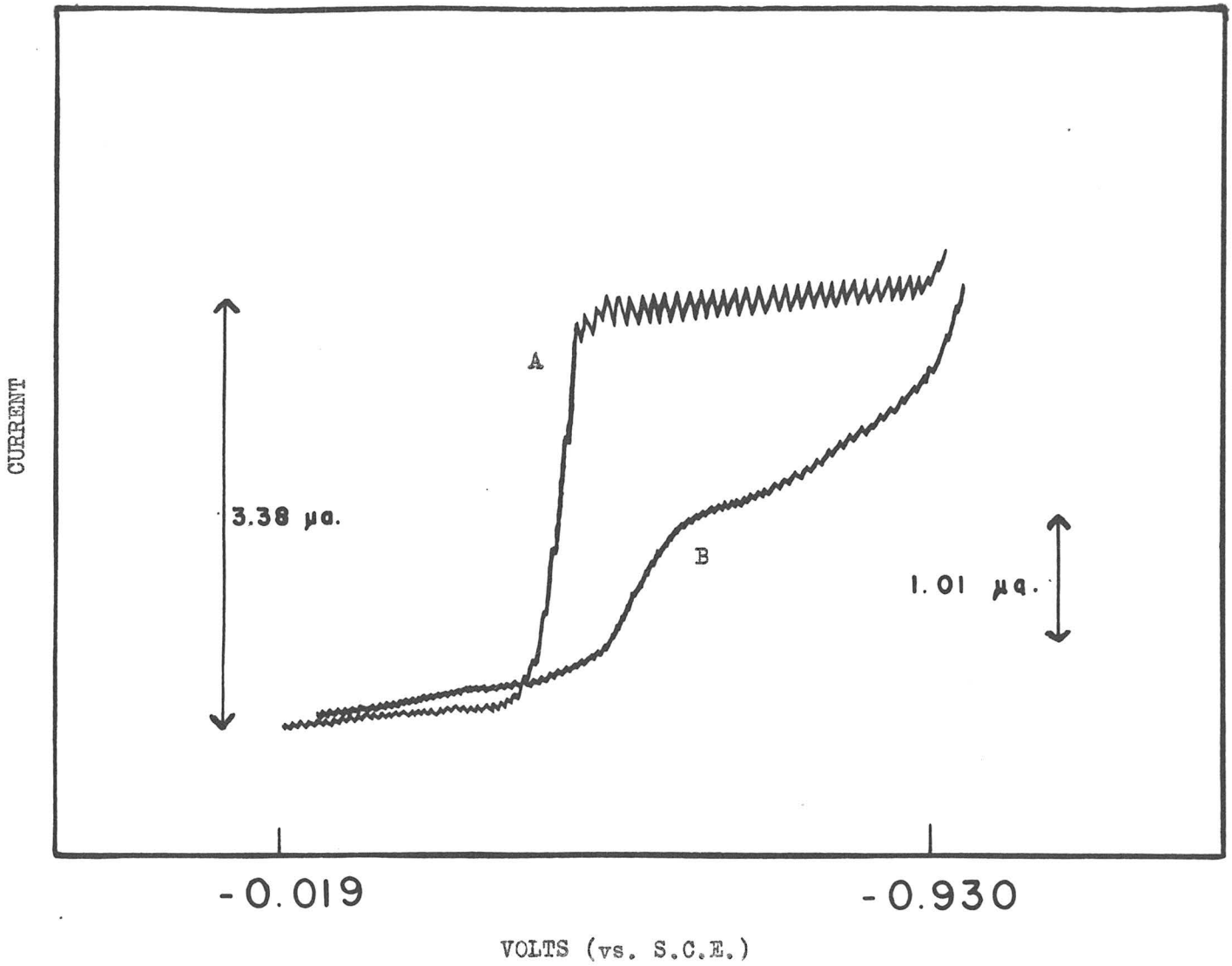


Figure 6: p-Hydroxyphenylazophenylarsonic Acid. A Comparison Between c.-v. Curves Obtained in the Absence and in the Presence of Albumin. Curve A was obtained from a solution 9.06 X $10^{-4}$ M. in dye, curve B from a solution 9.86 X $10^{-4}$ M. in dye and 7.99 X $10^{-6}$ M. in horse albumin. Both solutions were 0.15 M. in NaCl, 0.02 M. in veronal; pH 8

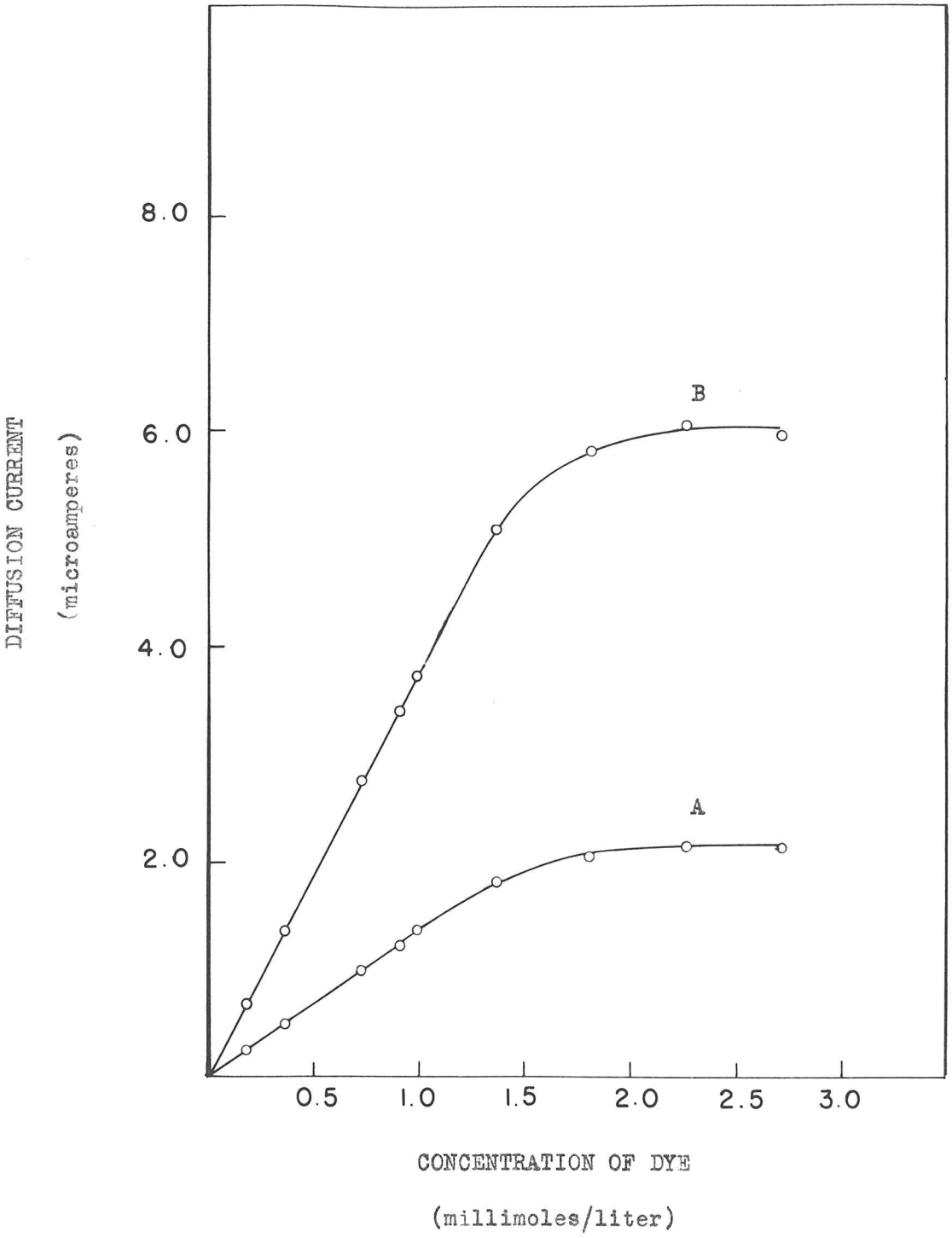


Figure 7: p-Hydroxyphenylazophenylarsonic Acid. The Variation of the Diffusion Current with Concentration of Dye in the Presence (Curve A) and in the Absence (Curve B) of Albumin (See Table V). All solutions were 0.15 M. in NaCl, 0.02 M. in veronal; pH 8. The solutions along curve A were $6.1 \times 10^{-6}$ M. in albumin

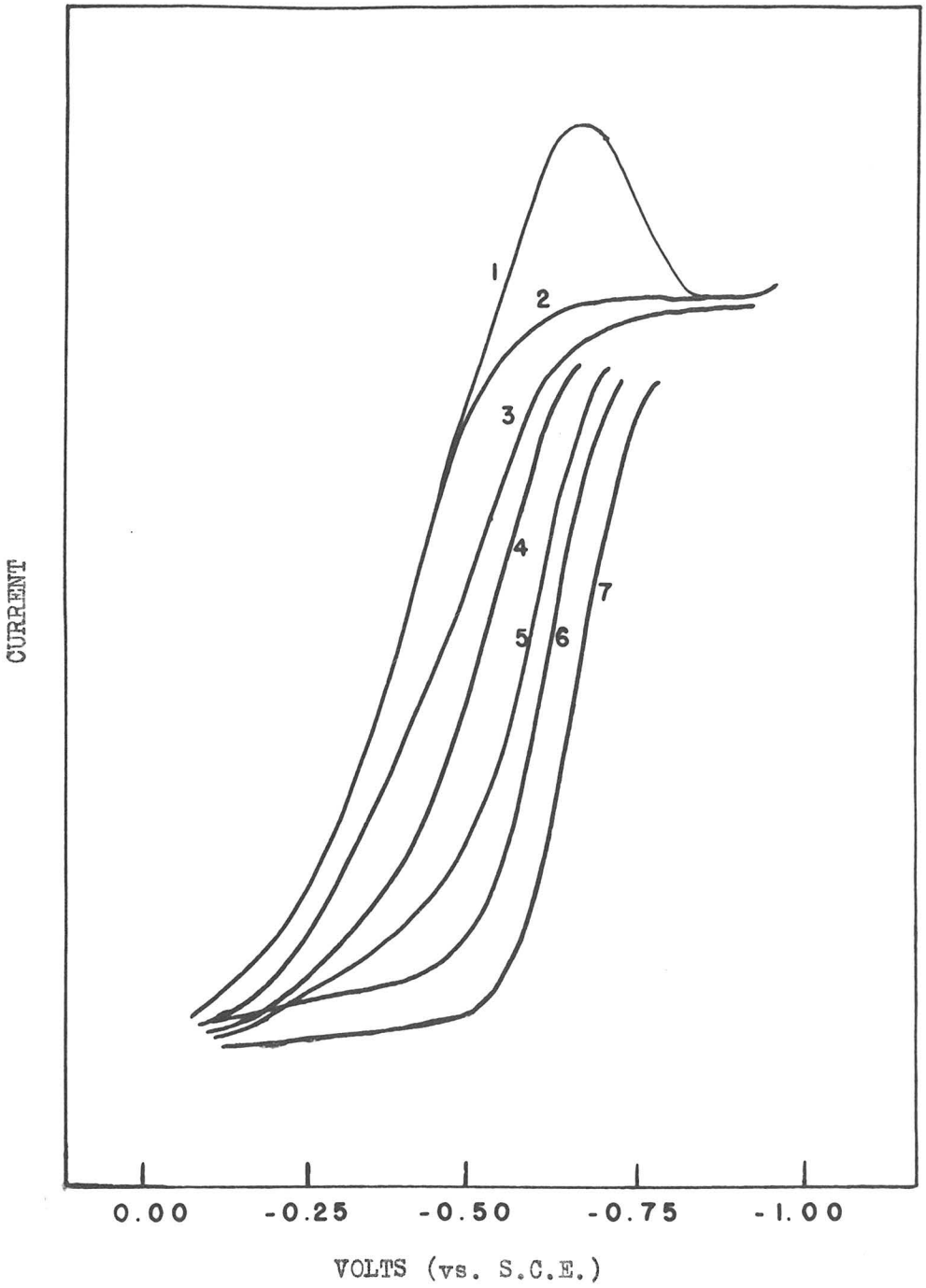


Figure 8: The Effect of Thymol on the c.-v. Curves of Cystine (See Table VI). All solutions are 0.001 M. in cystine, 0.15 M. in NaCl; pH 1 -

The concentrations of thymol are as follows:

1) 0.00 X $10^{-5}$ M.
2) 1.00 X $10^{-5}$ M.
3) 3.00 X $10^{-5}$ M.
4) 9.00 X $10^{-5}$ M.
5) 10.0 X $10^{-5}$ M.
6) 15.0 X $10^{-5}$ M.
7) 20.0 X $10^{-5}$ M.

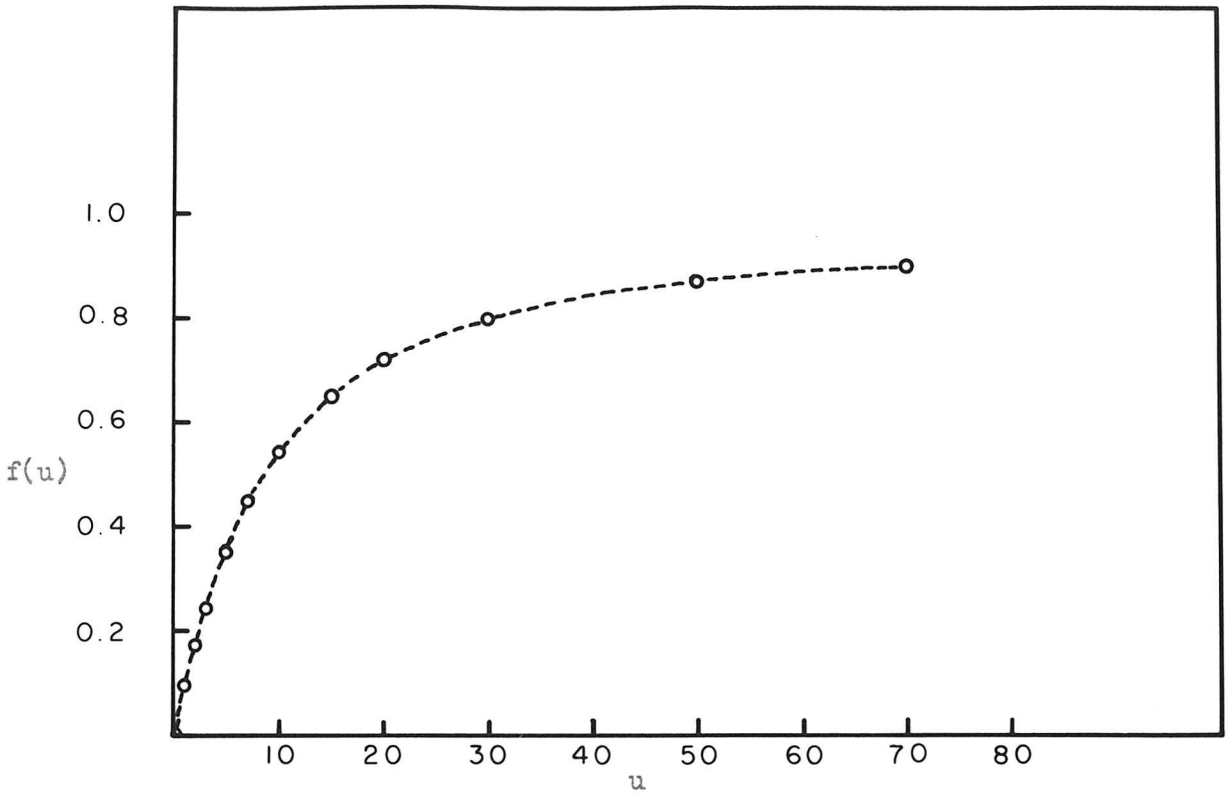


Figure 9: The Variation of the Function f(u) with u. (See Table VII and Equation (20))

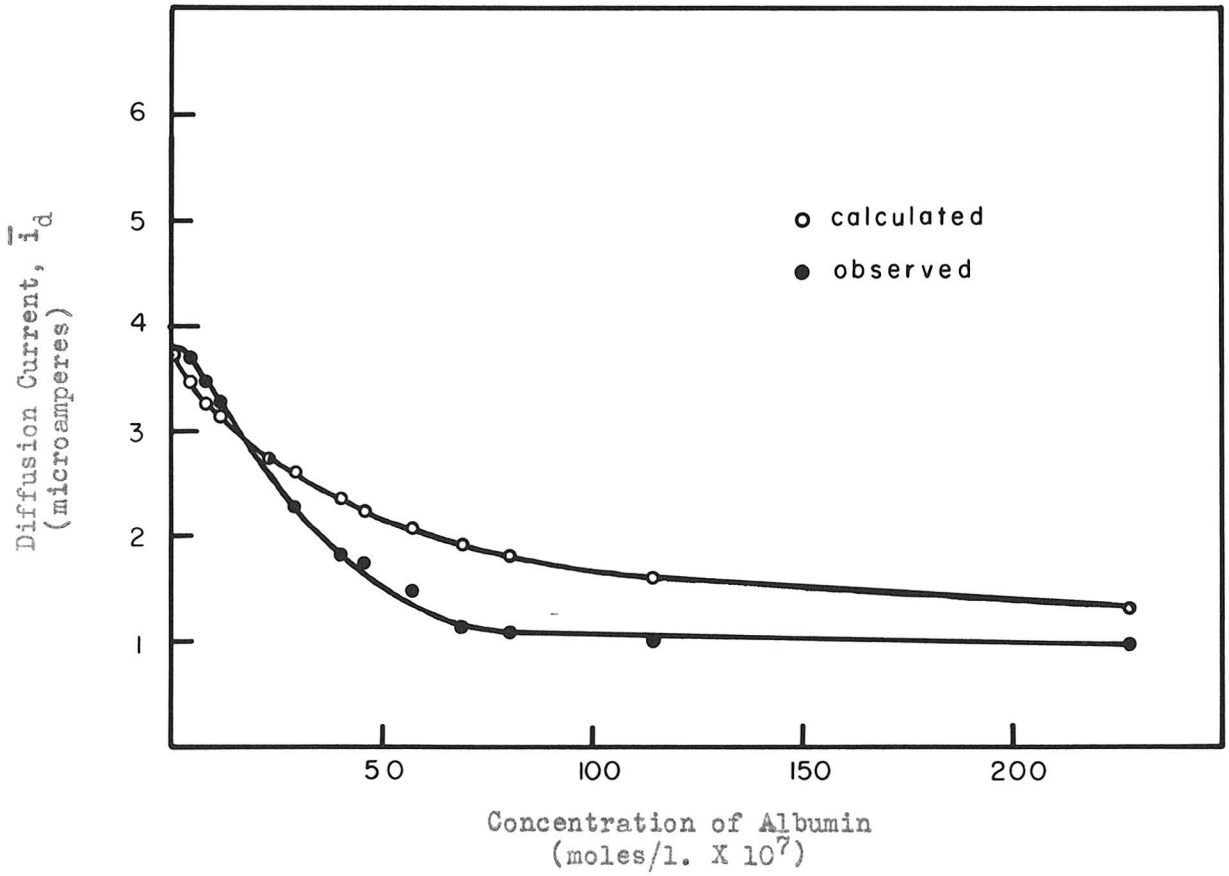


Figure 10: Comparison of the Observed and the Calculated Diffusion Current of HPA as a Function of the Albumin Concentration

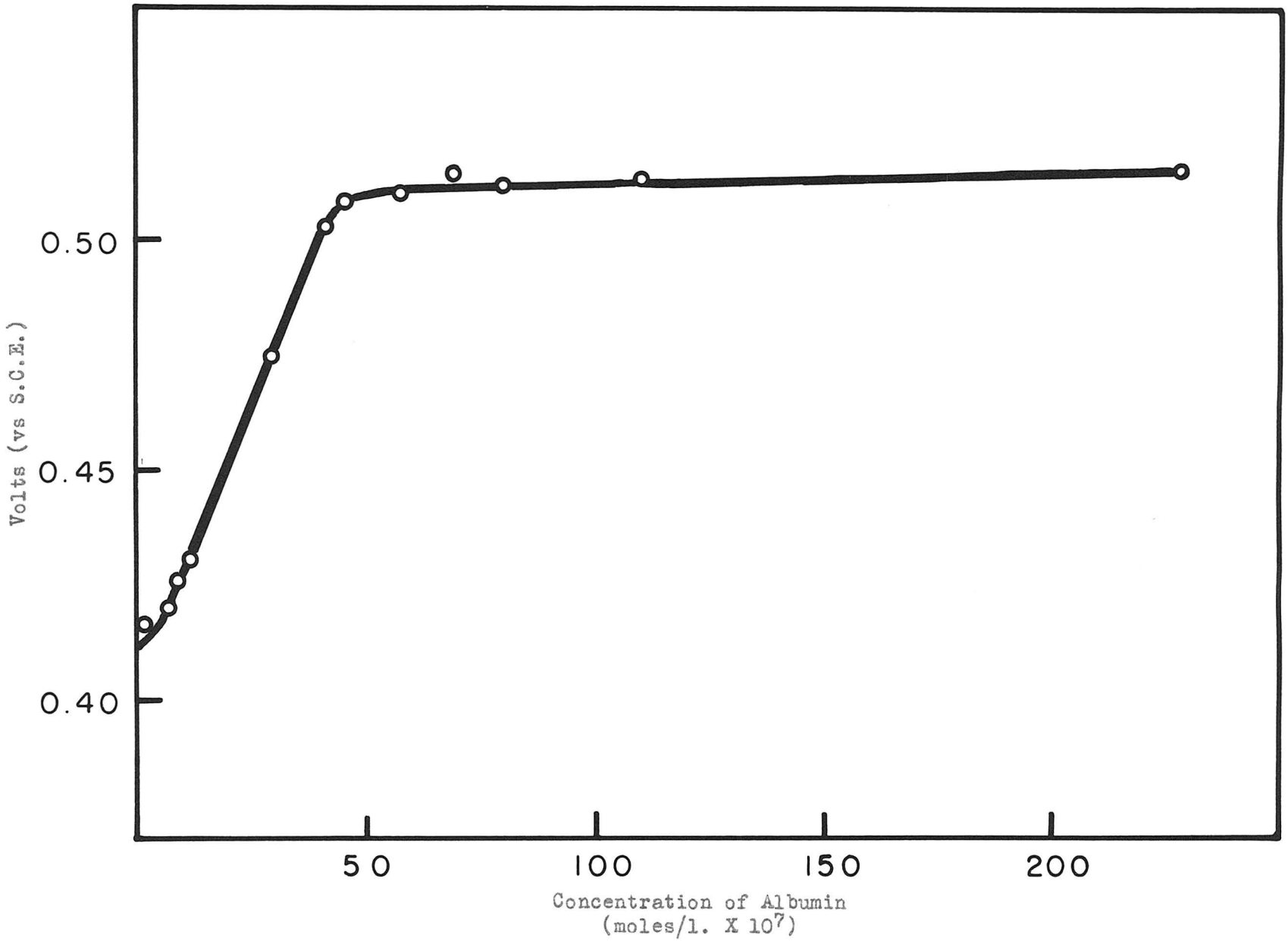


Figure 11: Variation of the Half-Wave Potential of HPA with Change in the Albumin Concentration

# Part II

## The Polarographic Analysis of Nitrite and of Nitrite-Nitrate Mixtures

[Reprinted from the Journal of the American Chemical Society, 68, 2665 (1946).]

CONTRIBUTION FROM THE GATES AND CRELLIN LABORATORIES OF CHEMISTRY, CALIFORNIA INSTITUTE OF TECHNOLOGY, No. 1031]

# The Polarographic Analysis of Nitrite and of Nitrite–Nitrate Mixtures[1]

BY BERTRAM KEILIN AND JOHN W. OTVOS[2]

A method for the polarographic determination of nitrate in the presence of uranyl ion in acid solution has been described by Kolthoff, Harris and Matsuyama.[3] Since in the earlier methods studied by Tokuoka and Ruzicka[4,5] in which other cations were used as "activators," the reduction potentials for nitrate and nitrite were always found to be identical, it was of interest to us to examine the polarographic behavior of nitrite in the presence of uranyl ion.

At the acid concentrations necessary for suppressing the hydrolysis of uranyl ion, all but a few per cent. of nitrite exists as nitrous acid and the similarity between nitrate and nitrite is thus greatly decreased. Nevertheless the waves for the two substances are very similar in appearance and occur at the same potential.

A method for the separate estimation of nitrate and nitrite in solutions containing both ions is described in this paper. Use is made of the additivity of the waves, and of a simple chemical conversion of nitrite to nitrate without the introduction of new ions which might interfere with the determination.

## Experimental

**Apparatus and Materials.**—A Heyrovsky Type XII Polarograph was used in all experiments. Measurements were made at 25°. Dissolved oxygen was removed by passing nitrogen through the solutions. All chemicals were of reagent grade. The sodium nitrite used in quantitative experiments was standardized against permanganate in acid solution, the primary standard being sodium oxalate.[6]

**Decomposition of Nitrous Acid.**—It is known that in cold dilute solutions and in the absence of air nitrous acid decomposes to nitric acid and nitric oxide; in the presence of oxygen, nitric acid alone is produced. Because of the instability of nitrous acid, a polarographic procedure for the determination of nitrite in acid solution must involve some error. Experiments performed in connection with this investigation have shown that in air and at concentrations which are of interest in polarography the decomposition of nitrous acid[7,8] is first order and that about six per cent. decomposes in a half hour at room temperature. If the nitrite solution is polarographed as soon as possible after it is acidified, the error arising from nitrous acid decomposition can be kept below 3%.

**Comparison of the Nitrous Acid and Nitrate Waves.**—Figure 1 shows a nitrous acid wave and a nitrate wave, each obtained with a solution $4 \times 10^{-4}$ $M$ in the nitrous acid[9] or nitrate, $2 \times$

(1) This paper is based in whole or in part on work done for the Office of Scientific Research and Development under Contract OEMsr-881 with the California Institute of Technology.

(2) Present address: Shell Development Company, Emeryville, California.

(3) I. M. Kolthoff, W. E. Harris and G. Matsuyama, THIS JOURNAL, **66**, 1782 (1944).

(4) M. Tokuoka, *Coll. Czechoslov. Chem. Comm.*, **4**, 444 (1932).

(5) M. Tokuoka and J. Ruzicka, *ibid.*, **6**, 339 (1934).

(6) J. S. Laird and T. C. Simpson, THIS JOURNAL, **41**, 524 (1919).

(7) Abel, *Z. physik. Chem.*, **148**, 337 (1930).

(8) Bray *et al.*, *Chem. Rev.*, **10**, 161 (1932).

(9) Concentrations of nitrous acid, as given in this paper, include both un-ionized and ionized forms.

$10^{-4}$ $M$ in uranyl acetate, 0.01 $M$ in hydrochloric acid, and 0.1 $M$ in potassium chloride. The two waves are almost identical in shape. There is no trace of the nitric oxide wave at $-0.77$ volt (*vs.* S.C.E.) reported by Heyrovsky and Nejedly[10] for acid solutions of nitrite, probably because nitrogen was bubbled through the solutions immediately before the polarograms were made.

In neutral or alkaline solutions the reduction potentials of nitrate and nitrite are known to become more positive in the presence of polyvalent cations.[5] This effect has been attributed to the formation of loose "ion pairs" which, because of their positive charge, facilitate the access of nitrate or nitrite to the negative electrode. Presumably the same phenomenon occurs with nitrate in acid solution in the presence of uranyl ion. Nitrous acid, however, is uncharged and should not require the assistance of polyvalent cations for its approach to the cathode. In preliminary experiments in this Laboratory, nitrous acid in the absence of uranyl ion has indeed been found to produce a wave at about $-1.0$ volt (*vs.* S.C.E.), which is approximately the half-wave potential of the uranyl-activated nitrite wave. This wave may correspond to that reported by Schwarz[11] for nitrite in acetic acid solution, which extends from $-0.6$ to $-1.6$ volts. Although the uranyl ion has little effect on the half-wave potential of the nitrous acid wave, its presence causes an increase in the nitrous acid diffusion current.

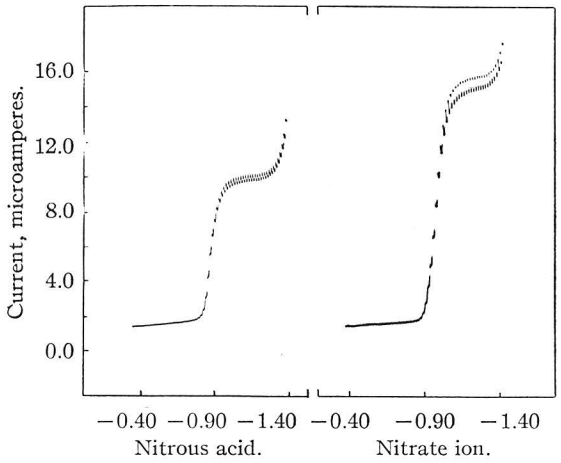


Fig. 1.—Comparison of nitrous acid and nitrate waves. Solutions are 0.1 $M$ in hydrochloric acid, 0.1 $M$ in potassium chloride, $2 \times 10^{-4}$ $M$ in uranyl acetate, and $4 \times 10^{-4}$ $M$ in nitrous acid and nitrate, respectively; $m^{2/3}t^{1/6} = 2.08$ mg.$^{2/3}$ sec.$^{-1/2}$.

The nitrous acid wave shown in Fig. 1 is a little over half as high as the nitrate wave, after correction has been made for the blank uranyl wave. The diffusion current constants for nitrous acid at several concentrations are given in Table I. For the more dilute solutions the concentration of uranyl ion was reduced to $5 \times 10^{-5}$ $M$ from the usual value of $2 \times 10^{-4}$ $M$. Over a hundred-fold concentration range of nitrous acid ($2 \times 10^{-5}$ $M$ to $2 \times 10^{-3}$ $M$), the mean value of $i_d/Cm^{2/3}t^{1/6}$ is 7.45 and the average deviation of the points from the mean is 4.5%. Probably a large part of the deviation is due to the instability of nitrous acid and variations in the time required to run a polarogram.

TABLE I

DIFFUSION CURRENT CONSTANT FOR NITROUS ACID AT 25°

$m^{2/3}t^{1/6} = 2.08$ mg.$^{2/3}$ sec.$^{-1/2}$ at $-1.2$ volts *vs.* S.C.E.; diffusion current is measured at $-1.2$ volts *vs.* S.C.E.; residual current at $-1.2$ volts = 2.00 microamperes

| Concn. of nitrous acid, millimoles/liter, $C$ | Diffusion current of nitrous acid, microamperes, $i_d$ | $K = i_d/Cm^{2/3}t^{1/6}$ |
|---|---|---|
| A. Solutions 0.1 $M$ in KCl, 0.01 $M$ in HCl, and $2 \times 10^{-4}$ $M$ in $UO_2(OOCCH_3)_2$ | | |
| 5.125 | 47.8 | 4.50[a] |
| 2.050 | 31.5 | 7.40 |
| 1.025 | 15.6 | 7.30 |
| 0.820 | 12.3 | 7.20 |
| .512 | 7.52 | 7.06 |
| .205 | 2.92 | 6.87 |
| .102 | 1.56 | 7.35 |
| .082 | 1.17 | 6.87 |
| .0512 | 0.87 | 8.16 |
| B. Solutions 0.1 $M$ in KCl, 0.01 $M$ in HCl, $5 \times 10^{-5}$ $M$ in $UO_2(OOCCH_3)_2$ | | |
| 0.102 | 1.66 | 7.83 |
| .082 | 1.32 | 7.74 |
| .0512 | 0.83 | 7.78 |
| .0205 | .324 | 7.60 |
| .0102 | .214 | 10.1[a] |
| .00512 | .111 | 10.4[a] |
| C. Average diffusion current constant | | 7.45 |

[a] Not included in the average.

The number of electrons involved in the reduction of nitrous acid can be calculated with the use of Ilkovic's equation:

$$i_d = 605nD^{1/2}Cm^{2/3}t^{1/6} \quad (1)$$

where $i_d$ is the average diffusion current obtained at the dropping mercury electrode in microamperes, $n$ is the number of faradays transferred per mole, $D$ is the diffusion coefficient of the reducible substance in cm.$^2$ sec.$^{-1}$, $C$ is its concentration in millimoles per liter, $m$ is the rate of flow of mercury in mg. sec.$^{-1}$ and $t$ is the drop time in seconds. The diffusion current constant, $K = i_d/Cm^{2/3}t^{1/6}$, as given in Table I, is 7.45. The value of $D$ for nitrite ion, calculated from its equivalent conductance,[12] is $1.92 \times 10^{-5}$ cm.$^2$ sec.$^{-1}$. With the assumption that the diffusion coefficient for nitrous acid is the same as that for nitrite ion, $n$ can be calculated from these figures

(10) J. Heyrovsky and V. Nejedly, *Coll. Czechoslov. Chem. Comm.*, **3**, 126 (1931).

(11) K. Schwarz, *Z. anal. Chem.*, **115**, 161 (1939).

(12) Niementowski and Roszkowski, *Z. physik. Chem.*, **22**, 147 (1897).

The value obtained for the electron transfer, $n$, is 2.8 faradays per mole.

Kolthoff, Harris and Matsuyama[3] report a five-electron reduction for nitrate in the presence of uranyl ion. The present result of 2.8 or 3 electrons for nitrous acid indicates that it, as well as nitrate, is reduced to nitrogen at the dropping mercury cathode in acid solution in the presence of uranyl ion.

It is interesting to compare this value of the electron transfer for nitrous acid, $n = 3$, with the value obtained by direct analysis of the nitrous acid wave according to the fundamental equation for a polarographic wave, first derived by Heyrovsky and Ilkovic.[13]

$$E_{d.e.} = E_{1/2} - \frac{0.0591}{n} \log \frac{i}{i_d - i} \qquad (2)$$

In this equation $E_{d.e.}$ and $i$ are corresponding values for the potential of the dropping mercury electrode and the current at any point on the wave, $E_{1/2}$ is the half-wave potential, and $n$ is the number of electrons involved reversibly in the reduction. When $\log i/(i_d - i)$ is plotted against the voltage, a slope is obtained which corresponds to a value of $n = 1$ (Fig. 2). An electron transfer of $n = 1$ was also obtained by Kolthoff, Harris and Matsuyama in an analysis of the nitrate wave, although the over-all reduction of nitrate appears to involve 5 electrons. It may be inferred that, under these conditions, neither the reduction of nitrous acid nor that of nitrate is reversible. A similar effect has been found by Orlemann and Kolthoff[14] in the irreversible reduction of iodate and bromate.

**Solutions Containing both Nitrate and Nitrite Ions.**—In polarograms of solutions containing both nitrate ion and nitrous acid, the diffusion current, above that due to the blank uranyl wave, is the sum of the diffusion currents due to nitrate ion and nitrous acid independently. In Table II, the observed diffusion currents of some solutions containing these ions together are compared with values calculated from the additivity relationship

$$i_d = m^{2/3}t^{1/6}(7.45C_1 + 13.8C_2) \qquad (3)$$

where $C_1$ and $C_2$ are the concentrations of nitrite and nitrate in millimoles per liter and $m$ and $t$ are expressed in the conventional units. The coefficients of $C_1$ and $C_2$ are the experimentally determined diffusion current constants reported here and in the paper of Kolthoff, Harris and Matsuyama.[3]

TABLE II

ADDITIVITY OF NITRATE AND NITROUS ACID WAVES

Solutions 0.1 $M$ in KCl, 0.01 $M$ in HCl, $2 \times 10^{-4}$ $M$ in $UO_2(OOCCH_3)_2$; $m^{2/3}t^{1/6} = 2.08$ mg.$^{2/3}$ sec.$^{-1/2}$

| Concn. of nitrate, millimoles/liter | Concn. of nitrous acid, millimoles/liter | Diffusion current, microamperes Obs. | Calcd. |
|---|---|---|---|
| 0.100 | 0.096 | 4.35 | 4.37 |
| .100 | .192 | 5.75 | 5.86 |
| .100 | .384 | 8.85 | 8.83 |
| .100 | .768 | 14.9 | 14.8 |

(13) J. Heyrovsky and D. Ilkovic, *Coll. Czechoslov. Chem. Comm.*, **7**, 198 (1935).

(14) E. F. Orlemann and I. M. Kolthoff, THIS JOURNAL, **64**, 1044 (1942).

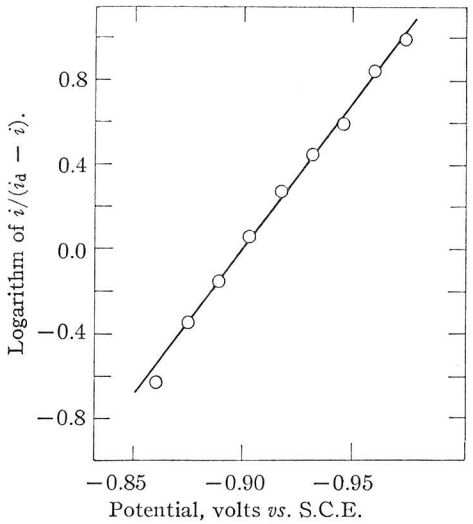


Fig. 2.—Analysis of nitrite reduction wave in 0.1 $M$ potassium chloride, 0.01 $M$ hydrochloric acid and $2 \times 10^{-4}$ $M$ uranyl acetate.

From a single polarogram of a solution containing uranyl ion, only a figure representing the weighted sum of nitrous acid and nitrate concentrations can be obtained. To obtain the concentrations of the substances separately by the methods described above it is necessary to run another polarographic experiment on an aliquot of the solution after altering the relative amounts of the two substances in a known way. It is convenient to do this by transforming one of them quantitatively to the other. A satisfactory and convenient method of achieving this transformation is the quantitative oxidation of nitrite to nitrate by hydrogen peroxide in acid solution.

$$HNO_2 + H_2O_2 \longrightarrow NO_3^- + H^+ + H_2O$$

If the solution is then made basic, the excess peroxide may be catalytically decomposed with manganese dioxide. The only products of these two reactions that remain in solution are nitrate, water and oxygen; no new ionic species are produced. The uranyl ion must not be added until the reactions described above are completed and the solution is again acidified.

A polarogram of the oxidized solution, after the addition of uranyl acetate, potassium chloride and hydrochloric acid in the usual concentrations, gives a diffusion current

$$i_d' = 13.8m^{2/3}t^{1/6}(C_1 + C_2) \qquad (4)$$

since all of the nitrite has been converted to nitrate. From equations (3) and (4), the separate concentrations $C_1$ and $C_2$ of nitrite and nitrate, respectively, can be calculated.

$$C_1 = \frac{i_d' - i_d}{6.35m^{2/3}t^{1/6}} \quad (5)$$

$$C_2 = \frac{i_d'}{13.8m^{2/3}t^{1/6}} - C_1 \quad (6)$$

**Procedure for the Polarographic Determination of Nitrite.**—For the determination of nitrite in solutions where its concentration is between $5 \times 10^{-5}$ and $5 \times 10^{-3}$ $M$, the following procedure is recommended.

Prepare two stock solutions, one being 0.2 $M$ in potassium chloride, 0.02 $M$ in hydrochloric acid, and $4 \times 10^{-4}$ $M$ in uranyl acetate; the other having the same composition except that it is only $1 \times 10^{-4}$ $M$ in uranyl acetate.

Dilute 25.00 ml. of the uranyl acetate stock solution to 50.00 ml. with redistilled water, bubble with nitrogen gas to make oxygen-free, and measure the apparent diffusion current due to the reduction of uranyl ion at a potential of −1.2 volts *vs.* S.C.E. This current is taken as the "blank" or "residual" current for the nitrous acid wave.

Measure a suitable volume of an unknown nitrite solution into a 50-ml. volumetric flask, add 25.00 ml. of the appropriate uranyl acetate stock solution and dilute to volume with redistilled water. (It may be necessary to make a preliminary run in order to determine the concentration of uranyl ion to be used. In general, if the final concentration of the nitrite ion is to be above $1 \times 10^{-4}$ $M$, the stock solution containing the higher concentration of uranyl acetate is used. If the concentration is below this value, the one containing the lower concentration is employed.) Make the resulting solution oxygen-free and measure the apparent diffusion current at a potential of −1.2 volts *vs.* S.C.E. Subtract the "residual" current due to the reduction of uranyl ion from the diffusion current to obtain the diffusion current due to nitrous acid. The amount of nitrite in the unknown solution can be found from this diffusion current by referring to a standard curve, which is constructed by plotting diffusion current against concentration. Such a plot is prepared with data, such as are given in Table I, that are obtained with known solutions.

**Analysis of Solutions Containing Both Nitrate and Nitrite.**—Divide the solution to be analyzed into two equal portions. Add to the first portion 25.00 ml. of the appropriate uranyl acetate stock solution, and dilute to 50.00 ml. with redistilled water. Make the resulting solution air-free, measure the apparent diffusion current, and subtract the "residual" current as described above to obtain the total diffusion current due to nitrate ion and nitrous acid. To the second portion, add 2 $N$ hydrochloric acid until it is just neutral and then add an excess of five drops. Add 1 ml. of 30% hydrogen peroxide and allow the mixture to stand at room temperature for thirty minutes. Add eight drops of 2 $N$ sodium hydroxide and then introduce a small quantity of manganese dioxide. After the evolution of gas has ceased, decant the solution quantitatively into a 50-ml. volumetric flask. Add three drops of 2 $N$ hydrochloric acid and then 25.00 ml. of the appropriate uranyl acetate stock solution, and dilute to volume. Measure the apparent diffusion current as before, and again subtract the "residual" current. From the two values of the diffusion current thus obtained, the concentrations of nitrite and nitrate originally present in the unknown solution may be calculated as described above.

**Interferences.**—In general, interferences which have been described for the estimation of nitrate[3] will also be encountered in this determination. The presence in solution of substances such as strong bases and phosphates, which precipitate the uranyl ion, or complex-formers such as citrate or tartrate will interfere, as will also those substances, such as oxalates and strong acids, which discharge at voltages near to that of nitrous acid. Sulfate ion in a concentration twenty times that of the nitrite was found to reduce the wave height somewhat.

**Acknowledgment.**—We wish to express our thanks to Mr. F. D. Ordway of this Laboratory for his kind assistance in carrying out the chemical analyses necessary for this work. We are also greatly indebted to Mr. Joseph C. Guffy of the University of Wisconsin for his interest in this problem and for many most helpful conversations on the subject.

## Summary

1. In the presence of uranyl ion, nitrous acid in dilute solutions of hydrochloric acid is reduced at the same potential at which nitrate is reduced (*ca.* −1 volt *vs.* S.C.E.). The diffusion current is proportional to the nitrous acid concentration when the ratio of uranyl ion to nitrous acid is above a critical minimum. The reduction of nitrous acid under these conditions involves three electrons, indicating a reduction to nitrogen, but analysis of the wave shows that the reduction is irreversible.

2. A solution containing both nitrate and nitrite ions can be analyzed for both constituents in two polarographic experiments. First, the diffusion current due to the two constituents in the original solution is measured. With another aliquot, the nitrite present is oxidized to nitrate and the diffusion current of the resulting solution is measured as before. The nitrite can be conveniently oxidized by hydrogen peroxide in acid solution, and the excess peroxide can be destroyed catalytically by manganese dioxide in basic solution.

3. Interferences are similar to those encountered by Kolthoff, Harris and Matsuyama[3] in the analysis of nitrate solutions, except that large amounts of sulfate seem to reduce the diffusion current.

PASADENA, CALIFORNIA RECEIVED JULY 18, 1946

# Part III

## An Electron Diffraction Investigation of the Structure of Some Organic Molecules

a) Some Cyclic Derivatives of Ethylene Glycol

b) Naphthalene and Anthracene

# AN ELECTRON DIFFRACTION INVESTIGATION OF THE STRUCTURE OF SOME ORGANIC MOLECULES

Part III of this thesis is devoted to an account of the results obtained in a series of molecular structure determinations by the electron diffraction method. It is convenient to describe the five compounds which were investigated in two sections. Section (a) is given to the structure determinations of ethylene glycol sulfite ester, ethylene glycol chlorophosphite ester, and ethylene glycol acetal, and section (b) to those of naphthalene and anthracene. The account of the work is preceded by a brief description of the electron diffraction method as practised in these laboratories.

The electron diffraction apparatus has been described by Brockway:[1] A collimated beam of electrons originating from a hot tungsten filament and accelerated through a potential drop of approximately 40,000 volts is allowed to intersect a stream of gas emanating from a pinhole in a nozzle placed just below the path of the beam. The electrons interact with the molecules of the gas and then fall upon a flat photographic plate which, after development, shows a radially symmetric diffraction pattern that to the eye appears to consist of a series of alternate maxima and minima.

The diffracted intensity, which is a function of the scattering angle, may be described as the resultant of the contributions from the incoherent and the atomic scattering, which are structure insensitive and decline monotonically with increasing angle, and from the molecular

scattering, which is the particular component of interest in the determination of the structure of the molecule. The intensity of this rapidly varying component of the diffraction pattern is estimated as a function of the angle of scattering by visual examination of the photographs, whereby the observer, consciously aiding the contrast-sensitive properties of his eye, separates this component of the total intensity from the rest. The observations are interpreted in accordance with the appearance of the photographs and in a manner such that the resultant "visual curve" will prove useful in comparing the experimental data with theoretical calculations made in accordance with the reduced intensity function,

$$I(q) = \frac{K}{\sum_i (Z_i - f_i)^2} \sum_i \sum_{i \neq j} \frac{(Z_i - f_i)(Z_j - f_j)}{r_{ij}} \sin\left(\frac{\pi r q}{10}\right), \qquad (1)$$

where $r_{ij}$ is the value assigned to the distance between the $i^{\underline{th}}$ and $j^{\underline{th}}$ atoms in the molecule, K is a constant, $Z_i$ is the atomic number and $f_i$ the x-ray form factor of the $i^{\underline{th}}$ atom, and $q = 40/\lambda \sin \theta/2$ (where $\theta/2$ is the angle of diffraction and $\lambda$ is the wave length of the electrons.)

In the interpretation of the experimental data, it is customary to use the radial distribution method[2,3] in order to obtain a probability distribution of the distances in the molecules. The radial distribution integral, approximated by a summation, provides a direct method for determining the frequency of the terms contributing to the intensity pattern described by equation (1); from the frequency of these terms, the interatomic distances occurring in the molecule may be deduced. The radial distribution function (RDI) is calculated from the equation,

$$rD(r) = \sum_{q=1}^{q_{max}} I_o(q)\, e^{-aq^2} \sin \frac{\pi rq}{10} , \qquad (2)$$

where $I_o(q)$ is an intensity function taken from the visual curve; a is usually so adjusted that $e^{-aq^2} = 0.1$ at $q = q_{max}$. The unobservable first maximum in the visual curve is first estimated roughly and is finally drawn to agree approximately with that of the theoretical intensity curves. Generally, models of the molecule in which the interatomic distances disagree with the information obtained from the RDI may be regarded immediately as representing incorrect structures.

For a final determination of the molecular structure and for an estimation of the probable limits of error, the correlation method is used.[4] Theoretical intensity functions, I(q), are calculated from equation (1) or (for molecules in which the atoms do not differ widely in atomic number) from the simplified theoretical scattering formula,

$$I(q) = K \sum_{i} \sum_{j}' \frac{Z_i Z_j}{r_{ij}} e^{-b_{ij}q^2} \sin \left(\frac{\pi rq}{10}\right) , \qquad (3)$$

where the symbols are those defined in the preceding discussion, except that the value assigned for the atomic number of hydrogen is 1.25. This value is required for $q < 15$ because of the substitution of $Z_i Z_j$ for $(Z_i - f_i)(Z_j - f_j)/\overline{(Z_i - f_j)^2}$ and is tolerable otherwise because of the temperature factor, $e^{-b_{ij}q^2}$, which is active in the terms of the summation corresponding to X. . .H distances. The temperature factor is applied to account for thermal vibrations which vary the interatomic distances somewhat about their mean value. The value given to b is usually 0.00016 for bonded X–H terms, 0.0003 for X—H terms through one angle, and in cyclic compounds,

zero for all other terms. X. . .H terms through more than one angle and H. . .H terms are usually omitted from the summation. Calculations involving the use of equations (1), (2) and (3) are made with punched cards on International Business Machines.[5]

The theoretical intensity curves calculated by equations (1) and (3) are compared with the visual curve; those which in the opinion of the observer are an acceptable representation of the appearance of the photographs usually fall within an ellipsoidal or hyperellipsoidal volume in parameter space if the structure can be determined uniquely. From this region of acceptability, the observer estimates the limits of error for each parameter and chooses the model which he believes to represent best the structure of the molecule. If the structure cannot be determined uniquely by the electron diffraction method, it is necessary to deal with two or more ellipsoidal volumes in parameter space. The estimation of the best model and of the limits of error completes the determination.

a) Some Cyclic Derivatives of Ethylene Glycol

A number of new compounds, involving hitherto unknown ring systems, were synthesized by Majima and Simanuki and by Lucas, Mitchell and Scully. Among these are ethylene glycol sulfite ester (I),[6] ethylene glycol chlorophosphite ester (II)[7,8] and ethylene glycol acetal (III).[9]

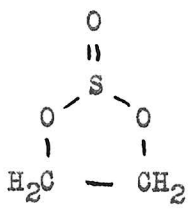

(I)

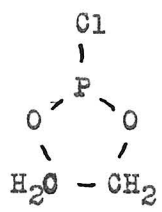

(II)

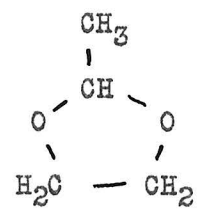

(III)

The interest in the molecular structure of these compounds centers about several points. They present new ring systems for investigation with respect to the planarity of the atoms and in addition offer an opportunity to the structural chemist for measuring some interatomic distances (e.g., single-bond sulfur-oxygen) which are not commonly found in molecules. To the organic chemist, the spatial configuration of the molecules (I), (II), and (III) is of interest with respect to the possibility of preparing geometric isomers of homologous derivatives. Compounds of the type (IV), for example should form geometrical isomers if atom X or atom Y is not coplanar with the remaining atoms in the ring.

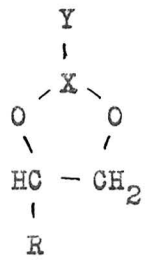

(IV)

R = any group other than H

In this investigation, some assumptions were made in calculating theoretical intensity curves for correlation with the visual curve. The general assumptions are described here and any special ones are presented below in connection with the compounds to which they apply. The bonded C-H distance was taken to be 1.09 Å. with a temperature factor applied as described previously. The plane of H-C-H was taken to be normal to that of C-C-O and to bisect the angle. Unless specific evidence could be obtained from the data, the angle C-C-H was adjusted by the method of least strain in which the deviation from $109^{\circ}28'$ is held constant for all angles about a particular carbon atom.

With the assumption that a plane of symmetry exists in the molecules, the structure of each may be completely described by the specification of three bond angles and four bond distances. Of the four bond distances, only three (expressed as ratios to the fourth) need be considered as parameters in determining the shape of the molecule. The fourth distance (the size parameter) is determined at the very last by a comparison of the positions of the main features in the visual curve with those in the best theoretical curve. Although the number of parameters is reduced to six, a complete determination of the limits of error by the correlation method still involves an almost impossibly long procedure. Consequently, in order to reduce further the number of necessary calculations, maximum use was made of the information to be obtained from the radial distribution function, and of some rational assumptions which were compatible with experience in the study of molecular structure. In the geometrical models considered, the bonded carbon-carbon and carbon-oxygen distances were arbitrarily assigned the value which was indicated in the respective RDI, and the group $O_{C-C}^{O}$ was taken to be coplanar. Other assumptions were made in the individual cases. Models were considered in which the remaining parameters were subjected to a systematic variation about the values obtained from the RDI. Theoretical intensity functions were calculated on the basis of these models, a "best fit" to the visual curve was obtained and a tentative set of the limits of acceptable variation of each of the parameters was determined on the basis of a qualitative comparison of the calculated curves with the visual curve. It was desired, furthermore, to extend these limits to include some measure of the possible errors incurred in arbitrarily fixing some of the shape parameters. Consequently, each

previously fixed parameter was assigned a "working deviation" from the fixed value; each was varied in turn by approximately this amount in a model having the other distances corresponding to those in the best curve obtained in the previous correlation procedure. The effects of these variations on the chosen calculated curve were noted and the tentative limits assigned previously to the determined parameters were revised to include the sum of these effects and to include an estimate of the experimental and random errors inherent in the method. Hence, the final statement of the limits of acceptable variation are to be interpreted as follows: if the arbitrarily fixed parameters are correct within the assigned working deviation, the limits of error of the determined parameters are as reported in the investigation. Thus the conclusions as to the limits of error of the structural parameters which were measured have been arrived at with a consideration of the validity of the assumptions which were made in their determination.

## EXPERIMENTS AND RESULTS

### i - Ethylene Glycol Sulfite Ester

The sample of ethylene glycol sulfite ester used in this investigation was prepared by Mrs. G. Guthrie by the action of thionyl chloride on ethylene glycol in methylene chloride solution.[6,9] The compound hydrolyzes rapidly in water and boils at 169-172°C. Purification was effected by vacuum distillation, and the fraction boiling at 61.2-61.8°C./12 mm. (uncorr.) was used in the electron diffraction experiments. The sample was admitted to the diffraction chamber through the standard high temperature nozzle which was maintained at approximately 100°C. The jet-to-film distance was 11.00 cm. The wave length of electrons in the present work was 0.06085 Å., determined against zinc oxide smoke.[10] The photographs showed features extending to q values of about 100.

The radial distribution function R of Figure 1 has strong maxima at 1.08, 1.42, 1.63, 2.46, and 2.95 Å. These distances are in complete agreement with a model of ethylene glycol sulfite ester in which the angle O-C-C is 111°, the ring oxygens and carbons are coplanar and the bond distances are as follows:

| | | |
|---|---|---|
| S - O | 1.64 Å. | (Single bond) |
| S = O | 1.42 | (Double bond) |
| C - O | 1.42 | |
| C - C | 1.52 | |
| C - H | 1.09 | |

However, the position of the sulfur atom relative to the assumed $^{O}\!\diagdown_{C - C}\!\diagup^{O}$

plane is not located definitely by the RDI. The peak at 2.95 Å. may correspond either to the sulfur-hydrogen distance in a model in which the ring system is entirely coplanar (B of Figure 1) or to the oxygen-carbon distance (through two angles) in a model in which the plane of O-S-O makes an angle of about 30° with that of O-C-C-O (C of Figure 1). The two theoretical intensity curves (B and C) were distinguishable only by an incipient doubling in the last maximum of curve A, the absence of which was felt to be confirmed upon reexamination of the photographs. The ring was assumed to be planar,* the C-H and S-H distances were fixed at 1.09 and 2.95 Å., respectively, and the ratios $\frac{C-C}{S=O}$ and $\frac{C-O}{S=O}$ were assumed to be $\frac{1.52}{1.42}$ and $\frac{1.42}{1.42}$, values which were in good agreement with the RDI peaks and with the results obtained for similar distances in other molecules.** The parameters S-O, ∠ C-C-O, and ∠ O-S=O were subjected to a systematic variation about the values indicated for them in the RDI. Some

---

* The author feels that this conclusion is somewhat uncertain since the region in which the difference occurs is low in intensity and difficult to interpret. In addition, there could probably be found a small change in some other parameter of the non-planar model which would bring the last feature back to coincidence with the visual curve without materially altering the rest of the curve. If non-planarity of the ring were proved, however, other results which are reported more definitely in this paper would not necessarily be invalidated, as the effect (on the other curves) of moving the sulfur atom out of the plane would undoubtedly be equally small.

** The value of 1.52 Å. is somewhat shorter than that usually accepted for the carbon-carbon bond distance. In order to account for the strength of the peak at 1.42 Å. in the RDI (compared to that at 1.63 Å.), it was necessary to take equal values for the S=O and C-O distances at 1.42 A., and to take a shorter distance for C-C than is usually found. It is of interest that in similar oxygen-containing compounds, the C-C distance may also be slightly short; viz., 1.51 ± 0.02 A. in diethyl ether,[11] 1.51 ± 0.03 A. in dioxane,[11] and 1.52 ± 0.02 A. in ethylene glycol.[12]

theoretical intensity functions are shown in Figure 1. Those based upon models in which ∠ O-C-C is 108° are characterized by too low an intensity in the region between q = 30 and q = 60 (D and E), whereas those based on models with ∠ O-C-C = 114° (I and J) are likewise unsatisfactory because of a common lack of prominence of the fourth maximum and also because of a doubled ninth minimum in place of the pronounced shelf which lies between the seventh maximum and the ninth minimum in the visual curve. A good fit to the visual curve is afforded by curve G, which corresponds to a model with S-O = 1.64 Å., ∠ C-C-O = 111°, and ∠ O-S=O = 106°.

In models corresponding to G, the previously fixed parameters were varied in turn by a small amount as described in the introduction to this section. The resultant curves are exemplified by K in which the C-C distance is increased by 0.01 Å. No material change may be noted. However, combined changes in these previously fixed parameters bring about variations in the theoretical intensity curves similar to those which occur as a result of changing the angle O-S=O, and to a lesser extent of changing the S-O distance. Consequently, upward revision of the error limits for these determined parameters was required.

An attempt was made to establish the rigidity of the O-S=O angles by assuming an entirely coplanar average structure in which the oxygen atom outside the ring vibrates symmetrically above and below the plane. This effect was simulated by applying appropriate temperature factors to the terms corresponding to distances which would be affected by such a vibration. It was concluded that though showing improvement in the relative width of the ninth and tenth maxima, these models are

outside the region of acceptability because of the incipient doubling of the eighth maximum in comparison with the seventh maximum and because of the shift in position of several of the main features. Similarly, models were calculated (A) in which the oxygen atom outside of the ring vibrates about the mean position assigned in Model G, in which the S=O bond makes an angle of 67° with its projection on the plane of the ring. Curve A is considered acceptable despite the disagreement with the visual curve in the last maximum; this discrepancy is not considered sufficient to rule out models of this type (see footnote page 74).

The values assigned to the structural parameters of ethylene glycol sulfite ester on the basis of this investigation and the probable limits of error are as follows:

| | | |
|---|---|---|
| C-H | 1.09 Å. | (assumed) |
| S-H* | 2.95 | |
| C-C* | 1.52 | (± 0.03 Å.) |
| C-O* | 1.42 | (± 0.02 Å.) |
| S=O* | 1.42 | (± 0.02 Å.) |
| S-O | 1.64 ± 0.05 Å. | |
| ∠ C-C-O | 111 ± 2° | |
| ∠ O-S O | 106 ± 3° | |

* These are the parameters fixed in the correlation procedure, the values for which are taken from the RDI. The quantities in parentheses are the variations of these distances within which the stated limits of error of the determined parameters hold.

The agreement between the intensity function for this model (which is based on a planar configuration of the ring) and the visual curve is shown (Table I) by a comparison of the positions of the main features. A non-planar ring structure is not definitely excluded.

Table I

Ethylene Glycol Sulfite Ester

| Min | Max | $q_{obs}$ | $q_G$ | $q_G/q_{obs}$ |
|---|---|---|---|---|
| 1 | | 7.77 | 7.3 | 0.940* |
| | 1 | 10.46 | 9.5 | 0.908* |
| 2 | | 13.59 | 12.0 | 0.883* |
| | 2 | 17.90 | 17.6 | 0.983 |
| 3 | | 22.96 | 22.8 | 0.993 |
| | 3 | 26.82 | 27.1 | 1.011 |
| 4 | | 31.40 | 31.3 | 0.997 |
| | 4 | 34.66 | 34.2 | 0.987 |
| 5 | | 38.50 | 38.4 | 0.997 |
| | 5 | 42.75 | 42.8 | 1.001 |
| 6 | | 46.92 | 46.9 | 1.000 |
| | 6 | 50.42 | 50.5 | 1.001 |
| 7 | | 54.50 | 54.7 | 1.004 |
| | 7 | 59.18 | 59.8 | 1.010 |
| 8 | | 66.49 | 66.8 | 1.005 |
| | 8 | ----- | ---- | ----- |
| 9 | | 69.76 | 70.6 | 1.012 |
| | 9 | 75.54 | 75.3 | 0.996 |
| 10 | | 82.26 | 80.8 | 0.981 |
| | 10 | 88.68 | 88.8 | 1.001 |
| 11 | | 95.44 | 95.3 | 0.998 |
| | | | Average (17 features) | 0.999 |
| | | | Average deviation | 0.007 |

* Not included in average

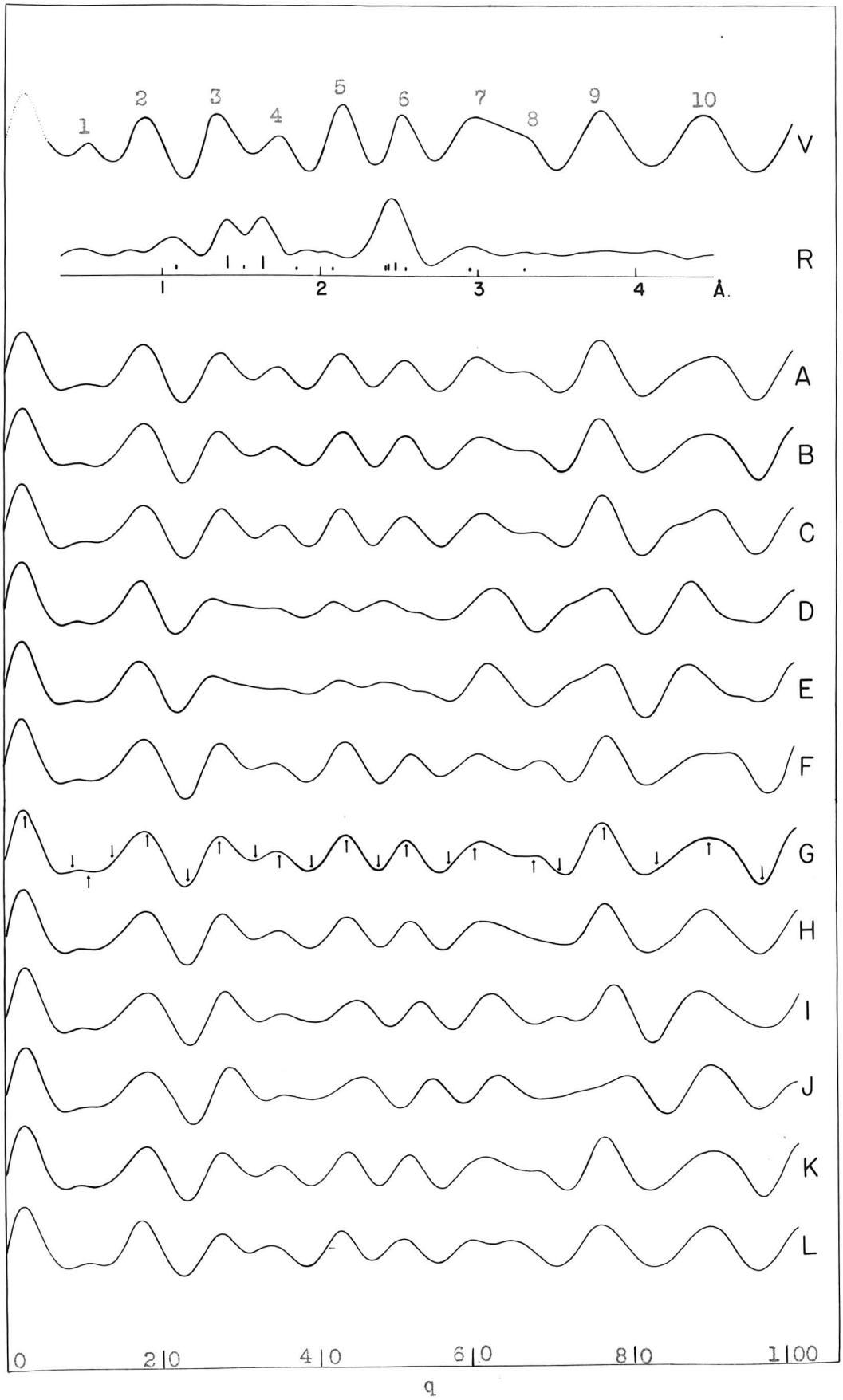


Figure 1: Electron Diffraction Curves for Ethylene Glycol Sulfite Ester

Table of Parameters (Figure 1)

Ethylene Glycol Sulfite Ester

| Model | S=O | S–O | C–C | ∠ C–C–O | ∠ O–S=O | ∠ C–O–S |
|---|---|---|---|---|---|---|
| | | Å. | | | | |
| A* | 1.41 | 1.64 | 1.52 | 111° | 106° | 108°30' |
| B | 1.41 | 1.64 | 1.52 | 111 | 106 | 108°30' |
| C | 1.41 | 1.64 | 1.52 | 108 | 106 | 102° |
| D | 1.42 | 1.67 | 1.52 | 108 | 103 | 108°30' |
| E | 1.42 | 1.67 | 1.52 | 108 | 106 | 108°30' |
| F | 1.42 | 1.61 | 1.52 | 111 | 106 | 108°30' |
| G | 1.42 | 1.64 | 1.52 | 111 | 106 | 108°30' |
| H | 1.42 | 1.64 | 1.52 | 111 | 109 | 108°30' |
| I | 1.42 | 1.64 | 1.52 | 114 | 106 | 108°30' |
| J | 1.42 | 1.61 | 1.52 | 114 | 109 | 108°30' |
| K | 1.42 | 1.64 | 1.53 | 111 | 106 | 108°30' |
| L | 1.42 | 1.64 | 1.52 | 111 | 106 | 129°30'** |

* Term in summation corresponding to non-bonded C---O distance at 3.28 Å. omitted.

** This is the mean position. The temperature factor $e^{-aq^2}$ with a 0.0003 was applied to the C---O distance at 3.86 Å.

All models

| | | |
|---|---|---|
| S=O | 1.42 Å. | (except A, B, and C) |
| C–O | 1.42 | |
| C–H | 1.09 | |
| S–H | 2.95 | |

ii - Ethylene Glycol Chlorophosphite Ester

The sample of ethylene glycol chlorophosphite ester used in this investigation was prepared by Mr. C. N. Scully by the action of phosphorus trichloride on ethylene glycol in methylene chloride solution.[7,8] The compound was purified by vacuum distillation and the fraction boiling at 42-43°/12 mm. was used in preparing electron diffraction photographs. The compound is of special interest because of the extremely high chemical activity of the chlorine atom. Hydrolysis occurs rapidly in water or in moist air with the evolution of hydrochloric acid; extensive decomposition of the pure material with the formation of a bright orange precipitate (probably phosphorus) was observable a few days after purification.

Diffraction photographs were taken at temperatures ranging from 20°C. to 100°C. with the use of a heated, glass nozzle designed by Dr. S. Claesson for high temperature work. In obtaining dense photographs, a beam-stop, designed by Mr. H. G. Pfeiffer, was placed between the jet and the film to reduce the background scattering. The jet-to-film distance was 10.93 cm. Features were observed at q values extending to about 105. The photographs were examined independently by this author and by four other investigators* and a visual curve (V of Figure 2) was drawn to represent the final compromise among these workers with respect to the interpretation of the diffraction pattern. The general agreement was good but some differences in the interpretation of fine structure in the pattern were registered by the various observers; e.g., in the prominence of the second and fifth maxima and in the extent of

---

* Dr. V. Schomaker, Dr. K. W. Hedberg, Mr. G. Guthrie, and Mr. H. G. Pfeiffer.

doubling in the ninth and eleventh maxima. In the assignment of limits of error by the correlation method, liberal allowance was made for these differences in interpretation. The finally chosen theoretical intensity curve satisfies all observers in that each of the features in contention is an acceptable compromise among the various observations.

The radial distribution function, R, is shown in Figure 2. Peaks are observed at 1.55, 2.11, 2.43 (diffuse), 2.85 and 3.20 Å. It is immediately striking that no maximum is observed at 1.76 Å., a position corresponding to the sum of the covalent bond radii of the atoms, for the P-O single-bond distance. The absence of this peak, coupled with the strength of the maximum at 1.54 Å., led to the conclusion that the P-O distance in the molecule is considerably shorter than might be predicted. An analysis of the first peak in the radial distribution curve (as a sum of Gaussian peaks of suitable area) indicated the following most probable interatomic distances in the molecule: C-O = 1.41 Å., C-C = 1.52 Å., P-O = 1.58 Å. The maximum at 2.11 Å. corresponds to the bonded P-Cl distance, which is considerably greater than 2.00-2.05 Å., observed for the P-Cl distance in $POCl_3$, $POF_2Cl$, $PSCl_3$, $PFCl_2$ and similar compounds. The diffuse peak at 2.43 Å. corresponds to the cross-ring distances (through one angle), P---C, O---O, and O---C, and the peaks at 2.85 and 3.20 Å. correspond respectively to the Cl---O and Cl----C distances. No geometrical model containing the indicated bond distances and a planar ring can be formulated which will satisfy the last three peaks in the RDI. For example, such a model with $\angle$ O-C-C = 107° gives reasonable agreement with the peak at 2.43 Å., but if the Cl---O distance be fixed at 2.85 Å., the Cl----C distance is found to be 3.67 Å., in severe disagreement with

3.20 Å. indicated in the RDI. The theoretical intensity function for this planar model, curve A, is shown in Figure 2. The general shape of the region comprising the first, second, and third maxima and minima is in severe disagreement with the visual curve.

An excellent fit to the RDI was afforded by a model in which the group $O_{C-C}^{O}$ was assumed planar with $\angle$ O-C-C = 107°. The position of the chlorine atom was fixed at a distance of 2.85 Å. from each oxygen and 3.20 Å., from each carbon. With the bond distances P-O = 1.58 Å. and P-Cl = 2.11 Å., the phosphorus is fixed in a position such that the plane of O-P-O makes an angle of about 30° with that of $O_{C-C}^{O}$.

For the correlation procedure, a number of assumptions were made: the ratios $\frac{C-C}{P-Cl}$ and $\frac{C-O}{P-Cl}$ were fixed at $\frac{1.52}{2.11}$ and $\frac{1.41}{2.11}$; the O-C-C angle was tentatively assigned a value of 107°. It is not to be inferred that the weak contribution of the C-C distance to the theoretical intensity curves is well-defined by the RDI, but since this term was of little significance in the summation and since the distance, 1.52 Å., in combination with the other bond distances as stated, resulted in the best fit to the first main peak in the RDI, this value was assumed to be best.

The remaining parameters were systematically varied as follows: $\angle$ C-O-P from 109 to 113°, $\angle$ O-P-Cl from 99 to 103°, and P-O from 1.55 to 1.64 Å. Equation (3) was used in all calculations except that resulting in curve JA. The non-bonded X. . .H distances were omitted in all except the finally accepted curve. Some representative theoretical intensity curves are shown in Figure 2. The effect on the curves of a variation in the P-O distance is shown by curves B, C, and D. In increasing the P-O distance, the main effects throughout are to strengthen the second maximum, to weaken the fifth maximum, to strengthen the feature which in

these curves occurs between the eighth and ninth maximum (but which in more acceptable curves occurs on the outside of the ninth maximum) and to decrease the doubling in the eleventh maximum. Curves with P-O as short as 1.55 Å. (B) invariably show an inacceptable reversal of the relative strength of the seventh and eighth maxima and of the corresponding minima. These discrepancies are corrected in curves with P-O = 1.58 Å. or somewhat greater. The sequence, curves C,E, and F exemplifies the effect of increasing the angle C-O-P from 109 to 111°. The result, in general, is to weaken the second maximum, to strengthen the fifth maximum, to move the doubling from the ninth minimum toward the ninth maximum, and from the eleventh maximum toward the eleventh minimum. The general effect of an increase in the angle O-P-Cl is exemplified by the sequence, curves G,H, and E. The second maximum is weakened, the fifth maximum becomes more prominent, and the feature which in curve G occurs as an asymmetry on the outside of the ninth maximum moves to the inside of the ninth minimum in curve E. The nature and the position of the eleventh maximum, which is strongly doubled in these curves, is altered somewhat by this variation, but apparently is not improved in comparison with the visual curve.

The theoretical intensity function which best combines the features of the curves described above corresponds to a model in which the P-O distance is 1.60 Å., and the angles C-O-P and O-P-Cl are 110° and 100°, respectively. This curve, I of Figure 2, compares well with the visual curve in many features. The nature of the region comprising the fifth and sixth maxima and minima is quite acceptable and the character

of the region between the sixth maximum and the eleventh minimum is very good in that the envelope covering the maxima and that covering the minima show respectively the concave upward and concave downward curvature which was finally agreed upon by all observers. A number of discrepancies, however, in comparison with the visual curve may still be noted. The second maximum appears to be too strong in comparison with the third, the seventh maximum is a trifle too strong compared to the sixth, the ninth maximum is too strongly doubled and the eleventh maximum appears to be too sharp. Definite improvement in all of these features is noted with the application of a temperature factor, $e^{-aq^2}$, to the term corresponding to the Cl-C distance (curve J). The value assigned to $\underline{a}$ is 0.0003 which corresponds to a distribution of distances about the mean in the form of a Gaussian curve with half-width equal to approximately 0.1 Å. An appreciably smaller value for $\underline{a}$ results in more doubling of the ninth maximum than we are willing to accept, whereas a larger value has no further noticeable effect on the curve.

The agreement of curve J with the visual curve is considered to be excellent. The ninth maximum was held to be a weak and indistinct feature, quite broad with perhaps a slight tendency toward doubling. The eleventh maximum was first drawn by this author to be strongly doubled much as shown in curve H, but after examination of three heavy pictures piled atop one another, it appears very likely that no such strong doubling exists, and that the eleventh maximum in curve J is an excellent representation of this feature. Other observers did not make a similar mistake in the interpretation of this feature. The second maximum in curve J is somewhat stronger in comparison with the first and third than had been drawn in the visual curve. Some improvement is noted in curve

JA in which the reduced intensity function, equation (1) was used instead of equation (3) to calculate the initial portion of the curve. Equation (1) is a closer approximation to the appearance of the photographs, especially in molecules containing atoms of widely differing atomic number. The shift in the second minimum in going from curve J to JA may be attributable to the use of a step function in approximating the dependence of f on q. The second maximum in curve JA is still somewhat stronger than is desirable but is acceptable for this difficultly interpretable region of the film.

During the course of the investigation, the effect of variations in the fixed parameters was investigated. Of the variations investigated, $\Delta(C\text{-}C) = 0.02$ Å., $\Delta(C\text{-}O) = 0.03$ Å. and $\Delta(\angle\ O\text{-}C\text{-}C) = 2^{\circ}$, the largest effect was shown by the last-named. Curve K corresponds to a model similar to that for curve G, but with the angle $O\text{-}C\text{-}C = 109^{\circ}$. Changes in these fixed parameters by the amounts indicated appear to be similar in effect on the curves to changes in the angles O-P-Cl and C-O-P of about $1/2^{\circ}$, and would appear to add this uncertainty to the determination of these parameters.

In the determination of the error limits, a good deal of weight was attached to the appearance of single features. The nature of the eleventh maximum is affected quite strongly by variations in the P-O distance, but not so strongly by changes in the angle parameters. Thus, from the correlation procedure alone, a limit of error of 0.02 Å. was assigned to the P-O distance. The eleventh maximum is certainly not so broad and doubled as is shown in curves with P-O = 1.58 Å., nor so sharp as is shown by curves with P-O = 1.64 Å. (L). Temperature factors improve this feature very little in these curves. A variation in the angles C-O-P and O-P-Cl have marked effects on several features: the fifth maximum,

the relative height of the seventh, eighth and ninth maxima, the shape of the ninth maximum, etc. A consideration of the relative changes brought about in these features have led to a limit of error of $2^{\circ}$ for each of the angle parameters C-O-P and O-P-Cl from the correlation procedure alone. A consideration of the average deviation of observed q values from those calculated and of the errors introduced by variations in the fixed parameters, led to the following structural parameters for ethylene glycol chlorophosphite ester:

| | |
|---|---|
| C-H | 1.09 Å. (assumed) |
| C-C | 1.52 ($\pm$ 0.02) Å.* |
| C-O | 1.41 ($\pm$ 0.03) Å.* |
| P-Cl | 2.11 ($\pm$ 0.02) Å.* |
| $\angle$ O-C-C | 107 ($\pm$ 2)$^{\circ}$ |
| P-O | 1.60 $\pm$ 0.04 Å. |
| $\angle$ C-O-P | 110 $\pm$ 2.5$^{\circ}$ |
| $\angle$ O-P-Cl | 100 $\pm$ 2.5$^{\circ}$** |

* These are the parameters fixed in the correlation procedure, the values for which are taken from the RDI. The quantities in parenthesis are the variations of these distances within which the stated limits of error of the determined parameters hold.

** The chlorine atom vibrates about this mean position such that the distribution of Cl-C distances is in the form of a Gaussian curve of half-width = 0.1 Å.

The positions of the main features of the visual curve are compared in Table II with those of curve J. There is good agreement with an average deviation of less than one percent.

Table II

Ethylene Glycol Chlorophosphite Ester

| Min | Max | $q_o$ | $q_J$ | $q_J/q_o$ | |
|---|---|---|---|---|---|
| 1 | | 6.47 | 6.4 | 0.989* | |
| | 1 | 9.48 | 9.5 | 1.002* | |
| 2 | | 11.58 | 11.7 | 1.010* | |
| | 2 | 15.04 | 15.4 | 1.024 | |
| 3 | | 17.15 | 17.5 | 1.020 | |
| | 3 | 19.67 | 20.0 | 1.017 | |
| 4 | | 24.16 | 24.2 | 1.002 | |
| | 4 | 29.39 | 29.1 | 0.990 | |
| 5 | | 35.34 | 34.9 | 0.988 | |
| | 5 | 37.72 | 37.5 | 0.994 | |
| 6 | | 40.21 | 39.9 | 0.992 | |
| | 6 | 43.05 | 42.5 | 0.987 | |
| 7 | | 47.31 | 47.2 | 0.998 | |
| | 7 | 50.98 | 51.1 | 1.002 | |
| 8 | | 54.98 | 55.0 | 1.000 | |
| | 8 | 58.56 | 58.6 | 1.001 | |
| 9 | | 62.75 | 62.4 | 0.994 | |
| | 9 | 66.64 | 66.1 | 0.992 | |
| 10 | | 73.84 | 73.8 | 0.999 | |
| | 10 | 78.11 | 78.1 | 1.000 | |
| 11 | | 83.21 | 82.9 | 0.996 | |
| | 11 | 88.97 | 89.3 | 1.004 | (center of gravity) |
| 12 | | 95.64 | 95.7 | 1.001 | |
| | 12 | 99.26 | 99.4 | 1.001 | |
| 13 | | 103.12 | 102.2 | 0.991 | |
| | 13 | 105.97 | 106.0 | 1.000 | |
| | | | Average (23 features) | 0.999 | |
| | | | Average deviation | 0.007 | |

* Not included in the average

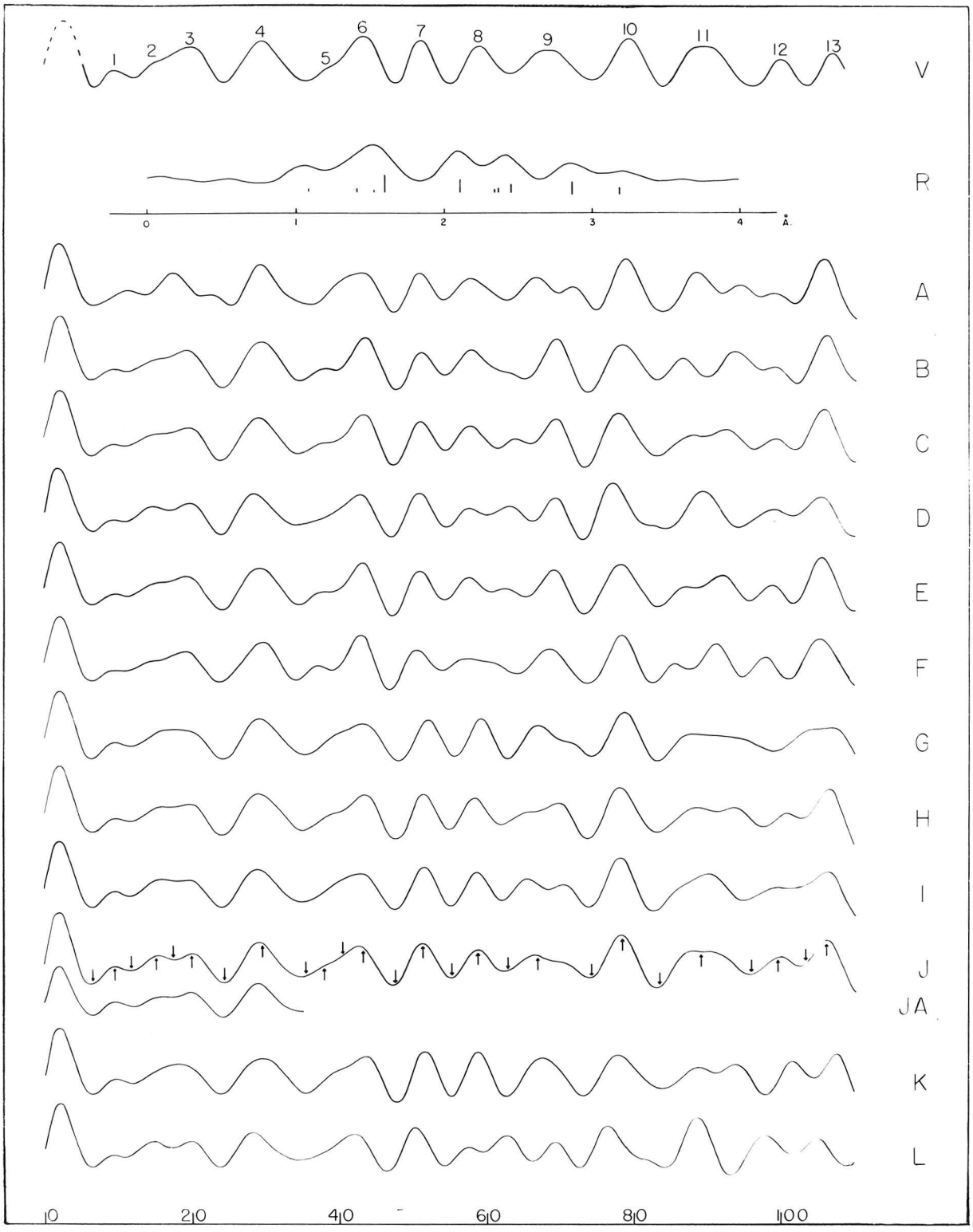


Figure 2: Electron Diffraction Curves for Ethylene Glycol Chlorophosphite Ester

Table of Parameters (Figure 2)

Ethylene Glycol Chlorophosphite Ester

| Model | P-O | ∠ O-P-Cl | ∠ C-O-P |
|---|---|---|---|
| A | 1.58 | 101° | 116° |
| B | 1.55 | 103 | 109 |
| C | 1.58 | 103 | 109 |
| D | 1.61 | 103 | 109 |
| E | 1.58 | 103 | 110 |
| F | 1.58 | 103 | 111 |
| G | 1.58 | 99 | 110 |
| H | 1.58 | 101 | 110 |
| I | 1.60 | 100 | 110 |
| J*† | 1.60 | 100 | 110 |
| JA*‡ | 1.60 | 100 | 110 |
| K | 1.58 | 99 | 110 |
| L | 1.64 | 103 | 110 |

All models

| | | |
|---|---|---|
| C-C | 1.52 Å. | |
| C-O | 1.41 | |
| P-Cl | 2.11 | (except model K in which P-Cl = 2.13 Å.) |
| ∠ C-C-O | 107° | |
| C-H | 109 | |

* The non-bonded hydrogen distances have been omitted from all theoretical intensity calculations except J and JA

† Temperature factor, $e^{-aq^2}$, applied to Cl-C distance (a = 0.0003)

‡ Model JA is similar to J except that the theoretical intensity function is calculated according to equation (1).

iii - Ethylene Glycol Acetal

The sample of ethylene glycol acetal used in this investigation was prepared by Mrs. G. Guthrie in an original two-step synthesis.[9] Di-n-amyl acetal was first prepared by the action of n-amyl alcohol on paraldehyde in the presence of dry hydrogen chloride gas. After purification, the di-n-amyl acetal was treated with ethylene glycol in the presence of p-toluenesulfonic acid. An exchange of the alkyl groups resulted with the formation of ethylene glycol acetal (b.p. = 82.5°C.) and the regeneration of amyl alcohol.

Electron diffraction photographs were taken at room temperature. The gas was admitted to the chamber through the standard low-temperature nozzle which, in one series of experiments, was equipped with a beam-stop. The jet-to-film distance was 10.95 cm. Features were observed on the photographs at q values extending to about 100. The visual curve, V, is shown in Figure 3.

Ethylene glycol acetal is a homologue of ethylenemethylene dioxide, the structure of which was determined by Dr. W. Shand.[11] He chose, as the best structure for his compound, a model in which the ratio $\frac{C-O}{C-C}$ is $\frac{1.42}{1.54}$ and the ring is coplanar with the angle O-C-C = 105°37'. However, the theoretical intensity curve corresponding to this model deviates markedly from his visual curve in two important features. I believe that this model is not the correct one for the structure of ethylenemethylene dioxide.

The estimated visual curves of ethylenemethylene dioxide and of ethylene glycol acetal show a great similarity which is borne out by a comparison of the diffraction photographs of the two compounds. The

region comprising the sixth and seventh maxima is broad and somewhat doubled and appears to be definitely weaker than the following eighth maximum as drawn by this author and by Dr. Shand. The general aspect of this region is denied by the model chosen by Shand.

The visual curve, V, and the radial distribution integral, R, of ethylene glycol acetal are shown in Figure 3. In the RDI, peaks were observed at 1.13, 1.44, 2.03, 2.30, 2.80, 3.18, and 3.60 Å., the last being quite diffuse. A good approximation to the maximum at 1.44 Å. was calculated from Gaussian curves representing C-O and C-C distances of 1.43 and 1.53 Å. respectively. The peak at 2.30 Å. is sharp, symmetrical, and of theoretical half-width, from which it may be inferred that the C--C, O--O, and O--C distances through one angle are all very close to this value.

An examination of the peak at 1.44 Å. in the RDI and a consideration of the structure determination of ethylenemethylene dioxide led to the conclusion that an attempt to resolve the two C-C or the two C-O distances would be futile. In the correlation procedure, it was deemed more profitable to determine the bond angles in the molecule than to attempt a redetermination of C-C and C-O distances for which the values indicated are in good agreement with those found by Shand[11] in similar compounds.* The

---

* Ethylenemethylene dioxide: C-C = 1.54 ± 0.05 Å.; C-O = 1.42 ± 0.03 Å.; all angles = 108°; probably planar.

Trimethylene oxide: C-C = 1.54 ± 0.03 Å.; C-O = 1.46 ± 0.03 Å.; ∠ C-C-C = ∠ C-C-O = 88.5 ± 3°; ∠ C-O-C = 94.5 ± 3°; probably planar within 15-20°.

1,4-Dioxane: C-C = 1.51 ± 0.04 Å.; C-O = 1.44 ± 0.03 Å.; ∠ C-O-C = 112 ± 5°; ∠ O-C-C = 109½ ± 5°; "chair" form.

1,3,5-Trioxane: C-O = 1.42 ± 0.03 Å.; ∠ C-O-C = ∠ O-C-O = 112 ± 3°; "chair" form.

ratio $\frac{C-C}{C-O}$ was held constant at $\frac{1.53}{1.43}$. The angle O-C-C in the ring was varied from 104° to 108°, the angle C-O-C from 105° to 109°, and the angle O-C-C' (C' is the carbon atom not contained in the ring) from 100 to 104°. Within the region of variation is found a smaller region of geometrically impossible models which, of course, could not be calculated. The calculation of theoretical intensity curves was carried out with the use of equation (3). A number of representative theoretical intensity curves are shown in Figure 3. In all except the finally accepted curve, non-bonded X. . .H terms were omitted from the summation. Curves A, B, and C correspond to models in which the five-membered ring is planar, with the ring angle, O-C-C, equal to 104, 106, and 108° respectively. Of these, only B, which is similar to Shand's chosen model of ethylenemethylene dioxide, is considered acceptable. A and C are inacceptable beyond q = 50. Of the models containing a non-planar five-membered ring, three types may be considered depending on the position of the carbon atom, C', relative to the two glycol carbon atoms in the ring. Curve D represents the "chair" form, and curve E the "cradle" form, in each of which the group $O_{C-C}^{O}$ is planar; curve F represents the "staggered ring" form, in which one of the glycol carbon atoms is above, and the other is below, the plane of O-C-O, and the projection of the C-C' bond bisects the angle O-C-O. The distances in each of these models are in reasonable agreement with the RDI. Curve E, corresponding to the "cradle" form, is in excellent qualitative agreement with the visual curve. The curves D and F are considered to be unacceptable because of the strong doubling of the sixth and seventh maxima. It is highly probable, however,

that acceptable models of the "chair" and staggered ring" form could be found. In the remainder of the correlation procedure, only models corresponding to the "cradle form" were considered. A number of these are shown (G, H, I, J, K). The acceptability of these curves, in general, had to be decided by the nature of the region comprising the sixth, seventh, and eighth maxima and minima.

An attempt to resolve the two different C-O distances in the molecule served to justify the original assumption that a definite result could not be obtained. The average of the C-O distances was determined to be 1.43 ± 0.03 Å., but a change of 0.05 Å. in the individual distances (holding the average constant) resulted in curves which were considered still acceptable. The application of a temperature factor to the term corresponding to the C---C distance at 2.84 Å., apparently does not change curve E by an appreciable amount in any feature. This may be inferred from curve M in which this term is omitted completely. The sixth and seventh maxima remain acceptable and the ninth maximum is weakened such that it approximates more closely the visual curve; this, however, occurs in a difficultly interpretable region of the film and is not considered significant.

A comparison of the positions of the main features in the visual curves with those in curve E is made in Table III. The structural parameters for ethylene glycol acetal are as follows:

| | |
|---|---|
| C-H | 1.09 Å. (assumed) |
| C-C (individual) | 1.53 (assumed) |
| C-O (individual) | 1.43 ± 0.05 A. |
| C-O (average) | 1.43 ± 0.03 A. |
| ∠ C-C-O | 106 ± 4° |
| ∠ C'-C-O | 101.5 ± 4° |
| ∠ C-O-C | 106.5 ± 4° |

Table III

Ethylene Glycol Acetal

| Min | Max | $q_o$ | $q_E$ | $q_E/q_o$ |
|---|---|---|---|---|
| 1 | | 8.26 | 7.5 | 0.908* |
| | 1 | 11.71 | 11.0 | 0.939* |
| 2 | | 14.83 | 14.1 | 0.951* |
| | 2 | 19.17 | 19.2 | 1.002 |
| 3 | | 24.55 | 24.4 | 0.994 |
| | 3 | 28.94 | 29.1 | 1.006 |
| 4 | | 32.87 | 33.9 | 1.031** |
| | 4 | 36.58 | 36.8 | 1.006 |
| 5 | | 40.86 | 40.3 | 0.986** |
| | 5 | 45.42 | 44.9 | 0.989 |
| 6 | | 49.75 | 50.1 | 1.007 |
| | 6 | 54.19 | 55.0 | 1.015** |
| 7 | | 58.41 | 57.8 | 0.990 |
| | 7 | 62.01 | 61.6 | 0.993** |
| 8 | | 66.89 | 66.9 | 1.000 |
| | 8 | 71.88 | 71.7 | 0.997 |
| 9 | | 76.80 | 76.2 | 0.992 |
| | 9 | 80.43 | 79.9 | 0.993 |
| 10 | | 84.02 | 83.4 | 0.993 |
| | 10 | 88.40 | 88.0 | 0.995 |
| 11 | | 93.62 | 93.3 | 0.997 |
| | 11 | 99.05 | 98.2 | 0.991 |
| | | | Average (19 features) | 0.998 |
| | | | Average deviation | 0.007 |

* Not included in the average

** In computing the average and average deviation, these quantities were given half weight since the measurements of $q_o$ were subject to errors introduced by the St. John effect.

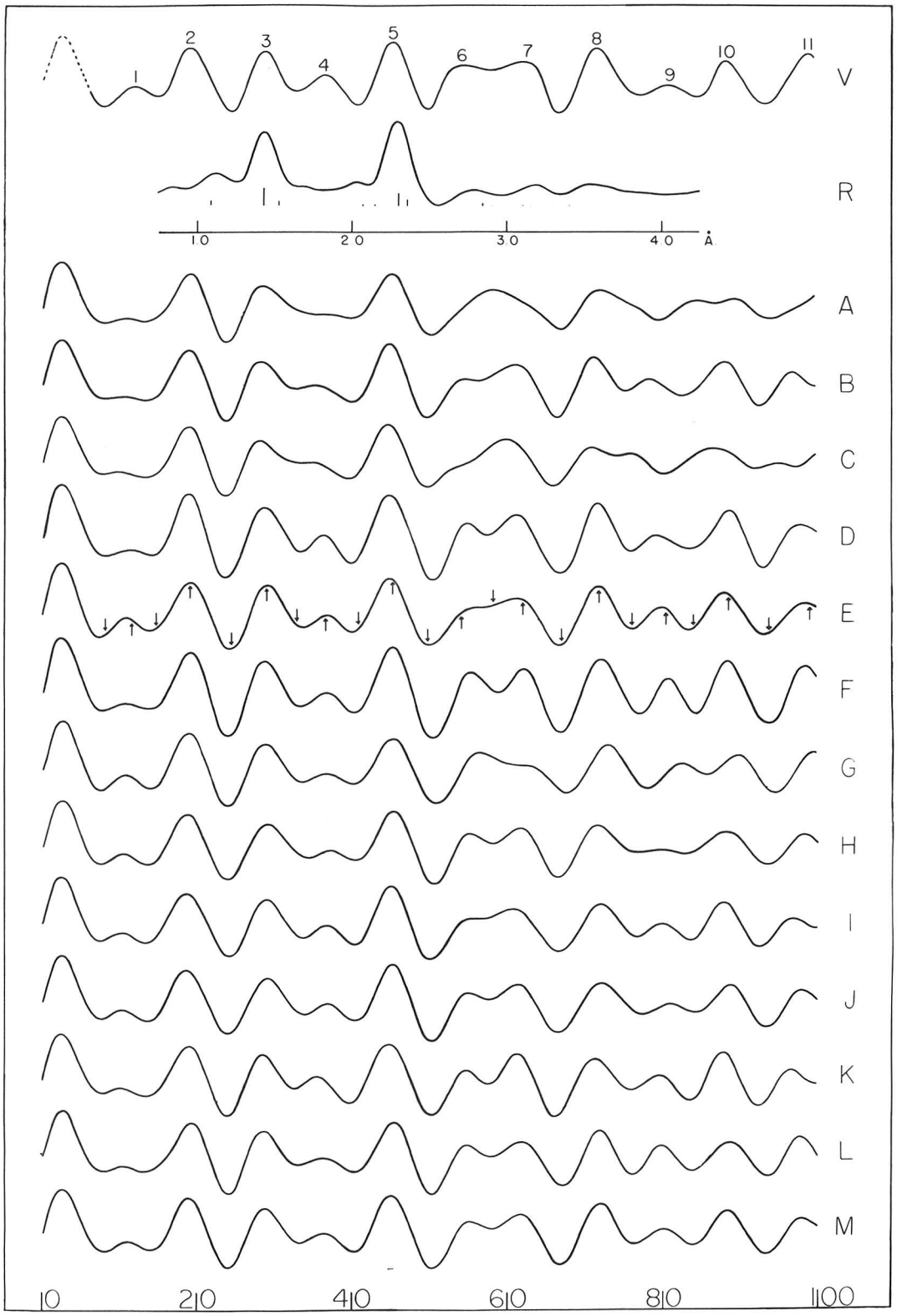


Figure 3: Electron Diffraction Curves for Ethylene Glycol Acetal

Table of Parameters (Figure 3)

Ethylene Glycol Acetal

| Model* | ∠ O-C-C | ∠ O-C-C' | ∠ C-O-C |
|---|---|---|---|
| A | 104° | 115° | 100° |
| B | 106 | 110 | 102 |
| C | 108 | 104 | 104 |
| D | 105°37' | 101°44' | 106°52' |
| E | 105°37' | 101°44' | 106°52' |
| F | 105°37' | 101°44' | 106°52' |
| G | 104 | 100 | 105 |
| H | 104 | 104 | 107 |
| I | 104 | 104 | 109 |
| J | 106 | 100 | 107 |
| K | 106 | 104 | 109 |
| L | 106 | 102 | 107 |
| M | 105°37' | 101°44' | 106°52' |

All models

| | | |
|---|---|---|
| C-O | 1.43 Å. | (except model M)** |
| C-C | 1.53 | |
| C-H | 1.09 | |

* The non-bonded hydrogen terms are omitted from all models except model E, in which all terms are included, calculated and temperature-factored as described in the introduction.

** In model M, the bonded C-O distances in the group $O_{C-C}^{O}$ are 1.40 Å., and in the group $O^{C}_{O}$ are 1.46 Å.

## DISCUSSION

The molecules of ethylene glycol sulfite ester, ethylene glycol chlorophosphite ester and ethylene glycol acetal have been found to contain several interatomic distances which are appreciably different from those which might have been predicted from a consideration of the covalent radii of the atoms. The most striking discrepancies are observed in the structure of the chlorophosphite ester. The value for the P-O bond distance, obtained in the present work, is 1.60 Å., considerably shorter than the theoretical distance for a normal covalent single-bond, calculated either from the covalent radii suggested by Pauling[13,14] (1.76 Å) or from the Schomaker-Stevenson relationship[15] (1.71 Å.). Indeed, the value 1.60 Å. just corresponds to one-half covalent double-bond character for each P-O distance, calculated from the Pauling radii and the Pauling formula for percent double-bond character. In addition, the P-Cl bond distance, 2.11 Å., in this molecule is significantly greater than that which is predicted from the same sources (2.09 Å. and 2.01 Å., respectively). According to theories of resonance, after Pauling,[16] the interpretation of these apparent anomalies may be made in terms of ionic or double-bonded structures which, in contributing to the state of the molecule, would be expected to affect the distances in a way indicated by the experimental results. Several possible structures are written below. In each of these, the adjacent charge rule and the octet rule for first row elements are satisfied. Structure (I) is a classical representation of a molecule in which normal covalent single-bond distances would be exhibited. If a structure of the type (II),

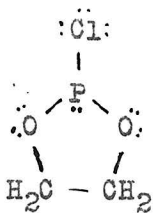

(I)

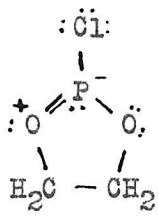

(II)

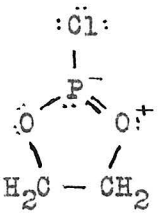

(IIa)

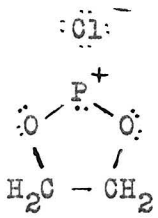

(III)

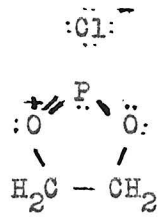

(IV)

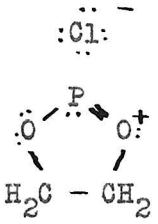

(IVa)

resonating with its equivalent, (IIa), completely described the state of the molecule, the P-O bond would have one-half double-bond character but the P-Cl bond would only be lengthened by about 0.05 Å. from the normal covalent distance.[15] This could not completely account for the discrepancies, especially since the unfavorable distribution of charge between the phosphorus and the oxygen atoms makes it unlikely that this structure would contribute to so great an extent to the state of the molecule. (III) would be expected to shorten the P-O bond distance by only 0.03 Å. Structure (IV), resonating with (IVa), might reasonably account for the observed structure of the molecule. In (IV) and (IVa), the coulomb attraction of unlike charges would be expected to be very weak in contrast to a normal $X\ Y^-$ ionic bond; in addition, since the

electronic configuration about the phosphorus in (IV) is different from that in (I), an extra van der Waals' repulsion between the electrons of $Cl^-$ and the unshared pair on the phosphorus may well account for the increase in the interatomic distance. The postulation of ionic character for the chlorine atom is in line with the high chemical activity observed in the molecule. Furthermore, if the molar refractivity of the chlorophosphite ester by compared with that of, say, the methoxyphosphite ester, 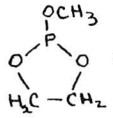 , which might be expected to exhibit a normal covalent structure analogous to (I), one observes an exaltation of refractivity in the chlorophosphite ester corresponding to approximately one-third of a double-bond.* This may or may not constitute evidence in favor of structures (IV) and (IVa) since the validity of the additivity rule for second row elements has not definitely been shown. However, Mitchell[7] has shown that, for phosphorus in a large number of compounds of the type discussed here, the additivity rule is quite reliable.

It may also be pointed out that an effect analogous to that reported here has been observed in nitrosyl chloride. In this compound, the N-O and N-Cl distances are 1.12 and 1.98 Å., respectively, instead of the calculated values 1.21 and 1.69 Å. This has been explained[18] by

---

* Mitchell[7] has carried out this calculation as follows: Assuming the average values for the atomic refractivity of carbon, hydrogen, and oxygen[17] and assuming the additivity of the atomic refractivity to yield the molar refractivity, values of the atomic refractivity of phosphorus were calculated from the experimental value for the methoxyphosphite ester and several of its homologues. Using an average of these values for phosphorus (the deviations being small), and using an average value for chlorine,[17] the molar refractivity of the chlorophosphite ester was calculated. The observed value deviated from the calculated value as indicated in the text.

resonance between the normal covalent structure, $:\ddot{\underset{\cdot\cdot}{Cl}}-\ddot{N}=\ddot{O}:$, and the ionic structure $:\ddot{\underset{\cdot\cdot}{Cl}}:^{-}\ :N\equiv O:^{+}$. The situation is similar in nitrosyl bromide.

The major difficulty in the proposal of structures (IV) and (IVa) is that the experimental results require that these contibute almost completely to the state of the molecule to the exclusion of any appreciable quantity of (I), which should represent a state of energy equal to or lower than that of (IV). One might be tempted to formulate structures which show two double-bonds or a triple-bond in the ring; these, however, are extremely unsatisfactory with respect to the distribution of charge. Consequently, for an interpretation of the results in terms of multiple and/or ionic bonds, one is forced to accept resonance between (IV) and (IVa) with perhaps a small contribution from (I) as representing the structure of the molecule. It may, of course, be that, as set forth by Pitzer[19] in a recent article and by others, the postulation of multiple bonds for other than first row elements is unjustified, but this language does present a plausible basis for the interpretation of many apparently anomalous results.

It should perhaps be pointed out that a number of anomalous P-O and P-Cl distances have previously been reported. In $P_4O_6$,[20] $P_4O_{10}$,[20] and $P_4O_6S_4$,[21] the "single-bond" P-O distances have the values 1.65, 1.62, and 1.61 Å., respectively. These correspond to something less than 50% double-bond character in the bond but, contrary to the statement of Hampson and Stosick, the distances cannot be satisfactorily explained on the basis of ionic or multiple-bond structures. In $PCl_5$, which has the form of a trigonal bipyramid, the two P-Cl bonds which are directed along

the three-fold axis of the molecule are 2.12 Å. in length. However, it is very probable that this is not analogous to the present work, since in $PCl_5$, the chlorine atoms suffer severe steric interactions, with those farthest from the central phosphorus atoms having the greater number of close Cl. . .Cl interactions. In ethylene glycol sulfite ester, the single-bond S-O distance has been determined to be 1.64 Å., significantly shorter than that predicted from the Pauling covalent radii or from the Schomaker-Stevenson modification (1.70 and 1.69 Å., respectively). In terms of multiple bonds the discrepancy corresponds to approximately 12 percent double-bond character in each S-O bond. No anomaly is necessarily indicated here, since structures of the type (V), resonating with (Va) may reasonably be written. Contributions from these will satisfactorily

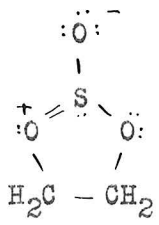

(V)

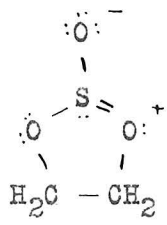

(Va)

account for the observations. The only value for a single-bond S-O distance that has previously been reported is that found by Westrink and MacGillavry[22] for the $\gamma$-modification of $(SO_3)_3$. Their value of 1.60 Å. is in more serious disagreement with predicted values than is the present work. However, no great precision is claimed for the atomic positions.

It is of interest that the C-C distance in each of the molecules appears to be slightly shorter than that usually found. This is in agreement with values for this distance in ethylene glycol, diethyl ether, and dioxane (see footnote, p. 92). These discrepancies found in the present work cannot, however, be considered significant since the limits of error of these distances have been assumed rather than determined.

## SUMMARY

A determination of the molecular structure of three compounds, ethylene glycol sulfite ester, ethylene glycol chlorophosphite ester, and ethylene glycol acetal has been carried out. In each compound, the minimum symmetry $C_s$-m and a planar configuration of the group $O_{C-C}^{O}$ was assumed. In the sulfite ester, the assumption of a planar ring led to a reasonable structure in good agreement with the data, although non-planar structures could not be excluded. The symmetry $C_{2v}$-Pmm was ruled out, but vibration of the O-S=O angle about the position finally assigned could not be proved or disproved. In the chlorophosphite ester, the ring is definitely non-planar; the plane of $O^{P}O$ makes an angle of about 30° with that of $O_{C-C}^{O}$. In the acetal, the favored structure contained a non-planar ring, but a range of planar ring models falls within the region of acceptability. In the three molecules, a number of anomalous distances are found and an interpretation of these apparent anomalies is discussed in terms of multiple and ionic bonds. The structural parameters of the three molecules are as follows:

Ethylene glycol sulfite ester

| | |
|---|---|
| C-H | 1.09 Å. (assumed) |
| S-H | 2.95 * |
| C-C | 1.52 ( ± 0.03) Å.* |
| C-O | 1.42 ( ± 0.02) * |
| S=O | 1.42 ( ± 0.02) * |
| S-O | 1.64 ± 0.05 Å. |
| ∠ C-C-O | 111 ± 3° |
| ∠ O-S O | 106 ± 3° |

Ethylene glycol chlorophosphite ester

| | |
|---|---|
| C-H | 1.09 Å. (assumed) |
| C-C | 1.52 ( ± 0.02) Å.* |
| C-O | 1.41 ( ± 0.03) * |
| P-Cl | 2.11 ( ± 0.02) * |
| ∠ O-C-C | 107 ( ± 2)° * |
| P-O | 1.60 ± 0.04 Å. |
| ∠ C-O-P | 110 ± 2.5° |
| ∠ O-P-Cl | 100 ± 2.5° |

The chlorine atom vibrates about its mean position such that the distribution of Cl---C distance is in the form of a Gaussian curve of half-width = 0.1 Å.

Ethylene glycol acetal

| | |
|---|---|
| C-H | 1.09 Å. (assumed) |
| C-C (individual) | 1.53 (assumed) |
| C-O (individual) | 1.43 ± 0.05 Å. |
| C-O (average) | 1.43 ± 0.05 |
| ∠ C-C-O | 106 ± 4° |
| ∠ C'-C-O | 101.5 ± 4° |
| ∠ C-O-C | 106.5 ± 4° |

C' is the carbon atom outside of the ring

* In these structure determinations, an attempt was made to estimate the additional errors brought into the investigation by the assumption of certain parameters in the molecules. The starred parameters are those fixed in the correlation procedure; the values were taken from the RDI. The quantities in parentheses are the variations of these distances within which the stated limits of error of the determined parameters hold.

ii Naphthalene and Anthracene

The stability and the characteristic aromatic properties of both naphthalene and anthracene have suggested the formulation of resonating structures for these compounds similar to those proposed by Kekulé for benzene. In benzene, the contribution of equivalent structures, whether they be of the Kekulé, the Dewar or the Claus-Armstrong-Baeyer type, results in complete six-fold symmetry in the molecule. In naphthalene, however, resonance between the nearly equivalent structures of lowest energy, (VI), (VII), (VIII), should result in a molecule in which the bonds have differing amounts of double-bond character (IX). The length of a C-C bond with 1/3 double-bond character should be, after Pauling,[18] 1.42 Å.; that of a bond with 2/3 double-bond character should be 1.37 Å. Similarly, in anthracene, resonance among the structures

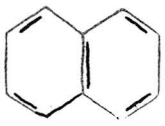

(VI)

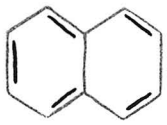

(VII)

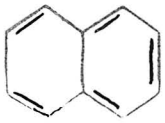

(VIII)

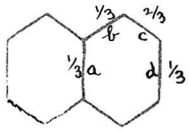


(IX)

(X), (XI), (XII) and (XIII), which are nearly equivalent and lowest in energy, should result in bonds with double-bond character as in (XIV).

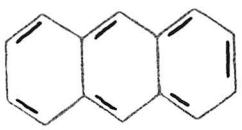

(X)

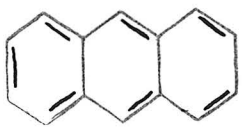

(XI)

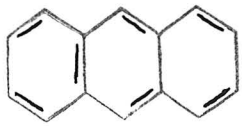

(XII)

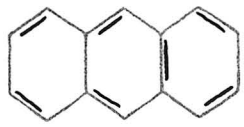

(XIII)

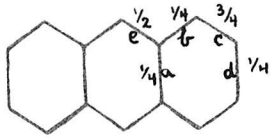


(XIV)

The lengths of C-C bonds with 1/4, 1/2, and 3/4 double-bond character should be 1.44, 1.39, and 1.355 Å. respectively.

A number of other treatments, inspired by quantum mechanics, have been given to the structure of naphthalene. In addition to the calculation by Pauling, which is outlined above, predictions of interatomic bond distances have been made by Lennard-Jones and Turkevich,[23] by Coulson,[24] by Penney[25] and by Brockway, Beach and Pauling.[26] The results of these calculations are summarized in Table IV. The bonds are designated a, b, c, and d as depicted in (IX) above.

Table IV

Theoretical Bond Lengths in Naphthalene

| | a | b | c | d | reference |
|---|---|---|---|---|---|
| $P_1$ [i] | 1.42 | 1.42 | 1.39 | 1.42 | 20 |
| $P_2$ [ii] | 1.40 | 1.44 | 1.39 | 1.42 | 26 |
| $C_1$ [iii] | 1.44 | 1.40 | 1.39 | 1.40 | 24 |
| $C_2$ [iv] | 1.42 | 1.41 | 1.38 | 1.40 | 24 |
| L-J [v] | 1.37 | 1.39 | 1.37 | 1.39 | 23 |
| Py [vi] | 1.42 | 1.40 | 1.38 | 1.40 | 25 |

i From consideration of double-bond character in each bond for equal contributions of (VI), (VII), and (VIII) (Pauling)

ii From Sherman's wave function[27] considering contributions of 42 possible structures (Brockway, Beach and Pauling)

iii From empirical consideration of bond interaction (Coulson)

iv From a valence-bond treatment of resonance (Coulson)

v From a molecular-orbital treatment (Lennard-Jones and Turkevich)

vi From a valence-bond treatment of resonance (Penney)

Theoretical treatments of the anthracene molecule have not been as numerous nor, in general, have the results been as precisely stated as was the case for naphthalene. The results of numerical calculations by Pauling and coworkers[18,26] and by Michailov[28] are summarized in Table V. The bonds are designated a, b, c, d, and e as depicted in (XIV) above.

Table V

Theoretical Bond Lengths in Anthracene

| | a | b | c | d | e | reference |
|---|---|---|---|---|---|---|
| $P_1$[i] | 1.44 | 1.44 | 1.355 | 1.44 | 1.39 | 18 |
| $P_2$[ii] | 1.474 | 1.453 | 1.395 | 1.446 | 1.425 | 26 |
| M[iii] | 1.44 | 1.416 | 1.375 | 1.41 | 1.396 | 28 |

i From consideration of double-bond character in each bond for equal contributions of (X), (XI), (XII), and (XIII) (Pauling)

ii From Sherman's wave function[27] (Brockway, Beach and Pauling) (by Michailov)

iii From a valence-bond treatment of resonance, after Penney[25] (Michailov)

Determinations of the structures of crystalline naphthalene[29] and anthracene[30] have been made by Robertson. The molecules were reported to be planar, with atoms at the corners of regular hexagons. The C-C bond distances were reported to be equal and, in each molecule, to have the length 1.41 Å. Pauling[26] has noted small deviations from regularity in Robertson's Fourier projection of the naphthalene molecule and has interpreted these to indicate that the carbon-carbon distances are not truly equal.

An electron diffraction investigation of the structure of naphthalene was carried out by Specchia,[31] but only an average value, 1.397 Å. was arrived at for the C-C bond distances.

The present work, a determination of the structures of naphthalene and anthracene in the gas phase, is a completion of an investigation begun in 1941 by Dr. Jurg Waser, who prepared electron diffraction photographs of the two compounds and calculated a number of theoretical curves for naphthalene. The large number of parameters which were to be determined in each molecule necessitated a procedure somewhat different from that which is usually followed in electron diffraction investigations. The distances reported by Robertson in naphthalene and anthracene were, for each case, in reasonable agreement with the peaks in the radial distribution function. Theoretical intensity functions which were calculated from these models, however, were not in full agreement with the visual curve. The parameters of the $D_{2h}$ model were varied individually about the values assigned in the Robertson model, which was used as a standard for comparison. From a consideration of the effects of each of these parameter variations on the theoretical intensity curves, it was possible to suggest a model, the intensity function for which would be in best agreement (in the range investigated) with experimental observations.

The estimation of limits of error for the individual parameters in naphthalene and anthracene is almost impossibly difficult, since the treatment of each problem by a systematic correlation procedure is not feasible. Consequently, I have attempted only to estimate the limits of error for the average bond distance, to determine the model which, in the

region of parameter space considered, appears to result in the best possible agreement with experimental observations, and to indicate the parameter variations to which the theoretical intensity functions are most sensitive.

In the parameter range investigated, the variations in the qualitative aspect of the theoretical curves are quite small; as a result, much of the comparison of these curves with the visual observations was made on the basis of the relative positions of the features. Indeed, the final choice of a favored model was based upon these considerations.

i Naphthalene

The electron diffraction photographs were taken by Dr. Waser with the use of the standard high-temperature nozzle. The jet-to-film distance was 10.91 cm. Features were observed at q values extending to about 100.

The visual curve, V, for naphthalene and the radial distribution function, R, are shown in Figure 4. Peaks are observed at 1.39, 2.20, 2.43, 2.78, 3.08, 3.73, and 4.20 Å. These distances are in reasonable agreement with the Robertson model. Some theoretical intensity functions for molecular models of symmetry $D_{2h}$ are also shown in Figure 4. The Robertson model (Curve A) is seen to be acceptable within the limits of experimental error. Similar models, with angles different from 120° become unsatisfactory (B and C) in the region of the tenth and eleventh maxima and also in the relative positions of many of the main features. The shift in these positions is much larger than that brought about by a change of 0.03 Å. in any bond distance. No combination of such changes

has been found which brings curves B and C back to coincidence with the observations. Consequently, it may be that the allowable variation in the angle is as little as $2^{\circ}$, although a precise statement cannot be made from this examination of a comparatively small number of curves.

A comparison of the relative positions of the main features in curves B-E and G-L with the visual curve led to the suggestion of a model, corresponding to curve F, which, in the range of parameters considered, best represents the appearance of the photographs. Curve F, after adjustment of the size parameter, corresponds to the following model:

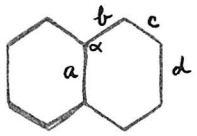


a $1.42_4$ Å.
b $1.40_4$
c $1.38_4$
d $1.40_4$
$\angle \alpha$ $120^{\circ}$

A conclusion concerning the average bond distance in naphthalene was reached in the following manner: for each of a large number of models (in the region of parameter space under consideration), the average bond distance was multiplied by the $\overline{q/q_o}$ for the corresponding theoretical intensity curve. The mean of the resultant set of numbers was taken as the average bond distance. The maximum deviation from the mean was taken as the probable limit of error. The value finally arrived at was $1.39_7 \pm 0.02$ Å.

Of the individual parameters, the angle $\alpha$ appears to be most precisely determinable by the electron diffraction method. The precision

in the individual bond distances, as might have been predicted from the relative effect of displacing the various atoms in the molecule, appears to be in the order b > c > d > a.

A number of errors in the interpretation of the photographs appear to have been made. The height of the fifth maximum was thought to be greater than that of the sixth, and the strength of the tenth maximum was overestimated. From reexamination of the photographs with particular reference to these features, it was estimated that curve F is a better representation of the photographs in these regions than is the visual curve. These errors are probably not serious since all theoretical intensity curves which were considered are similar in the particular aspects which were misinterpreted.

A comparison between the positions of the main features in the selected model, which is just Penney's (see Table IV, Py), it happens, and in Robertson's model with those in the visual curve is made in Table VI.

Table VI

Naphthalene

| Min | Max | $q_o$ | $q_F$ | $q_F/q_o$ | $q_A$ | $q_A/q_o$ |
|---|---|---|---|---|---|---|
| 1 | | 7.67 | 7.68 | (1.001)* | 7.60 | (0.990)* |
| | 1 | 10.08 | 10.04 | (0.996)* | 10.08 | (1.000)* |
| 2 | | 13.98 | 13.84 | 0.990 | 13.92 | 0.995 |
| | 2 | 17.70 | 18.12 | 1.023 | 17.84 | 1.008 |
| 3 | | 23.74 | 23.76 | 1.001 | 23.44 | 0.987 |
| | 3 | ----- | ----- | ----- | ----- | ----- |
| 4 | | ----- | ----- | ----- | ----- | ----- |
| | 4 | 28.96 | 29.60 | 1.022 | 29.44 | 1.017 |
| 5 | | 31.34 | 31.60 | 1.008 | 31.20 | 0.995 |
| | 5 | 33.92 | 34.12 | 1.006 | 34.24 | 1.009 |
| 6 | | 41.04 | 40.92 | 0.997 | 40.00 | 0.975 |
| | 6 | 44.12 | 44.40 | 1.006 | 44.40 | 1.006 |
| 7 | | 47.40 | 47.40 | 1.000 | 47.68 | 1.006 |
| | 7 | 49.24 | 49.96 | 1.015 | 50.40 | 1.024 |
| 8 | | 51.30 | 51.50 | 1.004 | 51.45 | 1.003 |
| | 8 | 53.63 | 53.96 | 1.006 | 53.73 | 1.002 |
| 9 | | 56.00 | 55.44 | 0.990 | 55.28 | 0.987 |
| | 9 | 59.52 | 60.04 | 1.009 | 59.84 | 1.005 |
| 10 | | 63.84 | 64.48 | 1.010 | 64.56 | 1.011 |
| | 10 | 66.72 | 67.36 | 1.010 | 67.28 | 1.008 |
| 11 | | 70.08 | 70.12 | 1.001 | 69.84 | 0.997 |
| | 11 | 72.88 | 72.80 | 0.999 | 72.48 | 0.995 |
| 12 | | 74.45 | 74.60 | 1.003 | 73.76 | 0.992 |
| | 12 | 75.76 | 76.44 | 1.009 | 76.32 | 1.007 |
| 13 | | 80.32 | 80.76 | 1.005 | 80.80 | 1.006 |
| | 13 | 82.80 | 82.40 | 0.995 | 83.44 | 1.008 |
| 14 | | 84.80 | 85.08 | 1.003 | 84.64 | 0.998 |
| | 14 | 87.84 | 87.88 | 1.000 | 87.72 | 0.996 |
| 15 | | 90.56 | 90.28 | 0.997 | 90.08 | 0.993 |
| | 15 | 93.60 | 92.92 | 0.993 | 92.32 | 0.986 |
| | | Average | | 1.004 | | 1.000 |
| | | Average deviation | | 0.008 | | 0.009 |

* Not included in the average

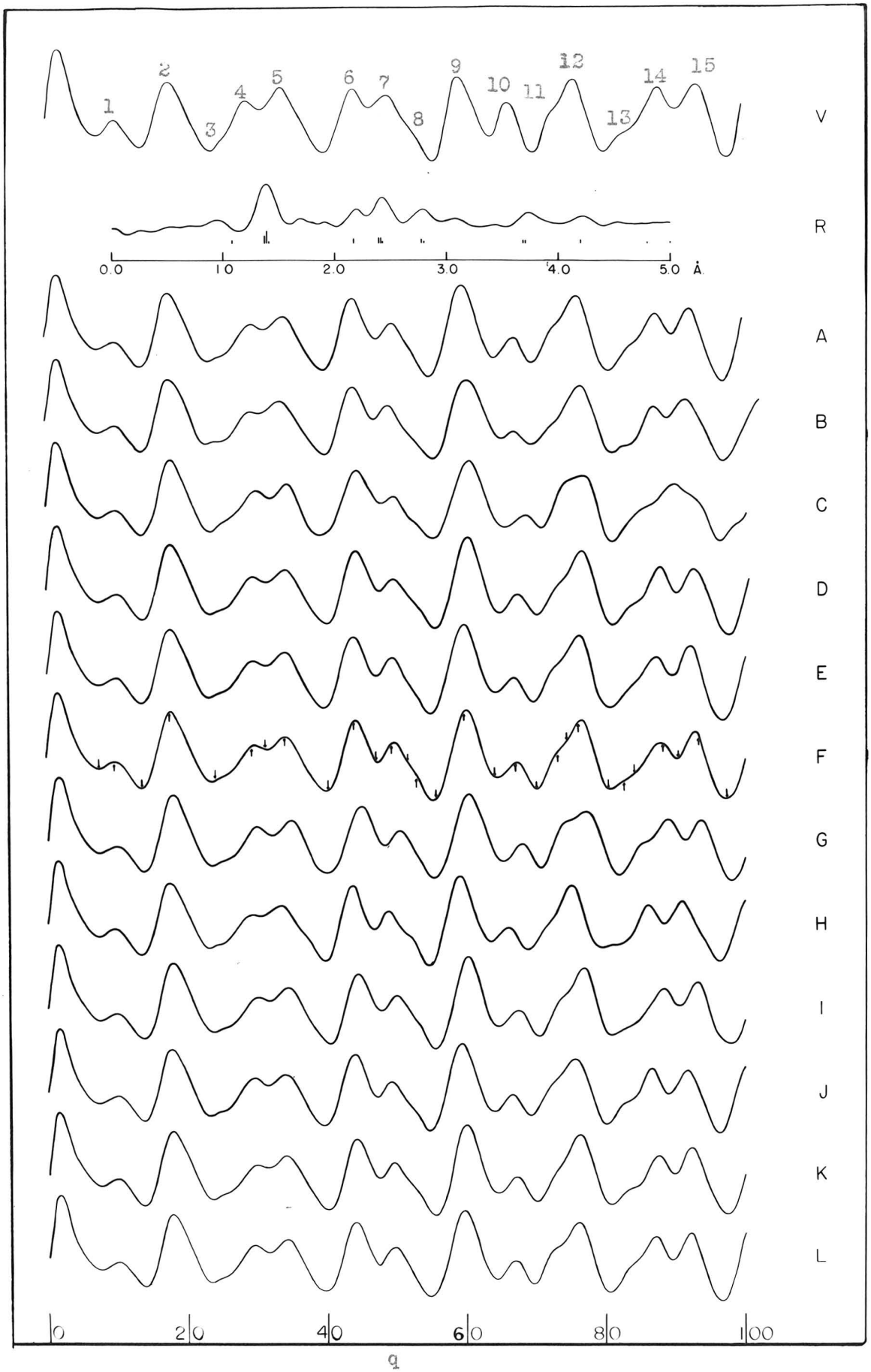


Figure 4: Electron Diffraction Curves for Naphthalene

Table of Parameters (Figure 4)

Naphthalene

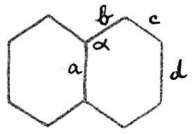


| Model | a | b | c | d | ∠α |
|---|---|---|---|---|---|
| A | 1.40 | 1.40 | 1.40 | 1.40 | 120 |
| B | 1.40 | 1.40 | 1.40 | 1.40 | 118 |
| C | 1.40 | 1.40 | 1.40 | 1.40 | 122 |
| D | 1.36 | 1.40 | 1.40 | 1.40 | 120 |
| E | 1.44 | 1.40 | 1.40 | 1.40 | 120 |
| F | 1.42 | 1.40 | 1.38 | 1.40 | 120 |
| G | 1.40 | 1.44 | 1.40 | 1.40 | 120 |
| H | 1.40 | 1.40 | 1.36 | 1.40 | 120 |
| I | 1.40 | 1.40 | 1.44 | 1.40 | 120 |
| J | 1.40 | 1.40 | 1.40 | 1.36 | 120 |
| K | 1.40 | 1.40 | 1.40 | 1.44 | 120 |
| L | 1.40 | 1.36 | 1.40 | 1.40 | 120 |

All models planar with symmetry $D_{2h}$

ii Anthracene

The electron diffraction photographs were taken by Dr. Waser under conditions similar to those in which pictures of naphthalene were prepared. The jet-to-film distances were 10.91 cm. and 20.25 cm.; pictures at the longer camera distance were taken to aid in the estimation of fine structure in the intensity pattern at small q values.

The visual curve, V, is shown in Figure 5. Peaks in the radial distribution function, R, are observed at 1.09, 1.41, 2.17, 2.42, 2.83, 3.37, 3.70, 4.19, and 4.98 Å. Beyond 5.5 Å., no significant peaks appeared in the RDI. The procedure followed in applying the correlation method was similar to that outlined in the introduction to part III b and to that used in determining the structure of naphthalene. The parameters of the $D_{2h}$ model, a, b, c, d, e, $\alpha$ and $\beta$ (as shown below), were varied individually about the values assigned in the Robertson model, A of Figure 5, which was used as a standard for comparison.

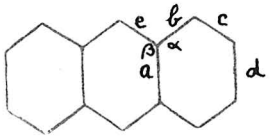


The attempt to determine individual bond distances in anthracene was of no avail. The differences in the theoretical intensity curves shown in Figure 5 are, for the most part, too small to permit one model to be chosen over other models on the basis of qualitative comparison. The best model was chosen on the basis of a comparison of the positions of the main features with those in the visual curve. Variations in the distances a or d (curve H, I, J, K) bring about such small changes in the intensity functions that extremely wide limits of error must be assigned to these

distances. On the other hand, an increase in either the distance b or e (curves G and O) brings about similar variations in the positions of the main features so that only an average of these two distances may be stated.

The Pauling model of anthracene (curve P), described in the introduction to this section, is considered to be within the acceptable region. The diffuse nature of the next-to-last maximum, the reversed asymmetry in the last minimum and the general disagreement in the positions of these features occur in a region in which the visual curve must be considered uncertain. Consequently, in the absence of more serious disagreement, curve P is considered acceptable. By comparison with the visual curve, G is best in agreement with observed data, the average deviation of $q_{calc}/q_{obs}$ being 0.007. Average deviations of $q_{calc}/q_{obs}$ for curves A, M, and O are 0.009, 0.009, and 0.010 respectively. Curve G, after adjustment of the size parameter, corresponds to the following model:

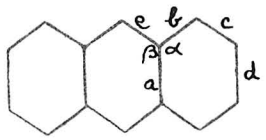


a $1.41_7$ Å.

b $1.43_7$

c $1.41_7$

d $1.41_7$

e $1.43_7$

$\angle\alpha$ 120°

$\angle\beta$ 120°

The average bond distance, determined as in naphthalene from a consideration of the $\overline{q/q_o}$ for each of a large number of curves, was found to be $1.41_9 \pm 0.02$ Å.

The most precisely determinable parameters in anthracene appear to be the angles $\alpha$ and $\beta$ ; these, however, can probably not be estimated with as much certainty as can the angle in naphthalene. The statement of the bond distances b, c, and e, is probably more precise than that of a and d, but less so than that of the angles $\alpha$ and $\beta$ . The quantitative changes in theoretical intensity curves brought about by variations in the distances b and e are such that their average is probably more precisely determinable than are the individual distances.

It should be pointed out that several distances in model G are in disagreement with their respective peaks in the RDI, although curve G is in good agreement with the visual curve. No explanation for the anomaly is offered.

A comparison of the positions of the main features in curve G with those in the visual curve is shown in Table VII.

Table VII

Anthracene

| Min | Max | $q_o$ | $q_G$ | $q_G/q_o$ |
|---|---|---|---|---|
| 1 | | 7.91 | 7.65 | 0.967 |
| | 1 | 10.30 | 10.20 | 0.990 |
| 2 | | 14.00 | 14.00 | 0.998 |
| | 2 | 16.85 | 17.30 | 1.027 |
| 3 | | 23.60 | 23.70 | 1.004 |
| | 3 | ----- | ----- | ----- |
| 4 | | ----- | ----- | ----- |
| | 4 | 28.72 | 28.60 | 0.996 |
| 5 | | 31.38 | 30.75 | 0.980 |
| | 5 | 34.34 | 33.25 | 0.968 |
| 6 | | 40.32 | 39.70 | 0.985 |
| | 6 | 43.44 | 43.40 | 0.999 |
| 7 | | 46.94 | 47.05 | 1.002 |
| | 7 | 49.73 | 49.40 | 0.993 |
| 8 | | 51.61 | 51.25 | 0.993 |
| | 8 | 53.63 | 53.25 | 0.993 |
| 9 | | 54.96 | 54.25 | 0.996 |
| | 9 | 59.13 | 58.95 | 0.997 |
| 10 | | 63.43 | 63.45 | 1.000 |
| | 10 | 65.54 | 65.60 | 1.001 |
| 11 | | 68.30 | 68.65 | 1.005 |
| | 11 | 71.39 | 71.00 | 0.995 |
| 12 | | 73.22 | 72.60 | 0.992 |
| | 12 | 75.42 | 74.60 | 0.989 |
| 13 | | 78.97 | 79.30 | 1.004 |
| | 13 | 82.04 | 81.60 | 0.995 |
| 14 | | 83.70 | 82.85 | 0.990 |
| | 14 | 85.08 | 85.80 | 1.008 |
| 15 | | 88.38 | 88.00 | 0.996 |
| | 15 | 90.74 | 90.30 | 0.995 |
| 16 | | 96.41 | 95.90 | 0.995 |

| | |
|---|---|
| Average | 0.995 |
| Average deviation | 0.007 |

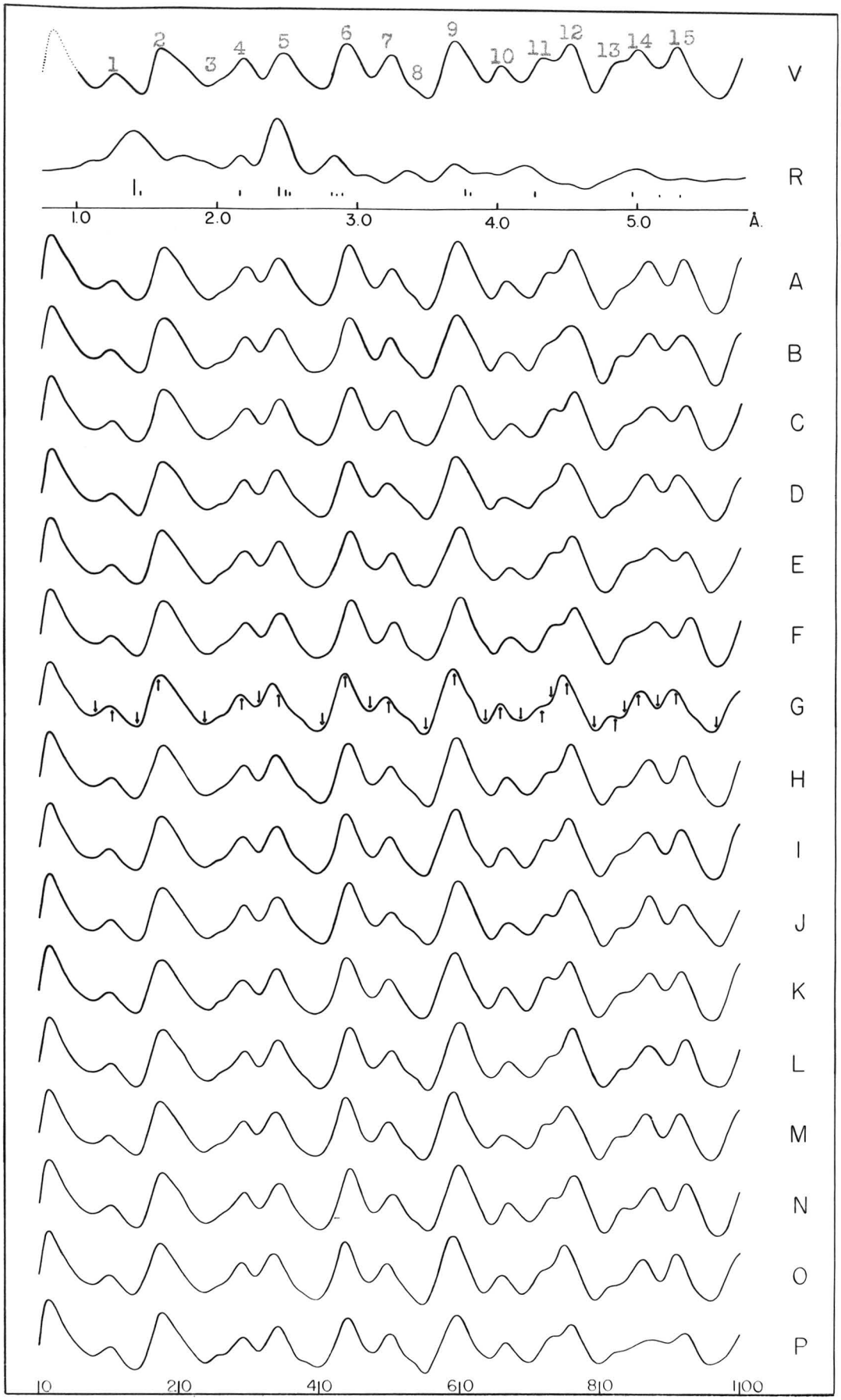


Figure 5: Electron Diffraction Curves for Anthracene

Table of Parameters (Figure 5)

Anthracene

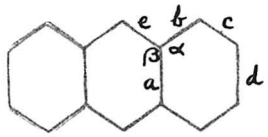


| Model | a | b | c | d | e | ∠α | ∠β |
|---|---|---|---|---|---|---|---|
| A | 1.41 | 1.41 | 1.41 | 1.41 | 1.41 | 120 | 120 |
| B | 1.41 | 1.41 | 1.41 | 1.41 | 1.41 | 120 | 118 |
| C | 1.41 | 1.41 | 1.41 | 1.41 | 1.41 | 120 | 122 |
| D | 1.41 | 1.41 | 1.41 | 1.41 | 1.41 | 118 | 120 |
| E | 1.41 | 1.41 | 1.41 | 1.41 | 1.41 | 122 | 120 |
| F | 1.41 | 1.41 | 1.41 | 1.41 | 1.37 | 120 | 120 |
| G | 1.41 | 1.41 | 1.41 | 1.41 | 1.45 | 120 | 120 |
| H | 1.41 | 1.41 | 1.41 | 1.37 | 1.41 | 120 | 120 |
| I | 1.41 | 1.41 | 1.41 | 1.45 | 1.41 | 120 | 120 |
| J | 1.37 | 1.41 | 1.41 | 1.41 | 1.41 | 120 | 120 |
| K | 1.45 | 1.41 | 1.41 | 1.41 | 1.41 | 120 | 120 |
| L | 1.41 | 1.41 | 1.37 | 1.41 | 1.41 | 120 | 120 |
| M | 1.41 | 1.41 | 1.45 | 1.41 | 1.41 | 120 | 120 |
| N | 1.41 | 1.37 | 1.41 | 1.41 | 1.41 | 120 | 120 |
| O | 1.41 | 1.45 | 1.41 | 1.41 | 1.41 | 120 | 120 |
| P | 1.44 | 1.44 | 1.355 | 1.44 | 1.39 | 120 | 120 |

All models planar with symmetry $D_{2h}$

## SUMMARY

The molecular structures of naphthalene and of anthracene have been determined by the electron diffraction method. The assumption of a planar structure with a molecular symmetry $D_{2h}$ leads to models in excellent agreement with the observed intensity function. The individual C-C bond distances could not be determined with a desirable degree of accuracy, but the average bond distance was determined within very narrow limits. The models which, in the regions investigated, were favored as being in best agreement with the visual observations were as follows:

Naphthalene

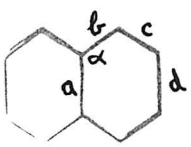


a $1.42_4$ Å.

b $1.40_4$

c $1.38_4$

d $1.40_4$

$\angle \alpha$ 120°

Average bond distance $1.39_7 \pm 0.02$ Å.

Anthracene

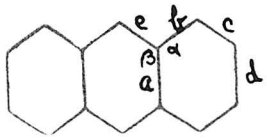


a $1.41_7$ Å.

b $1.43_7$

c $1.41_7$

d $1.41_7$

e $1.43_7$

$\angle \alpha$ 120°

$\angle \beta$ 120°

Average bond distance $1.41_9 \pm 0.02$ Å.

## REFERENCES


1. L. O. Brockway, Rev. Mod. Phys. 8, 231 (1936)
2. L. Pauling and L. O. Brockway, J.A.C.S. 59, 2181 (1937)
3. R. Spurr and V. Schomaker, J.A.C.S. 64, 2693 (1942)
4. L. Pauling and L. O. Brockway, J. Ch. Phys. 2, 867 (1934)
5. P. A. Shaffer, Jr., V. Schomaker and L. Pauling, J. Ch. Phys. 14, 659 (1946)
6. R. Majima and H. Simanuki, Prco. Imp. Acad. (Japan) 2, 544 (1926)
7. H. J. Lucas, F. W. Mitchell and C. N. Scully (to be published)
8. C. N. Scully, M. S. Thesis, Calif. Inst. of Tech. (1947)
9. M. Guthrie, B. A. Thesis, Reed College (1948)
10. C. S. Lu and E. W. Malmberg, Rev. Sci. Instr. 14, 271 (1943)
11. W. Shand, Jr., Ph.D. Thesis, Calif. Inst. of Tech. (1947)
12. J. Donohue, Ph.D. Thesis, Calif. Inst. of Tech. (1947)
13. L. Pauling and M. L. Huggins, Z. Krist. 87, 205 (1935)
14. L. Pauling and L. O. Brockway, J.A.C.S. 59, 1223 (1937)
15. V. Schomaker and D. P. Stevenson, J.A.C.S. 63, 37 (1941)
16. L. Pauling, The Nature of the Chemical Bond, Second Edition, Cornell University Press, Ithaca, N.Y. (1940), Chap. V.
17. Smiles, The Relation Between Chemical Constitution and Some Physical Properties, Longman, Green and Co., London (1910)
18. Reference 16, Chap. VIII
19. K. S. Pitzer, J.A.C.S. 70, 2140 (1948)
20. G. C. Hampson and A. J. Stosick, J.A.C.S. 60, 1814 (1938)
21. A. J. Stosick, J.A.C.S. 61, 1130 (1939)
22. Westrink and MacGillavry, Rec. trav. chim. 60, 794 (1941)
23. J. E. Lennard-Jones and J. Turkevich, Prov. Roy. Soc. (London) A158, 280 (1937)

24. C. A. Coulson, J. Ch. Phys. 7, 1069 (1939)

25. W. G. Penney, Proc. Roy. Soc. (London) A158, 306 (1937)

26. L. O. Brockway, J. Y. Beach and L. Pauling, J.A.C.S. 57, 2705 (1935)

27. J. Sherman, J. Ch. Phys. 2, 488 (1934)

28. B. Michailov, Acta Physicochimica U.R.S.S. XXI, 387 (1946)

29. J. M. Robertson, Proc. Roy. Soc. (London) A125, 542 (1929)

30. J. M. Robertson, Proc. Roy. Soc. (London) A140, 79 (1938)

31. G. Specchia, Nuovo Cimento XVIII, 102 (1941)

Propositions Submitted by Bertram Keilin

Ph.D. Oral Examination, November 23, 1949, 1:00 P.M., Crellin Conference Room

Committee: Professors V. Schomaker (Chairman), C. D. Anderson, R. M. Badger, S. J. Bates, C. Niemann, J. G. Kirkwood, and L. Pauling

1. a) The molecular structure of selenium tetrachloride in the gas phase has been reported by Lister and Sutton.[1] Prof. V. Schomaker has pointed out that at equilibrium selenium tetrachloride vapor is completely dissociated into $SeCl_2$ and $Cl_2$,[2] that the diffraction photographs obtained by Lister and Sutton may have been of such a mixture, and that their reported data, indeed, agree more fully with a $SeCl_2 + Cl_2$ model than with any of their $SeCl_4$ models. It would be interesting to compare photographs taken of an equilibrium mixture of gas with those taken of a flowing gas. The former would be obtained in the usual way from an equilibrium gas mixture, the latter, which might possibly be characteristic of a transient $SeCl_4$ gas species, would be obtained by allowing the vapor from $SeCl_4$ crystals to pass continuously across the path of the electron beam. The excess gas in the chamber should not prove troublesome in causing secondary scattering of the electrons since it will be expected to condense rapidly on the walls.

b) The structure of $SeCl_2$ may be determined in a diffraction experiment from the vapor over $Se_2Cl_2$.[3]

1. Lister and Sutton, Trans. Far. Soc., 37, 393 (1941)
2. Yost and Kircher, J.A.C.S., 52, 4680 (1930)
3. Wehrli, Helv. Phys. Acta, 9, 329 (1936)

2. The planar model favored by Shand[4] as representing the structure of ethylene-methylene dioxide results in a theoretical intensity curve which is in severe disagreement with his data (obtained from electron diffraction

experiments) at several points. I propose a non-planar structure for this molecule for which the corresponding theoretical curve is in full agreement with the observations.

4. Shand, Ph.D. Thesis, Calif. Inst. of Tech. (1946)

3. An attempted synthesis[5] of 1,3-dibromo-2-carbethoxypropane (I) failed because of the instability of an intermediate, dimethylolmalonic ester.[6] The recent literature has yielded information[7] from which it seems likely that compound (I) may be prepared in the following manner from pentaerithrytol:

$$C(CH_2OH)_4 \longrightarrow (HOCH_2)_2C(CH_2Br)_2 \longrightarrow (HOOC)_2C(CH_2Br)_2 \longrightarrow HOOC\text{-}CH(CH_2Br)_2$$

5. Keilin, M.S. Thesis, Calif. Institute of Tech. (1945)

6. Gault and Roesch, Bull. soc. chim., series 5, 4, 1410 (1937)

7. Mooradian and Cloke, J.A.C.S., 67, 942 (1945)

4. The present method[8] for preparing 1,3-cyclobutanedicarboxylic acid is highly unsatisfactory inasmuch as it involves a reaction in which the yield is about 10%. I propose that a more satisfactory yield would result from a malonic ester synthesis of this compound.[9,10]

8. Markownikoff and Krestownikoff, Ann. 208, 333 (1881).

9. Perkin, J.C.S., 51, 1 (1887)

10. Owen, Ramage and Simonsen, J.C.S., 153, 1211 (1938)

5. The expression obtained in this thesis (p. 32) for the diffusion current of a reducible ion or molecule in the presence of capillary-active substances implies a different dependence of the current on the time than does the Ilkovic equation.[11] A test of the validity of this equation may be made by a study of the dye-protein system by the oscillographic current-time method.[12]

11. Ilkovic, Coll. Czech. Chem. Commun., 6, 498 (1934)

12. Matheson and Nichols, Trans. Amer. Electrochem. Soc., 73, 193 (1938)

6. A further investigation of single-bond S-O and P-O distances would be of interest in connection with the apparently anomalous results reported in this thesis. The interatomic distances in dimethyl sulfate, dimethyl sulfite and trimethyl phosphate would be of great interest in determining the extent of the occurrence of these anomalous distances.

7. The permanent electric dipole moment of ethylene glycol chlorophosphite ester would be expected to be small ($\approx 1$ Debye unit) if these molecules contained normal covalent bonds. A determination of the moment would give much information concerning the contribution of multiple-bond or ionic structures to the state of this molecule.

8. In this thesis (p. 24), it has been reported that mercury droplets formed at a dropping electrode in a protein-containing saline solution remain as discrete globules at the bottom of the container if the potential of the electrode is more positive than -2.2 v. (vs. S.C.E.) during their formation, but will coalesce under the action of a platinum electrode at a potential more negative than -0.7 v. I propose the following explanation for the apparent anomaly: Adsorption of protein on the drop surface occurs when the potential of the drop is more positive than -0.7 v. The potential on a drop formed between -0.7 and -2.2 v. is rapidly dissipated after it leaves the electrode; however, if formed at a potential more negative than -2.2 v., the drop consists, at the surface, of a dilute sodium amalgam. The discharge of sodium from this amalgam, as the drop falls through the solution, maintains a potential sufficient to preclude the adsorption of protein.

9. Kolthoff and Lingane[13] state that in a 1% solution of gelatin, the diffusion current of a solution of lead ion is reduced to 50% of its normal value, and that this decrease may be attributed to the change in viscosity of the medium. I submit that the current decrease cannot be completely explained in this manner, but must be attributed at least in part, to adsorption of the protein on the mercury droplet.

13. Kolthoff and Lingane, Chem. Reviews, 24, 1-94 (1939)

10. The course in elementary quantum mechanics should be offered in the chemistry department more often than once in three years. Because of the importance of this subject to a full understanding of physical chemistry, it is a severe handicap for a student to spend one or two years in residence before being exposed to the rudiments. Furthermore, the scope of many other courses might be widened considerably if a knowledge of quantum mechanics were a required prerequisite.